

# **SYSTEMS BIOLOGY OF MAMMALIAN CELLS**

-

## **MATHEMATICAL MODELING FOR UNCOVERING METABOLIC COMPARTMENTATION**

Dissertation

zur Erlangung des Grades

des Doktors der Ingenieurwissenschaften

der Naturwissenschaftlich-Technischen Fakultät III

Chemie, Pharmazie, Bio- und Werkstoffwissenschaften

von

Averina Nicolae

Saarbrücken, Deutschland

2015

|                           |                                |
|---------------------------|--------------------------------|
| Tag des Kolloquiums:      | 20. November 2015              |
| Dekan:                    | Prof. Dr.-Ing. Dirk Bähre      |
| Berichterstatter:         | Prof. Dr.-Ing. Elmar Heinzle   |
| Zweiter Berichterstatter: | Prof. Dr. Volkhard Helms       |
| Vorsitz:                  | Prof. Dr. Gert-Wieland Kohring |
| Akad. Mitarbeiter:        | Dr. Judith Becker              |

*“Clouds are not spheres, mountains are not cones, coastlines are not circles, and bark is not smooth, nor does lightning travel in a straight line.”*

— Benoît B. Mandelbrot

*To my mother*

## Acknowledgments

Coming to Germany for pursuing a PhD has been the most life altering journey of my life. It was a long effort though which I have received immense support, both personally and professionally. Without all the people who involved themselves so generously, this thesis would not have existed. For this, I would like foremost to express my immense appreciation to Prof. Dr. Elmar Heinzle for trusting me to become one of his PhD students. I am delighted to thank him for giving me the opportunity to come to Saarland and have him not only as an exceptional supervisor, but also as an inspiring mentor for everything that concerns work, science and life. I am grateful for him allowing me the space to pursue my research in a personal manner and for his valuable insights and guiding.

I would also like to thank Prof. Dr. Volker Helms for gladly consenting to reviewing this thesis and being the second supervisor. I want to thank the thesis committee in advance for lending from their precious time for my defense. I want to express my tremendous appreciation to Dr. Susanne Kohring for her reliable, consistent care and for the logistic support she always so promptly provided.

I can only be grateful for receiving the best project partner one can wish for. My symbiosis with Dr. Judith Wahrheit produced great research and a friendship I will cherish for a lifetime. This thesis depended on the data that she so diligently pursued despite all the setbacks. I want to thank her for the vision, her inspirational drive and energy, and for all our scientific fights ... but let's call them discussions. Simone Beckers deserves my gratitude for all the many times she basically saved my life in Germany. Life as a foreigner is not particularly easy, and I would like to thank all the people who became my home away from home: my friends and colleagues Alexander Strigun and Christian Weyler for all the great scientific and other engaging conversations, Andreas Neuner for being my big brother here and to Jens, Tobias and Christian for their energizing attitude. My colleagues at Technische Biochemie created an excellent work atmosphere and I would like to thank Fozia, Michel, Klaus, Robert, Konstantin, Vassilis,

Susanne, Verena, Richa, Malina, Esther, Lisa, Saskia, Sebastian, Yeda, Steffen, Rene, Georg and Daniel for making the lab a great place to do science.

I would like to acknowledge the support of BMBF (German Federal Ministry of Education and Research) projects SysCompart [project ID 031555D] and OxiSys [project ID 031 5891 B] for funding, and that of SysCompart project coordinator Prof. An-Ping Zeng and all the other collaborators involved in SysCompart for all the fruitful contributions.

In Saarbrücken I was blessed to meet many amazing people that I can now call my friends, and I will thank all of them for the moral support, help and friendship throughout all these years.

Last, but obviously not least, my family deserves my deepest gratitude for their unconditional love and support, for believing in me and for encouraging me continuously.

## Abstract

Compartmentation contributes at controlling the mammalian metabolism and is important in aging and diseases. Systems biology methods were applied to study compartmentation between cytosol and mitochondria.

A mathematical modeling platform for non-stationary  $^{13}\text{C}$  metabolic flux analysis (Inst- $^{13}\text{CMFA}$ ) was developed and tested. It was then extended to model also extracellular labeling. First, fluxes were determined for the CHO-K1 cell line metabolism using only extracellular labeling and one labeled substrate. The results indicate that the cells adapt to sustain fast growth and to manage the complex media. Then, high resolution of compartment fluxes, reversibility and intracompartmental concentrations resulted by applying Inst- $^{13}\text{CMFA}$  to data from two labeling experiments. In both studies, pentose phosphate pathway carried a large flux. The produced NADPH is used by fatty acid synthesis and for mitigating oxidative stress. Differences in labeling were described by a model with pyruvate channeling.

Selectively permeabilized CHO-K1 cells were fed mitochondrial substrates. Using the elementary mode decomposition of the mitochondrial network, the observed extracellular rates were distributed into elementary mode fluxes. This evidenced activity of pathways and regulatory effects.

By combining more systems biology methods, this thesis constructed a larger picture for characterizing the complex metabolism of CHO-K1 cells and uncovered many new characteristics of metabolic compartmentation.

## Zusammenfassung

Die Kompartimentierung des Stoffwechsels trägt dazu bei den Stoffwechsel des Säugetiers zu regulieren. Methoden aus der Systembiologie wurden angewendet um die Kompartimentierung zu untersuchen.

Eine Modellierungsplattform für nichtstationäre  $^{13}\text{C}$  Stoffwechsel-Flussanalyse (Inst- $^{13}\text{CMFA}$ ) wurde erarbeitet und getestet. Die Plattform wurde erweitert um Änderungen in der extrazellulären Isotopenmarkierung aufzunehmen. Flüsse wurden für die CHO-K1 Zelllinien bestimmt durch die Verwendung von extrazellulärer Markierung. Flusswerte deuten darauf hin, dass sich die Zellen hinsichtlich schnellem Wachstum und der komplexen Medienzusammensetzung anpassen. Eine hohe Auflösung von Parametern wurde erreicht, indem Inst- $^{13}\text{CMFA}$  auf die Daten aus zwei Markierungsexperimenten angewendet wurde. In beiden Studien trug die Pentosephosphatweg einen hohen Fluss um NADPH zur Fettsäuresynthese und um oxidativen Stress zu vermeiden. Weiterhin lieferte das Channeling von Pyruvat eine Erklärung für Unterschiede Markierungen.

Selektiv permeabilisierten CHO-K1 Zellen wurden verschiedene Substrate zugeführt. Unter Anwendung der Elementarmoden Zerlegung auf das mitochondriale Netzwerk konnte die Aktivität von Stoffwechselpfaden und regulierenden Effekten belegt werden.

Indem weitere Methoden der Systembiologie angewandt wurden, trägt diese Dissertation dazu bei ein umfassenderes Bild des Stoffwechsels von CHO-K1 Zellen zu erstellen. Gleichzeitig wurden neue Fragen in Bezug auf Kompartimentflüsse aufgeworfen.

# Abbreviations

## Subscripts

c - cytosolic

ex - extracellular

m - mitochondrial

## Abbreviations

AA - amino acid

AKGDH -  $\alpha$ -ketoglutarate dehydrogenase

C<sub>4</sub> - 4-carbon dicarboxylic acid

CHO - Chinese hamster ovary

EMA - elementary mode analysis

FBA - flux balance analysis

G6P - glucose-6-phosphate

GC-MS - gas chromatography - mass spectrometry

GDH - glutamate dehydrogenase

GLS - glutaminase

HPLC - high performance liquid chromatography

IDH - isocitrate dehydrogenase

Inst-<sup>13</sup>C MFA - Non-stationary <sup>13</sup>C metabolic flux analysis

mAb - monoclonal antibody

MDH - malate dehydrogenase

ME - malic enzyme

MFA - metabolic flux analysis

MID - mass isotopomer distribution

MTHF - methyltetrahydrofolate

PCK - phosphoenolpyruvate carboxykinase

PCX - pyruvate carboxylase



|      |                                   |
|------|-----------------------------------|
| PDH  | – pyruvate dehydrogenase          |
| PEP  | – phosphoenolpyruvate             |
| PG   | – phosphoglycerate                |
| PPP  | – pentose phosphate pathway       |
| SHMT | – serine hydroxymethyltransferase |
| SSQD | – sum of square differences       |
| TCA  | – tricarboxylic acid              |

## Contents

|                                                                                                     |           |
|-----------------------------------------------------------------------------------------------------|-----------|
| <b>1. Introduction in systems biology for metabolism analysis of eukaryotic cells .....</b>         | <b>1</b>  |
| 1.1. Mitochondria .....                                                                             | 3         |
| 1.2. Systems biology of mammalian cells .....                                                       | 4         |
| 1.3. <sup>13</sup> C-based metabolic flux analysis .....                                            | 10        |
| 1.4. Non-stationary <sup>13</sup> C metabolic flux analysis .....                                   | 14        |
| 1.5. Dynamic metabolic flux analysis .....                                                          | 17        |
| 1.6. Elementary mode analysis .....                                                                 | 17        |
| 1.7. The Chinese hamster ovary cell line .....                                                      | 18        |
| <b>2. Platform for non-stationary <sup>13</sup>C metabolic flux analysis .....</b>                  | <b>27</b> |
| 2.1. Introduction .....                                                                             | 27        |
| 2.2. Theoretical aspects that require Inst- <sup>13</sup> CMFA .....                                | 27        |
| 2.2.1. Inst- <sup>13</sup> CMFA to study compartmentation .....                                     | 27        |
| 2.2.2. Reversibility .....                                                                          | 28        |
| 2.3. Platform structure .....                                                                       | 29        |
| 2.4. Platform testing .....                                                                         | 31        |
| <b>3. Non-stationary <sup>13</sup>C metabolic flux analysis of CHO cells in batch culture .....</b> | <b>35</b> |
| 3.1. Introduction .....                                                                             | 36        |
| 3.2. Materials and methods .....                                                                    | 38        |
| 3.2.1. Cell culture and experimental set-up .....                                                   | 39        |
| 3.2.2. Quantification of metabolites .....                                                          | 39        |
| 3.2.3. Analysis of isotopomer labeling patterns .....                                               | 39        |
| 3.2.3.1. Sample preparation .....                                                                   | 39        |
| 3.2.3.2. GC-MS measurements .....                                                                   | 39        |
| 3.2.3.3. Data analysis .....                                                                        | 40        |
| 3.2.4. Metabolic network models .....                                                               | 40        |
| 3.2.5. Non-stationary- <sup>13</sup> CMFA methodology .....                                         | 42        |
| 3.2.5.1. Metabolite balancing .....                                                                 | 42        |
| 3.2.5.2. Intracellular and extracellular carbon balance .....                                       | 43        |
| 3.2.5.3. Parameter estimation .....                                                                 | 44        |
| 3.3. Results and discussion .....                                                                   | 45        |
| 3.3.1. Cell growth and extracellular fluxes .....                                                   | 46        |

|           |                                                                                                                           |           |
|-----------|---------------------------------------------------------------------------------------------------------------------------|-----------|
| 3.3.2.    | Non-stationary labeling experiment .....                                                                                  | 47        |
| 3.3.3.    | Isotopomer labeling .....                                                                                                 | 48        |
| 3.3.4.    | Metabolic fluxes in the CHO-K1 cell line .....                                                                            | 51        |
| 3.3.5.    | Transport reversibility .....                                                                                             | 55        |
| 3.3.6.    | Confidence intervals calculation and sensitivity analysis .....                                                           | 56        |
| 3.4.      | Conclusions .....                                                                                                         | 59        |
|           | Supplementary data 3 .....                                                                                                | 62        |
| <b>4.</b> | <b>High resolution <math>^{13}\text{C}</math> metabolic flux analysis in CHO cells .....</b>                              | <b>63</b> |
| 4.1.      | Introduction .....                                                                                                        | 64        |
| 4.2.      | Materials and methods .....                                                                                               | 66        |
| 4.2.1.    | Cell culture .....                                                                                                        | 66        |
| 4.2.2.    | 4.2.2. Experimental set-up of labeling experiments .....                                                                  | 67        |
| 4.2.3.    | Quantification of extracellular metabolites .....                                                                         | 68        |
| 4.2.4.    | Analysis of isotopomer labeling patterns .....                                                                            | 68        |
| 4.2.4.1.  | Sample preparation .....                                                                                                  | 68        |
| 4.2.4.2.  | GC-MS measurement .....                                                                                                   | 68        |
| 4.2.4.3.  | Data analysis .....                                                                                                       | 69        |
| 4.2.5.    | Dynamic metabolic flux analysis .....                                                                                     | 69        |
| 4.2.6.    | Metabolic network for non-stationary $^{13}\text{C}$ MFA .....                                                            | 72        |
| 4.2.7.    | Flux space analysis .....                                                                                                 | 73        |
| 4.2.8.    | Non-stationary $^{13}\text{C}$ MFA .....                                                                                  | 73        |
| 4.3.      | Results and Discussion .....                                                                                              | 74        |
| 4.3.1.    | Cell growth and extracellular metabolite concentrations .....                                                             | 74        |
| 4.3.2.    | Labeling experiment .....                                                                                                 | 75        |
| 4.3.3.    | Dynamic metabolic flux analysis .....                                                                                     | 79        |
| 4.3.4.    | Flux space .....                                                                                                          | 81        |
| 4.3.5.    | Fittings of MIDs and model re-adaptation .....                                                                            | 81        |
| 4.3.6.    | Metabolic fluxes, compartmentation and channeling .....                                                                   | 85        |
| 4.3.7.    | Estimated intracompartmental pools .....                                                                                  | 90        |
| 4.4.      | Concluding discussion .....                                                                                               | 93        |
|           | Supplementary data 4 .....                                                                                                | 96        |
| <b>5.</b> | <b>Identification of active elementary flux modes in mitochondria<br/>using selectively permeabilized CHO cells .....</b> | <b>97</b> |
| 5.1.      | Introduction .....                                                                                                        | 98        |
| 5.2.      | Materials and methods/Experimental .....                                                                                  | 100       |

|                                                                                                     |            |
|-----------------------------------------------------------------------------------------------------|------------|
| 5.2.1. Cell culture.....                                                                            | 100        |
| 5.2.2. Preparation of mitochondrial medium .....                                                    | 100        |
| 5.2.3. Mitochondrial transport experiments .....                                                    | 101        |
| 5.2.4. Analytical determination of organic acids and amino acids .....                              | 102        |
| 5.2.5. Mitochondrial network .....                                                                  | 103        |
| 5.2.6. Elementary mode analysis .....                                                               | 106        |
| 5.2.7. Metabolic flux analysis .....                                                                | 107        |
| 5.3. Results and Discussion .....                                                                   | 107        |
| 5.3.1. Mitochondrial uptake and production of metabolites .....                                     | 107        |
| 5.3.2. Connection of tested substrates and observed products using elementary<br>mode analysis..... | 109        |
| 5.3.3. General characteristics .....                                                                | 110        |
| 5.3.4. Pyruvate and aspartate .....                                                                 | 112        |
| 5.3.5. Citrate.....                                                                                 | 115        |
| 5.3.6. $\alpha$ -ketoglutarate .....                                                                | 116        |
| 5.3.7. C <sub>4</sub> -dicarboxylates .....                                                         | 117        |
| 5.3.8. Glutamine and glutamate .....                                                                | 119        |
| 5.3.9. Serine.....                                                                                  | 121        |
| 5.4. Conclusions .....                                                                              | 123        |
| Supplementary data 5 .....                                                                          | 125        |
| <b>6. Conclusions and outlook.....</b>                                                              | <b>126</b> |
| <b>Research activities.....</b>                                                                     | <b>131</b> |
| <b>Appendix.....</b>                                                                                | <b>132</b> |
| Appendix to Chapter 1 .....                                                                         | 132        |
| Appendix to Chapter 3 .....                                                                         | 134        |
| Appendix to Chapter 4 .....                                                                         | 142        |
| Appendix to Chapter 5 .....                                                                         | 159        |
| <b>References .....</b>                                                                             | <b>182</b> |

## **Chapter 1**

### **1. Introduction in systems biology for metabolism analysis of eukaryotic cells**

“We are prone to thinking by analogy [...] but very little in our human experience is truly comparable to the immensely crowded, membrane-subdivided interior of a eukaryotic cell or the intricately layered structures of a mammalian tissue. So in our daily efforts to understand how cells work, we are faced with a challenge: how do we develop intuition that works at the microscopic scale?” (Flamholz et al., 2014). One could further ask “how does one harness the complexity of the eukaryotic cell to answer practical questions?” A complex problem requires a complex solution. Sustained research in molecular biology and the emergence of “*omics*” technologies supply vast information concerning the components, the structure and the interactions within the cell. However, without a rigorous modeling framework, this knowledge provides little insight on how the systems properties emerge, what are the goals of the cell and how its behavior could be predicted. Systems biology, an explosively developing scientific field, addresses the question by observing multiple components simultaneously and by integrating those using rigorous mathematical models (Sauer et al., 2007). Biological systems are inherently complex, and in the case of eukaryotic cells, structural organization and compartmentation adds another layer of complexity when compared to the prokaryotic cell, as it was noted for yeast (Castrillo and Oliver, 2011), mammalian cells (Niklas and Heinzle, 2012) or plants (Lucas et al., 2011).

Studying the metabolism of eukaryotic cells at systemic level is of essential importance for designing and improving recombinant organisms (Carinhas et al., 2012; Dietmair et al., 2012; Liu; Zurbriggen et al., 2012), with the goal of increasing yield or producing desired glycosylation pattern in therapeutic proteins. Concerning mammalian organisms, the development of new treatments or diagnosis strategies benefits greatly from an in depth understanding of disease mechanisms and drug toxicity at the metabolic level (Bugrim et

al., 2004; DeBerardinis and Thompson, 2012; Kell, 2006). The eukaryotic cell (Fig. 1.1) distinguishes itself from the prokaryotic cell by the separation of the nucleus and organelles from the cytosol using enclosure within a system of endomembranes. The major role of compartmentation is to confine metabolic processes to distinct compartments in which it is possible to create different environments with respect to metabolite concentrations, enzymes and pH. Metabolite and protein traffic between compartments and cytosol is tightly regulated by selective membrane permeability and via membrane transporters (Schell and Rutter, 2013). Isoenzymes enable the same reaction to occur in different subcellular compartments under sometimes very different conditions, especially related to substrate availability and cofactor concentrations. This confers the eukaryotic cell a high degree of flexibility in controlling metabolic pathways. The cytosol is structured by a 3D meshwork called cytoskeleton that provides spatial organization of the organelles in the cytoplasm and also confers shape to the cell (de Forges et al., 2012). Enzymes can associate in transient or permanent complexes favored by the 3D structure, leading to substrate channeling (Jandt et al., 2013; Zhang, 2011) in some metabolic pathways. Other than enhancing reaction rates, enzyme complexes can protect unstable intermediates, create microenvironments for otherwise kinetically unfavorable reaction and isolate toxic or inhibitory intermediates from the rest of the cell.

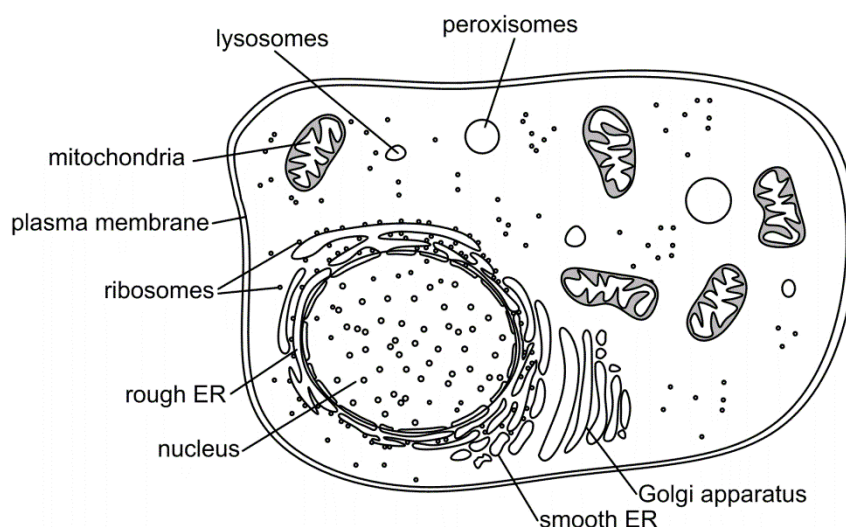


**Figure 1.1. Scheme of a mammalian cell**

### 1.1. Mitochondria

Mitochondria evolved as specific organelles by inclusion of protobacteria in the precursor of the eukaryotic cell. Although the mitochondrial genome contains a small number of genes coding for the respiratory complex and genes needed for mitochondrial replication, mitochondrial proteome contains a wealth of over 1000 proteins and varies highly depending on the organism and cell type (Friedman and Nunnari, 2014; Pagliarini et al., 2008). The mitochondrial metabolism is responsible for producing most of the energy in the eukaryotic cell by combining the TCA cycle activity with oxidative phosphorylation. Electrons are transferred from NADH or succinate to oxygen and ATP is produced from ADP by using the proton gradient generated by the electron transfer. Most NADH is produced by the TCA cycle through the oxidation of organic acids involved in the cycle. Mitochondrial carriers (Table 1.1) belonging to the mitochondrial carrier family (Kuan and Saier, 1993) are proteins encoded in the nucleus, and though they are characterized by relatively low homology, they share a common topology (Hamel et al., 2004). They are localized in the mitochondrial inner membrane and control the shuttling of various metabolites, cofactors and ions across the mitochondrial membrane. In the framework of cellular metabolism, the tightly regulated transport process is essential in maintaining distinct compartmented microenvironments and the membrane potential (Schell and Rutter, 2013).

Owing to evolution of different roles organelles play in the cell, their membranes exhibit distinct compositions (van Meer et al., 2008). In comparison to the plasma membrane, the mitochondrial membrane contains almost no sterols and includes cardiolipin, a lipid unique to the mitochondria. This property enables the use of detergents, e.g. digitonin or saponin, to selectively permeabilize only the plasma membrane, leaving the mitochondria intact (Kuznetsov et al., 2008; Niklas et al., 2011a). Such “ghost cells” can be utilized for respiration studies (Wahrheit et al., 2015), analysis of compartmented enzyme activity (Wahrheit et al., 2014b) or other studies of the mitochondrial metabolism.

Considering the central role the mitochondrial metabolism plays in the functioning of the eukaryotic cell, mitochondrial dysfunctions are responsible for many diseases e.g.

diabetes type II, cancer or neurodegenerative diseases (Balaban, 2010; Pagliarini et al., 2008; Palmieri, 2008; Wallace, 2012) and play a key role in the aging process (Bratic and Larsson, 2013). Also, the many bioprocesses that use eukaryotic cells for the production of small molecules or recombinant proteins rely on an optimal use of substrates and on the energy supplied by the TCA cycle (Klein et al., 2015).

### 1.2. Systems biology of mammalian cells

In the post-genomic era, where great amounts of genomic, transcriptome and proteomic data become available at a fast pace and sustained research effort is employed to coagulate this data into knowledge through systems biology, metabolism tends to be overlooked as the main reflection and influence of the physiological state of the cell (Ray, 2010). Metabolism is however the final manifestation of the entire genetic-transcriptome-proteomic apparatus. In-depth knowledge of the eukaryotic cell metabolism can impact how new treatments for diseases are conceived or the design of new strains and bioprocesses (Niklas and Heinzle, 2012). Compartmentation complicates systems biology studies of the metabolism because of the addition of new pools of the same metabolite (Fig. 1.2), the existence of compartmented isoenzymes and limited information on the properties of mitochondrial carriers (Wahrheit et al., 2011a).

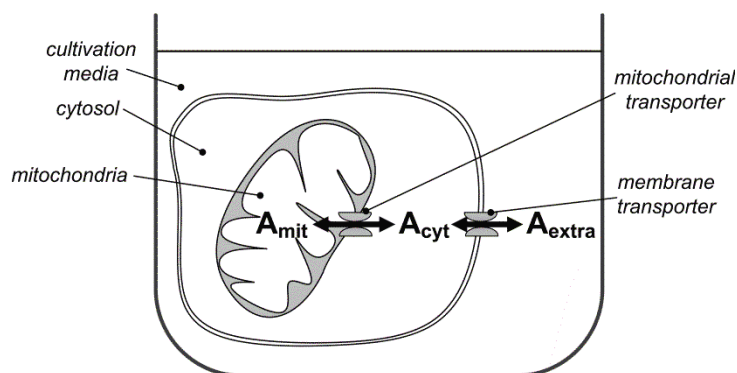


Figure 1.2. Compartmentation of metabolite *A* between the extracellular media (*extra*), cytosol (*cyt*) and mitochondria (*mit*). The connection between the pools is made via specific transporters.

Channeling effects and enzyme associations (al-Habori, 1995; Niklas et al., 2011b; Zhang, 2011) create permanent or temporary environments where certain metabolites are isolated from their bulk pools and reaction kinetics are very different compared to the *in vitro*



situation. Within this dissertation, the term “pool” will refer to a metabolite concentration confined to a cell compartment.

The metabolism of mammalian cells differs from that of plants and fungi due to its characteristic use of more and sometimes complex substrates and also the wider range of secreted metabolites. The central carbon metabolism (Fig. 1.3) is comprised of glycolysis, pentose phosphate pathway (PPP), mitochondrial transport, TCA cycle, anaplerotic and cataplerotic reactions and the amino acid metabolism. Although it differs greatly among organisms and cell types, a typical mammalian cell takes up glucose as the main carbon source, glutamine as carbon and nitrogen source, it can simultaneously take up and produce non-essential amino acids, it takes up essential amino acids mostly for protein synthesis and it can secrete lactate as a side product. Isoenzymes catalyze certain reactions from the TCA cycle, anaplerosis/cataplerosis or amino acid metabolism simultaneously in different compartments (Table 1.2).

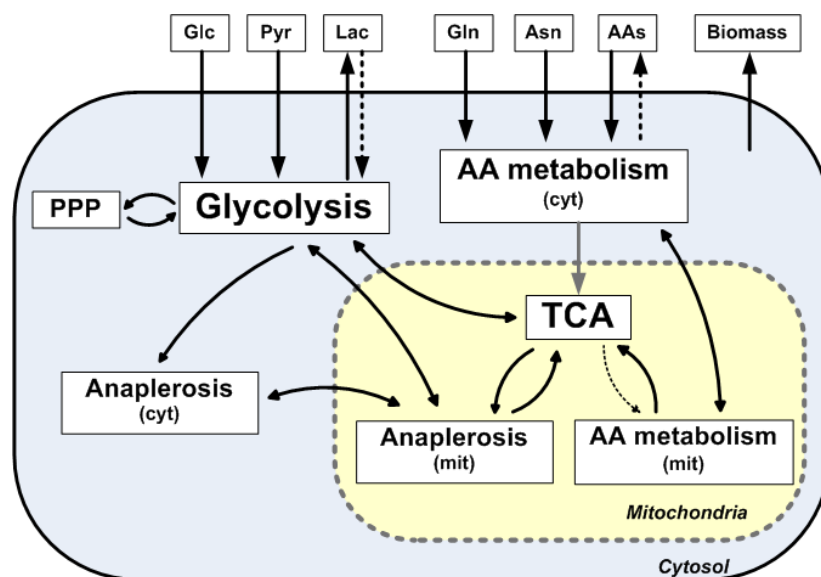


**Figure 1.3. General scheme of the mammalian cell metabolism.** Abbreviations: AA – amino acid; Asn – asparagine; Glc – glucose; Gln – glutamine; Lac – lactate; PPP – pentose phosphate pathway; Pyr – pyruvate.

From a systems biology point of view, characterizing the metabolism of a mammalian cell involves two main parts: establishing the topology of the metabolic network and in vivo flux analysis (Wahrheit et al., 2011a).

Table 1.1. Mitochondrial carriers in Baker's yeast (*Saccharomyces cerevisiae*), Chinese hamster (*Cricetulus griseus*) and human (*Homo sapiens*). <sup>1</sup> – from SGD (Christie et al., 2004); <sup>2</sup> – from CHOgenome (Hammond et al., 2012); <sup>3</sup> – from Human Genome Resources (Pruitt et al., 2000) .

| Nr | Mitochondrial carrier - substrate | Process                                                                                                                                                | <i>S. cerevisiae</i> <sup>1</sup>                  | CHO <sup>2</sup>                             | Human <sup>3</sup>                 | References                                                            |
|----|-----------------------------------|--------------------------------------------------------------------------------------------------------------------------------------------------------|----------------------------------------------------|----------------------------------------------|------------------------------------|-----------------------------------------------------------------------|
| 1  | pyruvate                          | $\text{Pyr}^-_c + \text{H}^+_c \rightarrow \text{Pyr}^-_m + \text{H}^+_m$                                                                              | YGL080W (MPC1)<br>YHR162W (MPC2)<br>YGR243W (MPC3) | Mpc1<br>Mpc2<br>LOC100772695<br>LOC103162130 | MPC1<br>MPC1L<br>MPC2              | (Bricker et al., 2012; Herzig et al., 2012)                           |
| 2  | NAD <sup>+</sup>                  | -                                                                                                                                                      | YIL006W/ YEL006W (YIA6/YEA6)                       | -                                            | -                                  | (Hildyard and Halestrap, 2003; Todisco et al., 2006)                  |
| 3  | citrate                           | $\text{Cit}_c + \text{Mal}_m \leftrightarrow \text{Cit}_m + \text{Mal}_c$<br>$\text{Cit}_c + \text{Pep}_m \leftrightarrow \text{Cit}_m + \text{Pep}_m$ | YBR291C (CTPi)                                     | Slc25a1                                      | SLC25A1 (CIC)                      | (De Palma et al., 2005; Gnani et al., 2009; Kaplan et al., 1995)      |
| 4  | oxaloacetate                      | $\text{Oaa}_c + \text{H}^+_c \leftrightarrow \text{Oaa}_m + \text{H}^+_m$                                                                              | YKL120W (OAC1)                                     | -                                            | -                                  | (Palmieri et al., 1999)                                               |
| 5  | pyrimidine nucleotide             | $\text{C/U/TTP}_c + \text{C/U/TDP}_m \rightarrow \text{C/U/TTP}_m + \text{C/U/TDP}_c$                                                                  | YBR192W (RIM2)                                     | Slc25a36<br>Slc25a33                         | SLC25A36<br>SLC25A33               | (Di Noia et al., 2014; Marobbio et al., 2006)                         |
| 6  | GTP/GDP                           | $\text{GDP}_c + \text{GTP}_m \leftrightarrow \text{GDP}_m + \text{GTP}_c$                                                                              | YDL198C (GGC1)                                     | -                                            | -                                  | (Vozza et al., 2004)                                                  |
| 7  | dicarboxylate                     | $\text{C}_4_c + \text{Pi}_m \leftrightarrow \text{C}_4_m + \text{Pi}_c$                                                                                | YLR348C (DIC1)                                     | Slc25a10<br>LOC100766192                     | SLC25A10 (DIC)                     | (Fiermonte et al., 1998; Palmieri et al., 1999; Pannone et al., 1998) |
| 8  | thiamine phosphate                | $\text{ThPP}_c \rightarrow \text{ThPP}_m$                                                                                                              | YGR096W (TPC1)                                     | Slc25a19                                     | SLC25A19 (DNC)                     | (Kang and Samuels, 2008; Marobbio et al., 2002)                       |
| 9  | phosphate                         | $\text{Pi}_c \leftrightarrow \text{Pi}_m$                                                                                                              | YJR077C (MIR1)                                     | Slc25a25<br>Slc25 A23                        | SLC25A25 (APC3)<br>SLC25A23 (APC2) | (del Arco and Satrustegui, 2004; Dolce et al., 1991;                  |

|    |                                     |                                                                                                                          |                                   |                                  |                                                                                                                                    |
|----|-------------------------------------|--------------------------------------------------------------------------------------------------------------------------|-----------------------------------|----------------------------------|------------------------------------------------------------------------------------------------------------------------------------|
|    |                                     |                                                                                                                          | Slc25a3                           | SLC25A24 (APC1)<br>SLC25A3 (PHC) | Phelps et al., 1991)                                                                                                               |
| 10 | citrate /<br>oxoglutarate           | $\text{Cit}_m + \text{AKG}_c \rightarrow \text{Cit}_c + \text{AKG}_m$                                                    | YMR241W (YHM2)                    | -                                | (Castegna et al., 2010)                                                                                                            |
| 11 | S-adenosylmethionine                | $\text{SAM}_c \leftrightarrow \text{SAM}_m$                                                                              | YNL003C (PET8)                    | Slc25a26                         | SLC25A26 (SAMC1)<br>(Marobbio et al., 2003)                                                                                        |
| 12 | ADP/ATP                             | $\text{ADP}_c + \text{ATP}_m \rightarrow \text{ADP}_m + \text{ATP}_c$                                                    | YBL030C<br>(PET9/AAC3)            | Slc25a4<br>Slc25a5<br>Slc25a31   | SLC25A4 (ANT1)<br>SLC25A5 (ANT2)<br>SLC25A6 (ANT3)<br>SLC25A31 (ANT4)<br>(Houldsworth and Attardi, 1988; Lawson and Douglas, 1988) |
| 13 | aspartate /<br>glutamate            | $\text{Glu}_c \leftrightarrow \text{Glu}_m$<br>$\text{Glu}_c + \text{Asp}_m \leftrightarrow \text{Glu}_m + \text{Asp}_c$ | YPR021C (AGC1)                    | Slc25a12<br>Slc25a13             | SLC25A12 (AGC1,<br>ARALAR1)<br>SLC25A13 (AGC2,<br>ARALAR2)<br>(Cavero et al., 2003;<br>Kobayashi et al., 1993)                     |
| 14 | succinate / fumarate                | $\text{Suc}_c + \text{Fum}_m \leftrightarrow \text{Suc}_m + \text{Fum}_c$                                                | YJR095W (SFC1)                    | -                                | (Palmieri et al., 1997)                                                                                                            |
| 15 | acylcarnitine,<br>basic amino acids | $\text{AcCAR}_c + \text{CAR}_m \leftrightarrow \text{AcCAR}_m + \text{CAR}_c$                                            | YOR100C (CRC1)                    | Slc25a20<br>Slc25a29             | SLC25A20 (CAC)<br>SLC25A29<br>(Huizing et al., 1997;<br>Porcelli et al., 2014; van<br>Roermund et al., 1999)                       |
| 16 | Calcium-binding<br>carrier protein  | $\text{ATP}_m/\text{ADP}_c + \text{Pi}_m \leftrightarrow \text{ATP}_m/\text{ADP}_c + \text{Pi}_c$                        | - (YMC3 in<br><i>P.pastoris</i> ) | SCaMC-1                          | SLC25A24<br>(Fiermonte et al., 2004)                                                                                               |
| 17 | $\alpha$ -ketoglutarate<br>/malate  | $\text{AKG}_m + \text{Mal}_c \leftrightarrow \text{AKG}_c + \text{Mal}_m$                                                | -                                 | Slc25a11<br>LOC100770598         | SLC25A11(OGC)<br>(Iacobazzi et al., 1992)                                                                                          |
| 18 | ornithine                           | $\text{Orn}_c + \text{H}^+_m \leftrightarrow \text{Orn}_m + \text{H}^+_c$                                                | ORT1                              | Slc25a15<br>Slc25a2              | SLC25A15 (ORC1)<br>SLC25A2 (ORC2)<br>(Fiermonte et al., 2003;<br>Palmieri et al., 2000)                                            |
| 19 | glutamate                           | $\text{Glu}_c \leftrightarrow \text{Glu}_m$                                                                              | -                                 | Slc25a18<br>Slc25a22             | SLC25A18 (GC2)<br>SLC25A22 (GC1)<br>(Fiermonte et al., 2002)                                                                       |
| 20 | oxoadipate                          | $\text{C5-C7 oxodicarboxylate}_c \rightarrow \text{C5-C7 oxodicarboxylate}_m$                                            | YPL134C (ODC1)                    | Slc25a21                         | SLC25A21 (ODC)<br>(Fiermonte et al., 2001;<br>Palmieri et al., 2001)                                                               |

|                                             |                     |   |                                                                                      |          |                 |                                                                 |
|---------------------------------------------|---------------------|---|--------------------------------------------------------------------------------------|----------|-----------------|-----------------------------------------------------------------|
| 21                                          | folate              | - | -                                                                                    | Slc25a32 | SLC25A32 (MFT)  | (Titus and Moran, 2000)                                         |
| 22                                          | uncoupling proteins | - | -                                                                                    | Slc25a7  | SLC25A7 (UCP1)  | (Boss et al., 1997; Cassard et al., 1990; Sanchis et al., 1998) |
|                                             |                     |   | -                                                                                    | Slc25a8  | SLC25A8 (UCP2)  |                                                                 |
|                                             |                     |   | -                                                                                    | Slc25a9  | SLC25A9 (UCP3)  |                                                                 |
|                                             |                     |   | -                                                                                    | Slc25a27 | SLC25A27 (UCP4) |                                                                 |
|                                             |                     |   | -                                                                                    | Slc25a14 | SLC25A14 (UCP5) |                                                                 |
| Not yet annotated                           |                     |   |                                                                                      |          |                 |                                                                 |
|                                             |                     |   | YHR002W (LEU5, involved in CoA transport in yeast mitochondria) (Prohl et al., 2001) |          | SLC25A40 (MCFP) |                                                                 |
|                                             |                     |   | MTCH1 (Palmieri, 2013)                                                               |          | SLC25A41        |                                                                 |
|                                             |                     |   | MTCH2                                                                                |          | SLC25A42        |                                                                 |
|                                             |                     |   | SLC25A16 (Mitochondrial carrier, Graves disease autoantigen) (Zarrilli et al., 1989) |          | SLC25A43        |                                                                 |
|                                             |                     |   | SLC25A28 (Mitoferrin2)                                                               |          | SLC25A44        |                                                                 |
|                                             |                     |   | SLC25A30 (KMCP1)                                                                     |          | SLC25A45        |                                                                 |
|                                             |                     |   | SLC25A33 (PNC1)                                                                      |          | SLC25A46        |                                                                 |
|                                             |                     |   | SLC25A34                                                                             |          | SLC25A47        |                                                                 |
|                                             |                     |   | SLC25A35                                                                             |          | SLC25A48        |                                                                 |
|                                             |                     |   | SLC25A36 (PNC2)                                                                      |          | SLC25A49        |                                                                 |
|                                             |                     |   | SLC25A37                                                                             |          | SLC25A50        |                                                                 |
|                                             |                     |   | SLC25A38                                                                             |          | SLC25A51        |                                                                 |
|                                             |                     |   | SLC25A39 (CGI-69)                                                                    |          | SLC25A52        |                                                                 |
|                                             |                     |   |                                                                                      |          | SLC25A53        |                                                                 |
| Required by metabolism but not yet assigned |                     |   |                                                                                      |          |                 |                                                                 |
|                                             |                     |   | glutamine transporter (Indiveri et al., 1998)                                        |          |                 |                                                                 |
|                                             |                     |   | neutral amino acids carrier (Cybulski and Fisher, 1977)                              |          |                 |                                                                 |

Metabolic network reconstruction aims at building a consistent network of metabolic events, i.e. reactions and transport, using biochemical knowledge. Biochemistry books, the metabolic network compilation by (Michal and Schomburg, 2012) and online databases (Hammond et al., 2012; Zhu et al., 2003) that collect and curate gene annotation, gene expression and proteomic data constitute the main starting points for building a metabolic network. Bioinformatics software can assist the otherwise cumbersome process of network reconstruction making the process automatic (Forth et al., 2010; Karp et al., 2010). Popular open source software like COBRA (Schellenberger et al., 2011) includes tools for constraint-based genome scale reconstruction and analysis.

**Table 1.2.** Isoenzymes from the central carbon metabolism of *Mus musculus*\* and their localization in cytosol and/or mitochondria.

| Enzyme                                                       | Compartment                         |                                                                         |
|--------------------------------------------------------------|-------------------------------------|-------------------------------------------------------------------------|
|                                                              | Cytosol                             | Mitochondria                                                            |
| Acetyl-Coenzyme A acetyltransferase                          | Acat2, Acat3                        | Acat1                                                                   |
| Aconitase                                                    | Aco1                                | Aco2                                                                    |
| Branched chain aminotransferase                              | Bcat1                               | Bcat2                                                                   |
| Fumarase                                                     | Fh1**                               | Fh1*                                                                    |
| Glutamic-oxaloacetic transaminase                            | Got1                                | Got2                                                                    |
| Glutamic pyruvic transaminase                                | Gpt                                 | Gpt2                                                                    |
| Isocitrate dehydrogenase                                     | Idh1 (NADP <sup>+</sup> -dependent) | Idh2 (NADP <sup>+</sup> -dependent), Idh3 (NAD <sup>+</sup> -dependent) |
| Lactate dehydrogenase                                        | Ldha, Ldhb                          | Ldhd                                                                    |
| Malate dehydrogenase                                         | Mdh1                                | Mdh2                                                                    |
| Malic enzyme                                                 | Me1 (NADP <sup>+</sup> -dependent)  | Me2 (NAD <sup>+</sup> -dependent), Me3 (NADP <sup>+</sup> -dependent)   |
| Phosphoenolpyruvate carboxykinase                            | Pck1                                | Pck2                                                                    |
| Serine hydroxymethyltransferase                              | Shmt1                               | Shmt2                                                                   |
| * (Blake et al., 2014)                                       |                                     |                                                                         |
| ** fumarase is present in the same form in both compartments |                                     |                                                                         |

Genome scale models of the mammalian cell metabolism include cofactor (e.g. NADH, NADPH, ATP, etc.) balance, but this can be a potential pitfall because of the lack of reliable respiration measurements, limited knowledge about futile cycles and uncertainties in the selectivity of enzymes for NAD<sup>+</sup> or NADP<sup>+</sup> (Wahrheit et al., 2011a). Missing links and inconsistencies in the network are corrected by reevaluating the model based on experimental observations. Once a consistent metabolic network was constructed, it can be used to determine the material flow from substrates to products by applying flux analysis methods. Genome scale models are modeled mathematically by converting them into stoichiometry matrices, where the rows correspond to the components, and the columns represent the reactions. Stoichiometry based modeling involves methods for flux balance analysis (Varma and Palsson, 1994; Xie and Wang, 1996; Zupke and Stephanopoulos, 1995), elementary mode analysis (Schuster et al., 2000), extreme pathway analysis (Wiback et al., 2003) or other constraint-based modeling that can include e.g. thermodynamics (Henry et al., 2007) or kinetics. Such methods can be used to understand cellular objectives, to obtain a feasible solution space for the metabolic fluxes under specific conditions or to simulate possible mutants/inhibitions *in silico*. All such models rely on the assumption of metabolic steady state, which means that: (1) intracompartmental concentrations do not change over time and (2) only one metabolic state of the cell is characterized.

### 1.3. <sup>13</sup>C-based metabolic flux analysis

Detailed metabolic flux analysis needs powerful tools to tackle complex networks as those of mammalian cells. Alternative pathways, intercompartmental transport and the presence of isoenzymes introduce new degrees of freedom in the network that weaken the resolution power of flux balance approaches. Flux balance analysis (FBA) methods rely on considering cofactor and electron balances. This can generate errors due to the uncertainty of cofactor preference of certain enzymes. Also, it is difficult to include oxidative phosphorylation uncoupling, futile cycles or electron leaking through the mitochondrial membrane. For answering questions regarding compartmentation,

metabolite exchange or channeling, while at the same time avoiding the use of cofactor and electron balances,  $^{13}\text{C}$  metabolic flux analysis ( $^{13}\text{CMFA}$ ) is currently method of choice.

The principle of using  $^{13}\text{C}$  substrate labeling is that, following the distribution of carbon in the metabolic network, the labeling pattern of intra- or extracellular metabolites contains information about the metabolic flux distribution. For a molecule, there are  $2^n$  possible arrangements of labeled and non-labeled carbon atoms, called carbon isotopomers, in which  $n$  is the number of carbon atoms in the molecule. A network is then built to trace the distribution of carbon from substrate(s) to metabolites and more specifically, to those for which the labeling pattern was sampled. Simulation of the  $^{13}\text{C}$  distribution throughout a metabolic network at steady state involves carbon-transfer rules and mass balances to compute the label distributions in the readout metabolites (Schmidt et al., 1997; Wahrheit et al., 2011a; Wiechert and de Graaf, 1997; Zupke and Stephanopoulos, 1994). For a typical reaction  $\mathbf{A} + \mathbf{B} \rightarrow \mathbf{C}$ , the isotopomer distribution vector of  $\mathbf{C}$  ( $IDV_C$ ) will be mapped from the isotopomer distribution vector of  $\mathbf{A}$  ( $IDV_A$ ) and  $\mathbf{B}$  ( $IDV_B$ ) using the isotopomer mapping matrices that maps  $\mathbf{A}$  to  $\mathbf{C}$  ( $IMM_{A \rightarrow C}$ ) and  $\mathbf{B}$  to  $\mathbf{C}$  ( $IMM_{B \rightarrow C}$ ) and element-wise multiplication  $\otimes$ :

$$IDV_C = (IMM_{A \rightarrow C} \times IDV_A) \otimes (IMM_{B \rightarrow C} \times IDV_B) \quad (1.1)$$

Known parameters, such as uptake fluxes  $v_{u,i}$  (eq. 1.2) and biomass fluxes  $v_{bio,i}$  (eq. 1.3), are determined by analyzing the extracellular metabolite concentrations (pools)  $C_i$  and biomass composition, then relating them to the cell number  $X$ , specific growth rate

$\frac{dX}{dt} \cdot \frac{1}{X}$  and the cell volume  $V_{cell}$ :

$$v_{u,i} = -\frac{dC_i}{dt} \cdot \frac{1}{X} \cdot \frac{1}{V_{cell}} \quad (1.2)$$

$$v_{bio,i} = Y_{i/X} \cdot \frac{dX}{dt} \cdot \frac{1}{X} \cdot \frac{1}{V_{cell}} \quad (1.3)$$

The intracellular fluxes  $v$  constitute the null space of the stoichiometric matrix  $S$  (eq. 1.4), that can be further divided to include the measured fluxes  $v_m$ :

$$\begin{aligned} S \times v &= 0 \\ S_m \times v_m + S_e \times v_e &= 0 \end{aligned} \quad (1.4)$$

where  $S_m$  – stoichiometric matrix corresponding to measured fluxes,  $S_e$  – stoichiometric matrix corresponding to estimated fluxes,  $v_e$  – estimated fluxes. In addition to the condition of metabolic steady state, in compartmented systems it is also necessary to assume that the volume ratio between compartments does not change. The mass balance in the three volumes for metabolite  $A$  in Fig. 1.2 can therefore be written as:

$$A_{extra}: \quad \frac{dC_{A,extra}}{dt} = Q_{A,in} - v_{A,uptake} \cdot X \cdot V_{culture} \cdot V_{cell} \quad (1.5)$$

$$A_{cyt}: \quad 0 = v_{A,uptake} - v_{A,cons,cyt} + v_{A,prod,cyt} - v_{A,transport} \quad (1.6)$$

$$A_{mit}: \quad 0 = v_{A,transport} - v_{A,cons,mit} + v_{A,prod,mit} \quad (1.7)$$

where:  $C_{A,extra}$  – concentration of  $A$  in the media,  $[\text{mmol} \times \text{L}^{-1}]$ ;  $Q_{A,in}$  – total feed of  $A$  in the culture media,  $[\text{mmol} \times \text{h}^{-1}]$ ;  $v$  – fluxes of uptake, consumption ( $_{cons}$ ), production ( $_{prod}$ ) and transport between compartments,  $[\text{mmol} \times (\text{L cell})^{-1} \times \text{h}^{-1}]$ ;  $X$  – cell density,  $[\text{cells} \times \text{L}^{-1}]$ ;  $V_{culture}$  – cultivation volume,  $[\text{L}]$ ;  $V_{cell}$  – cell volume,  $[\text{L cell}]$ .

A problem is then constructed that estimates the free parameters  $\Phi$  by fitting the simulated labeling patterns to labeling data retrieved from GC-MS (mass isotopomers) or  $^{13}\text{C}$ -NMR (positional enrichment) (Schmidt et al., 1999; Wittmann and Heinzle, 1999) using an optimization algorithm that minimizes the quadratic deviation estimator ( $f$ ) computed as the weighted sum of square differences between measured and computed MIDs (1.8).



$$\min f(\Phi) = \sum_{i=1}^{nr.meas.} \left( \frac{MID_i^{exp} - MID_i^{sim}}{MID_i^{exp}} \right)^2 \cdot \frac{1}{error_i}, \Phi \geq 0 \quad (1.8)$$

In  $^{13}\text{C}$ CMFA, the free parameters are the net and reversible fluxes at metabolic steady state. Classical  $^{13}\text{C}$ CMFA uses the isotopomer distributions sampled at labeling steady state.

Estimated flux distributions rely on several factors: (1) amount and quality of experimental data involving extracellular fluxes and labeling, (2) degree of complexity and correctness of the metabolic network, (3) numerical methods and performance of optimization algorithms. Sensitivity analysis or statistical methods e.g. Monte Carlo are then used to assess the influence of experimental errors and establish the confidence intervals for the estimated parameters (Antoniewicz et al., 2006; Wittmann and Heinzle, 2002; Yang et al., 2008). Experimental design can guide the choice of substrate labeling and the layout of an optimal set of measurements (Chang et al., 2008; Metallo et al., 2009). Software packages for  $^{13}\text{C}$ CMFA are available and can vary in their user-friendliness, open/closed source type, flexibility and the algorithms used for isotopomer balancing and parameter estimation (Millard et al., 2014; Quek et al., 2009b; Srouf et al., 2011; Zamboni et al., 2005).

Representative  $^{13}\text{C}$ CMFA applications for mammalian cells include the characterization of hybridoma cells metabolism and a comparison to flux analysis without using  $^{13}\text{C}$  labeling (Bonarius et al., 1998), unraveling compartmentation of pyruvate metabolism in pancreatic beta-cells (Lu et al., 2002), assessing the subtoxic effects of drugs on cardiomyocytes (Strigun et al., 2012), probing the metabolism of an inducible expression system in Chinese hamster ovary cells (Sheikholeslami et al., 2013) or using lactate labeling to characterize the metabolism of HEK cells (Henry et al., 2011). Efforts were made to establish cultivation media and techniques that help to maintain the metabolic steady state long enough until isotopic steady state is reached (Deshpande et al., 2009).

### 1.4. Non-stationary $^{13}\text{C}$ metabolic flux analysis

Ensuring metabolic steady state until isotopic steady state is reached is a mathematical necessity for applying  $^{13}\text{C}$ CMFA, but it can prove difficult in mammalian cell cultures. The required time scale is usually too large to maintain a stable metabolism. Substrates become depleted in the media and toxic products like lactate or ammonia accumulate, leading to significant changes in the metabolism and sometimes even to cell death. Also, exchange of metabolites with the media influences the intracellular labeling while increasing considerably the time needed to reach isotopic steady state. Although computationally and experimentally much more intensive than classical  $^{13}\text{C}$ CMFA, non-stationary  $^{13}\text{C}$ CMFA (Inst- $^{13}\text{C}$ CMFA) has the potential to overcome these difficulties by using the isotopomer dynamics at a short time scale, when the metabolism remains at steady state (Antoniewicz et al., 2007; Noh et al., 2007). For applying Inst- $^{13}\text{C}$ CMFA, the experimental isotopomer distributions are sampled over time and a mathematical model simulates the dynamics of isotopomers by integrating the carbon balance equations (eq. 1.9) starting from the moment when the labeled substrate was fed. For the system of reactions shown in (Fig. 1.4), the dynamic isotopomer balance depends on the intracompartmental concentration of  $D$  ( $C_D$ , [ $\text{mmol} \times (\text{L cell})^{-1}$ ]), on the fluxes producing  $D$  ( $v_{D,1}$  and  $v_{D,2}$ , [ $\text{mmol} \times (\text{L cell})^{-1} \times \text{h}^{-1}$ ]) and the fluxes consuming  $D$  ( $v_{D,out}$ , [ $\text{mmol} \times (\text{L cell})^{-1} \times \text{h}^{-1}$ ]):

$$C_D \cdot \frac{dIDV_D}{dt} = v_{D,1} \cdot (IMM_{A \rightarrow D} \times IDV_A) \otimes (IMM_{B \rightarrow D} \times IDV_B) + v_{D,2} \cdot (IMM_{C \rightarrow D} \times IDV_C) - v_{D,out} \cdot IDV_D \quad (1.9)$$

where  $IDV$  – isotopomer distribution vector,  $IMM$  – isotopomer mapping matrix. Following the substrate label switch, the isotopomer distribution of  $D$  changes gradually from non-labeled to labeled (Fig. 1.3), at a rate proportional to the  $v_{D,out} / Pool_D$  ratio.

In addition to extracellular fluxes and transient intracellular isotopomer distributions, Inst- $^{13}\text{C}$ CMFA (Fig. 1.5) also requires that at least some key intracellular concentrations are sampled experimentally (Noh and Wiechert, 2006). One major advantage is that Inst- $^{13}\text{C}$ CMFA permits the estimation of unknown intracompartmental, perhaps difficult to measure concentrations.

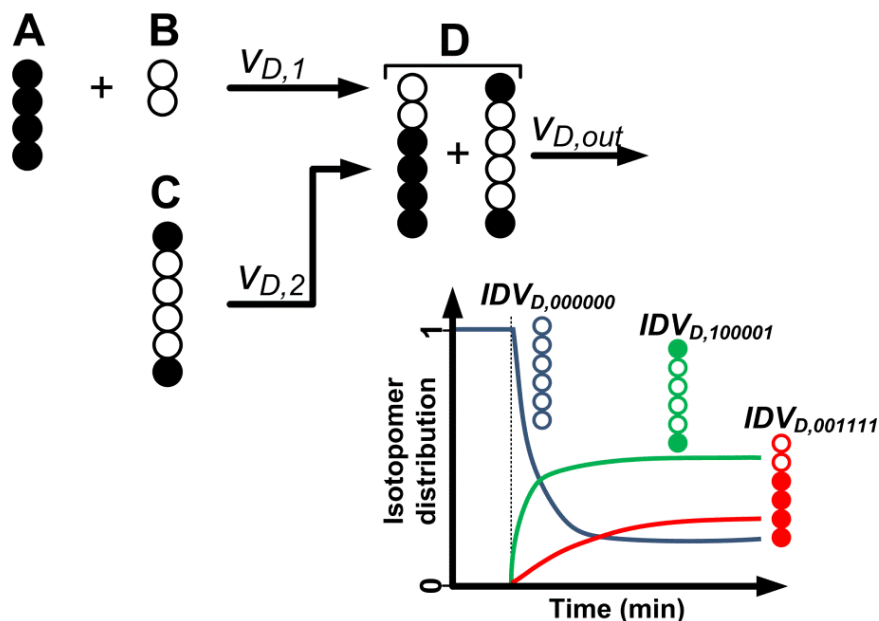


**Figure 1.4.** Example of a dynamical labeling experiment. Metabolite *D* is produced by two enzyme-catalyzed reactions from metabolites *A* and *B* in one reaction and from *C* in the second. The isotopomers of *D* corresponding to the labeling in *A*, *B* and *C*,  $IDV_{D,xxxxxx}$ , are formed at rates proportional to the fluxes  $v_{D,1}$  and  $v_{D,2}$  and inversely proportional with the intracompartamental pool of *D*.

The sampling time points and the labeled substrate or combination of substrates can be optimally chosen by applying experimental design strategies (Noh and Wiechert, 2006; Yang et al., 2014). Several software packages became recently available to tackle the numerical complexity of estimating metabolic fluxes using Inst- $^{13}\text{C}$ MFAs, of which some were published (Antoniewicz, 2013b; Kajihata et al., 2014; Young, 2014) and others are commercially available, like  $^{13}\text{C}$ Flux (<https://www.13cflux.net/>). Metabolic networks and flux maps are most comprehensible in graphical representation, for which visualization software was developed, like Omix (Noh et al., 2015).

Due to the complex experimental requirements, there are few published applications of Inst- $^{13}\text{C}$ MFAs. Using the transient labeling in intracellular metabolites lead to an extended topology and better characterization of methanol metabolism in *Pichia pastoris* compared to studies that used  $^{13}\text{C}$  labeling in proteinogenic amino acids (Jorda et al., 2014; Jorda et al., 2013).

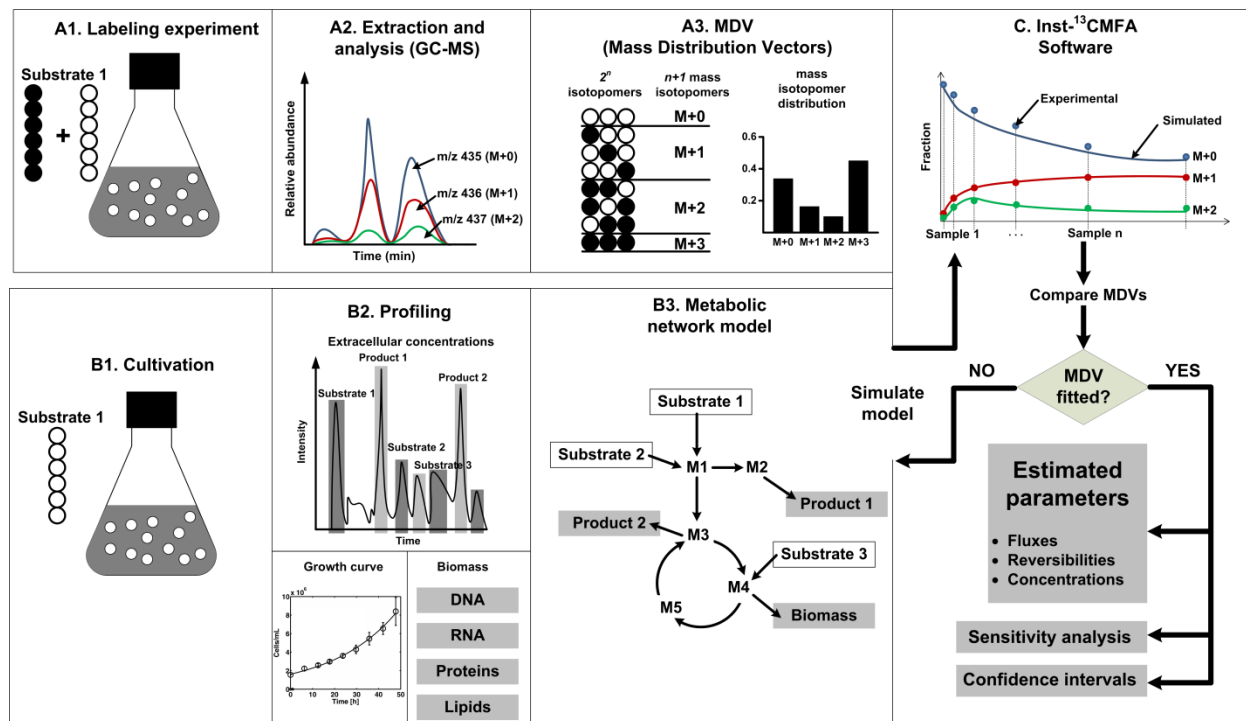


**Figure 1.5. Experimental and simulation scheme of non-stationary  $^{13}\text{C}$  metabolic flux analysis.** (A) In the labeling experiment (A1), a naturally labeled Substrate 1 is replaced with a  $^{13}\text{C}$ -labeled substrate. Labeled metabolites are sampled from the intra- and extracellular media, and then analyzed using mass spectrometry (A2) to determine the mass isotopomer distributions (A3). (B) Cultivation in non-labeled media (B1) provides the extracellular media and cells for cultivation profiling (B2) that determined the extracellular fluxes in the metabolic network (B3). (C) The metabolic network, mass distribution vectors (MDVs) and extracellular fluxes are data input for non-stationary  $^{13}\text{C}$  metabolic flux analysis (Inst- $^{13}\text{C}$ MFA) software that estimates the free parameters (fluxes, reversibilities and intracompartmental pools) by optimizing the fitting of the simulated MDVs. Once the estimation is considered successful, the confidence intervals of parameters are computed and sensitivity analysis is performed.

Plants use  $\text{CO}_2$  as the only carbon source, making steady-state  $^{13}\text{C}$ CMFA inapplicable but opening the door to many interesting applications of Inst- $^{13}\text{C}$ CMFA, as characterizing the leaf metabolism in *Arabidopsis thaliana* (Ma et al., 2014) or establishing subcellular compartmentation in various plant cells (Allen et al., 2007). Production of biopharmaceuticals using mammalian cells benefits greatly from a detailed understanding of the metabolism of relevant cell lines. Comprehensive flux maps were achieved with  $^{13}\text{C}$ CMFA and multiple labeled substrates in CHO cells (Ahn and

Antoniewicz, 2011) or extracellular labeling obtained after feeding [U- $^{13}\text{C}$ ] glucose to CHO-K1 cells in batch culture (Nicolae et al., 2014). Detailed metabolic aspects in cancer-like cells (Murphy et al., 2013) could be resolved at high resolution using isotopically nonstationary  $^{13}\text{C}$  flux analysis. Transient  $^{13}\text{C}$  labeling was also applied to study the neuronal metabolism in vivo (Gruetter, 2002) and the influence of hypoglycemia (Amaral et al., 2011).

### 1.5. Dynamic metabolic flux analysis

Despite the high resolution of  $^{13}\text{C}$ CMFA at determining the metabolic fluxes, sometimes the focus is to characterize mammalian metabolism over a longer time span. Capturing the dynamic change in metabolic fluxes in batch or fed-batch cultivations could help understanding the metabolic shifts in mammalian cell cultures (Niklas et al., 2011c) and the limiting effect of glutamine availability for CHO cells (Wahrheit et al., 2014a). Two main mathematical approaches exist for dealing with flux dynamics: one is to separate the flux timeline in phases for which the metabolism is considered to be at steady state (Antoniewicz, 2013a; Leighty and Antoniewicz, 2011) and another is to compute continuous flux values by fitting the extracellular concentrations with specific functions or with splines (Lequeux et al., 2010; Niklas et al., 2011c; Wahrheit et al., 2014a; Willemsen et al., 2015). Regardless of the approach, the extracellular fluxes are determined by fitting the extracellular concentrations and growth curve, determining the rates by numerical derivation and applying eq. 1.2 and 1.3, then the intracellular fluxes are computed using a stoichiometric model. Because the numerical derivation of splines and the experimental determination of concentrations are considerable sources of errors, Monte Carlo can be used to determine the standard deviations of the computed fluxes (Niklas et al., 2011c).

### 1.6. Elementary mode analysis

A very useful method for analyzing the topology of reaction networks, elementary mode analysis (EMA) decomposes the fluxes at steady state into *elementary modes* (Schuster et al., 2000) (Fig. 1.6). These are a set of vectors derived from the stoichiometric matrix, that have the following properties: (1) for a given network, there is an unique set of elementary

modes; (2) each elementary modes consists of the minimum number of reactions needed to exist as a functional metabolic unit, and cannot function if any reaction is removed and (3) the elementary modes are the set of all possible pathways that satisfy the previous condition (Papin et al., 2004). The metabolic fluxes at a given steady state can be expressed as a linear combination of the elementary fluxes. EMA provides a tool for stoichiometry-based approaches to characterize the structure of the metabolic network in mammalian cells (Orman et al., 2011) and evaluate the weight of each flux or to correlate the influence the uptake of a certain substrate has on the products. However, the decomposition of a flux distribution is usually not unique for large networks, and it can be made only by minimizing an objective function (Zhao and Kurata, 2009). Human blood cell network was a target for many pathways analysis studies to describe energy metabolism or to relate circulatory dysfunctions to enzymes (Cakir et al., 2004; Wiback and Palsson, 2002). Macroscopic reaction modes for CHO cells connecting substrates and products were constructed based on network decomposition in elementary modes (Provost et al., 2006).

### 1.7. The Chinese hamster ovary cell line

Both theoretical studies and bioproduction using mammalian cells require stable cells lines that can be cultivated in reproducible conditions. The Chinese hamster ovary (CHO) cell line was obtained by Puck in 1957 (Puck, 1985) from a female Chinese hamster (*Cricetulus griseus*). Nowadays, CHO are considered the mammalian equivalent of *E. coli* and are ideal model mammalian systems or for recombinant expressing heterologous proteins owing to: (1) their stable gene expression, (2) high yields of protein production, (3) the ability to produce glycosylated proteins compatible with humans, (4) powerful gene amplification systems, such as dihydrofolate reductase or glutamine synthetase-mediated gene amplification and (5) their ability to grow in serum-free media and suspension conditions found in large industrial bioreactors.

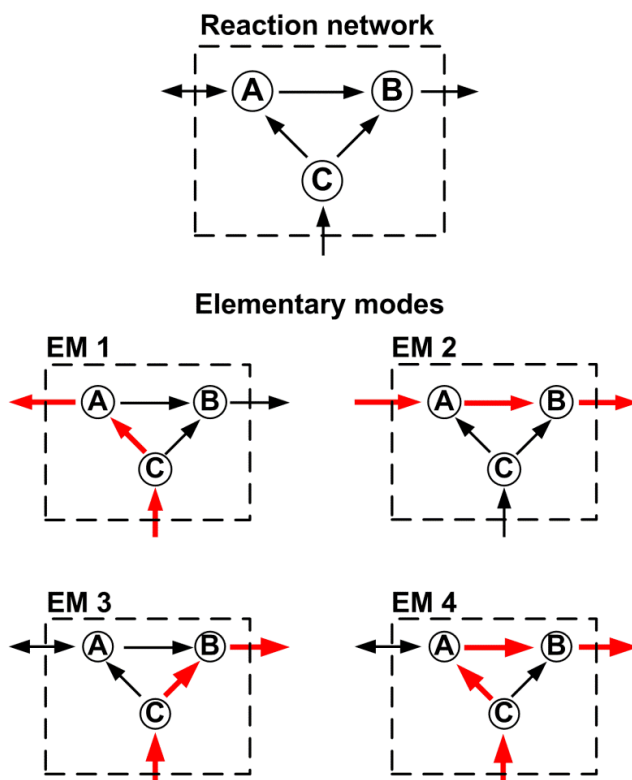


**Figure 1.6.** An example of elementary mode decomposition of a reaction network. EM – elementary mode. The red arrows represent each elementary mode. Adapted from (Papin et al., 2004)

CHO are therefore the main production cell line for biopharmaceuticals, responsible for nearly 70% of all recombinant therapeutic production (Jayapal et al., 2007; Kim et al., 2012). Considering the economical and scientific importance of CHO cells, there has been sustained effort in the field of systems biology to characterize the CHO cells (Table 1.3). Their genome was published in 2011 (Xu et al., 2011), sequenced from sorted chromosomes (Brinkrolf et al., 2013) and is available online at [www.chogenome.org](http://www.chogenome.org) (Hammond et al., 2012), a database that is continuously updated to include new annotations. Combining genome annotation using homology with *omics* studies that focused on unraveling the transcriptome (Becker et al., 2011; Hackl et al., 2011) and proteome (Baycin-Hizal et al., 2012) constitutes the foundation for the CHO systems biology era (Kildegaard et al., 2013).

## 1. Introduction

**Table 1.3. Timeline of “omics” and metabolic studies of the CHO cell line.** Abbreviations: CHO – Chinese hamster ovary; GS – glutamine synthetase; mAb – monoclonal antibody; PPP – pentose phosphate pathway; SHMT – serinehydroxymethyltransferase.

| “omics” studies of CHO cells                                                            | YEAR        | Metabolic studies of CHO cells                                                                                                                                                                                                                                                  | Cell line, culture type                       |
|-----------------------------------------------------------------------------------------|-------------|---------------------------------------------------------------------------------------------------------------------------------------------------------------------------------------------------------------------------------------------------------------------------------|-----------------------------------------------|
| Development of the CHO cell line (Puck, 1985).                                          | <b>1957</b> |                                                                                                                                                                                                                                                                                 |                                               |
| Mitochondria isolation in CHO cells (Madden and Storrie, 1987).                         | <b>1987</b> |                                                                                                                                                                                                                                                                                 |                                               |
|                                                                                         | <b>1996</b> | <ul style="list-style-type: none"> <li>Partitioning of serine and glycine metabolism was studied using [1-<sup>13</sup>C]- or [2-<sup>13</sup>C]glycine. Mitochondrial SHMT is the primary pathway for serine into glycine interconversion (Narkewicz et al., 1996).</li> </ul> | CHO K1<br><br>CHO glyA (lacks mSHMT activity) |
|                                                                                         | <b>1999</b> | <b>FIRST METABOLIC MODEL OF CHO</b> <ul style="list-style-type: none"> <li>A simplified model of the central carbon metabolism of CHO was used to study the consistency of mass balances when CHO cell are grown in complex media (Nyberg et al., 1999).</li> </ul>             | γ-CHO, continuous                             |
|                                                                                         | <b>2001</b> | <ul style="list-style-type: none"> <li>Metabolic flux redistribution in glutamate-based media. Regulation of glucose feed rate promotes efficient use of glucose and nitrogen source and lowers production of byproducts (Altamirano et al., 2001b).</li> </ul>                 | CHO TF 70R, suspension continuous             |
|                                                                                         |             | <ul style="list-style-type: none"> <li>Decoupling cell growth and product formation by generating a process with a growth phase and a stationary (producing) phase (Altamirano et al., 2001a).</li> </ul>                                                                       | CHO TF 70R, suspension batch                  |
| Two-dimensional electrophoresis map of CHO-K1 cell line proteins (Hayduk et al., 2004). | <b>2004</b> |                                                                                                                                                                                                                                                                                 |                                               |
|                                                                                         | <b>2005</b> | <ul style="list-style-type: none"> <li>Metabolism of CHO cells at low glucose concentration analyzed by determining intracellular metabolites. Amino acid catabolism and intracellular concentrations increased at reduced glucose availability (Lu et</li> </ul>               | CHO producing erythropoietin, monolayer       |



|                                                                                                                                                                                                                                                                                                                                                                                      |             |                                                                                                                                                                                                                                                                                                                                                                                                                                                                                    |                                                                                           |
|--------------------------------------------------------------------------------------------------------------------------------------------------------------------------------------------------------------------------------------------------------------------------------------------------------------------------------------------------------------------------------------|-------------|------------------------------------------------------------------------------------------------------------------------------------------------------------------------------------------------------------------------------------------------------------------------------------------------------------------------------------------------------------------------------------------------------------------------------------------------------------------------------------|-------------------------------------------------------------------------------------------|
|                                                                                                                                                                                                                                                                                                                                                                                      |             | al., 2005).                                                                                                                                                                                                                                                                                                                                                                                                                                                                        |                                                                                           |
|                                                                                                                                                                                                                                                                                                                                                                                      | <b>2006</b> | <ul style="list-style-type: none"> <li>• Macroscopic bioreaction model of CHO cell culture generated using elementary modes for each culture phase (Provost et al., 2006).</li> <li>• Metabolic characterization of recombinant CHO cells expressing glutamine synthetase (GS) in the medium with or without glutamine (Zhang et al., 2006).</li> </ul>                                                                                                                            | <p>CHO-320, suspension batch</p> <p>CHO-GS producing a recombinant protein, monolayer</p> |
| Genomic platform for CHO cells containing 28,000 CHO transcripts obtained using Sanger-based sequencing (Kantardjieff et al., 2009).                                                                                                                                                                                                                                                 | <b>2009</b> |                                                                                                                                                                                                                                                                                                                                                                                                                                                                                    |                                                                                           |
|                                                                                                                                                                                                                                                                                                                                                                                      | <b>2010</b> | <ul style="list-style-type: none"> <li>• Flux analysis of an underdetermined network of CHO generates flux ranges (Zamorano et al., 2010).</li> </ul>                                                                                                                                                                                                                                                                                                                              | CHO-320, suspension batch                                                                 |
|                                                                                                                                                                                                                                                                                                                                                                                      |             | <ul style="list-style-type: none"> <li>• Metabolic flux analysis of CHO cell metabolism in the late non-growth phase evidences a high PPP and low lactate production (Sengupta et al., 2010).</li> </ul>                                                                                                                                                                                                                                                                           | CHO-GS SF18, suspension batch                                                             |
|                                                                                                                                                                                                                                                                                                                                                                                      |             | <ul style="list-style-type: none"> <li>• Metabolic flux analysis of CHO cells in perfusion culture using <math>^{13}\text{C}</math>-labeled glucose (Goudar et al., 2010).</li> </ul>                                                                                                                                                                                                                                                                                              | n.s., perfusion                                                                           |
| <ul style="list-style-type: none"> <li>• CHO genome published (Xu et al., 2011).</li> <li>• Transcriptome unraveled by next-generation sequencing (Becker et al., 2011)</li> <li>• Next-generation sequencing of miRNA transcriptome (Hackl et al., 2011)</li> <li>• Metabolite profiling of CHO cells and identification of nutrient bottlenecks (Sellick et al., 2011a)</li> </ul> | <b>2011</b> | <ul style="list-style-type: none"> <li>• MFA of CHO cells at growth and non-growth phases using <math>[1,2-^{13}\text{C}]</math>glucose. Exponential phase: high glycolysis, lactate production, anaplerosis from pyruvate to oxaloacetate and from glutamate to <math>\alpha</math>-ketoglutarate, and cataplerosis through malic enzyme. Stationary phase: reduced glycolysis, lactate uptake, PPP flux, and reduced rate of anaplerosis (Ahn and Antoniewicz, 2011).</li> </ul> | CHO-K1, monolayer                                                                         |

|                                                                                                                                                                                                                                                                                                                                                                                                                                                                                    |             |                                                                                                                                                                                                                                                                                                                                                                                                                                                                                              |                                                                                           |
|------------------------------------------------------------------------------------------------------------------------------------------------------------------------------------------------------------------------------------------------------------------------------------------------------------------------------------------------------------------------------------------------------------------------------------------------------------------------------------|-------------|----------------------------------------------------------------------------------------------------------------------------------------------------------------------------------------------------------------------------------------------------------------------------------------------------------------------------------------------------------------------------------------------------------------------------------------------------------------------------------------------|-------------------------------------------------------------------------------------------|
| <ul style="list-style-type: none"> <li>• Proteomic analysis of CHO cells included the cellular proteome, secretome, and glycoproteome. A total of 6164 grouped proteins were identified from both glycoproteome and proteome (Baycin-Hizal et al., 2012).</li> <li>• Chinese hamster ovary database is made available as an online resource (Hammond et al., 2012).</li> <li>• Identification of the extracellular protein secretome in CHO cells (Slade et al., 2012).</li> </ul> | <b>2012</b> | <ul style="list-style-type: none"> <li>• Dynamic metabolic model of CHO cell culture based on decomposition provides sets of macroscopic bioreactions (Zamorano et al., 2012).</li> </ul>                                                                                                                                                                                                                                                                                                    | CHO-320, suspension batch                                                                 |
| <ul style="list-style-type: none"> <li>• CHO-K1 genome sequenced from sorted chromosomes (Brinkrolf et al., 2013).</li> <li>• Comparison of the <i>Cricetus griseulus</i> genome with that of six CHO cell lines highlights differences in genes related to bioproduction (Lewis et al., 2013).</li> </ul>                                                                                                                                                                         | <b>2013</b> | <ul style="list-style-type: none"> <li>• Kinetic model of CHO central carbon metabolism using Michaelis-Menten was used for studying the effect of sodium butyrate on CHO cells metabolism (Ghorbaniaghdam et al., 2013).</li> <li>• Flux balance analysis of Chinese hamster ovary cells before and after a metabolic switch from production to consumption showed that cells consuming lactate have a higher energy efficiency lactate producing cells (Martinez et al., 2013).</li> </ul> | CHO producing t-PA<br><br>CHO-XL99, suspension batch                                      |
|                                                                                                                                                                                                                                                                                                                                                                                                                                                                                    |             | <ul style="list-style-type: none"> <li>• Metabolic flux distributions of GS-CHO cell clones based on exometabolome profiling reveals that asparagine is the main source of nitrogen (Carinhas et al., 2013).</li> <li>• <sup>13</sup>C-MFA of a high expressing recombinant CHO cell line in fed-batch productions applied to determine changes in central metabolism that accompany growth and mAb production (Dean and Reddy, 2013).</li> </ul>                                            | CHOK1SV (producing IgG4 mAb), suspension batch<br><br>CHO producing mAb, suspension batch |

|                                                                   |      |                                                                                                                                                                                                                                                                                                                                                        |                                                         |
|-------------------------------------------------------------------|------|--------------------------------------------------------------------------------------------------------------------------------------------------------------------------------------------------------------------------------------------------------------------------------------------------------------------------------------------------------|---------------------------------------------------------|
|                                                                   |      | <ul style="list-style-type: none"> <li>• Parallel labeling using [1,2-<sup>13</sup>C]glucose and [U-<sup>13</sup>C]glutamine in parallel produced detailed flux maps of CHO cells (Ahn and Antoniewicz, 2013).</li> </ul>                                                                                                                              | CHO-K1, monolayer                                       |
|                                                                   |      | <ul style="list-style-type: none"> <li>• Steady state <sup>13</sup>CMFA applied to characterize CHO cell metabolism during four separate phases of a culture showed that a highly oxidative state of metabolism corresponds with peak antibody production (Templeton et al., 2013).</li> </ul>                                                         | mAb-producing CHO cell line, fed-batch                  |
|                                                                   |      | <ul style="list-style-type: none"> <li>• Comparative study of the intracellular flux distribution with and w/o the induction of recombinant protein synthesis studied using extracellular labeling showed that protein expression is correlated with changes in pathways related to ATP and NADPH formation (Sheikholeslami et al., 2013)</li> </ul>   | CHO producing anti-CD20 mAb, suspension batch           |
| 140 synthetic promoters for CHO engineering (Brown et al., 2014). | 2014 | <ul style="list-style-type: none"> <li>• Profiling of extracellular metabolites coupled with an analysis of intracellular distributions using 1-<sup>13</sup>C-pyruvate was used to trace metabolic rearrangements in different scenarios of asparagine and serine availability (Duarte et al., 2014).</li> </ul>                                      | CHOK1SV (producing IgG4 mAb), suspension batch          |
|                                                                   |      | <ul style="list-style-type: none"> <li>• <sup>13</sup>CMFA used to examine the effects of glutamine feeding on the metabolism and recombinant protein productivity of induced CHO cells. High TCA cycle at low glutamine levels and increased lactate production at high glutamine levels (Sheikholeslami et al., 2014)</li> </ul>                     | CHO producing mAb using a cumate gene-switch, fed-batch |
|                                                                   |      | <ul style="list-style-type: none"> <li>• Inst-<sup>13</sup>CMFA in CHO cells using only extracellular labeling showed that at exponential phase the metabolism ensures fast growth and mitigates oxidative stress. Compartmentation is used to control NAD(P)H availability and synthesis/catabolism of amino acids (Nicolae et al., 2014).</li> </ul> | CHO-K1, suspension batch                                |
|                                                                   |      | <ul style="list-style-type: none"> <li>• Glutamine feeding influence on CHO growth studied using dynamic metabolic flux analysis (Wahrheit et al., 2014a).</li> </ul>                                                                                                                                                                                  | CHO-K1, batch, fed-batch                                |

|             |                                                                                                                                                                                                                                                                           |                      |
|-------------|---------------------------------------------------------------------------------------------------------------------------------------------------------------------------------------------------------------------------------------------------------------------------|----------------------|
| <b>2015</b> | <ul style="list-style-type: none"> <li>• FBA applied to a large scale model and multivariate analysis to quantify intracellular metabolic fluxes of antibody-producing GS-CHO cells supplemented with different lots of wheat hydrolysates (Lee et al., 2015).</li> </ul> | CHO-GS producing mAb |
|-------------|---------------------------------------------------------------------------------------------------------------------------------------------------------------------------------------------------------------------------------------------------------------------------|----------------------|

In a typical culture of CHO cells, during the exponential growth phase, the CHO metabolism is characterized by a high glycolytic flux combined with a high lactate secretion flux. For protein production purposes, this state is highly inefficient due to low TCA cycle activity, glucose and media waste and the accumulation of lactate that alters the pH in the culture media. Later, depending on substrate availability, the culture can switch from producing to taking up lactate. This phase is characterized by slow growth but a high rate of protein production. The metabolism is responsible for handling the available substrates and supply the precursors related to growth and production. By reviewing the studies presented in Table 1.3, it is revealed that a deep understanding of the CHO cells metabolism is tightly correlated to improving recombinant protein production.

Compartmentation plays a key role in managing metabolites, and constitutes the major aspect to control the metabolism of eukaryotic cells. Dysfunctions in the mitochondrial metabolism are related to many widespread diseases. The aging process and many neurodegenerative diseases are correlated with changes in the mitochondria. Strain improvement for production of biopharmaceuticals relies on redirecting carbon and energy in the metabolic network. Mitochondria are at the core of the energy metabolism and are a partial location of the central carbon metabolism. Understanding compartmentation relates to gaining knowledge directed at engineering mammalian cell lines for optimized production or at designing novel treatments for diseases. Models of metabolism that include reaction compartmentation and mitochondrial transporter regulation are essential for describing the processes in the eukaryotic metabolism in a systemic manner. Consequently, both medicine and bioproduction would benefit greatly from a deeper understanding of the compartmentation of cellular processes.

This thesis sets the goal to understand better the compartmentation of the eukaryotic metabolism by applying a systems biology approach. To this goal, more mathematical modeling tools are developed that include compartmentation in the framework of the central carbon metabolism of mammalian cell. Through model building and model validation cycles, the task is to simultaneously determine details about the topology of compartmentation together with metabolic fluxes between the mitochondria and cytosol, all considered in the larger frame of the mammalian central carbon metabolism. The CHO-K1 cell line is used as a model mammalian system. In the chapters of this work are described the mathematical models in correlation to the specific knowledge that can be extracted by combining modeling with suitable experiments.

**Chapter 2:** Building and calibrating an Inst-<sup>13</sup>CMFA modeling platform using data from a labeling experiment in a continuous culture of *Saccharomyces cerevisiae*.

**Chapter 3:** Inst-<sup>13</sup>CMFA applied to a controlled batch culture of CHO-K1 cells aims to confirm that intracellular fluxes and reversibilities can be computed in a complex metabolic network by using only the labeling in extracellular metabolites. Experimental

labeling is fitted to the one computed using a model that simulates carbon and metabolite balance in both intra- and extracellular environments under the assumption of exponential growth.

**Chapter 4:** Taking Inst-<sup>13</sup>C MFA one step further, it was applied to a shake flask culture of CHO-K1 cells fed in parallel with [U-<sup>13</sup>C<sub>6</sub>] glucose and [U-<sup>13</sup>C<sub>5</sub>] glutamine. The goal is to perform the most detailed metabolic flux analysis to date with respect to compartmentation and to uncover details related to mitochondrial traffic and reaction compartmentation.

**Chapter 5:** Elementary mode analysis was applied to a model of the mitochondria to establish the contribution of enzymes and transporters to the mitochondrial metabolism. This was investigated by feeding several key substrates to selectively permeabilized CHO-K1 cells. By analyzing the flux values from each feeding experiment and the modes that achieve the conversion of substrates into observed products, it can be possible to determine key bottlenecks, regulatory effects and pathway activities in the mitochondria.

## Chapter 2

### 2. Platform for non-stationary <sup>13</sup>C metabolic flux analysis

#### 2.1. Introduction

As mentioned in Chapter 1, there are situations when steady state <sup>13</sup>C MFA is not applicable. Besides the practical aspects related to maintaining a stable metabolism throughout the duration of the labeling experiment, there are also situations determined by the structure of the carbon network that cannot be resolved using steady state <sup>13</sup>C MFA. Methods for quick quenching and sampling intracellular metabolites allow exploring of the information content of dynamic carbon labeling experiments. The goal of using any MFA method is to estimate intracellular fluxes. In order to reach this goal, Inst-<sup>13</sup>C MFA requires a complex software platform that handles heterogeneous types of data (extracellular fluxes, biomass composition, and mass isotopomer distributions), is capable of simulating the dynamic carbon balance model in a numerically stable manner, provides options for customization, enables checkpoints and offers a user-friendly interface where the simulations and parameter estimation are done efficiently.

#### 2.2. Theoretical aspects that require Inst-<sup>13</sup>C MFA

##### 2.2.1. Inst-<sup>13</sup>C MFA to study compartmentation

Due to compartmentation of metabolites and/or metabolic reactions, the labeling of certain metabolites can be different in the cytosol and mitochondria when using a labeled substrate. Activity of compartmented enzymes such as, e.g., mitochondrial malic enzyme and pyruvate carboxylase or cytosolic phosphoenolpyruvate carboxykinase, will differentiate the mitochondrial/cytosolic labeling patterns of the involved pools, i.e. malate, oxaloacetate and pyruvate. If inter-compartmental exchange occurs with high fluxes, transported metabolites will have similar labeling patterns in both compartments. Observing the proposed network, there are cases (Fig. 2.1) when alternative pathways cannot be distinguished even by using labeling.

One case (Fig. 2.1 a) is when there are several reaction pathways which connect one metabolite to a product, and they all transform the carbon backbone in the same manner. An example is the case for pyruvate dehydrogenase and pyruvate decarboxylase pathways leading both to mitochondrial acetyl-CoA. The second case (Fig. 2.1 b) is where a sampled metabolite originates from more precursor pools. By balancing metabolic fluxes and carbon it is mathematically impossible to determine compartment exchange fluxes and alternative synthesis pathways using only extracellular fluxes and steady state labeling patterns. An example of such a situation is the compartmentation of aminotransferases, which exist both in the cytosol and mitochondria and whose activity does not change the carbon backbone.

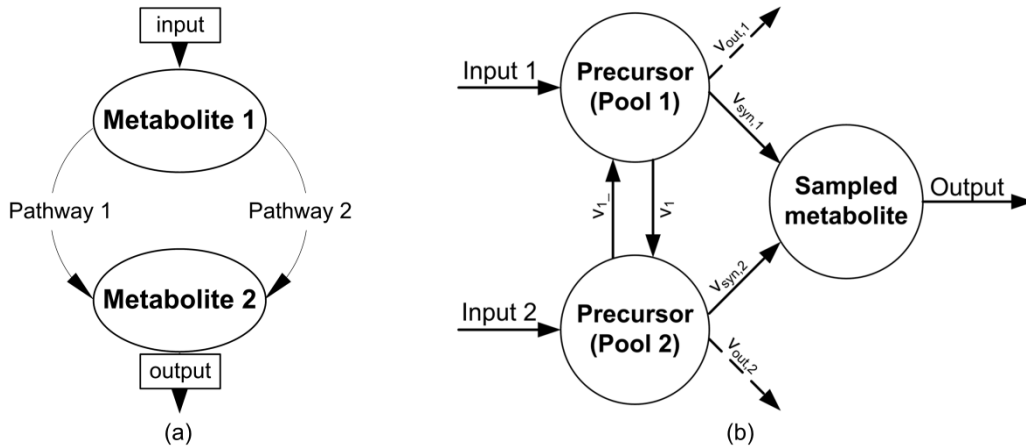


Fig 2.1. Model describing alternative synthesis pathways indistinguishable using labeling. (a) Alternative pathways which change the carbon backbone in the same way. (b) Compartmented identical reactions coupled with inter-compartmental exchange. The sampled metabolite originates via two pathways ( $v_{syn,1}$  and  $v_{syn,2}$ ) from a precursor compartmented in two pools (1 and 2). Reversible precursor transport is active ( $v_{1-}$ ,  $v_{-1}$ ) and pool draining into other metabolic reactions is considered measurable ( $v_{out,1}$ ,  $v_{out,2}$ ). Also input/output fluxes and labeling pattern are experimentally available.

### 2.2.2. Reversibility

It has already been shown that reversibility affects steady state labeling in several pathways (Follstad and Stephanopoulos, 1998). As Noh et al. (Noh and Wiechert, 2011) revealed by simulation, reversible fluxes affect the <sup>13</sup>C dynamics through the metabolic network. A backflow from a large pool into a small pool modifies the labeling dynamics of



both metabolites considerably, as it can be seen in Fig. 2.2. The labeling dynamics of A is slower if there is a reverse flux from a large pool B. Because many metabolic reactions take place close to equilibrium, reversibility changes label dynamics in the system without changing the isotopic steady state. Ignoring reversibility will therefore bias the estimation of intracompartmental concentrations. The steady state values depend only on the magnitude and ratio of metabolic fluxes (Fig. 2.2).

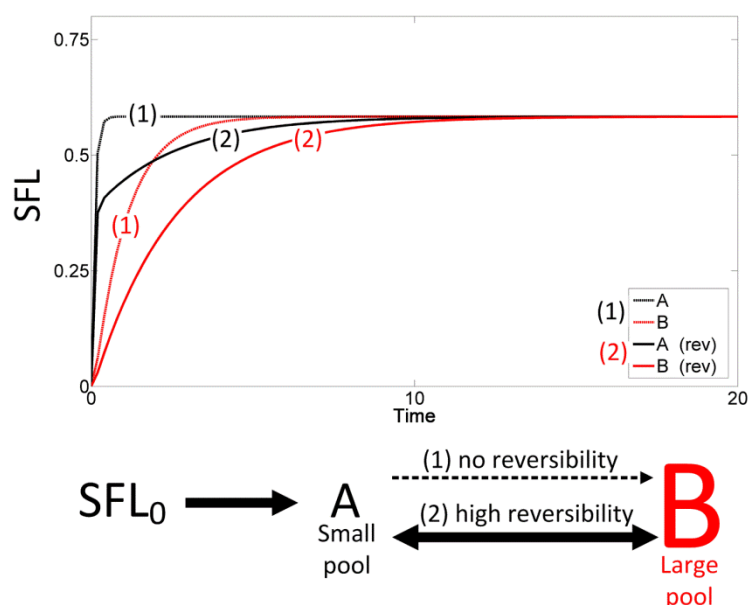


**Figure 2.2.** Summed fractional labeling (SFL) dynamics in a hypothetical reaction system. The label ( $SFL_0$ ) is introduced at time=0 and A and B become labeled at rates depending on the flux/pool ratio and reversibility. (1) there is no reversibility between A and B; (2) there is a high reversibility between A and B

### 2.3. Platform structure

A platform for simulating Inst-<sup>13</sup>CMFA experiments and for estimating parameters was built in Matlab®. At the core of the platform (Fig. 2.3) there is a system of differential equations for balancing the carbon in the metabolic network, which represents fundamentally the mathematical model of the dynamic carbon distribution through the metabolic network, from the labeled substrate to the sampled intra- or extracellular readout metabolites. Several procedures and functions were coded to:

- (1) generate atom mapping matrices from carbon transfer rules;

- (2) analyze the stoichiometric matrix, determine the degrees of freedom and select free fluxes;
- (3) compute intracellular fluxes for determined stoichiometric systems;
- (4) simulate the dynamic of isotopomers given a set of parameters;
- (5) compute the weighed sum of square differences (*SSQD*) from simulated and input MIDs (eq. 1.5);
- (6) determine the free parameters by minimizing the *SSQD* using numerical optimization;
- (7) perform sensitivity analysis;
- (8) plot the MID dynamics and sensitivity maps;
- (9) export the results in .csv or Microsoft Excel® form.

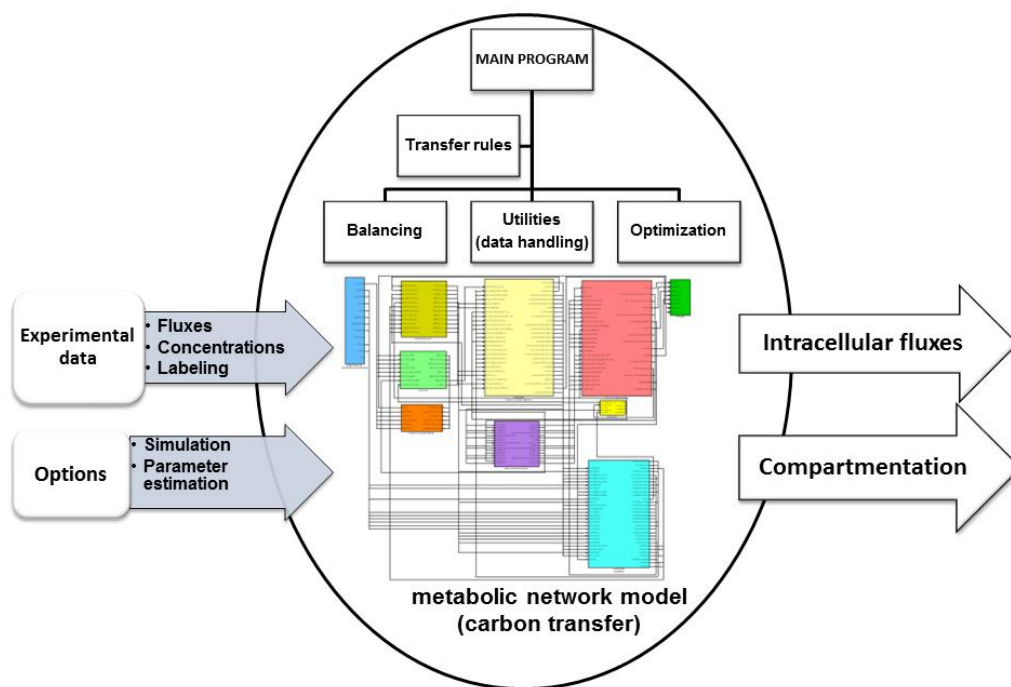


**Figure 2.3.** Scheme of the modeling platform for simulation and parameter estimation using non-stationary <sup>13</sup>C metabolic flux analysis. The main program handles the carbon transfer rules, procedures for balancing, data handling and optimization algorithms selection and/or customization, and also the simulation of the carbon balance through the metabolic network model. Data inputs: extracellular fluxes, intracellular concentrations and labeling. Combining data from more labeling experiments is possible. The user can input options related to the simulation and parameter estimation parameters.



Extracellular fluxes and transient mass isotopomer data from an experiment feeding [U-<sup>13</sup>C<sub>6</sub>]glucose and 50% [1-<sup>13</sup>C]glucose to a continuous culture of *S. cerevisiae* were obtained from (Hans, 2003). Although several parameter estimations and metabolic network modifications were attempted, the best fit failed to satisfy the  $\chi$ -squared test for model verification. Therefore, reliable parameter values could not be computed. However, the comprehensive data set was useful to test the functionality of the platform represented in Fig. 2.3. The model accurately described the labeling of intracellular alanine (Fig. 2.5), but it had difficulties to fit the amino acids whose labeling exhibited overshooting (Fig. 2.6), in particular the dynamics of the m+1 mass isotopomer of arginine and the steady state of the m+1 mass isotopomer of serine.

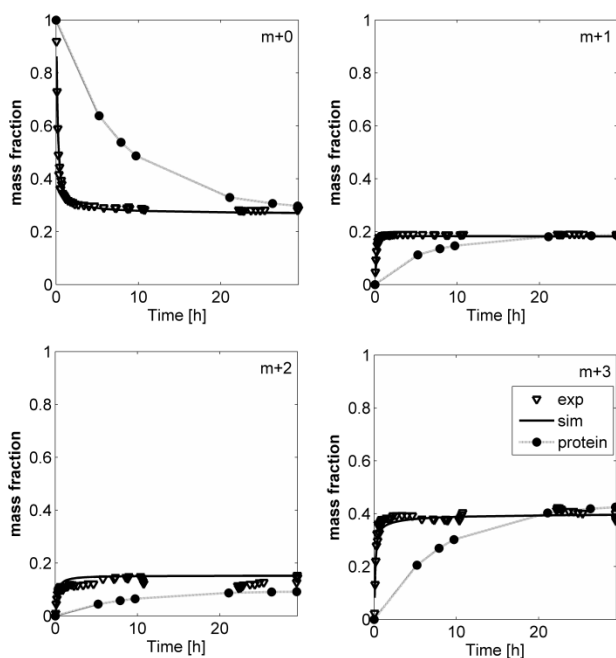


**Figure 2.5.** Dynamic distribution of intracellular alanine mass isotopomers from a carbon labeling experiment using a mixture of 50% [U-<sup>13</sup>C<sub>6</sub>]glucose and 50% [1-<sup>13</sup>C]glucose. Labeled substrate was fed to a continuous culture of *S. cerevisiae* until the labeling eventually reached a steady state in the proteinogenic amino acids (●). Intracellular metabolites were sampled by rapid quenching and then their labeling pattern was analyzed by GC-MS. A dynamic model carbon distribution in the *S. cerevisiae* central carbon metabolism was used to simulate the theoretical mass distributions (continuous line) which fitted best the experimental data (▽).

A model including the vacuole for storage of arginine was not successful for fitting the experimental overshooting, although it was able to simulate the qualitative behavior. Concerning serine labeling, the isotopomer model is not able to simulate a double overshooting (Fig. 2.6 d). It is very likely that the amino acids are cycled between protein synthesis and degradation (Belle et al., 2006) and that this process is also compartmented, as shown for yeast vacuoles (Horst et al., 1999).

The dataset was useful to calibrate the modeling platform and to test the performance of numerical algorithms for integration of differential equations and for optimization. In this respect, an integration algorithm for stiff systems of differential equations (Shampine and Reichelt, 1997) proved to be the fastest and the most stable from those tested. Random sets of fluxes that satisfy the numerical constraints imposed on the model by biochemistry (e.g. reaction direction) were generated using simulated annealing. The fastest converging optimization method was an internally reflective sequential quadratic programming optimization algorithm (Han, 1977). This algorithm accepts boundary and linear inequality constraints. A model simulation need approximatively 10 seconds on a 2.3 GHz QuadCore CPU, and the optimization algorithm performed around 2000 model runs before converging to a local minimum.

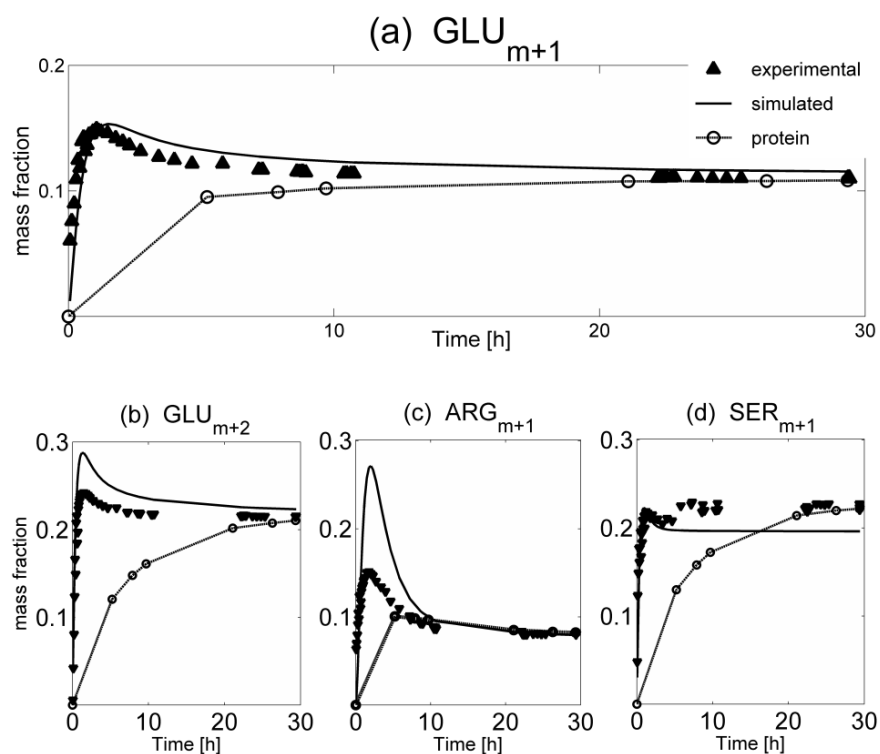


**Figure 2.6.** Nonlinear behavior of amino acids labeling dynamics manifested by certain mass isotopomers of metabolites from *S. cerevisiae* central carbon metabolism when a mixture of 50% [U-<sup>13</sup>C<sub>6</sub>]glucose and 50% [1-<sup>13</sup>C]glucose was fed to a continuous culture. Glutamate m+1(a) and m+2 (b), arginine m+1 (c) and serine m+1 (d) behavior was modeled for the experimental conditions using estimated values for intracellular fluxes and concentrations.

## Chapter 3

### 3. Non-stationary $^{13}\text{C}$ metabolic flux analysis of CHO cells in batch culture<sup>\*1</sup>

#### Abstract

Mapping the intracellular fluxes for established mammalian cell lines is important for scientific and economic reasons. However, this is being hampered by the complexity of metabolic networks, particularly concerning compartmentation.

Intracellular fluxes of the CHO-K1 cell line central carbon metabolism were successfully determined for a complex network using non-stationary  $^{13}\text{C}$  metabolic flux analysis. MIDs of extracellular metabolites were determined using  $[\text{U-}^{13}\text{C}_6]$  glucose. Compartmentation and transport reversibility proved essential to successfully reproduce the dynamics of the labeling patterns. Alanine and pyruvate reversibility changed dynamically even if their net production fluxes remained constant. Cytosolic phosphoenolpyruvate carboxykinase, mitochondrial malic enzyme and pyruvate carboxylase fluxes were successfully determined. Glycolytic pyruvate channeling to lactate was modeled. In the exponential growth phase, alanine, glycine and glutamate were excreted, and glutamine, aspartate, asparagine and serine were taken up. All these amino acids except asparagine were exchanged reversibly with the media. High fluxes were determined in the pentose phosphate pathway and the TCA cycle. The latter was fueled mainly by glucose but also by amino acid catabolism.

The CHO-K1 central metabolism in controlled batch culture is robust. It has the purpose to ensure fast growth on a mixture of substrates and also to mitigate oxidative stress. It achieves this by using compartmentation to control NADPH and NADH availability and by simultaneous synthesis and catabolism of amino acids.

<sup>\*1</sup>This chapter was published as: Nicolae, A., Wahrheit, J., Bahnemann, J., Zeng, A. P., Heinzle, E., 2014. *Non-stationary  $^{13}\text{C}$  metabolic flux analysis of Chinese hamster ovary cells in batch culture using extracellular labeling highlights metabolic reversibility and compartmentation*. BMC Syst Biol. 8, 50.

All experimental work described herein was carried out by Judith Wahrheit and Janina Bahnemann.

#### 3.1. Introduction

Economic importance and ease of cultivation make CHO cells a desirable candidate for metabolic studies in eukaryotic systems. Alongside with being the most important mammalian cell line for producing biopharmaceuticals (Butler and Meneses-Acosta, 2012; Kim et al., 2012; Walsh, 2010), CHO cells are able to grow in suspension cultures using chemically defined media (Deshpande et al., 2009), use multiple carbon sources simultaneously and maintain a stable metabolism for long periods in batch cultivations. This has led to a wealth of studies aimed at exploring CHO metabolism. After the decoding of the CHO-K1 cell line genome (Brinkrolf et al., 2013; Xu et al., 2011) and transcriptome (Becker et al., 2011), it can be expected that such studies will increase both in number and complexity. Metabolic flux analysis (MFA) of CHO cell cultures evolved from flux balancing analysis (Altamirano et al., 2001b) to more complex metabolic or isotopomer dynamic models (Ahn and Antoniewicz, 2012). Newer studies rely on  $^{13}\text{C}$ -MFA applied by fitting the summed fractional labeling (Ahn and Antoniewicz, 2011) or by fitting steady-state labeling data (Templeton et al., 2013) resulted from using in parallel more labeled substrates for determining the intracellular fluxes at metabolic steady state in different growth phases. However, the labeling patterns of the intracellular metabolites or of amino acids from hydrolyzed proteins that are usually needed for non-stationary  $^{13}\text{C}$ -MFA are obtained through a tedious methodology (Zamboni, 2011; Zamboni et al., 2009) and are susceptible to errors stemming mostly from the quenching/extraction phase (Dietmair et al., 2010; Wahrheit and Heinzle, 2013). In the absence of metabolite exchange with the media, intracellular labeling would reach steady state relatively fast, in the order of minutes for glycolytic intermediates and few hours for TCA cycle metabolites, as it was determined in *Pichia pastoris* (Jorda et al., 2013). In mammalian cells, exchange with the extracellular pools (Murphy et al., 2013) delays the intracellular isotopic steady state usually beyond the possibility to maintain metabolic steady state. Due to the large extracellular pools of amino acids, their exchange will transfer the time constant of the extracellular labeling process, which is in the order of days, to the intracellular labeling. One option is to use isotopic non-stationary metabolic flux analysis



### 3. Non-stationary $^{13}\text{C}$ MFA of CHO cells in batch culture

---

(Inst- $^{13}\text{C}$ MFA) applied at short time scales (Noh et al., 2007), but this approach has the drawback of requiring accurate determination of intracellular concentrations of metabolites (Noh and Wiechert, 2006).

Metabolite and reaction compartmentation is important for a realistic representation of the mammalian cell metabolism, but determining it raises supplementary demands from the experimental and modeling procedures, as reviewed in (Wahrheit et al., 2011a). In the exponential growth phase, a typical culture of CHO is characterized by high uptake rates of glucose and glutamine, the Warburg effect and the exchange of non-essential amino acids with the extracellular media (Deshpande et al., 2009; Provost et al., 2006). We can expect that by feeding a  $^{13}\text{C}$  labeled substrate, some of the extracellular metabolites will exhibit labeling patterns that can then be detected using GC-MS. As these metabolites will be enriched in  $^{13}\text{C}$  dynamically, non-stationary  $^{13}\text{C}$  metabolic flux analysis (Inst- $^{13}\text{C}$ MFA) applied to extracellular and intracellular isotopomers (Noack et al., 2010; Noh et al., 2006; Schmidt et al., 1997) provides a suitable framework to determine the intracellular fluxes. Extracellular pools have a large time scale for labeling (hours) compared to the intracellular pools (seconds/minutes), thus removing the need to sample intracellular pools provided that the labeling information in the extracellular metabolites is sufficient.

It is shown in this chapter that by using only the labeling patterns of extracellular metabolites produced by feeding  $[\text{U-}^{13}\text{C}_6]\text{glucose}$  as the only labeled substrate, intracellular fluxes can be successfully determined in a complex, compartmented metabolic network of the CHO-K1 cell line. In parallel, the aim is to prove that a simplified, non-compartmented model is not sufficient for describing the metabolism. The importance of considering reversibility when dealing with non-stationary isotopomer models is also underlined.

## 3.2. Materials and Methods

### 3.2.1. Cell culture and experimental set-up

The CHO-K1 cell line was kindly provided by the Institute of Cell Culture Technology (University Bielefeld, AG Noll, Germany). The cells were growing in suspension under serum and protein free conditions in the chemically defined medium TC-42 (TeutoCell AG, Bielefeld, Germany) supplemented with 4 mM L-glutamine (PAA, Germany). Precultures were cultivated in 125 mL baffled Erlenmeyer flasks (Corning Inc., Germany) at an initial cell density of  $0.4 \times 10^6$  cells/mL and a working volume of 50 mL on a shaking device (225 rpm) at 37°C and 5%  $\text{CO}_2$  in a humid atmosphere. For the main cultivation, cells were harvested during the exponential growth phase at a viability of  $\geq 98\%$  and resuspended in TC-42 medium with 100% [ $\text{U-}^{13}\text{C}_6$ ] glucose (99%, Euriso-Top, Saarbrücken, Germany). The main cultivation was performed in a Vario1000 bioreactor (Medorex e.K., Nörten-Hardenberg, Germany) at batch mode with a starting culture volume of 200 mL. The bioreactor was inoculated at a cell density of  $0.4 \times 10^6$  cells/mL. The cultivation temperature was kept constant at 37 °C and the impeller (3-blade marine propeller) speed was set to 300 rpm. During the cultivation, the pH value was controlled at 7.2 by gassing with  $\text{CO}_2$  and by using 0.5 M sodium carbonate solution. Dissolved oxygen was maintained at 30% of the saturation concentration. Samples were taken three times a day. Cell density and viability were determined by cell counting using the Trypan blue exclusion method. Supernatants were transferred into fresh tubes and stored at -20°C until further analysis. The average cell diameter was determined using an automated cell counter (Invitrogen, Darmstadt, Germany) in a separate experiment. This experiment was performed in a shaking incubator (2 inches orbit, 185 rpm, 37°C, 5%  $\text{CO}_2$  supply) using 250 mL baffled Erlenmeyer flasks (Corning Inc., Germany), an initial cell density of  $0.4 \times 10^6$  cells/mL, a working volume of 100 mL and using the same medium TC-42 medium (TeutoCell, Bielefeld, Germany) supplemented with 4 mM glutamine. Differences of cell diameters during the cultivation were maximum 5% and not taken into account. Cell volume was computed assuming the cells are spherical using a diameter of 10.6  $\mu\text{m}$ . Glutamine degradation kinetics were determined experimentally in a cell-free

### 3. Non-stationary $^{13}\text{C}$ MFA of CHO cells in batch culture

---

setup identical to the one employed for cell volume estimation. The determined glutamine degradation rate constant was  $kd_{\text{GLN}} = 0.0033 \text{ h}^{-1}$ .

#### 3.2.2. Quantification of metabolites

Quantification of glucose, organic acids and amino acids via HPLC was carried out as described previously by Strigun et al. (Strigun et al., 2011).

#### 3.2.3. Analysis of isotopomer labeling patterns

##### 3.2.3.1. Sample preparation

For determination of labeling patterns of lactate and amino acids, 50  $\mu\text{l}$  of supernatants were lyophilized, resolved in 50  $\mu\text{l}$  N,N-dimethylformamide (0,1 % pyridine) and incubated at 80°C for 30 min. 50  $\mu\text{l}$  N-methyl-N-t-butyltrimethylsilyl-trifluoro-acetamide (MBDSTFA) was added followed by another incubation at 80°C for 30 min for derivatization of metabolites into corresponding dimethyl-t-butylsilyl derivatives. For determination of the labeling pattern of pyruvate, lyophilized supernatants were resolved in 50  $\mu\text{l}$  pyridine containing 20 mg/ml methoxyamine hydrochloride and 50  $\mu\text{l}$  MSTFA (Macherey-Nagel, Düren, Deutschland) and incubated at 80°C for 30 min for derivatization into the methoxyamine-trimethylsilyl derivative. Derivatized samples were centrifuged at 13000 x g for 5 min at 4 °C and supernatants transferred into fresh glass vials with micro inlets.

##### 3.2.3.2. GC-MS measurements

Extracellular  $^{13}\text{C}$ -labeling dynamics were analyzed by gas chromatography mass spectrometry (GC-MS). The GC-MS measurements were carried out on a GC (HP 6890, Hewlett Packard, Palo Alto, CA, USA) equipped with an HP5MS capillary column (5% phenyl-methyl-siloxane diphenylpolysiloxane, 30 m  $\times$  0.25 mm  $\times$  0.25  $\mu\text{m}$ , Agilent Technologies, Waldbronn, Germany), electron impact ionization at 70 eV, and a quadrupole detector (Agilent Technologies). The injection volume was 1  $\mu\text{l}$  (7683B Autosampler, Agilent, Waldbronn, Germany; PTV-Injektor, Gerstel, Mühlheim a. d. Ruhr, Germany). Helium was used as carrier gas at a flow rate of 1.1 ml/min for analysis of lactate and amino acids or 0.7 ml/min for pyruvate analysis. The following temperature gradient was applied for lactate and amino acid analysis: 135°C for 7 min, 10°C/min up to

### 3. Non-stationary <sup>13</sup>CMFA of CHO cells in batch culture

---

162°C, 7°C/min up to 170°C, 10°C/min up to 325°C, 325°C for 2.5 min; inlet temperature: 140°C and heating with 720°C/min up to 320°C; interface temperature 320°C; quadrupole temperature 150°C. The temperature gradient for pyruvate analysis was as follows: 70°C for 1 min, 1°C/min up to 75°C, 5°C/min up to 315°C, 25°C/min up to 340°C, 340°C for 5 min; inlet temperature: 70°C and heating with 360°C/min up to 360°C; interface temperature 320°C; quadrupole temperature 280°C.

#### 3.2.3.3. Data analysis

After identification of metabolites in the scan mode using the NIST data bank, quantification of labeling enrichment was done in SIM (single ion monitoring) mode in two technical replicates using the following unique fragments (m/z) containing the complete carbon skeleton of metabolites: pyruvate 174, lactate 261, alanine 260, glycine 246, serine 390, aspartate 418, glutamate 432, glutamine 431. Mass isotopomer distributions were corrected for naturally occurring isotopes using the method of Yang et al. (Yang et al., 2009).

#### 3.2.4. Metabolic network models

Two metabolic networks were established based on experimental observations related to metabolite uptake and production and extracellular labeling. Both networks included: glycolysis; TCA cycle; anaplerotic reactions; synthesis of fatty acids, proteins and carbohydrates for biomass production; amino acid production and degradation. Transport from the extracellular media was reversible in both models for all metabolites with the exception of glucose, asparagine and essential amino acids. Mitochondrial transport of malate,  $\alpha$ -ketoglutarate, alanine, and reactions of transaminase, malate and lactate dehydrogenase were also reversible. The first model shown in Fig. 3.1 A considers the intracellular space without compartmentation. In the second model (Fig. 3.1 B), the mitochondrial reactions and pools are separated from the cytosol. Both models start from the annotation of the genomes of CHO-K1 and *Mus musculus* (Hammond et al., 2012; Kanehisa et al., 2014; Zhu et al., 2003). Enzyme localization was established using information from the MGI database and data from J. Wahrheit (Wahrheit et al., 2014b) who measured compartmented enzyme activity using a method adapted from Niklas et al.

### 3. Non-stationary $^{13}\text{C}$ MFA of CHO cells in batch culture

(Niklas et al., 2011a). Mitochondrial transport of alanine was included to explain the existence of alanine aminotransferases in both compartments. Metabolite pools were lumped where it did not influence the simulated labeling dynamics. Pentose phosphate pathway was reduced to one reaction where one carbon atom is lost for each G6P molecule and 5/3 molecules of PG are produced. Glycolysis was lumped to three fluxes transforming G6P into  $\text{PYR}_{\text{cyt}}$ .

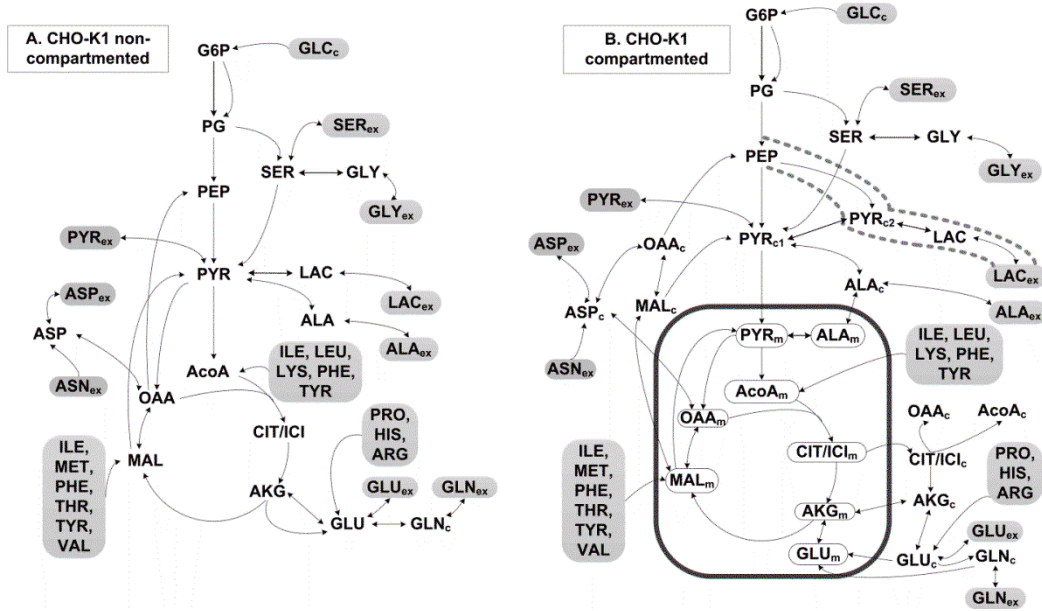


**Figure 3.1. Compartmented (A) and non-compartmented (B) networks of the CHO-K1 central metabolism used for simulations.** Irreversibility is indicated by simple arrows, and reversibility by double arrows. The reactions depicted in B are listed in detail in the Supplem. Table S3.1 together with fluxes and reversibilities determined. Subscripts meaning: *ex* – extracellular; *c* – cytosolic; *m* – mitochondrial. Abbreviations: AA – amino acids; AcoA – acetyl CoA; AKG –  $\alpha$ -ketoglutarate; ALA – alanine; ASN – asparagine; ASP – aspartate; CIT/ICI – citrate/isocitrate; G6P – glucose 6-phosphate; GLC – glucose; GLN – glutamine; GLU – glutamate; GLY – glycine; MAL – malate; OAA – oxaloacetate; PEP – phosphoenolpyruvate; PG – phosphoglycerate; PYR – pyruvate; SER – serine.

Isocitrate and citrate were condensed into one pool. Succinate, fumarate and malate were condensed into one pool. Two cytosolic pyruvate pools were used to describe metabolic channeling to lactate. Non-essential amino acids catabolism was lumped to three fluxes fueling the malate, acetyl-CoA and glutamate pool respectively. No carbon mapping was required in this case as essential amino acids are unlabeled. Glutaminase activity was

### 3. Non-stationary <sup>13</sup>CMFA of CHO cells in batch culture

---

mitochondrial (Xu et al., 2011) and glutamine synthetase was cytosolic (Hayward et al., 1986). Fatty acids, protein and storage carbohydrates composition of the cell was taken from Altamirano et al. (Altamirano et al., 2001b).

In total, the compartmented model consisted of 60 fluxes and 25 metabolites and the non-compartmented model of 42 fluxes and 16 metabolites. The complete flux list for the two models, together with the carbon transfer rules, is provided in the Supplem. Table S3.1.

#### 3.2.5. Non-stationary-<sup>13</sup>CMFA methodology

Isotopic non-stationary metabolic flux analysis (Inst-<sup>13</sup>CMFA) comprises: (1) metabolic steady-state balancing of intracellular metabolites for determining extracellular rates; (2) dynamic extracellular metabolite and isotopomer balance and (3) dynamic balances of intra-compartmental isotopomers.

##### 3.2.5.1. Metabolite balancing

Net extracellular rates  $v_{M\_ex}$  were determined for each extracellular metabolite  $M\_ex$  for the batch cultivation situation, under the assumption of metabolic steady state, by fitting the cell density  $X(t)$  and extracellular concentrations of metabolites  $C_{M\_ex}$  to an exponential growth model with specific growth rate  $\mu$  (eq. 3.1.a,b) and constant extracellular rates. Glutamine balance included first order degradation in the culture media (eq. 3.1.c).

$$dX/dt = \mu \cdot X(t) \quad (3.1.a)$$

$$dC_{M\_ex}/dt = v_{M\_ex} \cdot X(t) \quad (3.1.b)$$

$$dC_{GLN}/dt = v_{GLN} \cdot X(t) - kd_{GLN} \cdot C_{GLN}(t) \quad (3.1.c)$$

At intracellular metabolic steady state, the  $n$  metabolic fluxes that connect the  $m$  metabolites are constant and satisfy the material balance:

$$\mathbf{G} \cdot \mathbf{v} = \mathbf{0} \quad (3.2.a)$$

$$v_j = \varphi_j, \quad j = 1..R_{meas} \quad (3.2.b)$$

$$\alpha_i \leq v_i \leq \beta_i, \quad i = 1..n \quad (3.2.c)$$

### 3. Non-stationary <sup>13</sup>CMFA of CHO cells in batch culture

where  $G$  is the  $m \times n$  stoichiometric matrix and its null space  $v$  is the vector of net metabolic fluxes which are constrained by  $R_{meas}$  measured fluxes  $\varphi_j$  (eq. 3.2.b) and  $n$  inequalities (eq. 3.2.c) determined by flux direction. To reduce the number of parameters, the free fluxes were extracted from the network as described (Yang et al., 2008) to produce a determined stoichiometric system.

All biomass fluxes were computed considering the biomass composition listed in Suppl. Table S1.1 and Suppl. Table S1.2.

#### 3.2.5.2. Intracellular and extracellular carbon balance

The Inst- <sup>13</sup>CMFA framework developed in (Noh and Wiechert, 2006; Schmidt et al., 1997) was adapted to the case of batch culture cultivation. Isotopomer balances for extracellular (eq. 3.3) and intracellular (eq. 3.4) metabolites were solved together with the extracellular mass balances (eq. 1.a,b,c).

$$\frac{dIDV_{M\_ex}}{dt} = \frac{1}{C_{M\_ex}} \cdot \left[ X_{conc} \cdot (v_{M\_ex}^{in} \cdot IDV_{M\_cyt} - v_{M\_ex}^{out} \cdot IDV_{M\_ex}) - \frac{dC_{M\_ex}}{dt} \cdot IDV_{M\_ex} \right] \quad (3.3)$$

$$\frac{dIDV_{M\_in}}{dt} = \frac{1}{C_{M\_in}} \cdot \left( \sum_{j=1}^{R_M} v_j \cdot IDV_{M\_in,j} - v_{M\_in}^{out} \cdot IDV_{M\_in} \right) \quad (3.4)$$

with  $IDV_{M\_ex}$ ,  $IDV_{M\_cyt}$ ,  $IDV_{M\_in}$ , are the isotopomer distribution vectors of the extracellular, cytosolic and mitochondrial fractions of metabolite  $M$ .  $IDV_{M\_in,j}$  is the  $j^{th}$  reaction contribution to isotopomers of metabolite  $M$ , computed using isotopomer mapping matrices as described by Schmidt (Schmidt et al., 1997).  $X_{conc}$  is the cell volumetric concentration expressed in L cell / L media.  $C_{M\_ex}$  is the extracellular concentration of  $M$ ,  $v_{M\_ex}^{in}$  is the production flux of  $M$  expressed in  $\text{mmol} \times (\text{L cell})^{-1} \times \text{h}^{-1}$ ,  $v_{M\_ex}^{out}$  is the uptake flux,  $v_j$  is one of the  $R_M$  fluxes entering the intracompartmental pool of  $M$ ,  $C_{M\_in}$ , and  $v_{M\_in}^{out}$  is the flux exiting the pool. The metabolite and isotopomer balances from equations 1,2 and 4 are then solved simultaneously to obtain the time course of the mass isotopomer distributions. Isotopomer balancing employs absolute fluxes that can be computed from the net fluxes by introducing a reversibility parameter:

### 3. Non-stationary $^{13}\text{C}$ MFA of CHO cells in batch culture

---

$$rev_j = \frac{v_{j,reverse}}{v_j} \quad (3.5)$$

where  $v_j$  is the net flux and  $v_{j, forward}$  and  $v_{j, reverse}$  are the forward and respectively the reverse exchange fluxes, with  $v_{j, forward} - v_{j, reverse} = v_j$ ;  $v_{j, forward} \geq 0$  and  $v_{j, reverse} \geq 0$ .

The contribution of reaction  $j$  was computed using isotopomer mapping matrices (Schmidt et al., 1997) that trace carbon from the substrate to the reaction products. The initial mass distribution of all metabolites was computed considering the naturally occurring  $^{13}\text{C}$  fraction (1.1%) and the 99% atom purity of the employed  $^{13}\text{C}$  labeled substrate.

#### 3.2.5.3. Parameter estimation

The simulated time course of extracellular mass isotopomer distributions ( $MID$ ) was compared with the experimental values. The objective function to be minimized is expressed as the weighted sum of square differences between the experimentally determined and simulated  $MID$ s:

$$SSQD = (MID^{sim} - MID^{exp})^T \cdot \sum_{MID}^{-1} \cdot (MID^{sim} - MID^{exp}) \quad (3.6)$$

where  $SSQD$  is the objective function,  $MID^{sim}$  is the simulated  $MID$ ,  $MID^{exp}$  is the measured  $MID$  and  $\Sigma_{MID}$  is the measurement covariance matrix. The optimal solution was accepted when it satisfied the  $\chi$ -squared test for model verification with 95% probability, and  $N-p$  degrees of freedom, where  $N$  is the number of sampled points (size of  $MID^{exp}$ ) and  $p$  is the number of free parameters. To reduce the bias in the objective function generated by very small standard deviations, a minimum threshold of 0.005 was imposed. Accurate confidence intervals and sensitivity analysis of fluxes were computed according to (Antoniewicz et al., 2006). All the code was programmed and simulated in Matlab [MATLAB and Simulink Release 2013a, The MathWorks, Inc., Natick, Massachusetts, United States].

### 3.3. Results and discussion

#### 3.3.1. Cell growth and extracellular fluxes



### 3. Non-stationary <sup>13</sup>CMFA of CHO cells in batch culture

The cells exhibited exponential growth for 72 h (Fig. 3. 2) until glutamine became exhausted and a shift in metabolism was observed (data not shown). Estimated specific growth rate as fitted to eq. 3.1.a was  $\mu = 0.0401 \text{ h}^{-1}$ . Uptake and production of most metabolites was balanced, i.e. they were proportional to growth for the main carbon sources and produced metabolites (Fig. 3.2) and for other amino acids (Supplem. Fig. S 3.1). This means that metabolic steady state was maintained during the first 72 h of cultivation. Glucose constituted the main carbon source (Table 3.1), providing 65% of the total carbon entering the central carbon metabolism, with an uptake flux of  $371 \text{ mmol} \times (\text{L cell})^{-1} \times \text{h}^{-1}$ . Note that all fluxes are related to the cell volume specified by L cell. 39% of the glucose was converted to lactate. The observed pyruvate production rate was  $3.3 \text{ mmol} \times (\text{L cell})^{-1} \times \text{h}^{-1}$ .

**Table 3.1. Carbon sources for the central metabolism of the CHO-K1 cell line in batch culture during the exponential growth phase.** The contribution of AA1, AA2 and AA3 amino acid groups considers only catabolism. Abbreviations: AA1: amino acids catabolized to AcoA (isoleucine, leucine, lysine, phenylalanine, tyrosine); AA2: amino acids catabolized to four-carbon dicarboxylic acids (isoleucine, methionine, phenylalanine, threonine, tyrosine, valine); AA3: amino acids catabolized to glutamate (arginine, histidine, proline); AcoA: acetyl coenzyme A; AKG:  $\alpha$ -ketoglutarate; ASN: asparagine; ASP: aspartate; OAA: oxaloacetate.

\* Excluding requirements for protein synthesis

| Metabolite   | Target intracellular metabolite | Uptake flux<br>[mmol $\times$ (L cell) <sup>-1</sup> $\times$ h <sup>-1</sup> ] | Uptake flux<br>[Cmmol $\times$ (L cell) <sup>-1</sup> $\times$ h <sup>-1</sup> ] | Percentage of the total carbon-flux |
|--------------|---------------------------------|---------------------------------------------------------------------------------|----------------------------------------------------------------------------------|-------------------------------------|
| Glucose      | Pyruvate                        | 371.0                                                                           | 2226.2                                                                           | 64.9                                |
| Glutamine    | AKG                             | 66.4                                                                            | 331.9                                                                            | 9.7                                 |
| AA1*         | AcoA                            | 92.6                                                                            | 185.2                                                                            | 5.4                                 |
| AA2*         | Malate                          | 49.6                                                                            | 198.4                                                                            | 5.8                                 |
| AA3*         | AKG                             | 11.6                                                                            | 58.2                                                                             | 1.7                                 |
| ASP/ASN      | OAA                             | 68.1                                                                            | 272.3                                                                            | 7.9                                 |
| Serine       | Pyruvate, glycine               | 48.3                                                                            | 146.4                                                                            | 4.3                                 |
| <b>TOTAL</b> | -                               | -                                                                               | <b>3428.53</b>                                                                   | <b>100</b>                          |

### 3. Non-stationary $^{13}\text{C}$ MFA of CHO cells in batch culture

The glutamine uptake flux determined by fitting eq. (3.1.c) to the glutamine concentration over time was  $66.4 \text{ mmol} \times (\text{L cell})^{-1} \times \text{h}^{-1}$ , 16% smaller compared to the case when degradation was ignored. Glutamine uptake contributed with 10% to the total carbon pool.

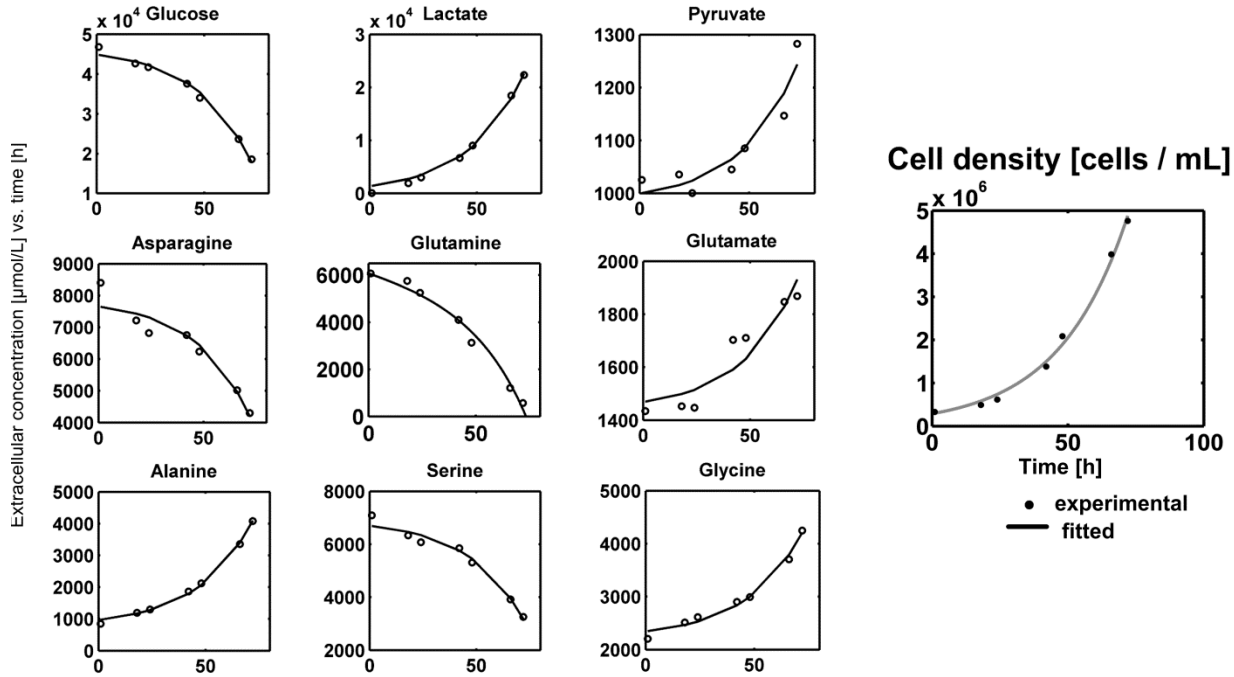


**Figure 3.2.** Culture profile of the CHO-K1 cells for the first 72 h during the exponential growth phase. Experimental values are shown with circles and calculated values are represented by solid lines.

The rest of the carbon feeding the central carbon metabolism, i.e. 25%, was obtained from amino acids catabolism.

Alanine, glycine and glutamate were produced (Fig. 3.3), while the other amino acids were taken up in excess of the quantity required for biomass synthesis. As a consequence of amino acids catabolism, a flux of  $92.6 \text{ mmol} \times (\text{L cell})^{-1} \times \text{h}^{-1}$  fueled the mitochondrial acetyl-CoA pool from the degradation of isoleucine, leucine, lysine, phenylalanine and tyrosine, while a flux of  $39.1 \text{ mmol} \times (\text{L cell})^{-1} \times \text{h}^{-1}$  cytosolic AcoA was directed towards fatty acids synthesis. The catabolism of excess isoleucine, methionine, phenylalanine, threonine, tyrosine and valine that remained after protein synthesis produced  $49.6 \text{ mmol}$

### 3. Non-stationary $^{13}\text{C}$ MFA of CHO cells in batch culture

---

$\times (\text{L cell})^{-1} \times \text{h}^{-1}$  succinate and fumarate (lumped into one pool of four carbon dicarboxylic acids, here represented as MAL in Fig. 3.1).

Metabolite dilution by growth was neglected due to negligible influence on the total mass balance.

#### 3.3.2. Non-stationary labeling experiment

The *MID* of extracellular pyruvate, lactate, alanine, glutamate, glutamine, aspartate, serine and glycine was sampled at 1, 18, 24, 42, 48, 66 and 72 h. During the exponential growth phase of 72 h none of the labeling reached steady state as shown in Fig. 3.4. Lactate and pyruvate exhibited similar labeling dynamics, however with different *MIDs* towards the end of the growth. This is surprising since lactate is obtained from pyruvate through the lactate dehydrogenase reaction. The predominant lactate fraction, i.e.  $\text{M}+3$ , increased to 0.85 and the pyruvate  $\text{M}+3$  fraction stabilized at 0.81, pointing towards glycolytic channeling to lactate achieved by the localized cooperation of glycolytic enzymes as observed in rapidly proliferating cells (Mazurek et al., 2001; Vander Heiden et al., 2010). From the produced amino acids, alanine, also derived from pyruvate, had a high  $\text{M}+3$  fraction. Glutamate and glycine  $\text{M}+2$  fractions increased slowly, with most of the change happening in the last 24 h due to the high number of producing cells present in the media., Extracellular aspartate, glutamine and serine were found to be labeled although they exhibited a net uptake. Glutamine fractional labeling, mostly the  $\text{M}+2$  isotopomer, increased sharply at the end of the phase, when very little glutamine remained in the media and the contribution of secreted glutamine played a large role to the labeling state.

### 3. Non-stationary $^{13}\text{C}$ MFA of CHO cells in batch culture

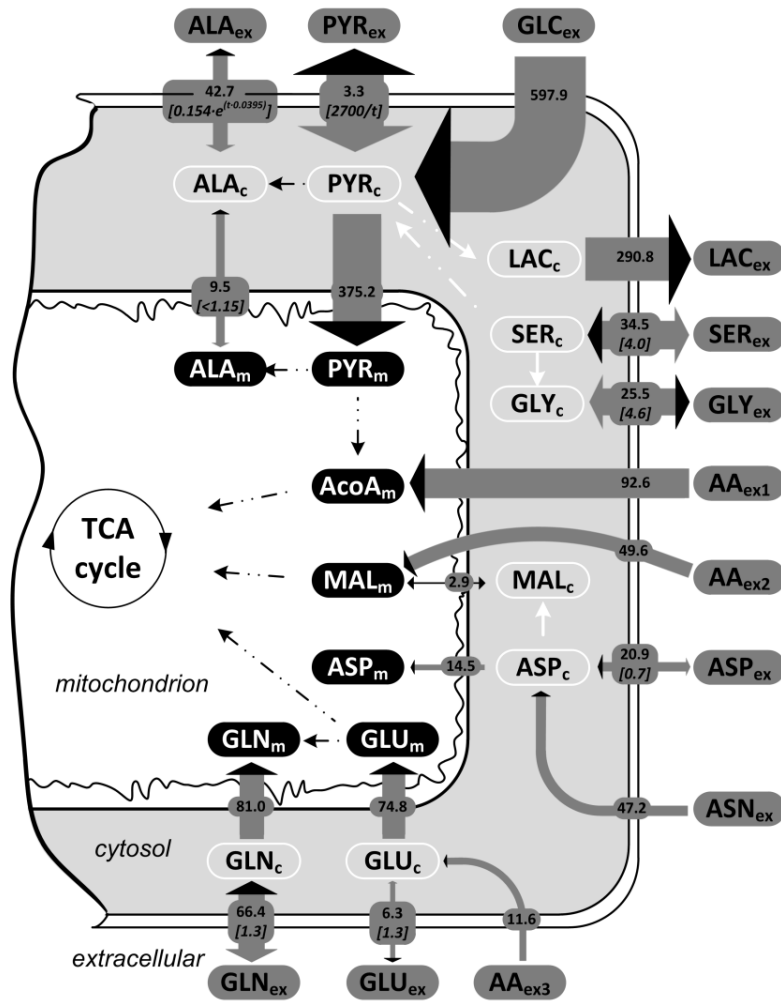


**Figure 3.3** Compartmentation of the CHO-K1 metabolism and the fate of extracellular metabolites. Net fluxes are indicated on the gray arrows in units of mmol product / (L cell × h), and reversibility parameter defined as *reverse flux/net flux* is shown in the square brackets (n.d. = not determined). The thickness of the gray arrows is proportional to the forward flux (=reverse flux + net flux), and shown qualitatively for the fluxes with variable reversibility. Net flux direction is shown by the black arrow heads. Amino acids catabolism is represented as the sum of the differences between amino acid uptake flux and flux required for protein production, reported to the metabolite derived from catabolism. Subscripts meaning: ex – extracellular; c – cytosolic; m – mitochondrial. Abbreviations: AA<sub>ex1</sub> – isoleucine, leucine, lysine, phenylalanine, tyrosine catabolized to acetyl-CoA; AA<sub>ex2</sub> – isoleucine, methionine, phenylalanine, threonine, tyrosine, valine catabolized to fumarate and succinate; AA<sub>ex3</sub> – arginine, histidine, proline catabolized to glutamate; AcoA – acetyl CoA; ALA – alanine; ASN – asparagine; ASP – aspartate; CIT/ICI – citrate/isocitrate; GLN – glutamine; GLU – glutamate; GLY – glycine; MAL – malate; PYR – pyruvate; SER – serine.

#### 3.3.3. Isotopomer fitting

Both the non-compartmented and compartmented isotopomer network models (Fig. 3.1) were fitted to the experimental mass distributions with the goal of determining unknown fluxes and reversibilities. The 7 sampling time points of the 8 metabolites produced a total number of 252 experimental *MIDs*.

Convergence to the optimal solution is difficult in isotopomer models (Srouf et al., 2011) and the parameter space of the objective function is marked by a multitude of local minima (Chen et al., 2007), making gradient-based algorithms unreliable. Consequently, a global optimization scheme was applied that had the following steps: (1) generate an initial random population of  $(40 \times p)$  parameter sets that satisfy constraints using a simulated annealing-based algorithm, (2) submit the population to a 50-generations genetic algorithm optimization, and (3) refine the best solution using a trust region reflective algorithm. Convergence to the optimal solution was verified by repeating the optimization scheme. One simulation took about 3 s, and the optimization procedure required about 40 h on a 2.3 GHz QuadCore CPU. All the numerical integration and optimization algorithms are found in Matlab toolboxes.

There were initial difficulties in fitting pyruvate and alanine labeling dynamics. As it was shown that reversibility greatly affects labeling dynamics (Noh and Wiechert, 2011), it was assumed that the transport reversibility parameter changes in time, even if the net fluxes remain constant. The decrease with time of pyruvate transport reversibility was mechanistically expressed using a hyperbolic function  $rev_{PYR} = \frac{rev_{PYR}^0}{time + \varepsilon}$ , where pyruvate transport reversibility  $rev_{PYR}$  decreases from a starting value  $rev_{PYR}^0$ . To avoid division by zero, a negligible correction factor  $\varepsilon$  was introduced. Alanine transport into the cell intensifies as extracellular alanine becomes exponentially more abundant. Transport reversibility was expressed in this case as  $rev_{ALA} = \alpha \cdot \exp(\beta \cdot time)$ , where  $\alpha$  and  $\beta$  are parameters to be determined.

### 3. Non-stationary $^{13}\text{C}$ MFA of CHO cells in batch culture

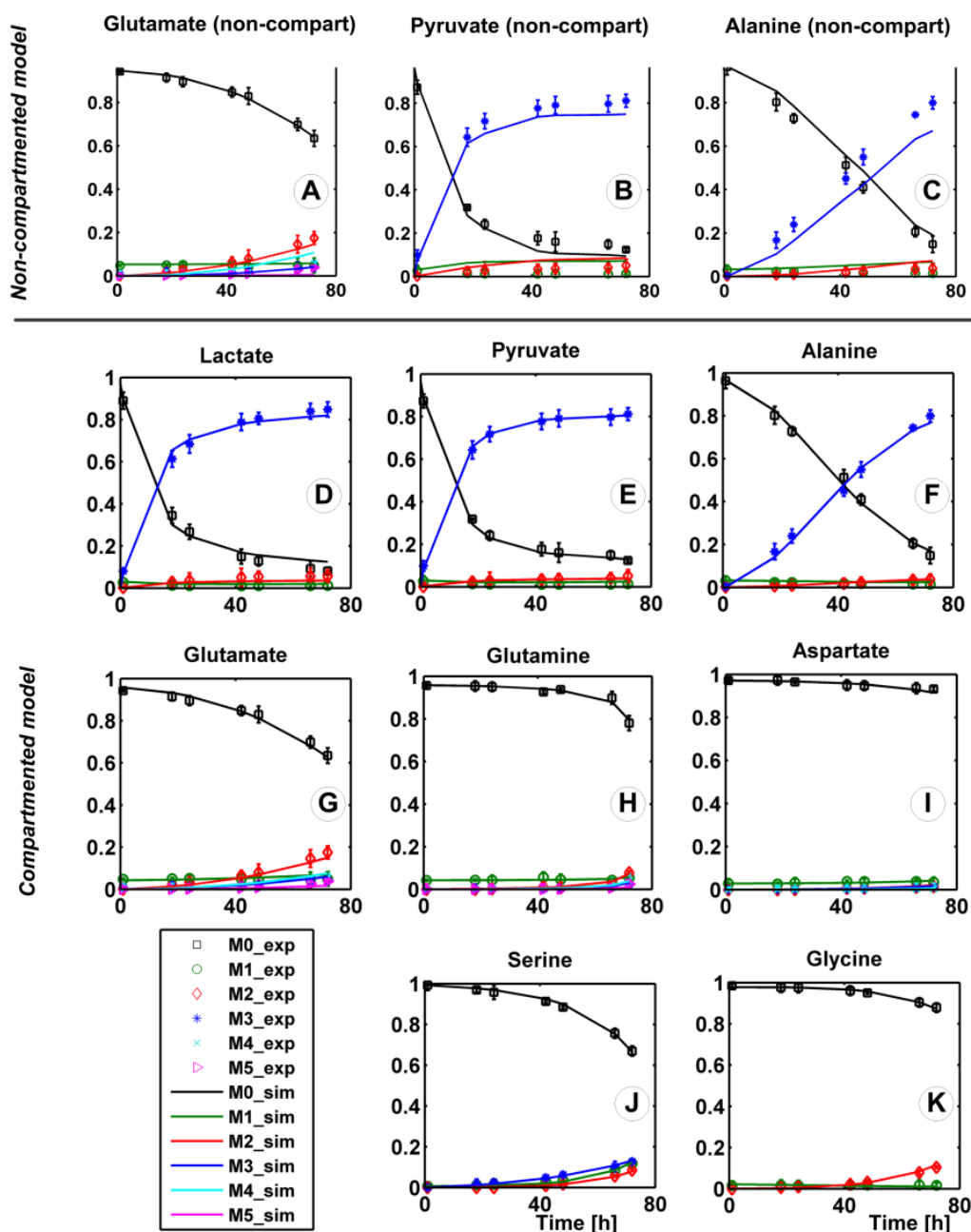


**Figure 3.4 Non-stationary  $^{13}\text{C}$  labeling experiment.** Experimental mass isotopomer distributions (symbols) with their standard deviations vs. simulated (line) mass isotopomer distributions of labeled extracellular metabolites. The plots A-C represent results from using the non-compartmented metabolic network specified in Figure 3.1 A. For the other eight plots (D-K), the compartmented model from Figure 3.1 B was simulated.

### 3. Non-stationary $^{13}\text{C}$ MFA of CHO cells in batch culture

---

The 24 free parameters of the non-compartmented model (Fig. 3.1 A) consisted of 5 fluxes, 18 reversibilities and the  $\text{CO}_2$  pool. At convergence, the model failed to fit the data with the minimized  $SSQD$  of 1572, larger than  $\chi^2(0.95, 252-24) = 264.2$ . Pyruvate, lactate, alanine and glutamate labeling were fit poorly even when transport reversibility was variable (Fig. 3.4). In consequence, the non-compartmented model was rejected. The low labeling content of pyruvate, alanine and lactate simulated with the non-compartmented model is explained by the lumping of the cytosolic and mitochondrial pyruvate pools. More than 30% of the carbon feeding the TCA cycle is not labeled, therefore it would be expected that the cataplerotic reactions catalyzed by phosphoenolpyruvate carboxykinase and malic enzyme will produce a large quantity of unlabeled pyruvate, which contradicts the experimental observations.

The compartmented model, consisting of 11 free fluxes and other 27 free parameters (reversibilities) depicted in Fig. 3.1 B, fitted the data successfully with the minimized  $SSQD = 249.0$  slightly smaller than  $\chi^2(0.95, 252-38) = 249.13$ . The poorer fit of the 66 and 72 h time points for lactate and 72 h for alanine can be explained by the metabolic shift towards the end of the growth phase. Exponential growth will add a larger contribution in the objective function to the labeling towards the end of the exponential phase compared to the beginning of the experiment because the rates of  $^{13}\text{C}$  accumulation in the extracellular media are much larger at high cell densities. This is best evidenced in Fig. 3.4 where glutamine, aspartate, serine and glycine do not become noticeably labeled until 40 h after the introduction of the labeled substrate.

#### 3.3.4. Metabolic fluxes in the CHO-K1 cell line

Glucose was converted to phosphoglycerate mostly by bypassing glycolysis (Fig. 3.5) through the pentose phosphate pathway (PPP). The estimated PPP flux was 80% of the total molar glucose input flux, a high activity contrasting with results obtained by Ahn and Antoniewicz for adherently growing CHO cells (Ahn and Antoniewicz, 2011) but observed for hybridoma (Bonarius et al., 1996) and cancer cells (Bensaad et al., 2006). A wide range of PPP activities, between 0-160 % of the glucose input flux, was determined for a highly-productive CHO line in fed-batch cultivation conditions at different growth

### 3. Non-stationary <sup>13</sup>CMFA of CHO cells in batch culture

---

phases (Templeton et al., 2013). The large quantities of cytosolic NADPH produced through PPP drive fatty acids synthesis and mitigate oxidative stress by reducing reactive oxygen species (Anastasiou et al., 2011; Schafer et al., 2009; Sengupta et al., 2010; Tuttle et al., 2000; Vizan et al., 2009), as it has also been proposed by Templeton et al. (2013). Overflow to lactate comprised 39% of the pyruvate produced from glycolysis. From the rest of the cytosolic pyruvate,  $42.7 \text{ mmol} \times (\text{L cell})^{-1} \times \text{h}^{-1}$  were converted to alanine, but most of it was transported into the mitochondria and converted to AcoA. The channeling flux from phosphoenolpyruvate to lactate was  $122.7 \text{ mmol} \times (\text{L cell})^{-1} \times \text{h}^{-1}$ , accounting for 42% of the total lactate being produced. The low reversibility of exchange between the two cytosolic pyruvate pools (Fig. 3.5) means that the channeled cytosolic pyruvate is practically separated from the cytosolic bulk pool. However, lactate was produced from both cytosolic pyruvate pools, indicating that glycolytic channeling is not the only lactate source in the cell. One possible explanation is that multi-enzyme complexes associated to membrane transporters, as characterized by Campanella et al. (2005), create a micro-compartmented environment in the cytosol. Glycolytic enzymes are partly associated and partly soluble, resulting in a mixed response in the lactate labeling.

The carbon flux in the TCA cycle originated mainly from acetyl-CoA derived from glycolytic pyruvate transported into the mitochondria (Fig. 3.5), with significant contributions from glutamine and essential amino acids catabolism. Such high activity of the TCA cycle and high connectivity with the glycolysis is in contrast with some previous reports of lower activity during exponential growth phase (Ahn and Antoniewicz, 2011; Quek et al., 2009a; Zamorano et al., 2010) but similar to (Goudar et al., 2010; Sengupta et al., 2010; Sheikholeslami et al., 2013). The differences can be assigned mainly to the use of different cell lines and cultivation conditions like media composition, aeration mode, pH control and culture type e.g. suspension or immobilized, batch or fed-batch. The lower lactate/glucose molar ratio of 0.78 reported herein means more pyruvate is available for use in the TCA cycle, thus making for a more efficient metabolism. Gluconeogenesis was active through phosphoenolpyruvate carboxykinase with 10% of the total flux entering the phosphoenolpyruvate pool, a fact explained qualitatively by the presence of M+2 lactate



### 3. Non-stationary $^{13}\text{C}$ MFA of CHO cells in batch culture

---

and pyruvate. In the absence of gluconeogenesis, only the M and M+3 mass isotopomers of these metabolites would be present after feeding fully labeled glucose. Malic enzyme activity was negligible in the cytosol, and this is in agreement with compartmented enzyme activity observed by Wahrheit et al. (2014b). This observation reaffirms that PPP was the main source of cytosolic NADPH. Mitochondrial malic enzyme was highly active, producing one third of the total mitochondrial pyruvate. However, a part of the mitochondrial pyruvate was recycled back into the TCA cycle via pyruvate carboxylase. Mitochondrial malate net transport flux was small and reversible. This explained the lack of M+1 labeling in lactate, alanine and pyruvate that would have been otherwise linked to the M+2 malate isotopomers that are expected to be obtained in the TCA cycle. As a consequence, the M+2 labeling in these metabolites relies on mitochondrial transport of citrate and on the activity of citrate lyase producing cytosolic acetyl-CoA and oxaloacetate, which is then further converted to phosphoenolpyruvate.

About one third of the total serine was produced from phosphoglycerate, using cytosolic glutamate for transamination. Serine was exchanged with the media, thus explaining extracellular labeling of serine. Half of the serine was not used for protein synthesis but was reversibly converted to glycine and C<sub>1</sub> units to sustain the high anabolic activity. Glycine was then secreted. The remaining excess of serine was converted to pyruvate. Alanine was synthesized mainly from cytosolic pyruvate in a highly reversible reaction. Connectivity between cytosolic and mitochondrial alanine pools and the direction of the mitochondrial alanine aminotransferase flux could not be determined. However, the transport flux of alanine to/from mitochondria was confined between -11.6 to 13.6 mmol  $\times$  L cell<sup>-1</sup>  $\times$  h<sup>-1</sup>, i.e.  $\pm 25\%$  of the alanine production flux. The flux of 68.1 mmol  $\times$  L cell<sup>-1</sup>  $\times$  h<sup>-1</sup> from asparagine and aspartate uptake to oxaloacetate was split through aspartate aminotransferases between cytosolic and mitochondrial oxaloacetate with a 3/1 ratio, but no other details could be inferred due to the low labeling level in extracellular aspartate.



Isocitrate dehydrogenase (IDH) activity in the cytosol could not be reliably determined. This is due to lack of information in directly connected metabolites citrate and  $\alpha$ -ketoglutarate, but also because it affects the labeling pattern in the same way as the mitochondrial isozyme. As a result, the fluxes in the mitochondrial/cytosolic citrate and  $\alpha$ -ketoglutarate loop could not be determined. Nevertheless, a net activity towards producing the high glutamate flux needed for cytosolic transamination reactions implies that  $\alpha$ -ketoglutarate is either produced in the cytosol by IDH or transported from the mitochondria into the cytosol. Mitochondrial glutamate pool was fed by transporting cytosolic glutamate into the mitochondria and by glutamine through glutaminase activity at comparable rates. In the mitochondria, glutamate was then converted to  $\alpha$ -ketoglutarate and fed into the TCA cycle through mitochondrial GDH. In the cytosol, the glutamate produced from  $\alpha$ -ketoglutarate in the various transaminase reactions was partially converted to glutamine, which was then exchanged with the media, leading to the presence of labeled glutamine in the media. In conclusion, simultaneous degradation and synthesis pathways for glutamine involve glutamine uptake, transport into the mitochondria and conversion to glutamate, glutamate dehydrogenation to  $\alpha$ -ketoglutarate,  $\alpha$ -ketoglutarate transport to the cytosol or citrate transport and citrate conversion to  $\alpha$ -ketoglutarate through cytosolic IDH activity, conversion of  $\alpha$ -ketoglutarate to cytosolic glutamate, and cytosolic glutamine synthesis.

#### 3.3.5. Transport reversibility

A very important part in modeling the extracellular labeling was considering the reversible exchange between the intracellular pools and the extracellular media, a phenomenon which affects the dynamics of the labeling process. All sampled extracellular non-essential amino acids except asparagine and proline, either produced or taken up, were exchanged with the culture media (Fig. 3.3). Even if the production flux of alanine remained constant throughout the cultivation, the fitting remained poor for alanine when considering a constant reversibility factor. There, the reversibility was estimated to increase with time. The function  $rev_{ALA} = 0.154 \cdot \exp(0.0359 \cdot \text{time})$  was used to compute the

### 3. Non-stationary <sup>13</sup>CMFA of CHO cells in batch culture

---

forward and reverse exchange fluxes (eq. 3.5), with both parameters being determined with a narrow confidence interval (Supplem. Table S3.1). Time is computed in hours. This successfully explained the dynamics of alanine labeling. The time constant of the reversibility function is a value close to the specific growth rate, pointing to the fact that alanine re-uptake is correlated to the extracellular concentration. Serine secretion flux, as computed with eq. 5, was up to 35 times higher than the net uptake flux. Glycine re-uptake flux was 4.6 times the net production flux. Aspartate, glutamate and glutamine exchange fluxes were in the same order with the net uptake/production flux, as expressed by the estimated reversibility parameter values of about 1. The confidence intervals for the transport reversibility parameters are larger than those for fluxes because at high reversibilities the labeling becomes less sensitive to small changes in reversibility.

Pyruvate transport reversibility is described by the function  $rev_{PYR} = \frac{2700}{time + 0.01}$ , where *time* is specified in hours. The hyperbolic function implies that at the beginning of the cultivation, the intense exchange of pyruvate (Garcia et al., 1994) eliminates the difference between the labeling of the intracellular and extracellular pools. Pyruvate re-uptake decreases because pyruvate concentration changes slightly (Fig. 3.1) while lactate accumulates in the media to reach high concentrations and competes with pyruvate for the monocarboxylate transporters (Halestrap and Price, 1999; Morris and Felmlee, 2008). Lactate transport reversibility parameter could not be estimated because at the beginning of the cultivation there is no lactate present in the media that could dilute the intracellular pool and affect the labeling dynamics.

#### 3.3.6. Confidence intervals calculation and sensitivity analysis

Most of the fluxes depicted in Fig. 3.5 were determined with narrow confidence intervals. Interval boundaries are not symmetrical due to the non-linear characteristics of the mathematical model. Determining both the flux and exchange in alternative pathways was not possible in the case of high reversibility e.g. for determining the compartmentation of alanine metabolism involving reversible transaminase reactions.

### 3. Non-stationary $^{13}\text{C}$ MFA of CHO cells in batch culture

---

The sensitivity coefficients provided quantitative information about the impact of the measured fluxes on the estimated flux values (Fig. 3.6 A). Sensitivity analysis also evidenced correlations between external fluxes and network pathways when  $[\text{U-}^{13}\text{C}_6]$  glucose is used. In this case, the *MIDs* of metabolites will depend on the interplay between the multitude of non-labeled carbon sources and the glucose feed, as opposed to organisms that use only one carbon source (Sellick et al., 2011a). The determination of anaplerotic fluxes relied on the supply of four carbon metabolites from amino acid catabolism.

Changes in the glutamine uptake flux (Fig. 3.6 A) affected most fluxes to a large extent. Nevertheless, the high influence was mainly computational, as any increase of the flux caused depletion of glutamine at the end of the cultivation and dramatically different labeling patterns. Glucose uptake flux affected the estimation of the PPP and TCA cycle fluxes. Errors in measuring glucose concentration over time will propagate in the values of these fluxes, as the glucose uptake flux determines the fraction of  $^{13}\text{C}$  entering the cell. Glucose-6-phosphate loses one  $^{13}\text{C}$  through oxPPP, therefore estimating the split between glycolysis and oxPPP depends highly on determining correctly all carbon sources. This explains the high sensitivity of the glycolysis/oxPPP split to all extracellular fluxes. Unexpected correlations were observed for the glycine production flux that influenced most anaplerotic and aminotransferase fluxes. Glycine is produced at the expense of serine, which is in turn produced from 3-phosphoglycerate, also converting glutamate to  $\alpha$ -ketoglutarate during transamination, and simultaneously converted to pyruvate, thus affecting the availability of both cytosolic pyruvate and glutamate.

Local sensitivity of the *SSQD* to free parameters computed as the normalized mean deviation of the objective function to variations in the estimated parameters shown in Fig. 3.6 B evidenced the determinable parameters and the redundant parameters. The notoriously difficult to determine anaplerotic fluxes of the phosphoenolpyruvate carboxykinase enzyme and mitochondrial malic enzyme induced a noticeable sensitivity in the objective function.

### 3. Non-stationary $^{13}\text{C}$ MFA of CHO cells in batch culture

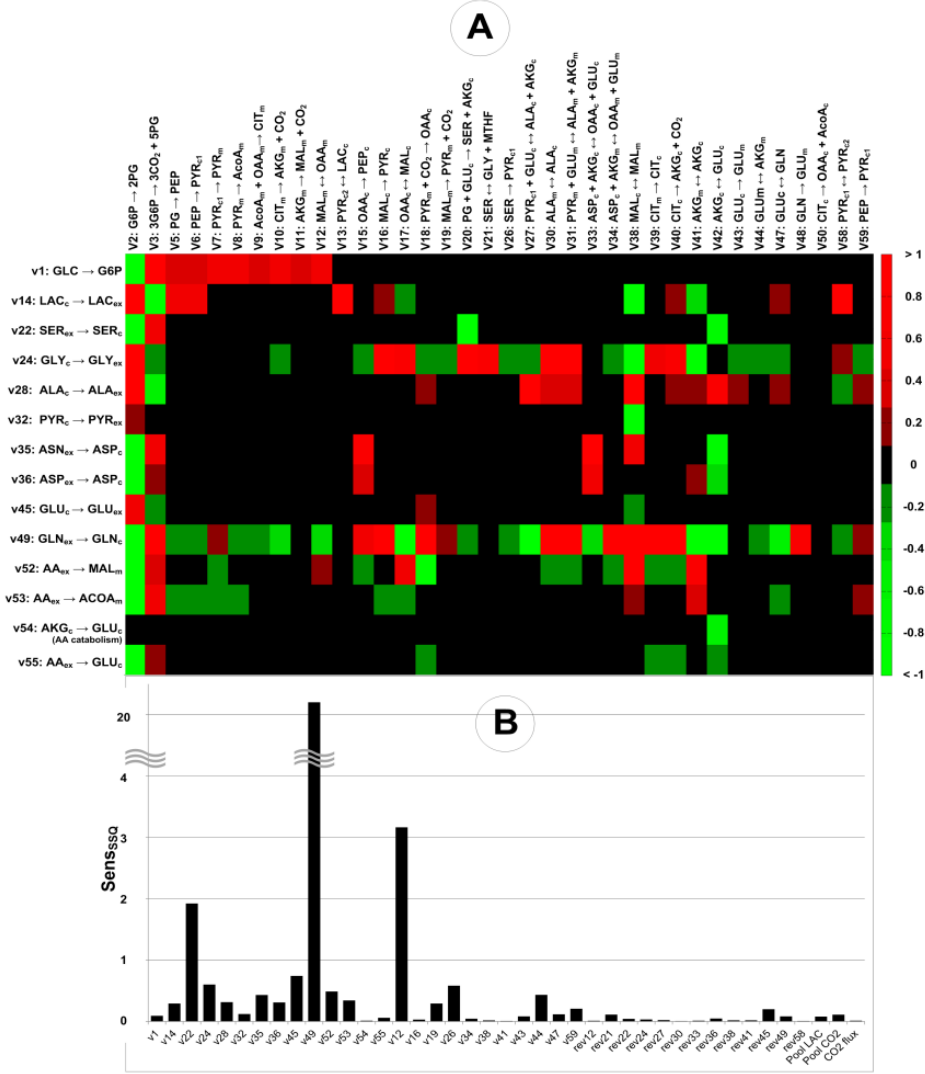


**Figure 3.6. Sensitivity analysis to measured fluxes and to parameters.** (A) Sensitivity of free fluxes to extracellular fluxes, computed for the compartmented network of CHO-K1 with  $[\text{U-}^{13}\text{C}_6]$  glucose as

substrate,  $\text{Sens}_{v_m}^{v_e} = \left( \frac{dv_e}{v_e^*} \right) \cdot \left( \frac{v_m^*}{dv_m} \right)$ , where  $\text{Sens}_{v_m}^{v_e}$  is the sensitivity of the estimated flux  $v_e$ , re-estimated

using values of the measured flux  $v_m$  at the border of the confidence interval.  $v_m^*$  - average measured flux.

(B) Normalized sensitivity of the objective function ( $\text{SensSSQ}$ ) to the free parameters (fluxes and rev=reversibilities) computed as mean value of SSQ resulted from perturbing each parameter 100 times:

$\text{SensSSQ} = \left( \frac{d\text{SSQ}}{\text{SSQ}^*} \right) \cdot \left( \frac{p_i^*}{dp_i} \right)$ , where  $\text{SSQ}^*$  is the optimized value of the objective function (eq. 3.6), and  $p_i^*$  is

the estimated value of parameter  $i$ . The rates  $v_i$  correspond to the rates in the network from Supplem. Table S3.1. Abbreviations: subscripts: c: cytosolic, ex: extracellular, m: mitochondrial; ALA: alanine; AcoA: acetyl coenzyme A; AKG:  $\alpha$ -ketoglutarate; ASN: asparagine; ASP: aspartate; CIT: citrate; G6P: glucose 6-phosphate; GLC: glucose; GLN: glutamine; GLU: glutamate; GLY: glycine; LAC: lactate; MAL: malate; OAA: oxaloacetate; PEP: phosphoenolpyruvate; PG: phosphoglycerate; PYR: pyruvate; SER: serine.

The increased network connectivity, obtained by coupling alanine or aspartate deamination to conversion of  $\alpha$ -ketoglutarate to glutamate, contributed to this fact. Oppositely, most intracellular reversibilities did not influence the parameter estimation results. This can be easily inferred from the fact that while reaction reversibility affects the dynamics of intracellular isotopomers, it does not mirror in the extracellular labeling apart from the reactions altering the carbon backbone. Also, in the situation where high values of the reversibilities resulted from estimation, local perturbations around these values will not influence the *MIDs*.

#### 3.4. Conclusions

In the present chapter it was shown that intracellular fluxes of the CHO-K1 cell line central carbon metabolism in batch culture can be determined for a complex network by making use solely of the mass isotopomers of extracellular metabolites resulted from feeding  $[\text{U-}^{13}\text{C}_6]$  glucose as the only labeled substrate. To this end, non-stationary  $^{13}\text{C}$  metabolic flux analysis proved an effective tool for unraveling important details of the CHO-K1 metabolism. Pathway compartmentation, e.g. of anaplerotic reactions and amino acid metabolism had to be considered for describing the mass isotopomer distribution. It can be reckoned that this fact plays an essential role in controlling the availability of NADH and NADPH in mitochondria and cytosol, but also in facilitating amino acid catabolism. A cancer-like high activity of the pentose phosphate pathway produced reducing NADPH partly to counteract the oxidative stress generated by the mitochondrial respiration and partly to fuel fatty acids biosynthesis. Cultivation conditions and different cells lines generate a wide range of metabolic fluxes, when considering previous studies concerned with the metabolism of CHO cells. Cytosolic pyruvate transport is reversible thousand-fold compared to the net production flux, indicating that although it is not a carbon source, pyruvate creates an extracellular environment (O'Donnell-Tormey et al., 1987) most probably by functioning as a balancing system for cytosolic NADH (Bucher et al., 1972). Considering that metabolite exchange with the media played a very important role in determining the intracellular fluxes, it is expected that future  $^{13}\text{C}$ MFA studies of

### 3. Non-stationary <sup>13</sup>CMFA of CHO cells in batch culture

---

mammalian cells metabolism will include this essential aspect. Compartmentation controls the simultaneous degradation and production of non-essential amino acids. Most likely, the CHO-K1 cells maintain the exponential growth phase under batch conditions by using a well-connected multi-pool system involving metabolite and reaction compartmentation, exchange with the media and inter-compartment exchange for controlling the metabolite and cofactor pools. Further studies on localizing enzyme and transporter activity together with sampling intra-compartmental concentrations would bring valuable contributions at elucidating the function of such cycling pathways. Accurate enzyme kinetics and thermodynamics (Henry et al., 2007) in mammalian cells would complement the modeling using Inst-<sup>13</sup>CMFA with information about reaction direction and reversibility. The knowledge gained through Inst-<sup>13</sup>CMFA depicts the CHO-K1 central metabolism as a robust, highly interconnected network that ensures fast growth and mitigates stress generated by reactive oxygen species and the accumulation of lactate in the culture media.

Due to the economic importance of CHO cells, efficient production processes leading to high product quality with minimum effort are of utmost importance. In-depth knowledge about CHO metabolism is expected to provide valuable assistance in identifying targets for metabolic engineering and guiding the design of feeding strategies leading to the development of efficient production processes. Overexpression, silencing or knockout of the specific glycolytic enzymes that associate with channeling glucose to lactate could either be used to study the control of the Warburg effect in cancer cells or for improving glucose utilization. However, as it was shown that compartmentation is important in managing metabolites, mitochondrial transporters are likely to constitute important targets for genetic modifications. Inter-compartmental transport of metabolites is a key factor in connecting the cytosol and the mitochondria energetically and it can be reckoned that modifying the genetic expression of transporters will have significant, perhaps surprising effects on the overall metabolism.

The proposed methodology of sampling the *MID* only in extracellular metabolites for determining intracellular fluxes using Inst-<sup>13</sup>CMFA has the potential of broader



### 3. Non-stationary $^{13}\text{C}$ MFA of CHO cells in batch culture

---

applications, as it circumvents the need to extract intracellular metabolites and it is non-invasive to cells. The information contained in the extracellular mass isotopomers has a higher resolution compared to the summed fractional labeling used previously. This is sufficient for resolving a complex metabolic network when more metabolites are produced and/or exchanged with the culture media. Therefore, future applications in the study of mammalian metabolism at physiological and pathological conditions, especially related to compartmentation, as reviewed in (Gutierrez-Aguilar and Baines, 2013), and oxidative stress, e.g. in cancer, neurodegenerative disorders and ageing are to be expected. Knowledge about the metabolism at the compartment level will be essential for identifying therapeutic targets and understanding disease mechanisms. Similarly, the method could be applied to other enzymatic systems or prokaryotic cells where extended metabolite exchange with the media occurs.

#### Supplementary data 3

**Supplem. Fig. S3.1. Complete culture profile of CHO-K1 cells during the exponential growth phase.** The lines represent the fitted concentration profiles to the experimental values (dots) and in the boxes are the determined extracellular rates [mmol/(L cell  $\times$  h)] together with the 95% confidence intervals. Glutamine uptake was determined by considering a spontaneous degradation rate of  $0.0033\text{ h}^{-1}$ . The exponential growth phase is shown in the last plot.

**Supplem. Table S3. 1. List of reactions in the non-compartmented central carbon metabolism of CHO-K1 (Table 1). List of metabolic reactions, fluxes and reversibilities in the compartmented central carbon metabolism of CHO-K1 cells (Table 2).** Carbon transfer rules are provided in the parentheses after each reaction. Reversible reactions are designated by double arrows. Reversibility is computed as the ratio between the reverse flux and the net flux.

**Supplem. Table S3.2. Experimental and simulated mass isotopomer distributions of extracellular metabolites and used standard deviations**

## Chapter 4

### 4. High resolution $^{13}\text{C}$ metabolic flux analysis in CHO cells<sup>\*2</sup>

#### Abstract

The metabolism of mammalian cells is characterized by compartmentation, metabolite exchange and channeling. Mass isotopomer distributions were determined from two parallel labeling experiments using  $[\text{U-}^{13}\text{C}_6]\text{glucose}$  and  $[\text{U-}^{13}\text{C}_5]\text{glutamine}$  as substrates in a CHO-K1 suspension culture. Using extra- and intracellular labeling dynamics non-stationary  $^{13}\text{C}$  metabolic flux analysis (INST- $^{13}\text{C}$ MFPA) was applied to resolve the metabolic fluxes in a complex metabolic network that included mitochondrial transport, metabolite compartmentation and channeling. Fluxes, reversibilities and intracompartmental concentrations were determined within narrow confidence intervals. The metabolism was characterized by pentose phosphate pathway activity of 90% and lactate production of 75% of the glucose uptake, low TCA cycle, low cataplerotic fluxes, and simultaneous catabolism and production of non-essential amino acids. Mitochondrial glutamate was converted to  $\alpha$ -ketoglutarate by aminotransferases while glutamate dehydrogenase flux was negligible. Malate and glutamate were cycled via several transporters between cytosol and mitochondria. Cytosolic NADH was partially transported into the mitochondria using the malate-aspartate shuttle and partially regenerated by cytosolic lactate dehydrogenase. The labeling dynamics of lactate and pyruvate indicate various metabolite channeling effects in the cytosol and the mitochondria as well as the existence of a mitochondrial lactate pool that serves most likely as intramitochondrial redox buffer. INST- $^{13}\text{C}$ MFPA combined with targeted parallel labeling experiments allowed to unravel great details of mammalian metabolism. Using this strategy, a comprehensive description of metabolic compartmentation including detailed insights in the  $\text{C}_3$  and  $\text{C}_5$  metabolism of CHO suspension cells was possible for the first time.

<sup>\*2</sup>A part of this chapter was submitted as an article to Metabolic Engineering Journal (February 2015). All experimental work described herein was carried out by Judith Wahrheit.

### 4.1. Introduction

In the context of a fast-developing biopharmaceutical industry (Birch and Racher, 2006; Walsh, 2010) and a continuous need to understand disease mechanisms at the molecular level, in-depth knowledge of mammalian cell metabolism is crucial. This requires a systems biology approach that integrates “*omics*” information to determine the metabolic network structure and function by using adequate computational tools. The major current challenge in metabolic flux analysis (MFA) of mammalian cells is to untangle the details related to compartmentation (Wahrheit et al., 2011a). Dysfunctions in metabolite management between compartments in mammalian cells can lead to a multitude of diseases (Balaban, 2010; Calvo et al., 2006; Duchen, 2004; Nassir and Ibdah, 2014; Palmieri, 2008). In addition, metabolite channeling (Jandt et al., 2013; Malaisse et al., 2004; Zhang, 2011), association of enzymes (Campanella et al., 2005), and microcompartmentation (Holthuis and Ungermann, 2013) are forms in which the eukaryotic metabolism is controlled by the cellular microstructure, but are only little understood.

Metabolic flux analysis of mammalian cells can rely just on flux balancing (Altamirano et al., 2001b; Bonarius et al., 1996; Sidorenko et al., 2008) or use also  $^{13}\text{C}$ -labeling information to resolve more complex metabolic networks (Amaral et al., 2011; Bonarius et al., 2001; Goudar et al., 2010; Niklas et al., 2011b). Non-stationary  $^{13}\text{C}$  metabolic flux analysis (INST- $^{13}\text{C}$ MFA) allows a detailed characterization of metabolic network function (Noh et al., 2006; Noh and Wiechert, 2006). By using the dynamics of mass isotopomer distributions (MIDs) it is possible to obtain detailed information about metabolic fluxes, reversibility and intracompartmental concentrations (Noh et al., 2007; Noh and Wiechert, 2011; Schmidt et al., 1997). However, the experimental and computational costs of this method are substantially higher when compared to other MFA methods (Fig. 4.1). INST- $^{13}\text{C}$ MFA also allows the estimation of intracompartmental concentrations by using only the labeling dynamics of selected metabolites (Wiechert and Noh, 2005). As a tool for

#### 4. High resolution $^{13}\text{C}$ metabolic flux analysis in CHO cells

---

detailed metabolic flux analysis, INST- $^{13}\text{C}$ CMFA proved to achieve the best resolution in resolving fluxes for cultured B-cells (Murphy et al., 2013). In eukaryotic cells, it was applied to study the metabolism of *Pichia pastoris* (Jorda et al., 2014), of hepatic cells (Hofmann et al., 2008; Maier et al., 2008) and of neurons (Amaral et al., 2011). I previously applied INST- $^{13}\text{C}$ CMFA using the extracellular MIDs of metabolites from a reactor batch culture of CHO-K1 suspension cells where  $[\text{U-}^{13}\text{C}_6]$  glucose was used as labeled substrate to determine the fluxes in a compartmented metabolic network as well as metabolite exchange with the media (Nicolae et al., 2014).

CHO cells are the main production cell line for biopharmaceuticals (Kim et al., 2012) and considered as the “mammalian equivalent of *E. coli*” given their relevance as mammalian model system (Jayapal et al., 2007). Economic importance made CHO cells a target for various MFA studies (Ahn and Antoniewicz, 2011; Altamirano et al., 2001a; Altamirano et al., 2001b; Duarte et al., 2014; Goudar et al., 2010; Nicolae et al., 2014; Nolan and Lee, 2010; Provost et al., 2006; Sengupta et al., 2010; Sheikholeslami et al., 2013; Templeton et al., 2013; Wahrheit et al., 2014a). The most detailed MFA studies used parallel labeling experiments and steady-state labeling to characterize the growth and the non-growth phases in monolayer CHO-K1 cells (Ahn and Antoniewicz, 2011),  $[\text{1-}^{13}\text{C}]$  glucose for analyzing an inducible expression system engineered into a CHO cell line (Sheikholeslami et al., 2013) or to characterize the metabolic shifts during antibody production in highly-productive CHO cell line (Templeton et al., 2013). Nevertheless, all previous studies did not succeed in untangling the traffic between mitochondria and cytosol, as these models did not fully take into consideration mitochondrial transport and metabolite compartmentation.

In the present work the CHO-K1 metabolism was studied by applying two labeled substrates,  $[\text{U-}^{13}\text{C}_6]$  glucose and  $[\text{U-}^{13}\text{C}_5]$  glutamine, to a shake flask batch culture of CHO-K1 suspension cells. The dynamics of intra- and extracellular MIDs was used to estimate the intracellular fluxes, reversibilities and intracompartmental concentrations by applying INST- $^{13}\text{C}$ CMFA. Such method produces a high-resolution analysis of the mammalian cell

## 4. High resolution $^{13}\text{C}$ metabolic flux analysis in CHO cells

metabolism, as it allows a detailed exploration of metabolic compartmentation, mitochondrial transport and metabolic channeling. The metabolic network resolved herein offers a new perspective of the complex CHO-K1 cells metabolism in particular and more generally on the intricate system of metabolic fluxes in mammalian cells.

|                   |                                                                                                                                                                                                                         |                        |                                                                                                                                                                                   |                      |
|-------------------|-------------------------------------------------------------------------------------------------------------------------------------------------------------------------------------------------------------------------|------------------------|-----------------------------------------------------------------------------------------------------------------------------------------------------------------------------------|----------------------|
| EXPERIMENTAL DATA | <b>BIOMASS QUANTIFICATION</b> <ul style="list-style-type: none"> <li>• Proteins</li> <li>• DNA, RNA</li> <li>• Carbohydrates</li> <li>• Fatty acids</li> </ul>                                                          | Metabolic steady state | <b>FBA</b><br>(+ objective function) <ul style="list-style-type: none"> <li>• Net fluxes</li> </ul>                                                                               | FLUX ANALYSIS METHOD |
|                   | <b>EXTRACELLULAR UPTAKE/ PRODUCTION</b> <ul style="list-style-type: none"> <li>• Organic acids</li> <li>• Amino acids</li> <li>• <math>\text{CO}_2</math>, <math>\text{O}_2</math>, <math>\text{NH}_3</math></li> </ul> |                        |                                                                                                                                                                                   |                      |
|                   | <b><math>^{13}\text{C}</math> LABELING</b> <ul style="list-style-type: none"> <li>• Organic acids</li> <li>• Amino acids</li> <li>• Macromolecules</li> </ul>                                                           | Steady state           | <b>STEADY-STATE <math>^{13}\text{C}</math>-MFA</b> <ul style="list-style-type: none"> <li>• Net fluxes</li> <li>• Exchange fluxes</li> </ul>                                      |                      |
|                   | <ul style="list-style-type: none"> <li>• Extracellular</li> <li>• Intracellular</li> </ul>                                                                                                                              | Transient              | <b>INST <math>^{13}\text{C}</math>-MFA</b> <ul style="list-style-type: none"> <li>• Net fluxes</li> <li>• Exchange fluxes</li> <li>• Intracompartmental concentrations</li> </ul> |                      |
|                   | <b>INTRACELLULAR CONCENTRATIONS</b> <ul style="list-style-type: none"> <li>• Organic acids</li> <li>• Amino acids</li> </ul>                                                                                            | Metabolic steady state |                                                                                                                                                                                   |                      |

**Figure 4.1.** Experimental requirements for metabolic flux analysis tools.

## 4.2. Materials and methods

### 4.2.1. Cell culture

The CHO-K1 cell line was kindly provided by the Institute of Cell Culture Technology of the University Bielefeld (Germany). The cells were grown in suspension culture under serum and protein free conditions in the chemically defined, protein-free TC-42 medium (TeutoCell, Bielefeld, Germany), supplemented with 6 mM L-glutamine (Sigma-Aldrich, Steinheim, Germany) from a 240 mM stock solution in  $\text{dH}_2\text{O}$ . Cultivation of the CHO-K1 cells was performed in baffled shake flasks (250 ml, Corning, New York, USA) in a shaking incubator (Innova 4230, New Brunswick Scientific, Edison, NJ, USA) at 135 rpm (2 inches orbit),  $37^\circ\text{C}$  and 5%  $\text{CO}_2$ .

### 4.2.2. Experimental set-up of labeling experiments

The pre-culture was carried out in a 250 ml baffled shake flask (Corning Inc., Germany) at an initial cell density of  $4 \times 10^5$  cells/ml and a working volume of 100 ml. For the tracer experiments, cells were harvested during the exponential growth phase and resuspended in TC-42 medium with 100% [ $\text{U-}^{13}\text{C}_6$ ] glucose (99%, Euriso-Top, Saarbrücken, Germany) or with 100% [ $\text{U-}^{13}\text{C}_5$ ]glutamine (99%, Cambridge Isotope Laboratories, Andover, MA, USA). Four parallel tracer experiments were performed, two replicates with fully labeled glucose and two replicates with fully labeled glutamine, respectively. The main cultures were inoculated at a start cell density of  $2 \times 10^6$  cells/ml in a start volume of 120 ml medium.

Extracellular samples of 0.5 ml were taken from all four cultivations every 6 h for cell counting, determination of extracellular metabolite concentrations and extracellular labeling dynamics. 50  $\mu\text{l}$  of the sample was diluted with PBS and mixed with Trypan Blue for determination of cell density, cell viability and average cell diameter using an automated cell counter (Invitrogen, Darmstadt, Germany). The sample was centrifuged (10,000 rpm, 5 min, Biofuge pico, Heraeus Instruments, Hanau, Germany), 300  $\mu\text{l}$  of the supernatant transferred to fresh tubes and stored at  $-20^\circ\text{C}$  for further analysis. The rest of the sample was used for pH determination (MP 220 pH Meter, Mettler-Toledo, Giessen, Germany).

Intracellular samples of 5 ml were taken alternately from the two replicates after 2 min, 10 min, 20 min, 30 min, 1h, 2 h, 4 h, 6 h, 12 h, 18 h, 24 h, 30 h, 36 h, 42 h and 48 h. Quenching and extraction for determination of intracellular metabolites was performed as described in detail recently (Wahrheit and Heinzle, 2013; Wahrheit and Heinzle, 2014a). In brief, a sample of 5 ml cell suspension was quenched in 45 ml ice-cold 0.9% sodium chloride solution and centrifuged for 1 min at  $2000 \times g$  in a pre-cooled centrifuge at  $0^\circ\text{C}$ . The supernatant was carefully decanted followed immediately by suction of residual liquid using a vacuum pump without touching the cell pellet. Washing was performed by carefully rinsing the cell pellet with 50 ml ice-cold 0.9% sodium chloride solution without

## **4. High resolution $^{13}\text{C}$ metabolic flux analysis in CHO cells**

---

resuspending the cells. After repeating the centrifugation step and removal of the supernatant, the cell pellet was frozen in liquid nitrogen. Intracellular metabolites were extracted twice in 100% methanol and once in water by repeated freeze-thaw cycles as described previously (Wahrheit and Heinzle, 2014b) and similar to (Sellick et al., 2011b). Extracts were dried in a centrifugal evaporator.

### **4.2.3. Quantification of extracellular metabolites**

Quantification of glucose, organic acids and amino acids via HPLC was carried out as described previously by Strigun et al. (Strigun et al., 2011).

### **4.2.4. Analysis of isotopomer labelling patterns**

#### **4.2.4.1. Sample preparation**

For determination of extracellular labeling dynamics, 50  $\mu\text{l}$  of supernatants were lyophilized, resolved in 50  $\mu\text{l}$  N,N-dimethylformamide (0.1 % pyridine) and incubated at 80°C for 30 min. 50  $\mu\text{l}$  N-methyl-N-t-butyldimethylsilyl-trifluoro-acetamide (MBDSTFA) was added followed by another incubation at 80°C for 30 min for derivatization of extracellular metabolites into corresponding dimethyl-t-butylsilyl derivatives. Dried cell extracts were resolved in 50  $\mu\text{l}$  pyridine containing 20 mg/ml methoxylamine and 50  $\mu\text{l}$  MSTFA (Macherey-Nagel, Düren, Deutschland) and incubated at 80°C for 30 min for derivatization of intracellular metabolites into corresponding methoxyamine-trimethylsilyl derivatives. Derivatized samples were centrifuged at  $13000 \times g$  for 5 min at 4 °C and the supernatants transferred into fresh glass vials with micro inlets.

#### **4.2.4.2. GC-MS measurements**

Extra- and intracellular  $^{13}\text{C}$ -labeling dynamics were analyzed by gas chromatography mass spectrometry (GC-MS). The GC-MS measurements were carried out on a GC (HP 6890, Hewlett Packard, Palo Alto, CA, USA) equipped with an HP5MS capillary column (5% phenyl-methyl-siloxane diphenylpolysiloxane, 30 m  $\times$  0.25 mm  $\times$  0.25  $\mu\text{m}$ , Agilent



#### 4. High resolution <sup>13</sup>C metabolic flux analysis in CHO cells

---

Technologies, Waldbronn, Germany), electron impact ionization at 70 eV, and a quadrupole detector (Agilent Technologies). The injection volume was 1 µl (7683B Autosampler, Agilent, Waldbronn, Germany; PTV-Injektor, Gerstel, Mühlheim a. d. Ruhr, Germany).

Helium was used as carrier gas at a flow rate of 1.1 ml/min for analysis of extracellular metabolites or 0.7 ml/min for analysis of intracellular metabolites. The following temperature gradient was applied for analysis of extracellular metabolites: 135°C for 7 min, 10°C/min up to 162°C, 7°C/min up to 170°C, 10°C/min up to 325°C, 325°C for 2.5 min; inlet temperature: 140°C and heating with 720°C/min up to 320°C; interface temperature 320°C; quadrupole temperature 150°C. The temperature gradient for analysis of intracellular metabolites was as follows: 70°C for 1 min, 1°C/min up to 75°C, 5°C/min up to 315°C, 25°C/min up to 340°C, 340°C for 5 min; inlet temperature: 70°C and heating with 360°C/min up to 360°C; interface temperature 320°C; quadrupole temperature 280°C.

##### 4.2.4.3. Data analysis

After identification of metabolites in the scan mode using the NIST data bank, quantification of labeling enrichment was done in SIM (selected ion monitoring) mode in at least two technical replicates. Unique fragments (m/z) containing the whole carbon backbone were chosen for secreted extracellular metabolites and selected intracellular metabolites of the central metabolism. Following fragments of extracellular metabolites (MBDSTFA derivatization) were analyzed: lactate 261, alanine 260, glycine 246, serine 390, aspartate 418, glutamate 432, glutamine 431. Identified fragments in cell extracts (MSTFA derivatization) were as follows: pyruvate 174, lactate 219, alanine 218, fumarate 245, malate 335, citrate 465, α-ketoglutarate 304, glycine 276, serine 278, aspartate 334, glutamate 348. Mass isotopomer distributions were corrected for naturally occurring isotopes using the method of Yang et al. (Yang et al., 2009).

##### 4.2.5. Dynamic metabolic flux analysis

The continuous time course of the metabolic fluxes was computed similar to Niklas et al. (2011) following the steps: (i) interpolation of the extracellular concentrations of

#### 4. High resolution $^{13}\text{C}$ metabolic flux analysis in CHO cells

---

metabolites and the cell density with a continuously derivable function, (2) computing the extracellular rates, and (3) computing intracellular fluxes based on a stoichiometric model. Cell density was interpolated using an exponential growth model. Extracellular concentrations of metabolites were interpolated using SLM (Shape Language Modeling), a user-developed fitting tool that uses customized splines (MATLAB 2012b, The Mathworks, Natick, MA, USA). To avoid overfitting and biological nonsense, all fitted values were constrained to positive values, not more than three splines per curve were used and, except where observed to be otherwise e.g. visual observation of metabolite production followed by uptake or vice versa, all fitting curves were constrained to be monotonous.

Water evaporation was taken into account by correcting the concentration values prior to interpolation using the experimentally determined evaporation rate. Both the evaporation rate and glutamine degradation kinetics were determined experimentally in a cell-free setup identical to the one employed during the cultivation. Extracellular fluxes were calculated in units of  $\text{mmol} \times (\text{L cell})^{-1} \times \text{h}^{-1}$  using the numerically differentiated concentration slopes  $\frac{dC_i}{dt}$ :

$$v_{u,i} = -\frac{dC_i}{dt} \cdot \frac{1}{X} \cdot \frac{1}{V_{\text{cell}}} \quad (4.1)$$

and by considering the spontaneous degradation of glutamine:

$$v_{u, \text{GLN}} = -\frac{dC_{\text{GLN}}/dt + kd_{\text{GLN}} \cdot C_{\text{GLN}}}{X \cdot V_{\text{cell}}} \quad (4.2)$$

where  $v_{u,i}$  is the uptake rate of metabolite  $i$ ,  $C_i$  is the fitted extracellular concentration,  $kd_{\text{GLN}}$  is the first order degradation constant of glutamine,  $X$  is the fitted cell density [ $\text{cells} \times \text{L}^{-1}$ ] and  $V_{\text{cell}}$  is the volume of one cell [L]. Biomass fluxes were calculated using the time-dependent growth rate:

#### 4. High resolution $^{13}\text{C}$ metabolic flux analysis in CHO cells

---

$$v_{bio,i} = Y_{i/X} \cdot \frac{dX}{dt} \cdot \frac{1}{X} \cdot \frac{1}{V_{cell}} \quad (4.3)$$

where  $v_{bio,i}$  is the biomass rate for metabolite  $i$  and  $Y_{i/X}$  is the biomass yield coefficient.

All biomass fluxes were computed considering the biomass composition listed in Suppl. Table S1.1 and Suppl. Table S1.2.

The stoichiometric model of the CHO-K1 metabolism was built based on pathway data presented by (Ahn and Antoniewicz, 2012) and adapted to accommodate experimental observations (Fig. 4.2). It comprises the main pathways in the central carbon metabolism: biomass production using proteins, fatty acids and carbohydrates; glycolysis, pentose phosphate pathway (PPP), tricarboxylic acid (TCA) cycle, and amino acids syntheses; and catabolism (Suppl. Table S4.1). Aminotransferase reactions were always coupled with the conversion of  $\alpha$ -ketoglutarate to glutamate. The stoichiometric model was simplified in the following way: compartmentation was neglected, anaplerotic reactions were lumped into one flux connecting phosphoenolpyruvate with oxaloacetate; and serine production and degradation reactions were modeled as one reversible flux between serine and pyruvate. The intracellular fluxes were calculated using the external fluxes according to network stoichiometry:

$$v_c = -\text{inv}(G_c) \times (G_m \times v_m) \quad (4.4)$$

where  $v_c$  and  $v_m$  are the arrays of intracellular and extracellular fluxes,  $G_c$  and  $G_m$  are the corresponding stoichiometric matrices. The  $G_c$  matrix must be invertible. Consequently, the stoichiometric model was modified as described above. Following all listed simplifications, the PPP flux could still not be calculated directly but was fixed in order to obtain an invertible  $G_c$ . The PPP was therefore set at 5% of the total glucose input flux, a value that suffices for DNA and RNA synthesis requirements and also limits the carbon loss in the reaction catalyzed by phosphogluconate dehydrogenase.

Numerical derivation is an important source of errors. In dynamic flux analysis, this issue can lead to computing fluxes lacking biological sense (e.g. a reversed TCA cycle). Noise amplification by derivation is mitigated by considering the measurement errors in the

## 4. High resolution $^{13}\text{C}$ metabolic flux analysis in CHO cells

computed flux values. Monte Carlo was applied to sample 1500 sets of extracellular concentrations using the average measured values perturbed normally with the standard deviations. Each set was then interpolated with piecewise splines and the metabolic fluxes were computed at the interpolation time points. Average flux values and flux standard deviations were calculated using the resulting flux sets.

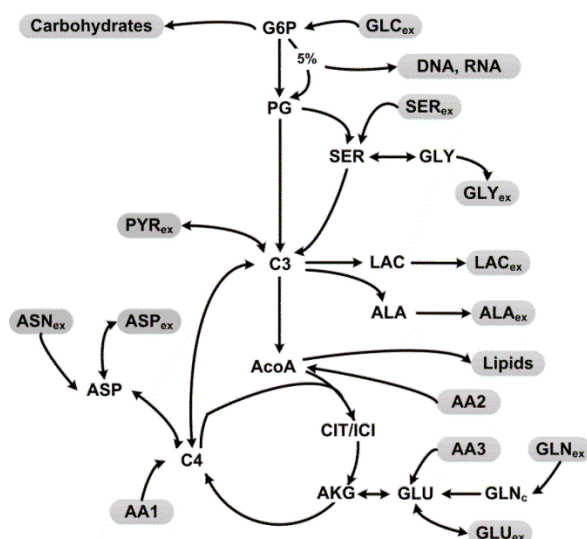


**Figure 4.2.** Simplified metabolic network of the CHO-K1 cell line central carbon metabolism. Subscripts: ex – extracellular. Abbreviations: AA1 – isoleucine, methionine, threonine, valine; AA2 – isoleucine, leucine, lysine, phenylalanine, tyrosine; AA3 – arginine, proline; AcoA – acetyl-coenzyme A; AKG –  $\alpha$ -ketoglutarate; ALA – alanine, ASN – asparagine; ASP – aspartate; C3 – phosphoenolpyruvate / pyruvate; C4 – malate / oxaloacetate; CIT – citrate; G6P – glucose-6-phosphate; GLC – glucose; GLN – glutamine; GLU – glutamate; GLY – glycine; LAC – lactate; PG – phosphoglycerate; PYR – pyruvate; SER – serine.

### 4.2.6. Metabolic network for non-stationary $^{13}\text{C}$ MFA

A detailed metabolic network of the CHO-K1 cell line was constructed using the annotated CHO genome database (Hammond et al., 2012), the *Mus musculus* genome (Zhu et al., 2003) and the KEGG Pathway database (Kanehisa et al., 2014). Information about enzyme compartmentation, mitochondrial transporters and metabolic channeling was included when available. The network included compartmentation of cytosolic and mitochondrial alanine and aspartate aminotransferases, cytosolic glutamine synthesis and mitochondrial glutaminase, cytosolic and mitochondrial isocitrate dehydrogenase. Concerning mitochondrial carriers, the following were considered: irreversible pyruvate

#### 4. High resolution $^{13}\text{C}$ metabolic flux analysis in CHO cells

---

carrier (confirmed by own mitochondrial studies, unpublished data), reversible dicarboxylate carrier, irreversible citrate carrier, reversible  $\alpha$ -ketoglutarate carrier, reversible glutamate carrier, reversible aspartate-glutamate carrier, reversible alanine transport and irreversible glutamine transport into the mitochondria. In addition, the network was modified using enzyme activity localization determined by Wahrheit et al. (2014b). The pathways producing macromolecules e.g. carbohydrates, proteins, fatty acids, nucleic acids were included as sink fluxes for precursor metabolites. The catabolism of amino acids was lumped into fluxes feeding target metabolite pools. For the detailed reaction list and the carbon transfer rules see (Supplem. Table S 4.2).

##### 4.2.7. Flux space analysis

Constraints imposed by extracellular fluxes and reaction direction limit the possible flux space. Convex analysis applied to calculating the flux polytope could be computationally cumbersome. This fact was circumvented by using Monte Carlo sampling to generate the flux space (Wiback et al., 2004). A total of 10000 flux sets was generated within the designated constraints and using the stoichiometry of the detailed model. The boundaries of the flux space were further used as constraints for the non-stationary  $^{13}\text{C}$  MFA.

##### 4.2.8. Non-stationary- $^{13}\text{C}$ MFA

Metabolite and carbon balancing for both intracellular and extracellular metabolites was applied for simulating the mass isotopomer distribution (MID) of selected metabolites over time. The mathematical modeling procedure of non-stationary  $^{13}\text{C}$  metabolic flux analysis (INST- $^{13}\text{C}$ MFA) is the same as described and applied by Nicolae et al. (2014). In the present study intracellular MIDs were available therefore intracompartmental concentrations of metabolites with sampled MIDs could be estimated. The sampled MID of a metabolite is the average of the mitochondrial and cytosolic values, weighed by the intracompartmental concentrations of that metabolite. The total mitochondrial volume was set to be 20% of the total cell volume, as estimated from STED microscopy (personal communication, Uwe Jandt), higher than reported for HeLa cells and a different cell line

## 4. High resolution $^{13}\text{C}$ metabolic flux analysis in CHO cells

of CHO cells (Gandhi and Samuels, 2011; Ross and Mel, 1972) but comparable to the average for mammalian cells or rat liver (Else and Hulbert, 1985; Weibel et al., 1969). Exact 3D data are, however, still lacking. For all the metabolites that were included in the model but for which the MIDs were not sampled, the intracompartmental pool values took negligible values of 0.1 mmol/L cell. The accepted standard deviation of extracellular MIDs in the objective function was 0.01 and of intracellular MIDs it was 0.03.

### 4.3. Results and Discussion

#### 4.3.1. Cell growth and extracellular metabolite concentrations

Growth and extracellular metabolite concentrations were determined from four biological replicates. The CHO-K1 cells maintained exponential growth for the whole cultivation period of 48 h (Fig. 4.3). The parallel cultivations were reproducible as is evident from the low standard deviations in (Fig. 4.3, Fig. 4.4 and Supplem. Table 4.4). The estimated specific growth rate was  $\mu = 0.034 \text{ h}^{-1}$  (Fig. 4.3). Glucose, glutamine, pyruvate, serine, asparagine, aspartate and essential amino acids were taken up (Fig. 4.4). Lactate, alanine, glutamate and glycine were produced throughout the cultivation period. By the end of the 48 h cultivation, 60% of the glucose was converted to lactate. Although the specific growth rate was constant, the specific uptake and production rates generally decreased over the 48h, the most marked trend being observed for lactate production (Fig. 4.4). However, no switch from production to uptake or vice-versa was observed.

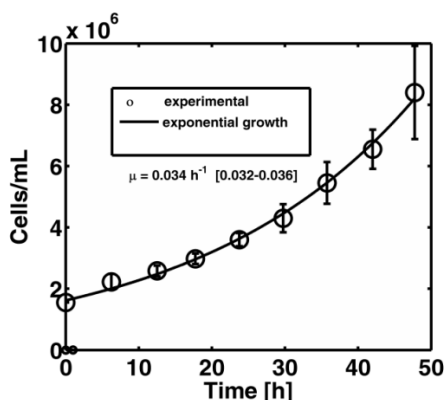


**Figure 4.3.** Growth profile of the CHO-K1 cells in 250 ml baffled shake flask with a working volume of 120 mL and the determined specific growth rate  $\mu$ . The values represent the average of 4 parallel cultivations

## 4. High resolution $^{13}\text{C}$ metabolic flux analysis in CHO cells

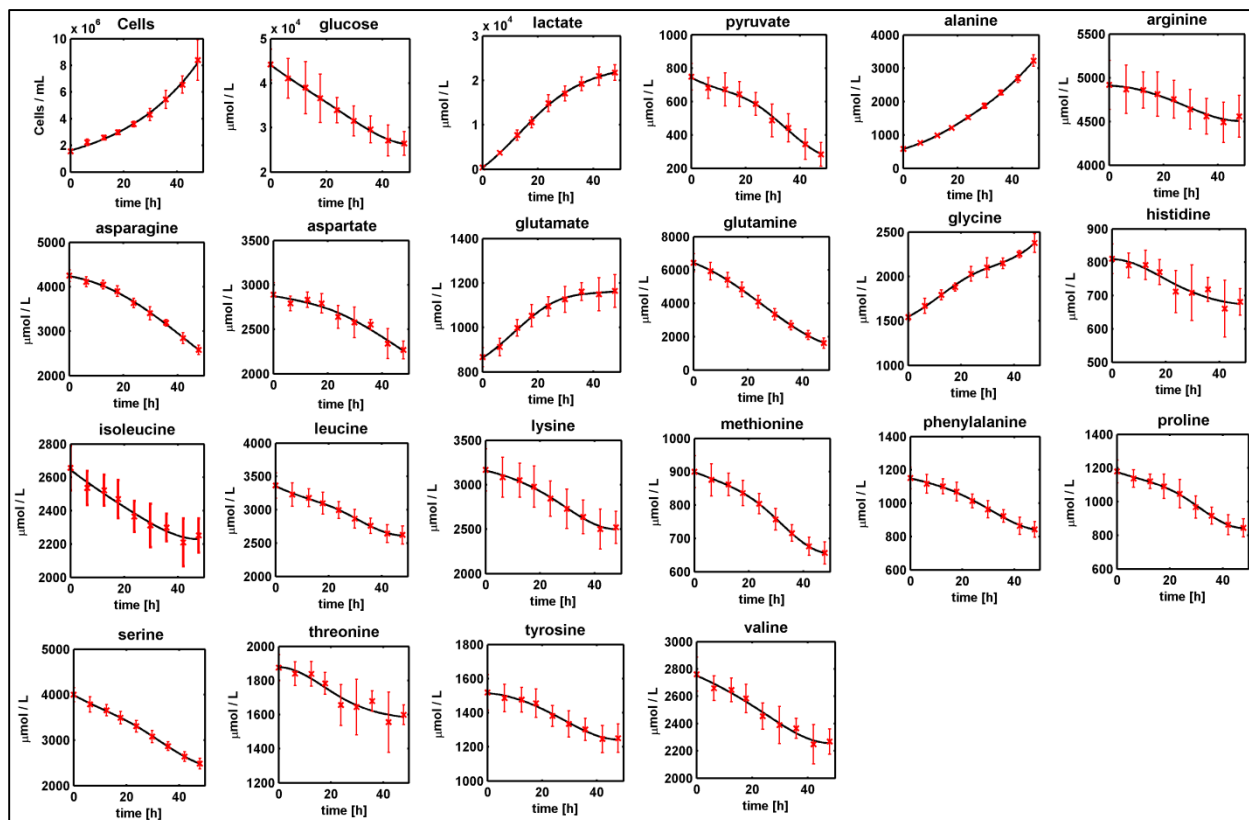


**Figure 4.4.** Cell density (cells / mL) and extracellular metabolites concentrations ( $\mu\text{mol} / \text{L}$ ) for a 48 h cultivation of CHO-K1 cells in 250 ml baffled shake flask with a working volume of 120 mL. The lines represent the piecewise spline interpolations and the red bars are the standard deviation computed from 4 parallel cultivations

### 4.3.2. Labeling experiment

Extracellular MIDs were determined from two biological replicates. For determination of the time courses for intracellular labeling dynamics, MIDs were obtained alternatively from two parallel cultivations for each labeled substrate. In the experiment where  $[\text{U-}^{13}\text{C}_6]$  glucose was used, the sampled metabolites became labeled gradually, and no steady state was reached after 48 h (Fig. 4.5 A). The general trend was an increase of the labeled fraction, the exception being intracellular lactate, whose  $\text{M}_3$  mass fraction decreased after 36 h. The mass isotopomer with the highest proportion for pyruvate, lactate and alanine was  $\text{M}+3$ , while for metabolites related to the TCA cycle e.g. citrate,  $\alpha$ -ketoglutarate, fumarate and malate, it was the  $\text{M}_2$ . Lactate and alanine pools were labeled differently

#### 4. High resolution $^{13}\text{C}$ metabolic flux analysis in CHO cells

---

intra- and extracellularly. This evidence supports the hypothesis of metabolic compartmentation of these two metabolites. Partitioning of lactate dehydrogenase activity, either by channeling (Jandt et al., 2013; Malaisse et al., 2004; Perez-Bercoff et al., 2011) or in cellular compartments (Baba and Sharma, 1971; Brooks et al., 1999; Gladden, 2004; Hashimoto and Brooks, 2008; Lemire et al., 2008; Philp et al., 2005; Sagrista and Bozal, 1987) can also be inferred by comparing the intracellular labeling of pyruvate and lactate. During the first 24 h, intracellular pyruvate and lactate follow similar labeling patterns. At 18 h after inoculation, a switch in the partitioning of lactate dehydrogenase was evident from diverging labeling patterns of intracellular pyruvate and lactate.

In the first 2 h, the labeling in pyruvate exhibited a sharp overshooting of the  $\text{M}+3$  fraction, that was manifested later also in lactate (Fig. 4.5 B). A similar overshooting behavior was observed in the  $\text{M}+4$  isotopomer of malate, and it transmitted to aspartate. When  $[\text{U-}^{13}\text{C}_5]$  glutamine was used as the  $^{13}\text{C}$  label source, no labeling was observed in serine and glycine, indicating there is no gluconeogenesis. Pyruvate and lactate displayed a sharp overshooting in the first 2 h in all mass isotopomers (Fig. 4.5 B). However, after 12 h, the labeling of pyruvate and lactate returned close to the natural labeling state, indicating the absence of fluxes that connect glutamine to pyruvate. The  $\text{M}+4$  fraction in aspartate, fumarate and malate increased until 18 h, and then it decreased in favor of the non-labeled fraction. This is most likely the result of a metabolic shift occurring around 18 h after inoculation. The shift is mirrored in glutamine and glutamate labeling, where the non-labeled fraction increased steadily after 24 h. The metabolic shift consists most likely of a decrease in the ratio between glutaminolysis and glycolysis in contributing to the TCA cycle. The specific uptake and production rates were therefore computed for the period of 0-18 h by fitting the model of exponential balanced growth in batch culture to the sampled extracellular concentrations (Fig. 4.4).

Aspartate, fumarate and malate had similar labeling patterns on both labeled substrates, suggesting a high degree of connection and exchange between these metabolites. The MID curves that exhibited overshooting returned to a smooth behavior after 2 h on both labeled substrates. Overshooting can be assigned to a stress response of the cells to media



change at the beginning of the culture (Wellen and Thompson, 2010). The stress response is characterized by very high metabolic rates that quickly convert the fed substrates after being resuspended to replenish the depleted intracellular pools. Once these pools were replenished, the metabolism followed a steady state behavior as can be seen in (Fig. 4.4). Since there is no observable difference in the cell number and extracellular concentrations in the first two hours, assessing the extracellular fluxes during this brief period and proving the existence of metabolic steady state required for metabolic flux analysis tools is not possible.

##### 4.3.3. Dynamic metabolic flux analysis

Flux changes throughout the 48 h cultivation period reflected the observation in the MIDs, namely that a shift in metabolism occurs after 18 h (Fig. 4.6). Glucose uptake flux decreased markedly and the relatively high standard deviation in glucose concentration measurement (Fig. 4.4) propagated in the computed fluxes. The initial slope of the interpolation curves is a significant source of uncertainty in the flux values computed in the first 10 h, as it can be observed by the high values of estimated standard deviations (Fig. 4.6.A). The metabolic shift occurring after approx. 20 h is marked by a decrease in the lactate production rate compared to the main extracellular fluxes: glucose uptake (Fig. 4.6.B), glutamine uptake (Fig. 4.6.D) and alanine production (Fig. 4.6.E).

Remarkably, the specific growth rate remained constant despite decreasing uptake rates of carbon sources. It can therefore be inferred that the cells are programmed for maximizing growth regardless of the availability of carbon sources. It is also very likely that the uptake and processing rates of glucose and glutamine depend on their extracellular concentrations. Owing to the sharply decreasing uptake rates of carbon sources, after 20 h from the inoculation, the carbon sources were deployed almost exclusively for sustaining growth and metabolite secretion. This led to an arrest of the TCA cycle (Fig. 4.6 A), which can explain the switch observed in lactate and pyruvate labeling (Fig. 4.5 A).

#### 4. High resolution $^{13}\text{C}$ metabolic flux analysis in CHO cells

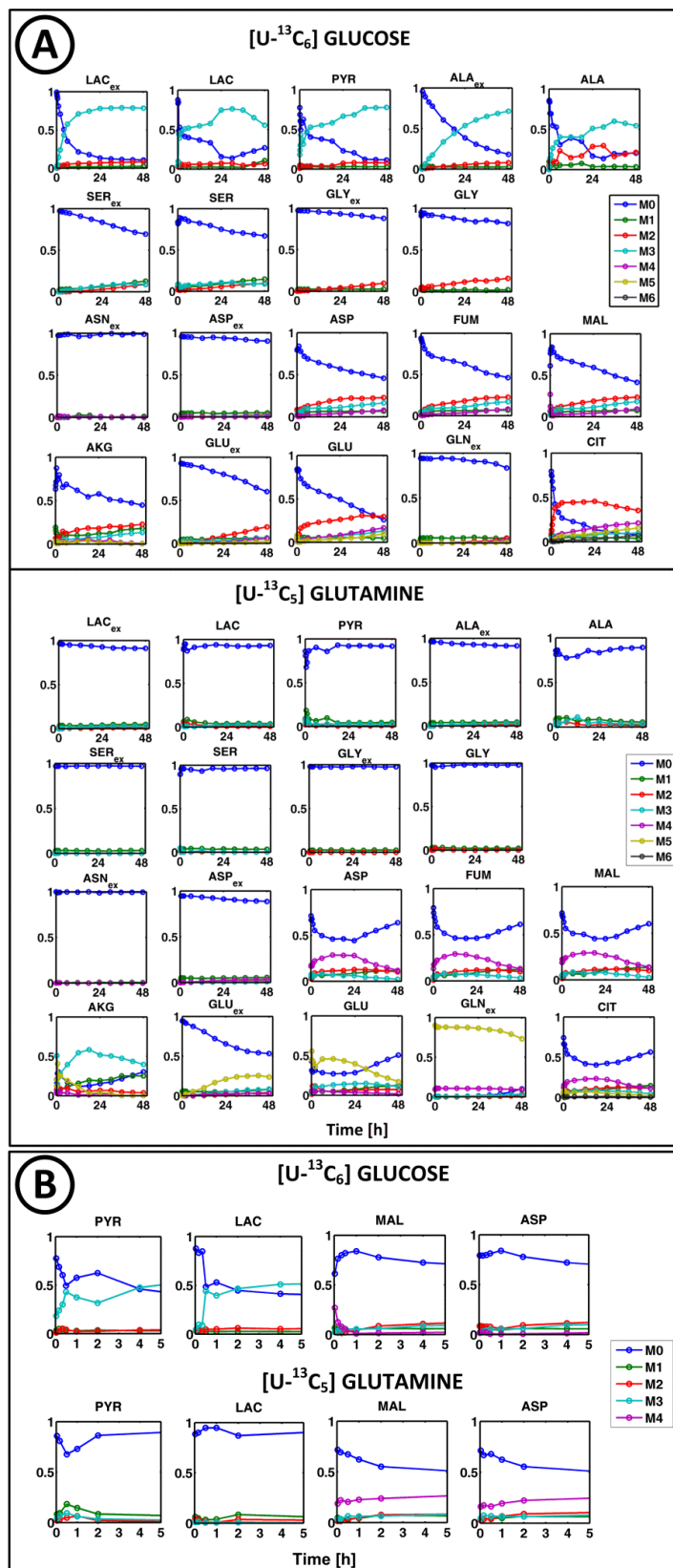


**Figure 4.5.** (A) Experimentally determined mass isotopomer distributions of intracellular and extracellular (subscript ex) metabolites during the 48 h of the labeling experiment using  $[\text{U-}^{13}\text{C}_6]$  glucose and  $[\text{U-}^{13}\text{C}_5]$  glutamine as substrates. (B) The first 5 h of the labeling experiment using  $[\text{U-}^{13}\text{C}_6]$  glucose and  $[\text{U-}^{13}\text{C}_5]$  glutamine as substrates showing the overshooting behavior in intracellular pyruvate (PYR), lactate (LAC), malate (MAL) and aspartate (ASP). Abbreviations: AKG –  $\alpha$ -ketoglutarate; ALA – alanine; ASN – asparagine; ASP – aspartate; CIT – citrate; FUM – fumarate; GLN – glutamine; GLU – glutamate; GLY – glycine; Lac – lactate; MAL – malate; PYR – pyruvate; SER – serine.

#### 4. High resolution $^{13}\text{C}$ metabolic flux analysis in CHO cells

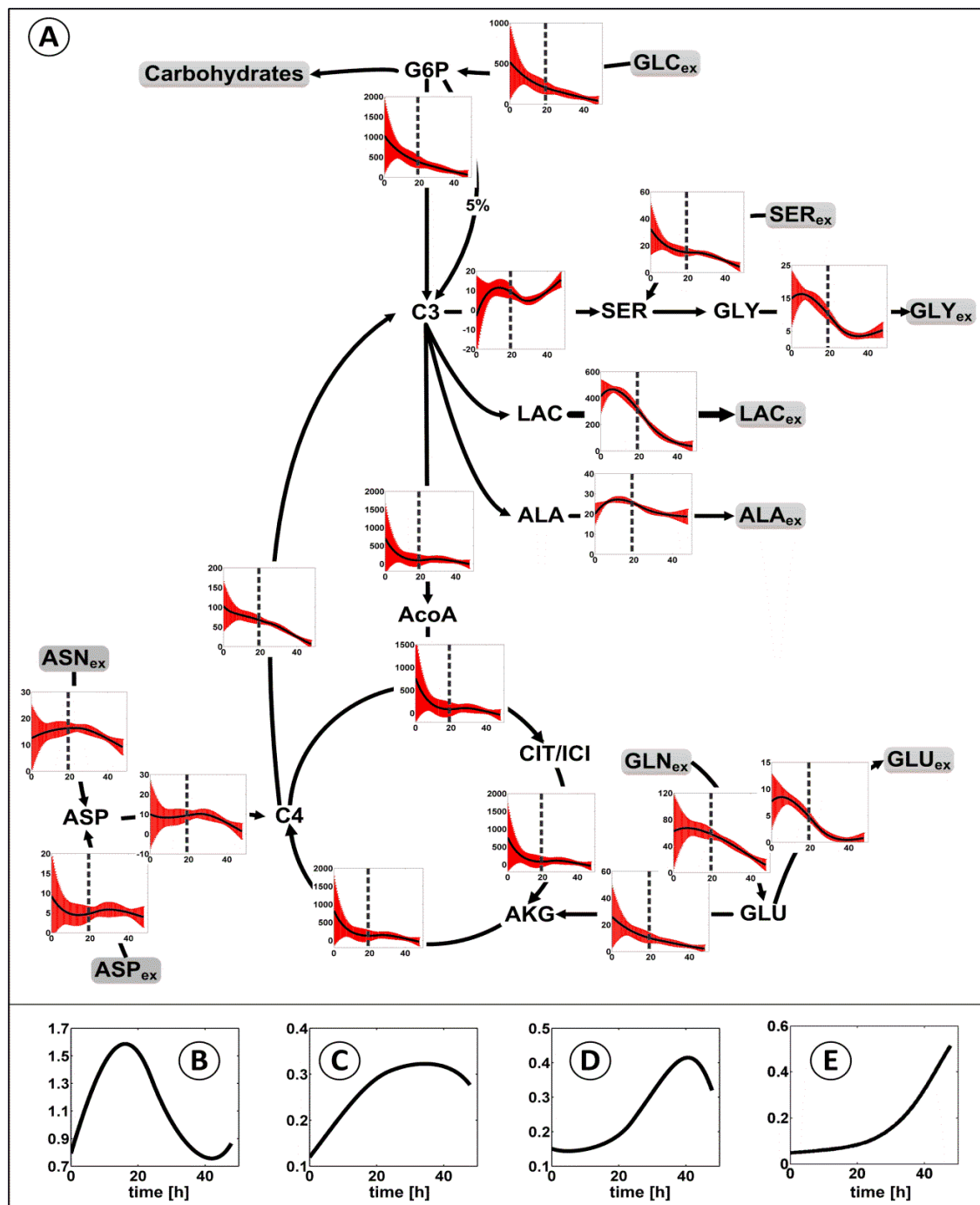


**Figure 4.6.** (A) Dynamics of fluxes in the metabolic network of CHO-K1 cells. The fluxes (black lines,  $\text{mmol} \times \text{L cell}^{-1} \times \text{h}^{-1}$ ) and their standard deviations (red bars) were determined from 1500 Monte Carlo simulations that fitted with piecewise splines normally perturbed extracellular. Dynamics of flux ratio between (B) lactate secretion and glucose uptake, (C) glutamine uptake and glucose uptake, (D) glutamine uptake and lactate secretion and (E) alanine secretion and lactate secretion. Subscripts: *ex* – extracellular. Abbreviations: AKG –  $\alpha$ -ketoglutarate; ALA – alanine; ASN – asparagine; ASP – aspartate; CIT – citrate; FUM – fumarate; GLN – glutamine; GLU – glutamate; GLY – glycine; Lac – lactate; MAL – malate; PYR – pyruvate; SER – serine

### 4.3.4. Flux space

The flux space for the detailed network of the CHO-K1 cell was computed using as constraint the extracellular fluxes computed for the first 18 h of cultivation and default boundary constraints for the free fluxes. Many fluxes were limited only by the default boundaries (Fig. 4.7). This outcome is not surprising considering the large number of degrees of freedom in the flux space i.e. 13. Fluxes in glycolysis and TCA cycle were limited by substrate uptake, i.e. glucose and glutamine. Pentose phosphate pathway consumes one carbon atom, making its flux inversely proportional to the flux in the TCA cycle. Interestingly, in the majority of cases the estimated fluxes did not match the fluxes with the highest frequency of occurrence in the flux space. Most of the fluxes estimated using  $^{13}\text{C}$  labeling data lie near the boundaries of the flux space.

### 4.3.5. Fitting of MIDs and model re-adaptation

For applying INST- $^{13}\text{C}$ MFPA, it was considered that the cells were at metabolic steady state between 2-18 h after the beginning of the labeling experiments (Deshpande et al., 2009; Noh et al., 2006). This is a valid assumption for most metabolites, as it was shown by fitting the extracellular concentrations to an exponential growth using constant yield coefficients (Fig. 4.4). The MIDs of 15 extracellular and intracellular metabolites, 5 time points for  $[\text{U-}^{13}\text{C}_6]$  glucose and 4 time points for  $[\text{U-}^{13}\text{C}_5]$  glutamine were sampled, totaling 675 experimental MID points (Fig. 4.8, Supplem. Table 4.3). Because of the highly noisy data, the MIDs of intracellular alanine and  $\alpha$ -ketoglutarate were excluded from the objective function. After several trials in which no successful fitting was obtained, the initial model was modified to include: (1) two pools of cytosolic pyruvate, of which one is channeled to lactate that is then directly secreted, (2) two pools of mitochondrial pyruvate, of which one is converted to acetyl-CoA via pyruvate dehydrogenase, (3) a pool of mitochondrial lactate, (4) cytosolic synthesis of glutamine and (5) serine degradation to pyruvate.

The parameter estimation was conducted using two strategies in parallel: one used a genetic optimization algorithm as described earlier (Nicolae et al., 2014), and the other

#### 4. High resolution $^{13}\text{C}$ metabolic flux analysis in CHO cells

---

used the following procedure: (1) generate 1000 random initial points that satisfy constraints, (2) use the point that produced the smallest value of the objective function as the starting point of a gradient-based algorithm and (3) find the minimum using the trust region reflective algorithm. The second optimization strategy was repeated 30 times, and it provided the best fit of the MIDs. One simulation took about 6.5 s, and the optimization procedure required about 6 days on a 2.3 GHz QuadCore CPU. A total of 64 parameters were estimated, of which 13 were free fluxes, 29 were flux reversibilities, 20 were intracompartmental pools and 2 additional parameters that expressed the non-labeled  $\text{CO}_2$  flux entering the cytosol and the mitochondria. This flux was needed to evaluate the labeling dynamics of  $\text{CO}_2$  used by carboxylation reactions.

The best fit (Fig. 4.8) resulted in a minimized weighted sum of square differences value of 665, which is smaller than the criteria for fitting  $\chi^2(0.95, 675-64) = 670$ . Most of the MIDs of metabolites were reasonably well fitted, with the exception of lactate when  $[\text{U-}^{13}\text{C}_6]$  glucose was used. Because the labeling of extracellular lactate is different from the labeling of intracellular lactate (Fig. 4.8), new cytosolic pyruvate pools from which lactate can derive were included in the model. While this assumption produced a much better approximation of lactate labeling, it is still possible that other metabolic configurations involving more sophisticated channeling and compartmentation are responsible for the observed labeling pattern in lactate.

Confidence intervals were computed accordingly to (Antoniewicz et al., 2006) and were very narrow for most estimated parameters (Suppl. Table S4.2). This is a strong indication that fitting simultaneously the intracellular MIDs from two parallel labeling experiments that used two different labeled substrates validates INST- $^{13}\text{C}$ MFAs as an effective methodology for untangling the details of complex metabolic networks, as it was already described by (Murphy et al., 2013).

## 4. High resolution $^{13}\text{C}$ metabolic flux analysis in CHO cells

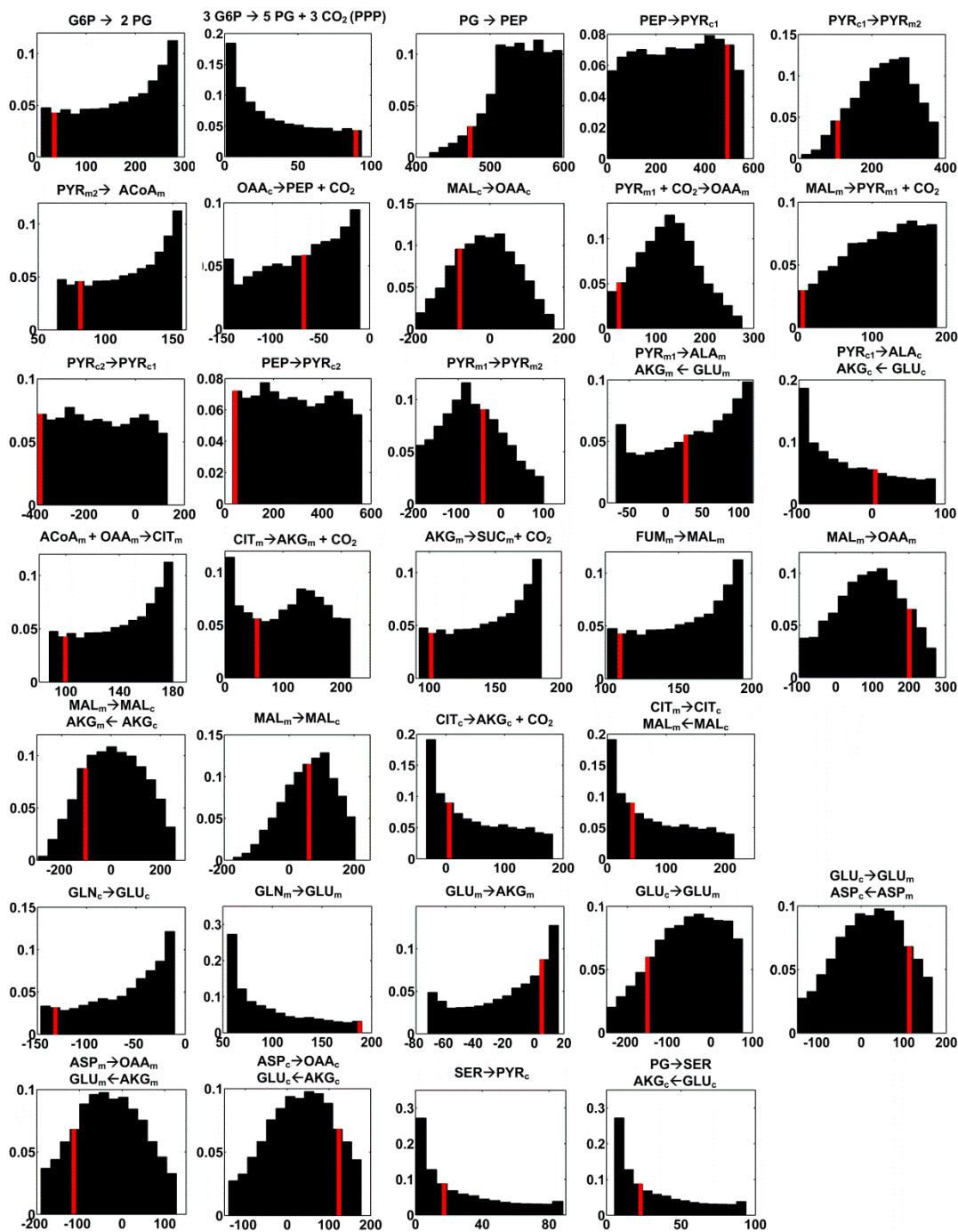


**Figure 4.7.** Flux space of the metabolic network of CHO-K1 cell representing the flux frequency distribution computed by Monte Carlo random sampling of 10000 flux sets that satisfied imposed constraints. The fluxes are expressed in  $[\text{mmol} \times \text{L cell}^{-1} \times \text{h}^{-1}]$ . The red line represents the fluxes estimated using INST- $^{13}\text{C}$ MFA. Subscripts meaning: c – cytosolic; m – mitochondrial; Abbreviations: ACoA – acetyl-CoA; ALA – alanine; ASP – aspartate; CIT – citrate; FUM – fumarate; GLC – glucose; G6P – glucose-6-phosphate; PG – phosphoglycerate; PEP – phosphoenolpyruvate; GLN – glutamine; GLU – glutamate; MAL – malate; OAA – oxaloacetate; PPP – pentose phosphate pathway; PYR – pyruvate; SER – serine; SUC – succinate.

#### 4. High resolution $^{13}\text{C}$ metabolic flux analysis in CHO cells

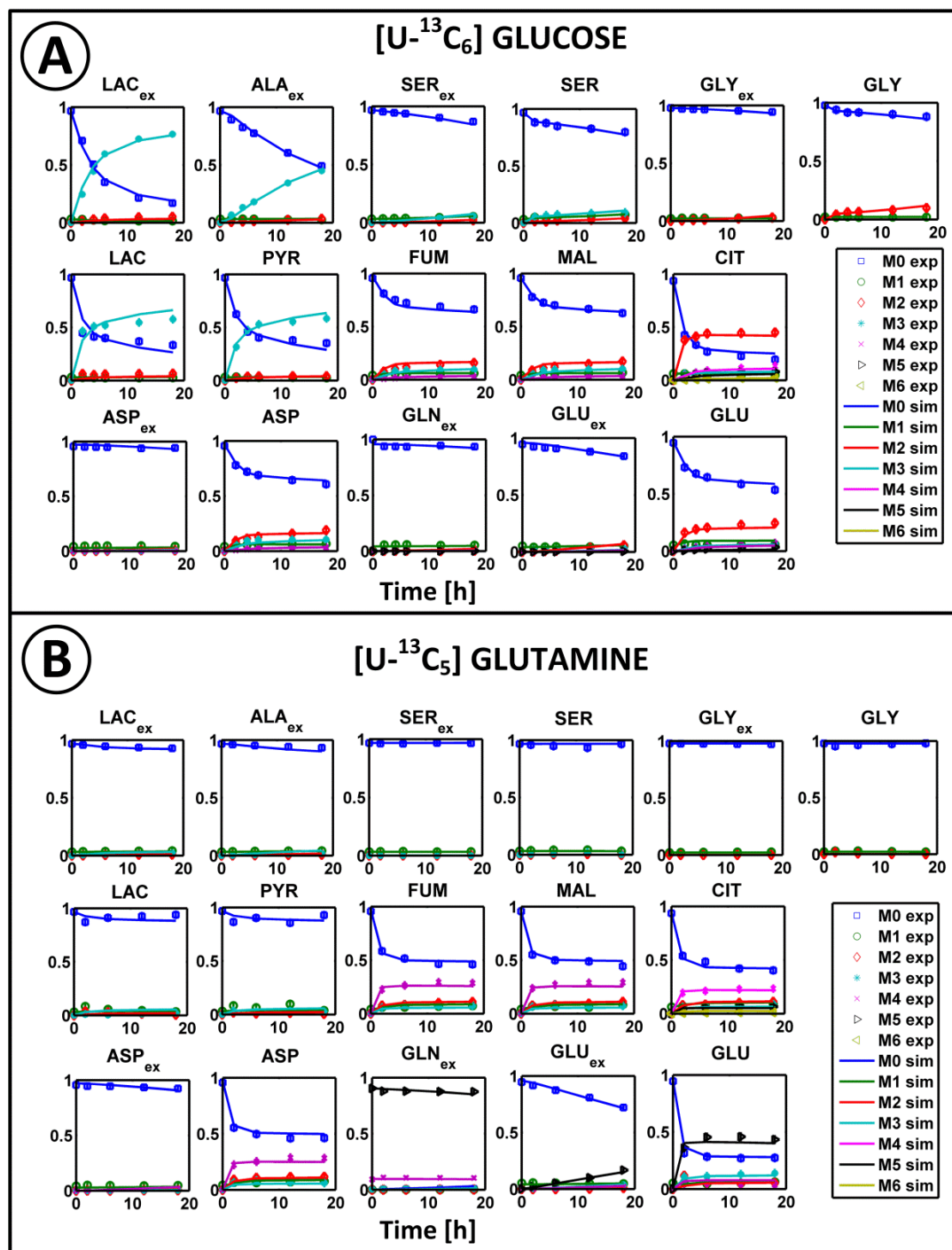


**Figure 4.8.** Mass isotopomer distributions (MIDs) of sampled metabolites during the first 18 h of cultivation of CHO-K1 suspension cells with (A)  $[\text{U-}^{13}\text{C}_6]$  glucose and (B)  $[\text{U-}^{13}\text{C}_5]$  glutamine. The values of the extracellular MIDs are the average of two biological replicates and the intracellular MIDs are obtained alternatively from two parallel cultivations for each labeled substrate. The continuous lines represent the best simulated fit of the MIDs. Subscripts meaning: ex – extracellular. Abbreviations: exp – experimental; sim – simulated; ALA – alanine; ASP – aspartate; CIT – citrate; FUM – fumarate; GLN – glutamine; GLU – glutamate; GLY – glycine; LAC – lactate; MAL – malate; PYR – pyruvate; SER – serine.

### 4.3.6. Metabolic fluxes, compartmentation and channeling

Glycolysis was the main carbon source of the CHO-K1 cell metabolism (Fig. 4.9 A). Consistent with our previous finding for the CHO-K1 cell line cultivated in a reactor batch culture (Nicolae et al., 2014), most of the glucose-6-phosphate was metabolized by the oxidative branch of the pentose phosphate pathway (PPP) and not by the upper glycolysis. 75% of the glucose was converted to lactate that was then secreted. The remaining glucose was converted to pyruvate that was transported to the mitochondria. In previous studies of this CHO-K1 cell line, it was found that partial glycolytic channeling resulted in two cytosolic pyruvate pools (Nicolae et al., 2014; Wahrheit et al., 2014b), a phenomenon observed before in CHO cells (Ahn and Antoniewicz, 2013; Deshpande, 2008) and also in other mammalian cells (Campanella et al., 2005; Cruz et al., 2001; Peuhkurinen et al., 1983; Zwingmann et al., 2001). In the present study, the channeling effect was less pronounced, as the two cytosolic pyruvate pools were estimated to be strongly connected (Fig. 4.9 A). However, active exchange from pyruvate towards a second cytosolic dead-end lactate pool had to be included. Also, the exchange between the extracellular and intracellular lactate pool was significant. This exchange must be considered to describe the MIDs dynamics of intracellular lactate and pyruvate. Furthermore, the model was expanded by a mitochondrial lactate pool and channeling of mitochondrial pyruvate to describe the difference in labeling between extracellular and intracellular lactate. Heterogeneously distributed pyruvate dehydrogenase in the mitochondrial matrix as found in fibroblasts (Margineantu et al., 2002) supports the assumption that a part of the pyruvate entering the mitochondria is converted to acetyl-CoA without mixing with the mitochondrial pyruvate pool (Fig. 4.9 B). These results are similar to those of Ahn et al. (Ahn and Antoniewicz, 2013).



#### 4. High resolution $^{13}\text{C}$ metabolic flux analysis in CHO cells

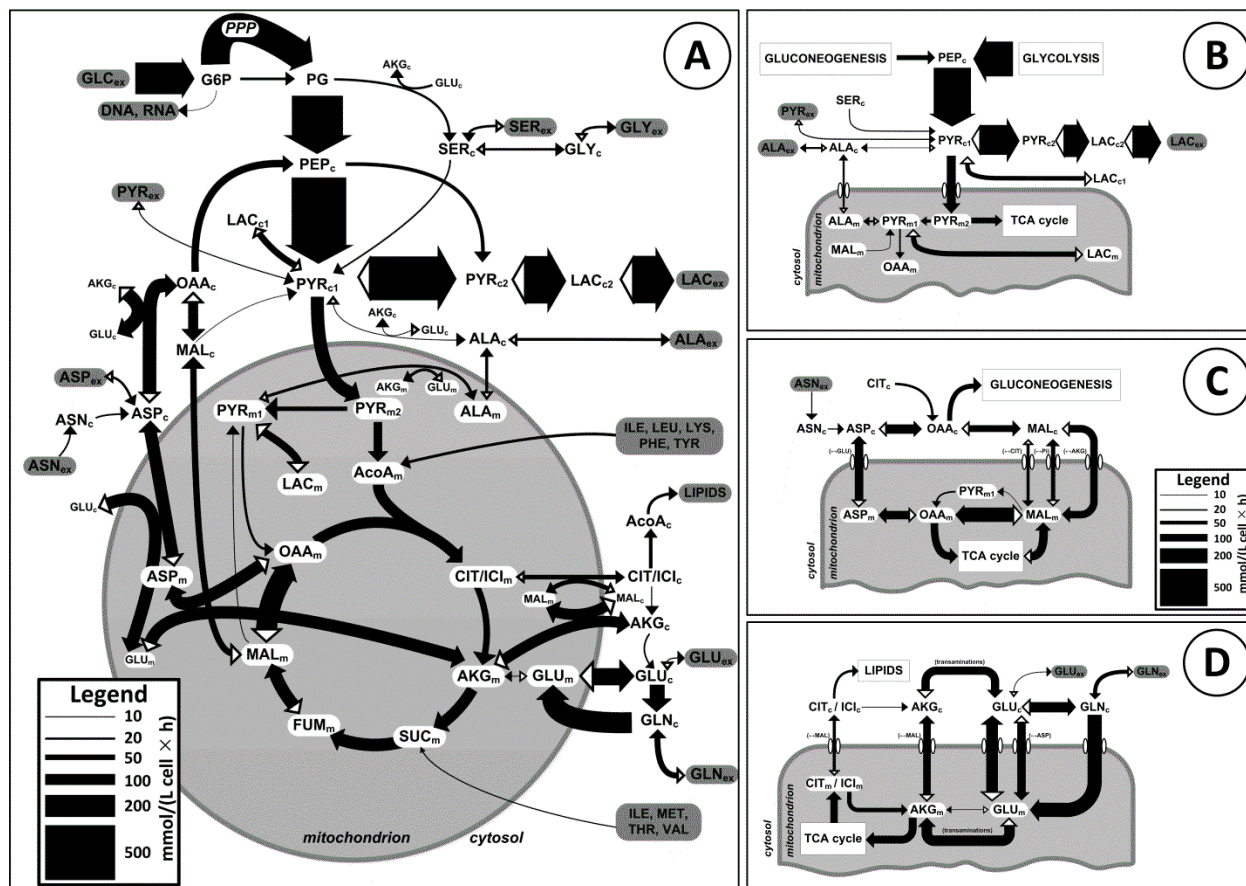


**Figure 4.9.** (A) Metabolic fluxes of the central carbon metabolism of CHO-K1 cells in the 2 – 18 h period of cultivation estimated using non-stationary  $^{13}\text{C}$  metabolic flux analysis. (B) Glycolysis and pyruvate metabolism compartmentation in CHO-K1 cells. (C) Metabolism of oxaloacetate (OAA), aspartate (ASP) and malate (MAL) in CHO-K1 cells. (D) Metabolism of glutamine (GLN), glutamate (GLU),  $\alpha$ -ketoglutarate (AKG) and citrate (CIT) in CHO-K1 cells. The thickness of the lines is proportional to the net flux values, except for the fluxes connecting  $\text{PYR}_{\text{m1}}$ - $\text{LAC}_{\text{m}}$  and  $\text{PYR}_{\text{c1}}$ - $\text{LAC}_{\text{c1}}$ , where they represent the exchange flux (the net flux being 0). The full arrows indicate the direction of the net flux, and the empty arrows indicate a reversible flux. Subscripts meaning: c – cytosolic; ex – extracellular; m – mitochondrial; Abbreviations: AcoA – acetyl-CoA; ALA – alanine; ASN – asparagine; ASP – aspartate; CIT – citrate; FUM – fumarate; GLC – glucose; G6P – glucose-6-phosphate; PG – phosphoglycerate; PEP – phosphoenolpyruvate; GLN – glutamine; GLU – glutamate; GLY – glycine; ICI – isocitrate; ILE – isoleucine; LAC – lactate; LEU – leucine; LYS – lysine; MAL – malate; MET – methionine; OAA – oxaloacetate; PHE – phenylalanine; PYR – pyruvate; SER – serine; SUC – succinate; THR – threonine; TYR – tyrosine; VAL – valine.

#### 4. High resolution $^{13}\text{C}$ metabolic flux analysis in CHO cells

---

Mitochondrial channeling results in two pyruvate pools, observed when  $[\text{U-}^{13}\text{C}_6]$  glucose is used: one with high  $^{13}\text{C}$  fractional labeling produced in the glycolysis that is channeled to acetyl-coA, and a second larger one replenished with  $^{12}\text{C}$  by cataplerotic reactions. Activity of mitochondrial lactate dehydrogenase was already confirmed in various tissues, e.g. heart mitochondria (Brooks et al., 1999), breast cancer cells (Hussien and Brooks, 2011), muscle cells (Hashimoto et al., 2006), liver cells (Brooks et al., 1999; Kline et al., 1986), astrocytoma (Lemire et al., 2008) and neurons (Hashimoto et al., 2008). Mitochondrial metabolism of lactate occurs when lactate is being metabolized as a carbon source, due to its high intracellular concentration (Brooks et al., 1999). However, in our case, lactate was secreted by the cells and it constituted a dead end metabolite in the mitochondria. It can therefore be assumed that the role of lactate in the mitochondria is to function as a buffer for NADH, a mediator of redox states between compartments (Gladden, 2004).

Glycolytic pyruvate and glutamine constituted the main fuels of the TCA cycle as previously shown for this cell line (Wahrheit et al., 2014a; Wahrheit et al., 2014b). The catabolism of essential amino acids was limited to a small flux feeding the acetyl-CoA pool. Otherwise, the uptake of essential amino acids was mostly restricted to the requirements for protein synthesis also previously found for this cells line (Wahrheit et al., 2014b).

At the cytosol-mitochondria boundary, most mitochondrial transporters carried significant fluxes. The mitochondrial pyruvate carrier (Bricker et al., 2012; Herzig et al., 2012) was the only connection between glycolysis and the TCA cycle, providing most of the mitochondrial pyruvate, as the mitochondrial malic enzyme activity was estimated to be very low (Fig. 4.9 B), consistent with enzyme assays (Wahrheit et al., 2014b). The aspartate-malate shuttle (Fig. 4.9 C) was constituted by export of mitochondrial aspartate via the glutamate-aspartate carrier (Cavero et al., 2003; Lane and Gardner, 2005) and import of cytosolic malate in the mitochondria via the malate- $\alpha$ -ketoglutarate carrier. Cytosolic aspartate was converted to oxaloacetate by the activity of aspartate aminotransferase. Cytosolic malate dehydrogenase converted oxaloacetate to malate and

#### 4. High resolution $^{13}\text{C}$ metabolic flux analysis in CHO cells

---

consumed a part of the cytosolic NADH. Another transporter that facilitated the transport of malate in the mitochondria was the malate-citrate carrier. Malate was transported in exchange for citrate, which was used in the cytosol for fatty acids synthesis (Gnoni et al., 2009; Zara et al., 2005). Although malate is transported in the mitochondria with a net flux, partial cycling of malate between mitochondria and cytosol occurred. The malate carrier exchanged mitochondrial malate for cytosolic phosphate (Fiermonte et al., 1999; Mizuarai et al., 2005) (Fig. 4.9 C). Phosphoenolpyruvate carboxykinase activity was modest but could serve as a starting point of gluconeogenesis. However, complete gluconeogenesis did not occur because neither serine nor glycine was labeled when [U- $^{13}\text{C}_5$ ] glutamine was used as tracer (Fig. 4.8 B).

Glutamine uptake in the mitochondria was 3.6 times higher than the net glutamine uptake from the medium. This is the result of a considerable cytosolic synthesis of glutamine from glutamate (Fig. 4.9 D). It was previously observed in CHO-K1 cells that the glutamine synthesis pathway is active even at high glutamine consumption rates (Nicolae et al., 2014). In the mitochondria, glutamine feeds the TCA cycle via glutamate that is converted to  $\alpha$ -ketoglutarate not by NADH-producing glutamate dehydrogenase, but by transamination reactions. Aspartate was synthesized in the mitochondria, exported and re-converted to oxaloacetate in the cytosol. Alanine synthesis was estimated to occur mostly in the mitochondria. Glutamate transporter carried a high flux leaving the mitochondria (Fig. 4.9 D). Glutamate was procured in the cytosol either via transport from the mitochondria or transamination of  $\alpha$ -ketoglutarate. Cytosolic glutamate was used to fuel glutamine synthesis and as an antiport partner to the aspartate-glutamate transporter. Despite the high activity detected *in vitro* for cytosolic IDH (Wahrheit et al., 2014b), this did not reflect in the labeling patterns, regardless of the reaction direction that was considered. Even setting the labeling of the  $\text{CO}_2$  pool as a free parameter did not result in the estimation of a significant activity. The role of such a high activity of cytosolic isocitrate dehydrogenase could be to control variations of the cytosolic NADPH content and stress response (Lee et al., 2002).

#### 4. High resolution $^{13}\text{C}$ metabolic flux analysis in CHO cells

---

In what concerns compartmentation of NADH and NADPH metabolism (Table 4.1), the excess of cytosolic NADH produced in the glycolysis is consumed by lactate dehydrogenase and malate dehydrogenase that is part of the malate shuttle. Cytosolic NADPH is provided only by the PPP since it was found by MFA that the activity of cytosolic malic enzyme was virtually absent. This agrees with earlier data of enzyme assays (Wahrheit et al., 2014b). The very low activity of mitochondrial malic enzyme means that little or even no mitochondrial NADPH was produced via this route. Oxidative stress (Tuttle et al., 2000; Vizan et al., 2009) that can be induced by futile cycles of disulfide bond formation and breaking during protein folding is an important consumer of NADPH (Tyo et al., 2012). This might indicate cytosolic NADPH supply as a limit for recombinant protein production. Enhancing the NADPH producing pathways could be a target for genetic modification in industrially relevant CHO strains (Klein et al., 2015). A large part of the cytosolic NADPH (21%) is used for fatty acid synthesis. Mitochondrial NADPH must be supplied by other reactions, most likely the transhydrogenase or NADP-dependent isocitrate dehydrogenase (Ceccarelli et al., 2002; Hatefi and Galante, 1977). It was shown by previous enzyme assays that around 90% of mitochondrial IDH activity is NADP-dependent (Wahrheit et al., 2014b).

All aminotransferase reactions and also many of the transport reactions were determined to be highly reversible (Suppl. Table S4.2). The shapes of the MID curves are strongly influenced by reversibility (Noh and Wiechert, 2011). Transport reversibility explained the reduced summed fractional labeling when  $[\text{U-}^{13}\text{C}_6]$  glucose was used as a substrate, as the intracellular labeling was diluted by the large extracellular pool of non-labeled metabolites, consistent with our previous observations (Nicolae et al., 2014).

Using intracellular labeling and two labeling experiments improved considerably the resolution and quality of estimated fluxes (Suppl. Table S4.2) compared to our previous study, where the same cell line was used but only extracellular labeling and one labeling experiment in a batch reactor cultivation (Nicolae et al., 2014). Now it was possible to establish the compartmentation of alanine synthesis and to solve the cytosolic and mitochondrial isocitrate –  $\alpha$ -ketoglutarate – glutamate cycling. Extracellular fluxes are

#### 4. High resolution $^{13}\text{C}$ metabolic flux analysis in CHO cells

---

highly dependent on the cultivation conditions as also reported earlier (Nicolae et al., 2014). Many observations are consistent with the earlier ones made in a bioreactor culture: (1) almost complete diversion of glucose-6-phosphate through the PPP, (2) absence of cytosolic malic enzyme activity, (3) similar phosphoenolpyruvate-carboxykinase activities, (4) simultaneous uptake and production of glutamine, (5) simultaneous uptake and production of serine and (6) excessive exchange of metabolites with the extracellular media. There were however also some significant differences compared to the reactor cultivation performed earlier (Nicolae et al., 2014): (1) reduced glucose uptake (~80% of the previous), (2) higher lactate production from glucose (75% compared to 39%) , (3) smaller TCA cycle flux, (4) reduced catabolism of essential amino acids, (5) low mitochondrial malic enzyme activity and (6) reduced uptake of asparagine. The metabolic flux map determined is probably the most complex to date for mammalian cells with respect to metabolic compartmentation, mainly because known mitochondrial transporters were incorporated into the flux model applied. The results of studies that use  $^{13}\text{C}$ MFAs to unravel the eukaryotic cell metabolism are highly dependent on the network structure. Changes in the network structure, e.g. the existence of other mitochondrial transporters, can lead to differences in some estimated fluxes due to non-linearity of isotopomer balances. It is therefore difficult to compare our results with previous  $^{13}\text{C}$ MFA studies of CHO cells. A high activity of the PPP was observed in the early exponential growth phase in a previous study that applied INST- $^{13}\text{C}$ MFA of CHO cells (Nicolae et al., 2014). A high PPP was found to be a characteristic of the late non-growth phase (Ahn and Antoniewicz, 2011; Sengupta et al., 2010) or late-exponential phase (Templeton et al., 2013). A high production of NADPH (Table 4.1) is required to counteract the oxidative stress induced by reactive oxygen species generated by mitochondrial respiration (Schafer et al., 2009; Vizan et al., 2009).

##### 4.3.7. Estimated intracompartmental pools

The use of INST- $^{13}\text{C}$ MFA and the MIDs of intracellular metabolites required the simultaneous estimation of fluxes, reversibilities and intracompartmental concentrations

---

#### 4. High resolution $^{13}\text{C}$ metabolic flux analysis in CHO cells

---

of certain metabolites. Estimated intracompartmental concentrations rely on the mitochondrial volume ratio determination. Using the available sampled intracellular MIDs (Fig. 4.8), the intracompartmental concentrations of 7 metabolites were estimated (Fig. 4.10) and the average intracellular concentration of another 2 (Fig. 4.10 A). Interestingly, pyruvate and lactate cytosolic concentrations were very low (Fig. 4.10 A) and considerably higher in the mitochondria. Lactate and pyruvate concentration distributions and the considered channeling effects explained the difference between extracellular and intracellular labeling in lactate when  $[\text{U-}^{13}\text{C}_6]$  glucose was used (Fig. 4.8 A). Association of pyruvate dehydrogenase to the mitochondrial pyruvate transporter could explain the transport of pyruvate in the mitochondria against a concentration gradient, because the complex can use imported pyruvate to produce acetyl-CoA without interfering with the mitochondrial pool. Malate and fumarate had almost identical MID dynamics (Fig. 4.8). This makes simultaneous determination of intracompartmental concentrations not possible. Fumarate intramitochondrial concentration was set to a low value (0.1 mmol/L cell). The estimated malate intracompartmental concentration had an upper value of 5.2 mmol/L cell in the mitochondria and 3.9 mmol/L cell in the cytosol, and lower values of 2.1 mmol/L cell and 0.8 mmol/L cell respectively. Given that high exchange between compartments quickly balances labeling between compartments, the exact values of malate concentration for each compartment cannot be determined. The  $\alpha$ -ketoglutarate concentration was high in the cytosol whereas citrate had a high concentration in the mitochondria. The high cytosolic  $\alpha$ -ketoglutarate concentration together with a low cytosolic concentration of citrate might be the reason why the observed activity of cytosolic isocitrate dehydrogenase towards  $\alpha$ -ketoglutarate synthesis was virtually zero as was also found by flux analysis in cancer cells (Metallo et al., 2012). Alanine had comparable concentrations in both compartments. Aspartate was concentrated in the mitochondria, but only the upper threshold of the cytosolic concentration could be estimated. A relatively high intracellular concentration of serine and glycine was also determined. The most concentrated metabolite was glutamate, with a mitochondrial concentration reaching almost 50 mmol/L cell, which might explain why

#### 4. High resolution $^{13}\text{C}$ metabolic flux analysis in CHO cells

---

glutamate is exported from the mitochondria to the cytosol. However, only the upper boundary of the cytosolic concentration of glutamate could be estimated (Fig. 4.10 A).

Citrate, glutamate and aspartate are exported with net fluxes from the mitochondria following the concentration gradient, while  $\alpha$ -ketoglutarate is exported against the concentration gradient. A high cytosolic  $\alpha$ -ketoglutarate concentration might be required to assist the various transamination reactions. All metabolites except  $\alpha$ -ketoglutarate were more concentrated in the mitochondria than in the cytosol. Also, the estimated concentrations of amino acids are higher than reported intracellular concentrations for CHO cells (Hansen and Emborg, 1994; Lu et al., 2005). By applying INST- $^{13}\text{C}$ CMFA, the average intracompartmental concentrations value might be overestimated as an effect of assigning negligible values to concentrations that are not estimated. However, since the dynamics of the MIDs depends on the pool size / flux ratio, the intracompartmental concentrations cannot be higher than their estimated upper boundary. Parameter estimation using INST- $^{13}\text{C}$ CMFA instead of experimental determination has the advantage that the concentrations are estimated *in vivo*, without the risk of metabolite leakage during quenching and extraction (Dietmair et al., 2010; Sellick et al., 2009; Wahrheit and Heinzle, 2014a; Wahrheit et al., 2011b). In addition, INST- $^{13}\text{C}$ CMFA provided a method to estimate intracompartmental concentrations of key metabolites of the central carbon metabolism, which was not yet achieved experimentally.

##### 4.3.8. Energy requirement and production

The energy requirement and production in the CHO-K1 cells was computed based on the intracellular fluxes (Fig. 4.9) and reaction stoichiometry (Suppl. Table 4.2). Excluding oxidative phosphorylation and mitochondrial ATP transport, the balance for ATP is positive in both compartments (Table 4.1). The main source of cytosolic ATP is glycolysis, and in the cytosol it is produced in the reaction catalyzed by succinate dehydrogenase, along with  $\text{FADH}_2$ . There is a small deficit of cytosolic NADH (i.e. electrons) which could be covered by reactions that were not included in the model. The value also falls within the standard deviation of the lactate secretion flux (Suppl. Fig. 4.1), which influences

#### 4. High resolution $^{13}\text{C}$ metabolic flux analysis in CHO cells

directly the flux of the reaction catalyzed by lactate dehydrogenase, where NADH is a cofactor, and also in the error for estimating the glycolysis flux based on glucose uptake.

As mentioned in subchapter 4.3.6, the high cytosolic NADPH production (Table 4.1) is most likely used to mitigate oxidative stress and to fuel fatty acid synthesis. The oxidation of NADH will consume  $348.8 \text{ mmol} \times (\text{L cell})^{-1} \times \text{h}^{-1} \text{ O}_2$ . Considering a 1/2.5 ratio of NADH/ATP and 1/1.5 for  $\text{FADH}_2/\text{ATP}$  for the process of oxidative phosphorylation (Hinkle, 2005) and the total consumption of NADH during this process, the total estimated production of ATP is  $1603.9 \text{ mmol} \times (\text{L cell})^{-1} \times \text{h}^{-1}$ , which is obviously much higher than the requirements for protein and nucleic acids production. Such a high production of ATP clearly points to the existence of futile cycles and various processes that consume energy in the CHO-K1 cells and are not related to the central carbon metabolism or growth. This reinforces the assumption that the CHO-K1 cells do not have as a cell objective optimal use of energy and resources, as bacteria are assumed to have, but another cell objective that at the moment one can only speculate about.

**Table 4.1.** Cofactor fluxes in the cytosol (c) and mitochondria (m) computed based on the intracellular fluxes in CHO-K1 cells for the 0-18h cultivation period

| Cofactor                             | Flux                                                             |
|--------------------------------------|------------------------------------------------------------------|
| *excluding oxidative phosphorylation | [ $\text{mmol} \times \text{L cell}^{-1} \times \text{h}^{-1}$ ] |
| $\text{ATP}_c^*$                     | 146.                                                             |
| $\text{ATP}_m^*$                     | 114.5                                                            |
| $\text{NADH}_c$                      | -33.0                                                            |
| $\text{NADH}_m$                      | 501.6                                                            |
| $\text{NADPH}_c$                     | 467.5                                                            |
| $\text{NADPH}_m$                     | 8.2                                                              |
| $\text{FADH}_{2m}$                   | 114.5                                                            |
| $\text{GTP}_c$                       | -66.4                                                            |
| $\text{GTP}_m$                       | -23.1                                                            |



#### 4. High resolution $^{13}\text{C}$ metabolic flux analysis in CHO cells

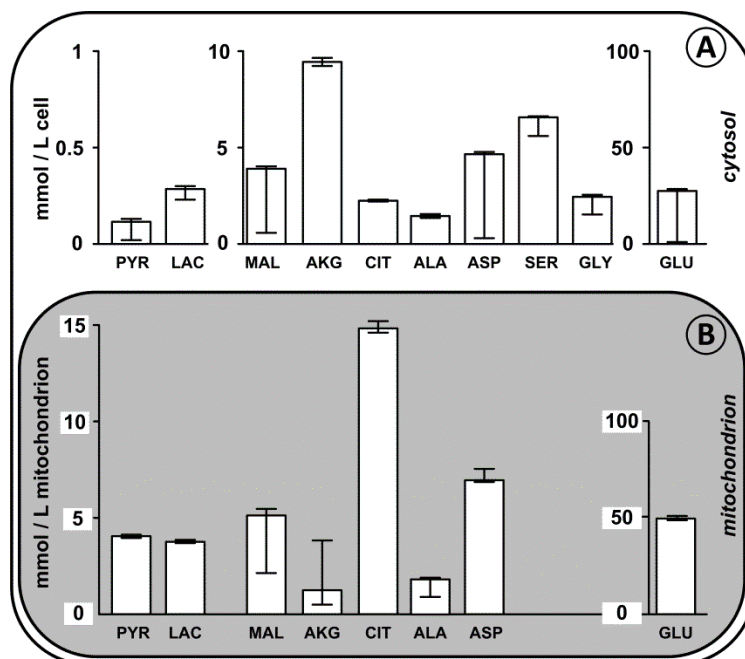


**Figure 4.10.** Cytosolic and mitochondrial concentrations of metabolites estimated using non-stationary  $^{13}\text{C}$  metabolic flux analysis by assuming a mitochondrial volume ratio of 20%. The error bar represents the 95% confidence interval evaluated by refitting the model until the minimized objective function took the value of  $\chi^2(0.95, \text{nr. experimental points} - \text{nr. parameters})$ . Abbreviations: AKG –  $\alpha$ -ketoglutarate; ALA – alanine; ASP – aspartate; CIT – citrate; GLU – glutamate; GLY – glycine; LAC – lactate; MAL – malate; PYR – pyruvate; SER – serine.

#### 4.4. Concluding Discussion

The fluxes and reversibility of the probably most complex metabolic network to date were estimated by applying INST- $^{13}\text{C}$ MFPA and using the intracellular and extracellular MID dynamics of metabolites obtained from two parallel labeling experiments with  $[\text{U-}^{13}\text{C}_6]$  glucose and  $[\text{U-}^{13}\text{C}_5]$  glutamine as labeled substrates. The labeling of MIDs was used during the exponential growth phase in the 2 – 18 h interval when the cells were at metabolic steady state. In the first 2 h of the labeling experiment, the MIDs of intracellular metabolites indicated a stress response to the cultivation condition. After 18 h, the metabolic state of the cells changed, visible by a shift in the MIDs of the metabolites. Most of the parameters were determined with narrow confidence intervals. They included: (1) metabolic fluxes in cycles and alternative pathways, (2) flux reversibility and (3) intracompartmental concentrations. This confirms that INST- $^{13}\text{C}$ MFPA

#### 4. High resolution $^{13}\text{C}$ metabolic flux analysis in CHO cells

---

is a powerful method that can resolve the metabolic fluxes in a network that included multiple mitochondrial transporters, reaction reversibility, metabolite exchange with the media and metabolite channeling. Consistent with our previous estimation for the CHO-K1 cell line (Nicolae et al., 2014), most of the glucose-6-phosphate was directed to the PPP, resulting in a high production of NADPH. Oxidative stress and fatty acid synthesis are the two main consumers of the cytosolic NADPH. The activity at the mitochondria – cytosol boundary is complex, involving intense metabolite trafficking and cycling. Malate and glutamate are both imported and exported via various mitochondrial carriers with the purpose of managing NADH distribution in the two compartments and providing antiport partners for other metabolites. The anaplerotic and cataplerotic fluxes were negligible with phosphoenolpyruvate-carboxykinase being the highest cataplerotic flux. The aspartate-malate shuttle consumed cytosolic NADH and produced mitochondrial NADH. Aspartate and alanine were synthesized in the mitochondria, and then transported to the cytosol. However, this is only a single metabolic state of the CHO-K1 cells. It was evidenced that there are significant differences between the metabolic fluxes in CHO-K1 cells in different cultivation setups (shake flask vs. reactor), even if the two cultivations used the same cell line and the same media and the sampling was done during the exponential growth phase.

A most interesting finding was related to the different labeling patterns in intracellular and extracellular lactate, which could not be explained by cytosol-mitochondria compartmentation. Four pyruvate pools were included, two dead-end lactate pools and extracellular lactate production channeling for modeling the observed difference in labeling. The results show that a large mitochondrial lactate pool is maintained, most likely to control the mitochondrial NADH content. Also, due to channeling of lactate production, the cytosolic lactate concentration is very small. Because the fitting of intracellular lactate left room for improvement, it is possible that the network configuration around the pyruvate nodes consists of more complex micro-compartmented structures (al-Habori, 1995). Such complexity is both a hindrance and an opportunity for INST- $^{13}\text{C}$ MFA to characterize metabolic networks. Observed

#### **4. High resolution $^{13}\text{C}$ metabolic flux analysis in CHO cells**

---

mitochondrial pyruvate channeling could be caused by the partial association between the recently discovered pyruvate transporter and pyruvate dehydrogenase. A systems biology approach that combines biological knowledge from experiments that unravel the spatial structure of the mammalian cell metabolism with realistic mathematical models is the strategy to follow when studying metabolic networks. Ideally, such strategy accepts feedback for guiding future experiments and creating new modeling paradigms that include the spatial organization of the metabolism.

### Supplementary data 4

**Supplem. Figure 4.1.** Cultivation profile of the CHO-K1 cells culture during 48 h in 250 ml baffled shake flask with a working volume of 120 mL. The represented extracellular concentrations are in  $[\mu\text{mol} / \text{L}]$  and the time is in [h]. The values represent the average from 4 parallel cultivations. The curves are the fitted values of extracellular concentrations simulating an exponential growth model with balanced growth (metabolic steady state) over the first 18 h.

**Supplem. Table S4.1.** List of reactions used in the stoichiometric model for dynamic metabolic flux analysis.

**Supplem. Table S4.2.** List of metabolic reactions, fluxes and reversibilities in the central carbon metabolism of CHO-K1 estimated for the first 2 – 18 h cultivation period. Carbon transfer rules are given in the parentheses for each reaction. Reversible reactions are indicated by double arrows. Reversibility is computed as the ratio between the reverse flux and the net flux. The 95% confidence interval was evaluated by refitting the model until the minimized objective function took the value of  $\chi^2(0.95, \text{nr. experimental points} - \text{nr. parameters})$ .

**Supplem. Table S4.3.** Experimental (exp) and simulated (sim) mass isotopomer distributions of extracellular metabolites and standard deviations (SD) used in simulations. (\_ex – extracellular; \_cell – intracellular);

**Supplem. Table S4.4.** Extracellular concentrations sampled in a 100 mL shake flask culture of CHO-K1 cells. (AVG – average from 4 parallel cultivations; SD – standard deviation)

### Chapter 5

#### 5. Identification of active elementary flux modes in mitochondria using selectively permeabilized CHO cells<sup>\*3</sup>

##### Abstract

The mitochondrial metabolism of the economically important Chinese hamster ovary (CHO) cells was accessed using selective permeabilization. Key substrates were tested without and with addition of ADP. Based on quantified uptake and production rates, it was possible to determine the contribution of different elementary flux modes to the metabolism of a substrate or substrate combination. ADP stimulated the uptake of most metabolites, directly by serving as substrate for the respiratory chain, thus removing the inhibitory effect of NADH, or as allosteric effector. Addition of ADP favored substrate metabolization to CO<sub>2</sub> and did not enhance the production of other metabolites. The controlling effect of ADP was more pronounced when metabolites were supplied to the first part of the TCA cycle: pyruvate, citrate,  $\alpha$ -ketoglutarate and glutamine. In the second part of the TCA cycle, the rates were primarily controlled by the concentrations of C<sub>4</sub>-dicarboxylates. Without ADP addition, the activity of the pyruvate carboxylase – malate dehydrogenase – malic enzyme cycle consumed the ATP produced by oxidative phosphorylation, preventing its accumulation and maintaining metabolic steady state conditions. Aspartate was taken up only in combination with pyruvate, whose uptake also increased, a fact explained by complex regulatory effects. Isocitrate dehydrogenase and  $\alpha$ -ketoglutarate dehydrogenase were identified as the key regulators of the TCA cycle, confirming existent knowledge from other cells. It was shown that selectively permeabilized cells combined with elementary mode analysis allow in-depth studying of the mitochondrial metabolism and regulation.

<sup>\*3</sup>A version of this chapter was submitted as an article to Metabolic Engineering Journal (November 2014). All experimental work described herein was carried out by Judith Wahrheit, Christian Weyler and Yannic Nonnenmacher.

### 5.1. Introduction

Eukaryotic cells are able to tune their complex metabolism through compartmentation. This involves confining reactions to designated compartments and controlling the access of metabolites through specific transporters. Mitochondria play an important part in the organization of the eukaryotic cell metabolism (Wahrheit et al., 2011a). They work as the powerhouse of the cell, being responsible for the TCA cycle, oxidative phosphorylation and other essential reactions in the central carbon metabolism. Furthermore, mitochondria play a key role in the signaling processes leading to apoptosis (Kroemer et al., 2007). Mitochondrial dysfunctions are associated with the aging process and with a wide range of human diseases (Calvo et al., 2006; Duchen, 2004; Lemasters, 2007; Moreno-Sanchez et al., 2014; Nassir and Ibdah, 2014; Raimundo et al., 2011; Thiele et al., 2005). Metabolite traffic between cytosol and mitochondria is mediated by carriers. These carriers, excellently reviewed by Palmieri (Palmieri, 2013), have important roles in physiological and pathological processes (Gutierrez-Aguilar and Baines, 2013). Studies related to mitochondrial function and metabolism focused on isolated features, like respiration and the respiratory chain (Frezza et al., 2007; Kuznetsov et al., 2008) or on the function of single mitochondrial transporters. Even after the advent of the systems biology era, studies of the mitochondrial metabolic network as a whole remain scarce (Balaban, 2006). So far, the most complex studies related to mitochondrial metabolism used enzyme kinetics, but their results are limited by insufficient knowledge about regulation and parameter values (Wu et al., 2007). Studying the mitochondrial metabolism in whole cells is complicated by the overlapping with other cellular reactions and by the limited accessibility of the mitochondria. Selective permeabilization using digitonin (Kuznetsov et al., 2008) is a simple and efficient way to access mitochondria while maintaining their functionality (Bahnemann et al., 2014).

Because mitochondria are capable of taking up several metabolites, either alone or in combination, process them through their metabolic network and secrete resulting metabolites, new methods are required for analyzing the data obtained from studies of

## 5. Identification of elementary flux modes in mitochondria

---

the mitochondrial metabolism. Elementary Mode Analysis (EMA) (Papin et al., 2004; Schuster et al., 2000) based on network stoichiometry generates all minimal subsets of reactions that can function as standalone metabolic units. Any observed flux distribution can be written as a linear combination of elementary modes. Therefore, the contribution of a reaction to the metabolic fluxes can be assessed by determining its participation and its flux values in the elementary modes. EMA has been used to study metabolic networks (Kaleta et al., 2009; Schwartz and Kanehisa, 2006), discover targets for metabolic engineering and drug development (Beuster et al., 2011) and to identify high-yield mutants of producer strains (Carlson et al., 2002; Neuner and Heinzle, 2011). The main application of EMA remains the microbial metabolism because available genome annotations and the relatively small network size allow genome-scale analyses. Stoichiometric analysis is however gaining an increasingly important role in studying mammalian cells (Orman et al., 2010; Orman et al., 2011; Schiff and Purow, 2009; Zamorano et al., 2012).

CHO cells are the mammalian workhorse in the biotechnology industry, responsible for the biggest share of biopharmaceuticals production (Jayapal et al., 2007; Walsh, 2010). The wealth of studies using CHO cells as model system has led to them being nicknamed the “mammalian equivalent of *E. coli*” (Puck, 1985). They are characterized by the ability to grow in suspension cultures using chemically defined media, can reach high cell densities and high product titers of recombinant proteins. The availability of recently published CHO genome and other omics data (Becker et al., 2011; Brinkrolf et al., 2013; Hackl et al., 2011; Xu et al., 2011) facilitates network studies.

The application of mitochondria-wide metabolic networks adds a new dimension to the analysis of mitochondrial metabolism. It permits access for studying interactions of several processes, e.g. transport, metabolite conversion, respiration as well as their control. This can be done in a most directed way by using intact mitochondria made accessible by selective permeabilization of the cell membrane. EMA was used to study the metabolism of CHO-K1 mitochondria made accessible through selective permeabilization.

## 5. Identification of elementary flux modes in mitochondria

---

Key substrates were screened for their ability to be metabolized by the permeabilized cells, both alone or with addition of ADP. The uptake and production of metabolites was then quantified. The observations were used to compute the contribution of mitochondrial elementary modes to the metabolic flux distribution in each tested case. Therefore, this analysis reaches beyond mere metabolic flux analysis by providing additional information, e.g. on the coupling of processes or on the control of metabolic pathways. Furthermore, the effect of ADP stimulation was quantified and metabolic bottlenecks were evidenced. Overall, it was demonstrated that great opportunities arise by applying this methodology to study the mitochondrial metabolism. For future studies it can easily be combined with other well-established methods, e.g. respiration analysis.

### 5.2. Materials and methods/Experimental

#### 5.2.1. Cell culture

Cultivation of the CHO-K1 cells was performed in baffled shake flasks (250 ml, Corning, New York, USA) in a shaking incubator (Innova 4230, New Brunswick Scientific, Edison, NJ, USA) at 135 rpm (2 inches orbit), 37°C and 5% CO<sub>2</sub>. The cells were cultivated in chemically defined, protein-free TC-42 medium (TeutoCell, Bielefeld, Germany), supplemented with 6 mM L-glutamine (Sigma-Aldrich, Steinheim, Germany) from a 240 mM stock solution in dH<sub>2</sub>O. The cells were passaged at the latest 72 h after inoculation and seeded with a cell density of  $4 - 5 \times 10^5$  cells/mL.

#### 5.2.2. Preparation of mitochondrial medium

The mitochondrial medium used in this study was derived from different media used for the assessment of respiration in isolated mitochondria (Madeira, 2012) and optimized with respect to osmolarity and ionic strength. The composition of the mitochondrial medium was as follows: 9.6 mM K<sub>2</sub>HPO<sub>4</sub>, 2.4 mM KH<sub>2</sub>PO<sub>4</sub>, 80 mM KCl, 75 mM sorbitol, 2 mM MgCl<sub>2</sub> and 100 µM EGTA. The pH was set to 7.4 with 5 N KOH. The individual components have been chosen to minimize interactions with the downstream analytics (MALDI-ToF, HPLC).



### 5.2.3. Mitochondrial transport experiments

The experimental set-up is schematically depicted in Fig. 5.1 and the different tested substrates and substrate combinations are listed in Table 5.1. CHO-K1 cells were harvested from a culture in the early exponential growth phase (48 - 50 h after inoculation) by centrifugation (5 min,  $125 \times g$ , Labofuge 400R, Function Line, Heraeus Instruments, Hanau, Germany). The supernatant was discarded quantitatively and the cells were resuspended in mitochondrial medium. Afterwards, the cell number was determined using an automated cell counter (*Countess® Automated Cell Counter*, Invitrogen, Karlsruhe, Germany) and set to  $10^7$  cells/mL by adding mitochondrial media. Selective permeabilization of the cytosolic membrane was performed by adding 0.01 % (w/v) digitonin from a 1% stock solution in dH<sub>2</sub>O and verified under the microscope using the Trypan blue exclusion method. 5 mL of permeabilized cell suspension were transferred into a 50 mL filter-tube bioreactor (TPP, Trasadingen, Switzerland) containing 5 mL of the respective substrate solution (2-fold concentrated in respiration medium). The final cell concentration was  $5 \times 10^6$  cells/mL, the final concentration of tested substrates was 4 mM. Considering that the average cell diameter of the CHO line was 10.6  $\mu\text{m}$ , a corresponding cell volume of  $6.23 \times 10^{-16} \text{ m}^3$  (=0.6 pL) was calculated. Cytosolic volume was therefore diluted with a factor of at least about 3200. Afterwards, incubation was performed for 150 min in a shaking incubator (Innova 4230, New Brunswick Scientific, Edison, NJ, USA) at 135 rpm (2 inches orbit), 37°C and 5 % CO<sub>2</sub>.

For experiments without ADP-stimulation, 400  $\mu\text{L}$  samples were taken every 30 min. The samples were centrifuged (5 min,  $6000 \times g$ , Biofuge pico, Heraeus Instruments, Hanau, Germany) and the supernatants were frozen for subsequent analysis. For experiments with ADP-stimulation, 100  $\mu\text{L}$  of 100 mM ADP (resolved in respiration medium) were added every 30 min. 350  $\mu\text{L}$  samples were taken before and after each addition of ADP. The samples were centrifuged (5 min,  $6000 \times g$ , Biofuge pico, Heraeus Instruments, Hanau, Germany) and the supernatants were frozen at -20°C for subsequent analysis.

## 5. Identification of elementary flux modes in mitochondria

Metabolites in these samples were identified using MALDI-ToF and quantified using HPLC.

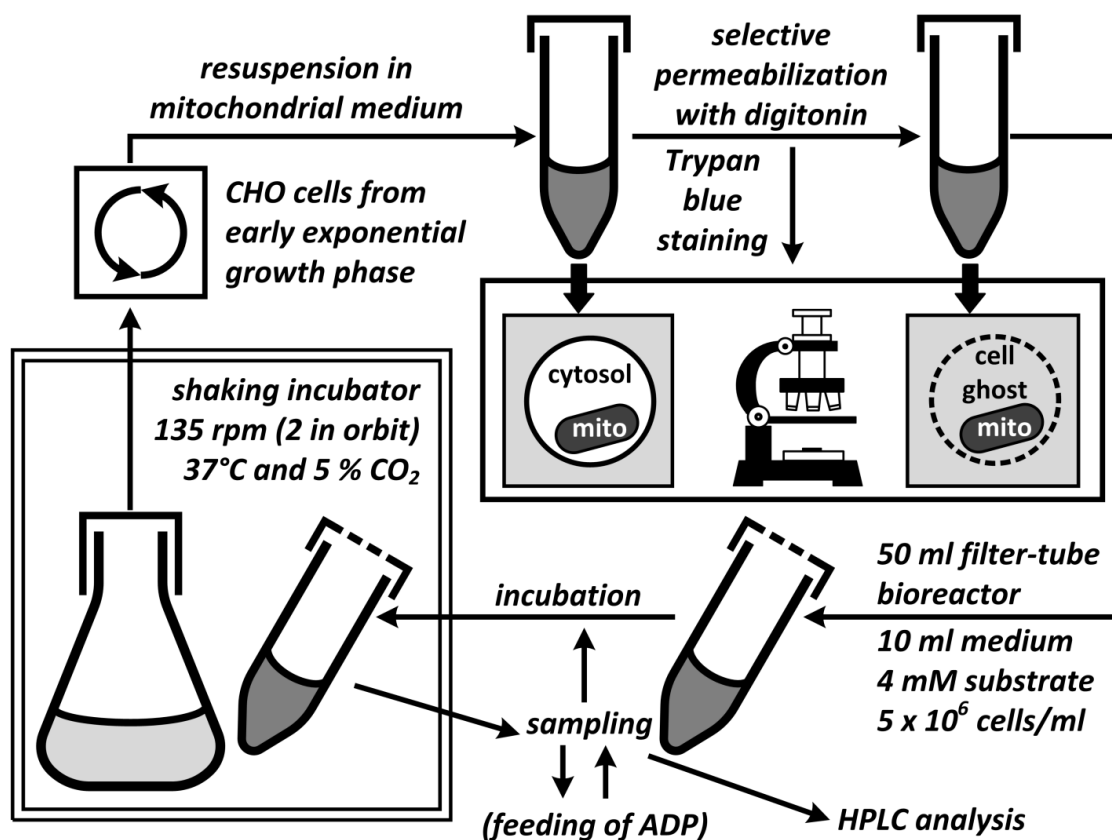


**Figure 5.1.** Experimental set-up for mitochondrial transport studies. CHO cells from the early exponential growth phase were harvested and resuspended in mitochondrial medium. Selective plasma membrane permeabilization with 0.01% (w/v) digitonin was microscopically verified using Trypan blue staining. Permeabilized cells were transferred into filter-tube bioreactors, mixed with a mitochondrial substrate and incubated in a shaking reactor for mitochondrial transport studies. Sampling (and ADP feeding) was performed every 30 min.

### 5.2.4. Analytical determination of organic acids and amino acids

Quantification of tested substrates and resulting products was performed by different established HPLC methods as described previously (Strigun et al., 2011). In the presence of ADP, citrate could not be quantified at low concentrations because of an unresolvable overlay of metabolite peaks in the chromatogram. Identification of organic acids was confirmed by MALDI-TOF MS (matrix-assisted laser desorption/ionization time-of-flight mass-spectrometry) analysis.

## 5. Identification of elementary flux modes in mitochondria

**Table 5.1.** Substrates and substrate combinations used for metabolization by selectively permeabilized CHO-K1 cells.

| without ADP stimulation |                         | with ADP stimulation |                              |
|-------------------------|-------------------------|----------------------|------------------------------|
| No.                     | Substrate(s)            | No.                  | Substrate(s)                 |
| 1a                      | pyruvate                | 1b                   | pyruvate, ADP                |
| 2a                      | pyruvate, aspartate     | 2b                   | pyruvate, aspartate, ADP     |
| 3a                      | citrate                 | 3b                   | citrate, ADP                 |
| 4a                      | $\alpha$ -ketoglutarate | 4b                   | $\alpha$ -ketoglutarate, ADP |
| 5a                      | succinate               | 5b                   | succinate, ADP               |
| 6a                      | fumarate                | 6b                   | fumarate, ADP                |
| 7a                      | malate                  | 7b                   | malate, ADP                  |
| 8a                      | glutamine               | 8b                   | glutamine, ADP               |
| 9a                      | glutamate               | 9b                   | glutamate, ADP               |
| 10a                     | aspartate               | -                    | -                            |
| 11a                     | serine                  | -                    | -                            |

Since the analytes were negatively charged, the mass spectrometer (ABI 4800, Applied Biosystems, Foster City, USA) was operated in negative ion mode. The used laser is a Nd:YAG solid-state laser (neodymium-doped yttrium aluminum garnet) emitting UV radiation with a wavelength of 355 nm by third harmonic generation. The laser intensity was set to 3700 and the number of shots per spot was 1250. The flight distance of the ions was doubled by using the reflector-mode, thus achieving an improved mass accuracy. Prior to MALDI-TOF MS measurements, the samples were diluted 1:10 with dH<sub>2</sub>O. This was necessary due to the high content of phosphate in the buffer (12 mM), which might disturb the measurement by signal suppression. 30  $\mu$ L of diluted sample were mixed with 30  $\mu$ L of matrix (9 mg/mL 9-aminoacridine in methanol) and 0.5  $\mu$ L of this mixture were spotted on a 384-spot MALDI target (Applied Biosystems, Foster City, USA).

### 5.2.5. Mitochondrial network

The model of the mitochondrial reaction network of the CHO-K1 cells (Fig. 5.2) was reconstructed using the published genome annotation (Hammond et al., 2012). The connection with the extramitochondrial medium is made through carrier-mediated transport for large molecules (e.g. amino acids, organic acids, ATP/ADP) and free diffusion for small uncharged molecules i.e. O<sub>2</sub>, CO<sub>2</sub> and NH<sub>3</sub>. The initially formulated


## 5. Identification of elementary flux modes in mitochondria

---

network model was reduced by removing reactions and metabolites that cannot contribute to the observed uptake and production. Information about compartmentation of enzyme activity as determined by Wahrheit et al. (Wahrheit et al., 2014b) for the same cell line was also considered. Accordingly, mitochondrial NADP<sup>+</sup>-dependent malic enzyme (ME) was active and mitochondrial PEP carboxykinase was not active. Carriers that transport C<sub>4</sub>-dicarboxylates did not discriminate between succinate and malate. With the exception of  $\alpha$ -ketoglutarate, glutamine, oxygen and pyruvate, all other metabolites are transported reversibly. NAD(P)<sup>+</sup> transhydrogenase was added to account for transferring electrons from NADPH to NADH. The applied stoichiometry of oxidative phosphorylation was 2.5 moles of ATP per mole of NADH and 1.5 moles of ATP per mole of FADH<sub>2</sub> (Hinkle, 2005). In our model, succinyl-CoA ligase used only ADP, and isocitrate dehydrogenase (IDH) isoenzymes and glutamate dehydrogenase (GDH) used only NAD<sup>+</sup>. Phosphate and NH<sub>3</sub> transport were not included in the stoichiometric model. The contribution of extramitochondrial reactions could be excluded because most of the possible reactions involving the added substrates or metabolites exported from the mitochondria require either cofactors (NADH, NADPH, etc.) or other reaction partners that were not present in the extramitochondrial media. Due to more than 3000-fold dilution by the selective permeabilization procedure, these metabolites had concentrations too low to be detectable. Also, systems for regenerating cofactors are absent. In order to prove these assumptions we demonstrated that pyruvate consumption was strictly dependent on mitochondrial activities (Suppl. Fig. S1). Pyruvate consumption was completely prevented by inhibition of the mitochondrial pyruvate carrier using  $\alpha$ -cyano-4-hydroxycinnamate. The only possible extramitochondrial reactions are those that do not need any other substrates than those sampled in the media, e.g. fumarase that only requires water as co-substrate.

## 5. Identification of elementary flux modes in mitochondria

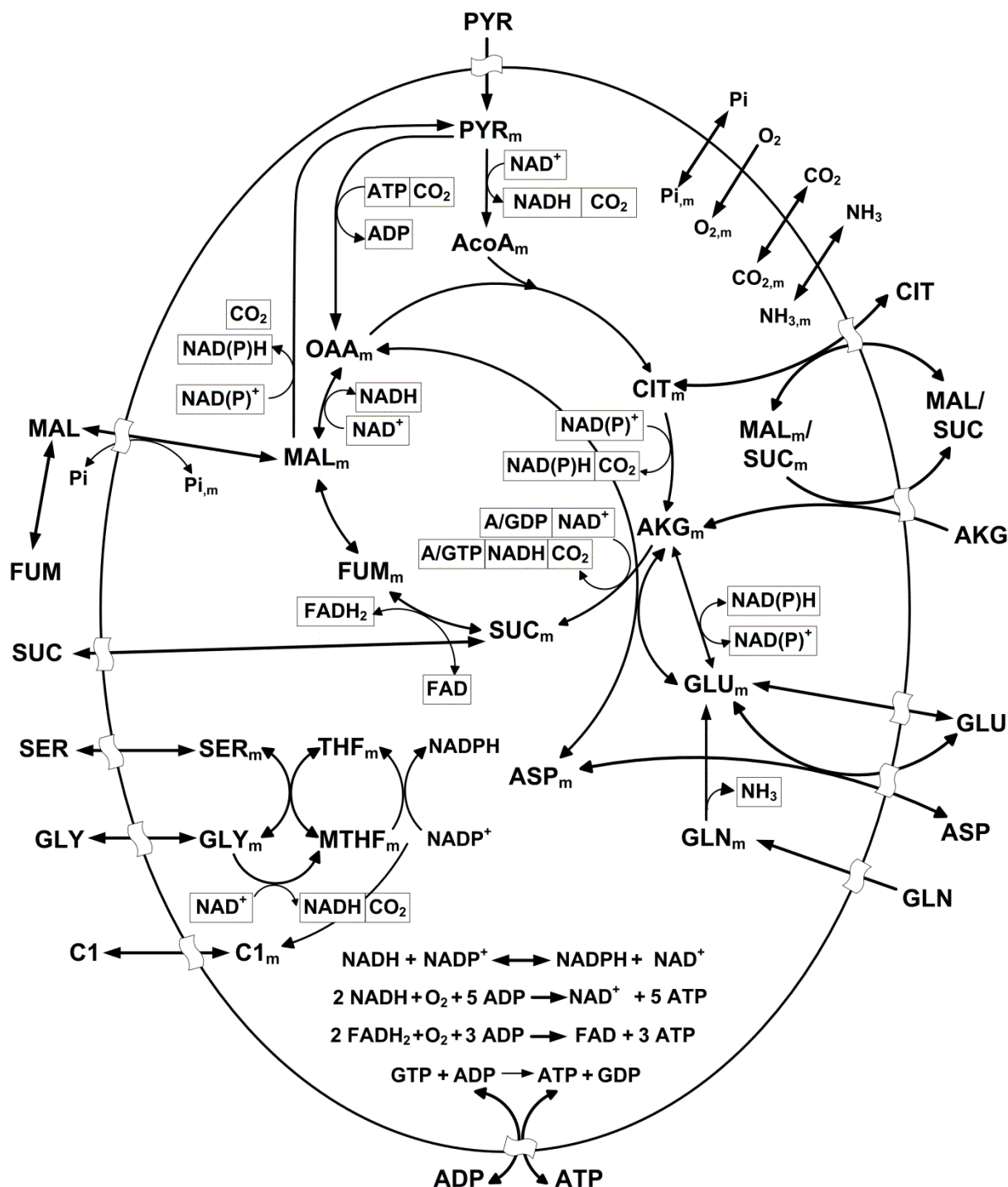


**Figure 5.2.** Metabolic network of the CHO-K1 mitochondria built based on genome annotation.  - Mitochondrial carrier. Subscripts: *m* - mitochondrial. Abbreviations: AcoA - acetyl-CoA; AKG - α-ketoglutarate; ASP - aspartate; C1 - one-carbon units; CIT - citrate; FUM - fumarate; GLN - glutamine; GLU - glutamate; GLY - glycine; MAL - malate; MTHF - 5-methyltetrahydrofolate; OAA - oxaloacetate; PYR - pyruvate; SER - serine; SUC - succinate; THF - tetrahydrofolate

### 5.2.6. Elementary mode analysis

The elementary modes of the mitochondrial network were computed using the *EFMtool* software (Terzer and Stelling, 2008). An algorithm was then used to identify, from all the elementary modes, the modes that can contribute to the conversion of each tested substrate or substrate combinations. This meant: (1) selecting the modes that take up any combination of the tested substrates from Table 5.1 and then (2) selecting the modes that exclude production of metabolites that were not observed. All possible modes involving CO<sub>2</sub> were included, though CO<sub>2</sub> itself was not measured. The selection is listed in the Suppl. Table S1. An observed flux set  $v$  can be expressed as a linear combination of elementary modes

$$v = \sum_{j=1}^M \alpha_j \cdot EM_j \quad (5.1)$$

where  $M$  is the total number of elementary modes described by the column vectors  $EM$  containing the mode stoichiometry. The size of matrix  $EM$  is  $R \times M$ , where  $R$  is the number of reactions. The weight coefficients  $\alpha_j$  are usually not unique, as the number of elementary modes can exceed the dimension of the flux cone. By simplifying the  $EM$  matrix using the experimental observations and the selection algorithm, a new matrix  $EM^\#$  was defined that contains only the transport reactions results. The size of the new matrix will be  $R^\#$  by  $M^\#$ , where  $R^\#$  is the number of transport reactions that contribute to the observed extracellular fluxes and  $M^\#$  is the number of modes selected using the algorithm. The mode flux  $\alpha$  representing the contribution of each mode to the measured fluxes was computed when the matrix  $EM^\#$  was invertible:

$$\alpha = EM^{\#-1} \times v \quad (5.2)$$

In some cases, assumptions were made in order to obtain an invertible  $EM^\#$ . These are described in the Results and Discussion section, separately for each tested substrate.

### 5.2.7. Metabolic flux analysis

Mitochondrial fluxes were computed for each feeding situation (Table 5.1) using the stoichiometry of the network from Fig. 5.2, the computed extracellular rates and by assuming no pyruvate carboxylase activity in the presence of ADP. The complete stoichiometry and the results are given in Supplem. Table S5.2.

## 5.3. Results and Discussion

### 5.3.1. Mitochondrial uptake and production of metabolites

In a previous study, a high-throughput respiration screening method was applied to verify the uptake and metabolization of a range of potential mitochondrial substrates (Wahrheit et al., 2015). The outcome of this screening served as starting point to design further in-depth mitochondrial studies.

Here, an extended experimental set-up (Fig. 5.1) was used to investigate the mitochondrial metabolism of CHO cells. The mitochondrial metabolism in selectively permeabilized cells was stimulated by addition of selected substrates or combinations of substrates and quantified mitochondrial uptake and production of metabolites (Table 5.2) by fitting the extracellular concentrations over time (Supplem. Fig. S5.2).

Metabolite uptake and production rates remained constant over time (Supplem. Fig. S5.2). This proves that the mitochondria remained intact and functioned at metabolic steady state throughout the sampling period. It was already shown by Deshpande et al. (Deshpande et al., 2009) that CHO cells can be maintained at metabolic steady state in defined media. Mitochondrial uptake of aspartate alone was not observed. However, aspartate was taken up when fed in combination with pyruvate. Uptake rates of single substrates increased in the order of glutamate, serine, pyruvate, citrate,  $\alpha$ -ketoglutarate, malate, glutamine, and succinate, with the uptake rate for succinate being 7.3 times (C-mol/C-mol) higher than that of glutamate (Table 5.2). Addition of ADP stimulated the uptake and excretion of metabolites by the mitochondria. With feeding of ADP, uptake

## 5. Identification of elementary flux modes in mitochondria

rates were all higher, increasing in the order of aspartate, pyruvate, malate, succinate, citrate,  $\alpha$ -ketoglutarate, and glutamine (Table 2). In this case, the uptake rate of glutamine was 4.6 times higher than the uptake of aspartate (C-mole/C-mole). It was observed that the highest impact of ADP on stimulating the uptake of citrate and  $\alpha$ -ketoglutarate. ADP addition doubled the uptake of aspartate, from 6.1 to 12.2 fmol / (cell  $\times$  min), but not of pyruvate, that increased only by 3.7 fmol / (cell  $\times$  min) when both substrates were fed in combination.

In accordance with previous mitochondrial studies using respiration analysis (Wahrheit et al., 2015), the following trends were observed: (1) stimulation of mitochondrial metabolism by addition of ADP, (2) without addition of ADP the highest respiration and uptake was observed on succinate, (3) relatively minor impact of ADP on stimulating the metabolization of malate and succinate, (4) relatively higher impact of ADP stimulation on the uptake of citrate and glutamine.

**Table 5.2.** Uptake and production rates of metabolites by the selectively permeabilized CHO-K1 cells [fmol / (cell  $\times$  min)] and the computed 95% confidence intervals (C.I.) given in square brackets. n.m. – not measured.

| No. | Substrate                      | Uptake rate<br>[95% C.I.]                     | Product                                          | Production rate<br>[95% C.I.]                               |
|-----|--------------------------------|-----------------------------------------------|--------------------------------------------------|-------------------------------------------------------------|
| 1a  | pyruvate                       | 4.6 [3.4, 5.7]                                | CO <sub>2</sub>                                  | n.m.                                                        |
| 1b  | pyruvate<br>ADP                | 14.2 [12.6, 15.9]<br>n.m.                     | CO <sub>2</sub><br>ATP                           | n.m.<br>n.m.                                                |
| 2a  | pyruvate<br>aspartate          | 11.9 [10.2, 13.5]<br>6.1 [4.0, 8.2]           | glutamate<br>CO <sub>2</sub>                     | 3.0 [2.5, 3.6]<br>n.m.                                      |
| 2b  | pyruvate<br>aspartate<br>ADP   | 15.6 [13.8, 17.3]<br>12.2 [6.9, 17.6]<br>n.m. | glutamate<br>CO <sub>2</sub><br>ATP              | 6.7 [5.4, 8.0]<br>n.m.<br>n.m.                              |
| 3a  | citrate                        | 5.6 [3.7, 7.5]                                | CO <sub>2</sub>                                  | n.m.                                                        |
| 3b  | citrate<br>ADP                 | 38.0 [25.4, 50.6]<br>n.m.                     | CO <sub>2</sub><br>ATP                           | n.m.<br>n.m.                                                |
| 4a  | $\alpha$ -ketoglutarate        | 12.7 [8.1, 17.3]                              | fumarate<br>CO <sub>2</sub>                      | 0.48 [0.46, 0.50]<br>n.m.                                   |
| 4b  | $\alpha$ -ketoglutarate<br>ADP | 40.2 [30.8, 49.6]<br>n.m.                     | fumarate<br>CO <sub>2</sub><br>ATP               | 2.5 [2.2, 2.7]<br>n.m.<br>n.m.                              |
| 5a  | succinate                      | 24.5 [19.1, 29.9]                             | fumarate<br>malate<br>citrate<br>CO <sub>2</sub> | 2.2 [1.7, 2.8]<br>14.5 [11, 17.9]<br>1.9 [0.9, 2.8]<br>n.m. |



## 5. Identification of elementary flux modes in mitochondria

|       |                           |                                             |                                                         |                                                             |
|-------|---------------------------|---------------------------------------------|---------------------------------------------------------|-------------------------------------------------------------|
| 5b    | succinate<br>ADP          | 30.5 [27.1, 33.9]<br>n.m.                   | fumarate<br>malate<br>citrate<br>CO <sub>2</sub><br>ATP | 2.1 [1.5, 2.8]<br>14.6 [10.7, 18.5]<br>n.m.<br>n.m.<br>n.m. |
| 6a/7a | malate<br>fumarate        | 14.6 [10.2, 19]<br>1.9 [0.9, 2.9]           | citrate<br>CO <sub>2</sub>                              | 4.9 [3.7, 6.0]<br>n.m.                                      |
| 6b/7b | malate<br>fumarate<br>ADP | 19.7 [14.6, 24.8]<br>1.7 [0.9, 2.5]<br>n.m. | citrate<br>CO <sub>2</sub><br>ATP                       | n.m.<br>n.m.<br>n.m.                                        |
| 8a    | glutamine                 | 20.0 [17.9, 22.1]                           | glutamate<br>aspartate<br>CO <sub>2</sub>               | 14.4 [11.4, 17.4]<br>3.3 [2.4, 4.2]<br>n.m.                 |
| 8b    | glutamine<br>ADP          | 44.7 [35.7, 53.7]<br>n.m.                   | glutamate<br>aspartate<br>CO <sub>2</sub><br>ATP        | 19.0 [15.4, 22.6]<br>11.4 [9.98, 12.9]<br>n.m.<br>n.m.      |
| 9a    | glutamate                 | 2.69 [1.22, 4.16]                           | aspartate<br>CO <sub>2</sub>                            | 3.38 [2.61, 4.15]<br>n.m.                                   |
| 9b    | glutamate<br>ADP          | 3.99 [-14.2, 22.2]<br>n.m.                  | aspartate<br>CO <sub>2</sub><br>ATP                     | 15.5 [13.0, 18.0]<br>n.m.<br>n.m.                           |
| 11a   | serine                    | 4.5 [2.3, 6.7]                              | glycine                                                 | 2.6 [2.0, 3.2]                                              |

### 5.3.2. Connection of tested substrates and observed products using elementary mode analysis

The mitochondrial elementary modes that connect tested substrates and observed products were selected. A total of 1780 elementary modes were generated by applying the *EFMTool* (Terzer and Stelling, 2008) to the network shown in Fig. 5.2, reduced as described in the Materials and Methods section and summarized in Supplem. Table S5.2. The partitioning of a substrate metabolism into different modes was calculated (Fig. 5.3), which was selected using the criteria specified in Supplem. Table S5.1. The production rate of a metabolite from a substrate or a combination of substrates is a linear combination of all modes that achieve the conversion. The case presented in Fig. 5.3 allows to compute the mode fluxes through A, B and C if the uptake of Substrate 1 and Substrate 2, as well as the production of Product 1 and Product 2 are measured. However, there were situations when the matrix describing the linear system relating mode fluxes to external fluxes (eq. 2) was not invertible. The contribution of each mode to the metabolism of all substrates was calculated without supplementary assumptions with the

## 5. Identification of elementary flux modes in mitochondria

---

following exceptions: (1) when pyruvate and aspartate were used together (Table 5.2), (2) when succinate and malate were used with ADP because citrate could not be experimentally determined, and (3) when glutamate was used, due to experimental noise. Situations that require reuptake of metabolites via antiport were also removed as including them would result in futile cycling between mitochondria and the extramitochondrial media. The selected modes and their computed contribution to each observed flux are given in Supplem. Table S5.3.

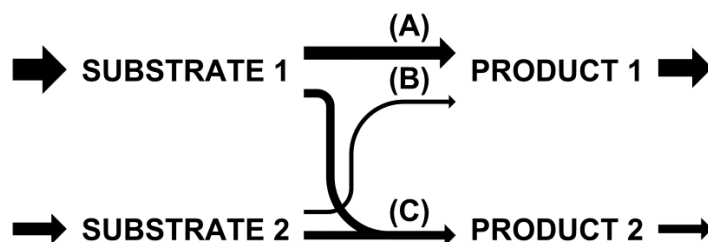


**Figure 5.3** - Example of establishing the partitioning of Substrate 1 and Substrate 2 into the elementary modes (A), (B) and (C) for yielding Product 1 and Product 2. The thickness of the arrows indicates the theoretical flux through each elementary mode.

### 5.3.3. General characteristics

While in the majority of cases a full metabolization to CO<sub>2</sub> was possible, many substrates led to partial TCA cycle activity and to secretion of metabolites. All experiments where ADP was supplied exhibited higher uptake rates for all tested substrates. This happens mainly because (1) ADP increases the availability of NAD<sup>+</sup> via the respiratory chain and (2) ADP stimulates pyruvate dehydrogenase, isocitrate dehydrogenase and  $\alpha$ -ketoglutarate dehydrogenase (AKGDH), three key enzymes responsible for controlling the TCA cycle (Michal and Schomburg, 2012; Strumilo, 2005). In the modes where ADP is not supplied, the pyruvate carboxylase (PCX) – malate dehydrogenase (MDH) – malic enzyme (ME) cycle is highly active to consume the excess of ATP produced by oxidative phosphorylation. It was shown earlier that ME is active in the mitochondria of the CHO-K1 cell line (Wahrheit et al., 2014b). PCX was found in the mitochondria of mouse cells (Da Cruz et al., 2003; Mootha et al., 2003) and was also evidenced as a necessary flux in CHO cells (Goudar et al., 2010; Nicolae et al., 2014; Sheikholeslami et al., 2013; Templeton

## 5. Identification of elementary flux modes in mitochondria

---

et al., 2013). Using  $^{13}\text{C}$  metabolic flux analysis (Nicolae et al., 2014), a PCX flux equivalent to  $1.56 \text{ fmol} / (\text{cell} \times \text{min})$  was calculated. The activity *in vivo* is approx. 150-fold times smaller than the maximum activity computed for permeabilized cells in the absence of ADP. This fact indicates the regulatory effect of ATP/ADP ratio on the PCX. The PCX – MDH – ME cycle is the rate-limiting element in metabolizing substrates in the absence of ADP since  $\text{NAD}^+$  and FAD are not regenerated in the respiratory chain, while accumulated ATP and NADH inhibit most enzymes involved in the TCA cycle (Michal and Schomburg, 2012). ME was responsible for replenishing pyruvate from malate to produce the acetyl-CoA required for initiating the citrate synthase reaction when pyruvate was not added. The modes that use the PCX – MDH – ME cycle to consume ATP were not considered when computing the mode fluxes with added ADP, although it would be theoretically possible for them to contribute to the observations. Using this assumption, the cells dispose of the produced ATP only by antiport with ADP. This is a valid assumption considering that PCX is strongly inhibited by high ADP concentrations (Keech and Utter, 1963; Walter and Stucki, 1970).

In the mitochondria, glutamate dehydrogenase and isoenzymes of IDH can use both  $\text{NAD}^+$  and  $\text{NADP}^+$  as cofactors. NADPH produced by  $\text{NADP}^+$ -dependent malic enzyme, glutamate dehydrogenase and IDH is oxidized by the transhydrogenase enzyme and NADH is produced. The conversion of NADPH is coupled with pumping  $\text{H}^+$  out of the mitochondria thereby contributing to building up the proton gradient across the inner mitochondrial membrane. Another pathway for transferring reducing factors from NADPH to NADH is by the reverse functioning (towards isocitrate) of the  $\text{NADP}^+$ -dependent IDH and isocitrate consumption by the  $\text{NAD}^+$ -dependent IDH (Sazanov and Jackson, 1994). Also, ATP synthesis can become partially uncoupled from respiration through the presence of uncoupling proteins (Boss et al., 2000; Moreno-Sanchez et al., 2014) or reduced due to proton and electron leakage (Jastroch et al., 2010). This can change the stoichiometry of using reducing equivalents to produce ATP, hence of the computed activity of the PCX – MDH – ME cycle when ADP is not provided. However, uncoupling proteins were not found to be expressed in wild-type CHO cells (Pecqueur et

## 5. Identification of elementary flux modes in mitochondria

---

al., 2008) but were shown to play a role in other cells concerning thermogenesis, protection against oxidative stress, export of fatty acids or mediation of insulin secretion (Mozo et al., 2006). One can therefore assume that the effect of uncoupling is negligible for balancing ADP/ATP.

### 5.3.4. Pyruvate and aspartate

Pyruvate fed alone sustained a complete TCA cycle. Upon stimulation with ADP, the pyruvate uptake flux increased 3.1 times (Table 5.2). Mitochondrial metabolism of pyruvate requires an active mitochondrial pyruvate carrier and all mitochondrial enzymes that metabolize pyruvate to  $\text{CO}_2$  (Figure 5.4 A1, 5.4 B1). When pyruvate and aspartate were fed together, the two metabolites had a reciprocal stimulating effect. In a separate experiment, aspartate alone was not taken up. The uptake of pyruvate in the presence of aspartate increased 2.6 times compared to the uptake of pyruvate alone. A double amount of aspartate was taken up per amount of glutamate produced (Table 5.2). Four possible elementary modes can be used to explain the observations: (1) uptake of pyruvate to produce  $\text{CO}_2$ , (2) co-uptake of pyruvate and aspartate to produce  $\text{CO}_2$  and one mole of glutamate per mole of aspartate, (3) uptake of aspartate to produce  $\text{CO}_2$  and one mole of glutamate per two moles of aspartate and (4) uptake of aspartate to produce only  $\text{CO}_2$ . Aspartate uptake through the glutamate-aspartate carrier occurs with equimolar secretion of glutamate. Glutamate must be partially re-transported into the mitochondria through a different carrier (Fiermonte et al., 2002) to account for the aspartate uptake/glutamate secretion rate ratio of 2. Surprisingly, the stoichiometry of the mode with co-uptake of pyruvate and aspartate (mode (2)), where aspartate provides one mole of oxaloacetate and pyruvate provides one mole of acetyl-CoA to fuel the TCA cycle, does not match the observed rates. Therefore, aspartate (Fig. 5.4 A3, B3) and pyruvate (Fig. 5.4 A2, B2) must be metabolized individually. Although aspartate is only taken up in combination with pyruvate, its metabolization happens via modes that exclude pyruvate. This is possible by mutual activation of modes, i.e. activation of rate controlling enzymes.

## 5. Identification of elementary flux modes in mitochondria

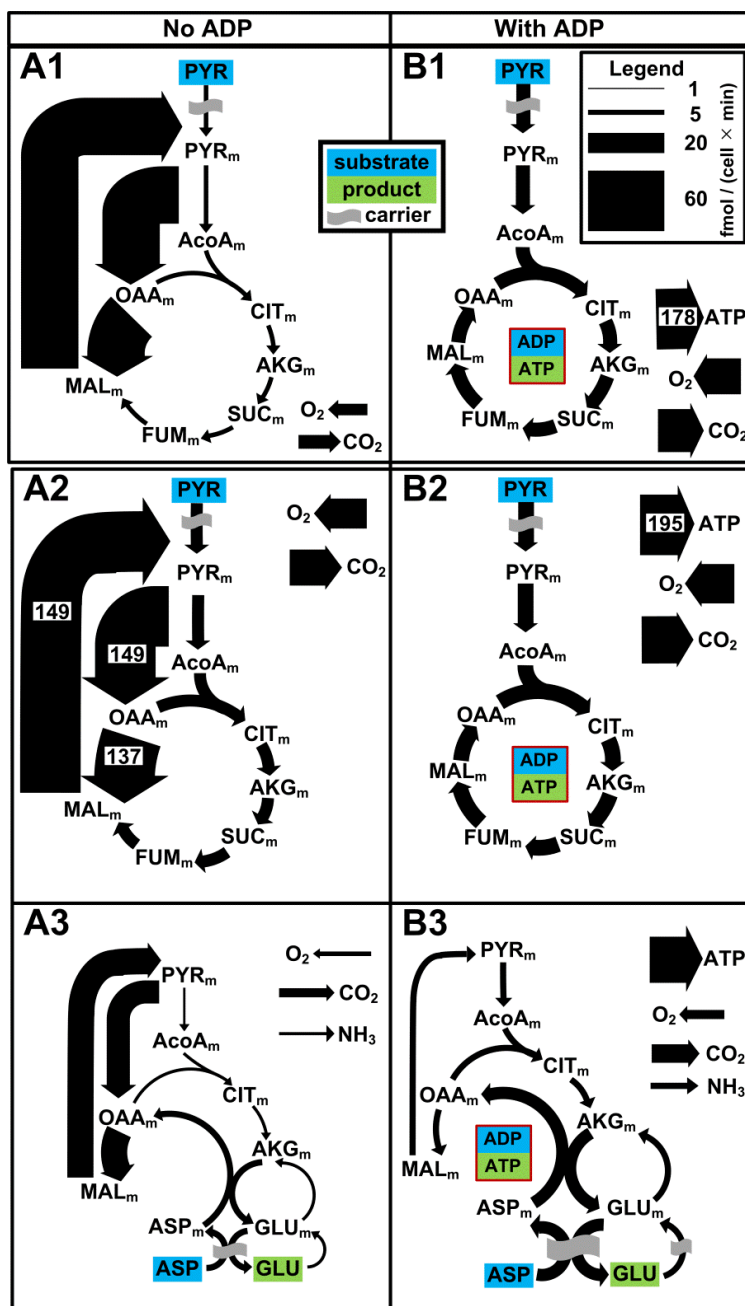


**Figure 5.4.** Fluxes of the mitochondrial elementary modes determined after feeding the permeabilized cells pyruvate (A1, B1) and a combination of pyruvate and aspartate (A2, A3, B2, B3). Modes from lines 1 and 2 metabolize pyruvate to CO<sub>2</sub>. Modes from line 3 metabolize aspartate to glutamate and CO<sub>2</sub>. The modes in the A-column do not use supplied ADP, and the modes in the B-column contained ADP as substrate. The fluxes higher than 60  $\text{fmol} / (\text{cells} \times \text{min})$  are indicated by numbers on the corresponding arrow. Subscripts: m - mitochondrial. Abbreviations: AcoA - acetyl-CoA; AKG - α-ketoglutarate; ASP - aspartate; CIT - citrate; FUM - fumarate; GLU - glutamate; MAL - malate; OAA - oxaloacetate; PYR - pyruvate; SUC - succinate.

## 5. Identification of elementary flux modes in mitochondria

---

The first regulatory step in the conversion of aspartate is aspartate aminotransferase, which is controlled by products and substrates following complex kinetics (Cascante and Cortes, 1988). This enzyme converts aspartate to oxaloacetate simultaneously with converting  $\alpha$ -ketoglutarate to glutamate. Glutamate is exchanged when aspartate enters the mitochondria (Fig. 5.2). Production of  $\alpha$ -ketoglutarate in the TCA cycle is needed to sustain the outflow of glutamate (Fig. 5.4 A3). Aspartate accumulation was observed in retina cells treated with an inhibitor of the mitochondrial pyruvate carrier (Du et al., 2013), which suggests that aspartate needs pyruvate for metabolization. Although oxaloacetate could exert product inhibition on PCX (Barden et al., 1972), it is consumed by MDH to produce malate, while the acetyl-CoA synthesized from pyruvate activates PCX (Jitrapakdee and Wallace, 1999), thus favoring the PCX-MDH-ME cycle towards hydrolyzing the ATP produced from the intramitochondrial pool of ADP in the respiratory chain. ME activity could be another bottleneck in the conversion of pyruvate and aspartate in the absence of ADP. It was shown that  $\alpha$ -ketoglutarate inhibits mitochondrial ME and MDH in brain cells (McKenna et al., 1995). Therefore, ME activity depends on the efficiency of  $\alpha$ -ketoglutarate removal from the mitochondria as glutamate.

Addition of ADP to the pyruvate-aspartate mixture did not change the pyruvate uptake flux, compared to when pyruvate and ADP were used. The most probable limitation in this case is pyruvate transport into the mitochondria, which was shown to influence the respiration capacity in yeast (Timon-Gomez et al., 2013) and is suspected to regulate pyruvate metabolism in cancer cells (Schell and Rutter, 2013). Aspartate uptake flux increased although the aspartate/glutamate ratio remained close to 2 (Table 5.2), comparable to the case without ADP. This result strengthens the assumption that the mode which uses aspartate to produce glutamate and  $\text{CO}_2$  is responsible for aspartate metabolism by the mitochondria.

Pyruvate catabolism to  $\text{CO}_2$  is limited to approx. 15 fmol/ (cell  $\times$  min) in all the three cases where other substrates were used together with pyruvate (i.e. ADP, aspartate,

## 5. Identification of elementary flux modes in mitochondria

---

aspartate and ADP). In a previous study of CHO-K1 metabolism (Nicolae et al., 2014), the *in vivo* computed rate of pyruvate transport into the mitochondria was 4 fmol/ (cell × min), which is in the same order of magnitude. This suggests the existence of a tightly controlled upper threshold in the mitochondrial pyruvate metabolism achieved using the pyruvate transporter and/or allosteric control by the pyruvate dehydrogenase complex.

### 5.3.5. Citrate

It was observed no metabolite production when citrate was used as substrate, also when ADP was added. Because citrate is taken up by antiport with C<sub>4</sub>-carboxylates, these were taken up again via the dicarboxylate carrier (Fig. 5.5 A, B) thus explaining their absence in the extramitochondrial medium. For this, several mechanisms can be assumed: (1) the dicarboxylate carrier can take up dicarboxylates at very low extramitochondrial concentrations, (2) reuptake of C<sub>4</sub>-carboxylates occurs via a mechanism that bypasses their dilution into the media by maintaining a high concentration in the inter-membrane space, (3) there is a mitochondrial carrier that takes up citrate alone, (4) there is cooperation between the citrate (Gnoni et al., 2009) and the dicarboxylic carriers. When ADP was added, there was a significant stimulation of citrate metabolization (Fig. 5.5 B), citrate being the metabolite taken up with the highest carbon flux and the substrate that produced the highest activity of the TCA cycle (Supplem. Table S5.2).

ADP and citrate have a joint activating effect on IDH, which is a limiting step of the TCA cycle as previously found for this cell line by Wahrheit et al. (Wahrheit et al., 2014b). The effect is also in qualitative accordance with respiration studies performed on selectively permeabilized CHO-K1 cells (Wahrheit et al., 2015), where a high stimulation of respiration was observed when citrate was used together with ADP. Citrate is known to inhibit citrate synthase (Williamson and Cooper, 1980), which would in this case be a bottleneck in the TCA cycle. However, citrate is consumed quickly by enzymes downstream the TCA cycle, IDH and AKGH, leading to low citrate and isocitrate concentrations and a release of its inhibiting effect.

## 5. Identification of elementary flux modes in mitochondria

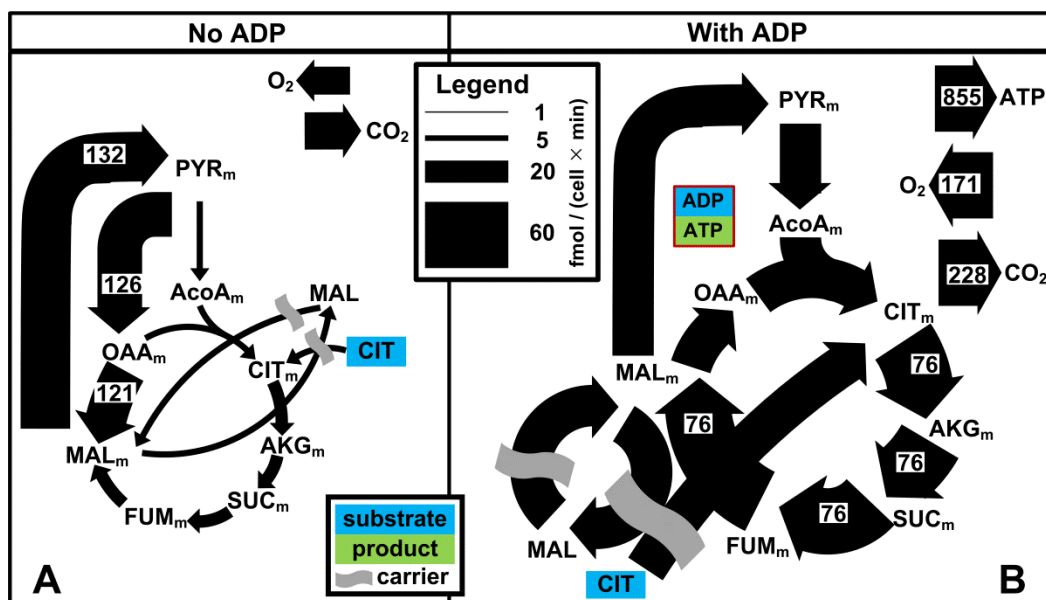


**Figure 5.5. Fluxes of the mitochondrial elementary modes that completely oxidize citrate to CO<sub>2</sub>.** Mode A does not contain added ADP, and mode B uses ADP as substrate. The fluxes higher than 60 fmol/(cell × min) are indicated by numbers on the corresponding arrow. Subscripts: m – mitochondrial. Abbreviations: AcoA – acetyl-CoA; AKG – α-ketoglutarate; CIT – citrate; FUM – fumarate; MAL – malate; OAA – oxaloacetate; PYR – pyruvate; SUC – succinate.

Citrate and isocitrate uptake by the mitochondria is not a typical physiological event described for the metabolism of mammalian cells. In contrast, citrate is usually transported from the mitochondria to supply the fatty acid synthesis in the cytosol. However, given the high cytosolic IDH activity (Wahrheit et al., 2014b), it is possible that in a physiological state the excess of NADPH generated by the pentose phosphate pathway (Nicolae et al., 2014) drives the reaction towards consuming α-ketoglutarate. A reversed functioning of the IDH (Metallo et al., 2012) has been described before for mammalian metabolism. Isocitrate and citrate are then produced from cytosolic α-ketoglutarate and then taken up by the mitochondria to be used in the TCA cycle.

### 5.3.6. α-ketoglutarate

Similarly to citrate, α-ketoglutarate could sustain a complete TCA cycle (Fig. 5.6 A). And similar to citrate, α-ketoglutarate enters the mitochondria using the α-ketoglutarate-dicarboxylate antiporter (Fig. 5.6 A, B1, B2) and the reuptake of malate via the C4-dicarboxylate carrier. Malate reuptake is not quantitative, as seen in the presence of a



## 5. Identification of elementary flux modes in mitochondria

small quantity of fumarate in the extramitochondrial media (Table 5.2, 4a), produced most probably by extramitochondrial fumarase activity. Though it was shown for astrocytes that  $\alpha$ -ketoglutarate inhibits ME (McKenna et al., 1995), this effect was not manifested in our experiments, considering the high metabolization rate in the absence of ADP and hence the high ME flux (Fig. 5.6 A). This means that in the mitochondria,  $\alpha$ -ketoglutarate concentration was maintained low even when the concentration in the media was high. With addition of ADP, the activation of IDH and AKGDH results in a 3-fold increase in  $\alpha$ -ketoglutarate uptake rate.

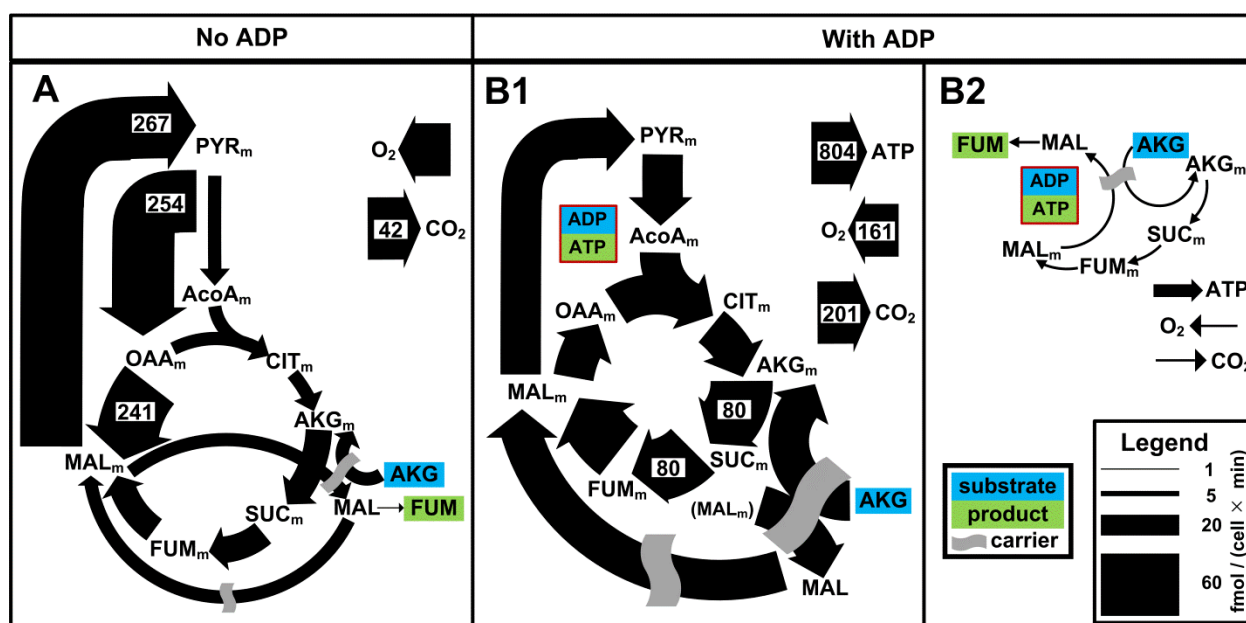


**Figure 5.6. Fluxes of the mitochondrial elementary modes that completely oxidize  $\alpha$ -ketoglutarate to CO<sub>2</sub> in the absence of ADP (A), with added ADP (B<sub>1</sub>) and the mode that produces extramitochondrial fumarate in the presence of ADP (B<sub>2</sub>).** The fluxes higher than 60 fmol/ (cell × min) are indicated by numbers on the corresponding arrow. Subscripts: *m* – mitochondrial. Abbreviations: AcoA – acetyl-CoA; AKG –  $\alpha$ -ketoglutarate; CIT – citrate; FUM – fumarate; MAL – malate; OAA – oxaloacetate; PYR – pyruvate; SUC – succinate.

### 5.3.7. C<sub>4</sub>-dicarboxylates

Succinate and malate were metabolized by the mitochondria with a relatively high rate, both with and without addition of ADP. They were transported through the dicarboxylate carrier, which requires mitochondrial phosphate antiport (Fiermonte et al., 1998). Phosphate is then replenished through another transport system e.g. via the phosphate

## 5. Identification of elementary flux modes in mitochondria

carrier (Hamel et al., 2004). Extracellular fumarate was converted to malate before being taken up in a fast equilibrium reaction, probably by extramitochondrial fumarase activity (Supplem. Fig. S5.2). The equilibrium reaction explains the presence of fumarate in the media when malate is produced from succinate (Fig. 5.7 A4, B4).

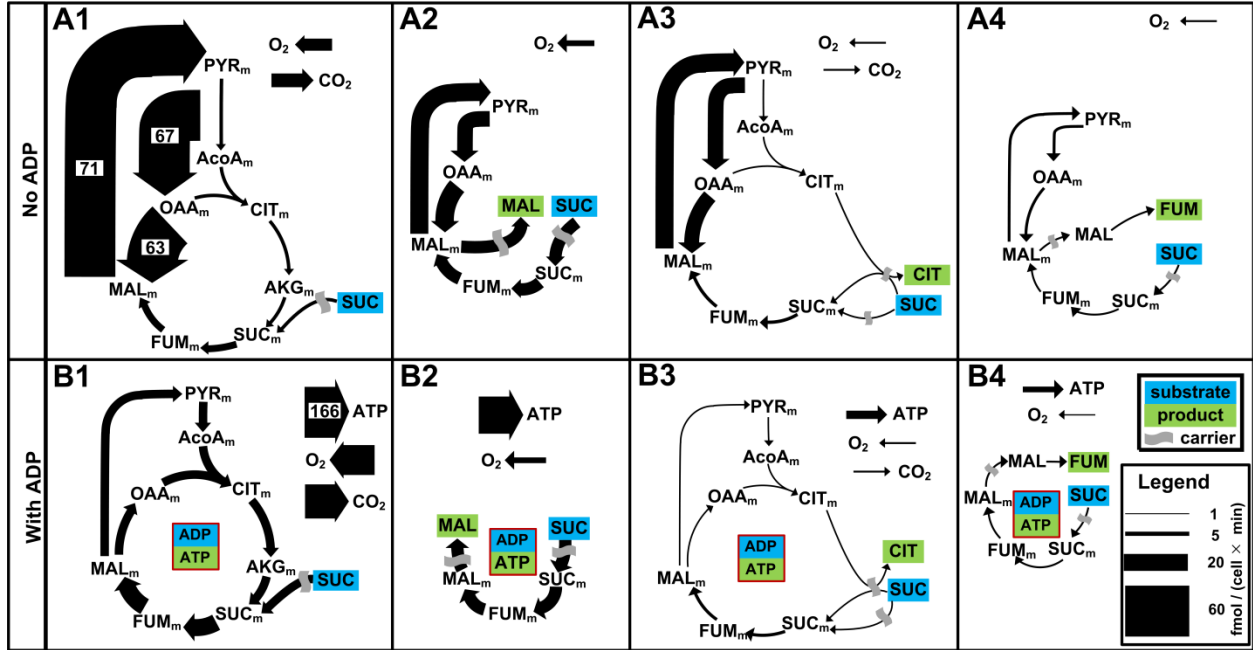


**Figure 5.7.** Fluxes of the mitochondrial elementary modes that metabolize succinate to CO<sub>2</sub> (A1, B1), succinate to malate (A2, B2), succinate to citrate and CO<sub>2</sub> (A3, B3) and succinate to fumarate (A4, B4). The modes in the A-column do not use supplied ADP, and the modes in the B-column contained ADP as substrate. The fluxes higher than 60 fmol/ (cell × min) are indicated by numbers on the corresponding arrow. Subscripts: m – mitochondrial. Abbreviations: AcoA – acetyl-CoA; AKG –  $\alpha$ -ketoglutarate; CIT – citrate; FUM – fumarate; MAL – malate; OAA – oxaloacetate; PYR – pyruvate; SUC – succinate.

Addition of ADP increased the metabolization rate of succinate to CO<sub>2</sub> 2.5 times (Fig. 5.7 A1, B1) and of malate 1.7 times (Fig. 5.8 A1, B1). Succinate was converted to malate with the same rate in both non-stimulated (Fig. 5.7 A2) and stimulated (Fig. 5.7 B2) cases. It can be inferred that fast pathway kinetics between succinate and malate and reduced activity in disposing of malate in the TCA cycle leads to accumulation that favors malate secretion instead of full metabolization. Compared to the high metabolization rates observed for citrate and  $\alpha$ -ketoglutarate, the supply of C<sub>4</sub>-dicarboxylates resulted in a lower activity of the TCA cycle. This implies that the second part of the TCA cycle, involving C<sub>4</sub>-

## 5. Identification of elementary flux modes in mitochondria

---

dicarboxylates, is mainly controlled by the concentrations of C<sub>4</sub>-dicarboxylates and less by the availability of cofactors. The metabolic steady state and therefore the intramitochondrial C<sub>4</sub>-dicarboxylates concentrations are maintained by removing the excess from the mitochondria via the dicarboxylate carrier. Complete catabolism to CO<sub>2</sub> in the absence of ADP was 17% for succinate and 48% for malate, and with ADP it was increased to 33% and 60% respectively. Citrate production from either succinate (Fig. 5.7 B<sub>3</sub>) or malate (Fig. 5.8 B<sub>2</sub>) suggests that high cytosolic concentrations of dicarboxylates induce *de novo* fatty acids synthesis by providing citrate to the cytosol, as it was shown on mouse models (Mizuarai et al., 2005).

Analytical determination of citrate was difficult in the presence of ADP due to an overlay of metabolite peaks in the chromatogram. Although the uptake fluxes of C<sub>4</sub>-dicarboxylates increased, the modes were computed under the assumption that the citrate secretion rate did not increase. This assumption relied on the fact that ADP enhances significantly the metabolization of citrate, as it was shown above (Fig. 5.5 B). Also, the situation when citrate is produced and then taken up for metabolization to CO<sub>2</sub> is equivalent to a mode that metabolizes C<sub>4</sub>-dicarboxylates to CO<sub>2</sub>. It is therefore unlikely that citrate will accumulate in the media when ADP is added.

### 5.3.8. Glutamine and glutamate

Mitochondria of permeabilized cells took up glutamine via the glutamine carrier (Hassanein et al., 2013; Indiveri et al., 1998) and used it to produce mostly glutamate, with a conversion of glutamine to glutamate (computed as the glutamate production flux to glutamine uptake flux) of 72% in the absence of ADP (Fig. 5.9 A<sub>3</sub>). By adding ADP, the conversion to glutamate decreased to 42% (Fig. 5.9 B<sub>3</sub>) although the net production rate increased by 32%. The glutamine uptake rate of the permeabilized cells was approx. 50 times higher than determined *in vivo* (Nicolae et al., 2014).

## 5. Identification of elementary flux modes in mitochondria

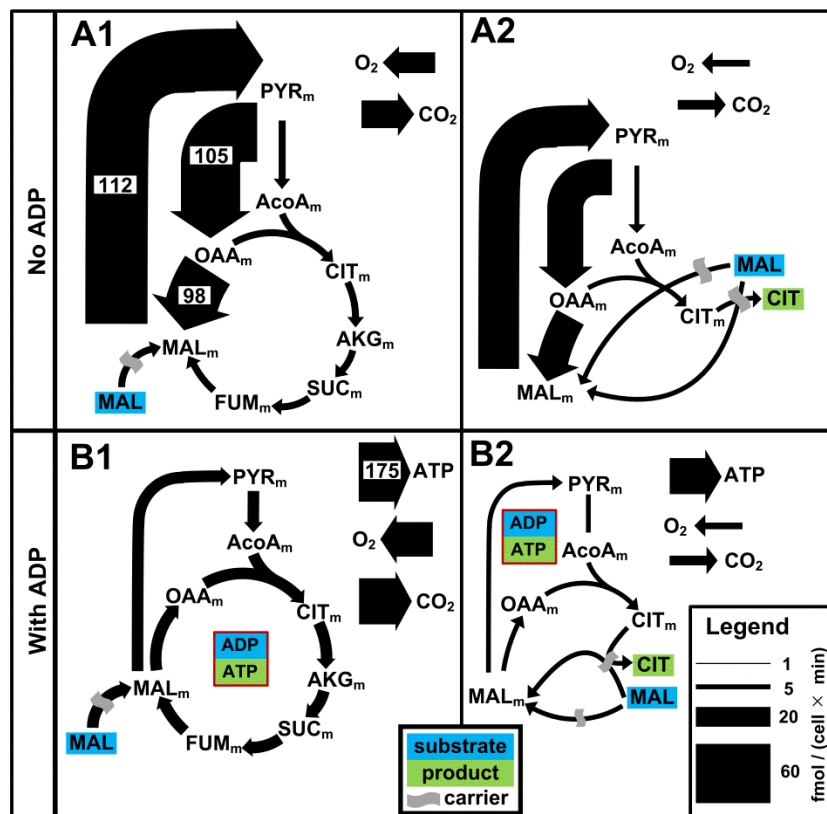


**Figure 5.8. Metabolic fluxes of the mitochondrial elementary modes that metabolize malate to CO<sub>2</sub> (A1, B1) and malate to citrate and CO<sub>2</sub> (A2, B2).** The modes in the A-column do not use supplied ADP, and the modes in the B-column contained ADP as substrate. The fluxes higher than 60 fmol / (cell × min) are indicated by numbers on the corresponding arrow. Subscripts: m – mitochondrial. Abbreviations: AcoA – acetyl-CoA; AKG – α-ketoglutarate; CIT – citrate; FUM – fumarate; MAL – malate; OAA – oxaloacetate; PYR – pyruvate; SUC – succinate.

Glutamate leaves the mitochondria through a different transport system than the aspartate-glutamate carrier, most likely the glutamate carrier (Fiermonte et al., 2002). The glutamate carrier has been shown to operate in the reverse direction, hence by removing glutamate from the mitochondria when it is produced in excess. The supply of cytosolic glutamate could then be used *in vivo* for transamination, e.g. the production of alanine, and also for glutamine synthesis, as it was described previously (Nicolae et al., 2014; Wahrheit et al., 2014a). When compared to the glutamine derivate α-ketoglutarate, the TCA cycle flux was four times smaller on glutamine than on α-ketoglutarate in the absence of ADP and half when ADP was supplied. Glutamine metabolism must therefore

## 5. Identification of elementary flux modes in mitochondria

---

be regulated before glutamine reaches the TCA cycle as  $\alpha$ -ketoglutarate. Because GDH is activated by ADP (Fang et al., 2002), glutamine catabolism to  $\text{CO}_2$  by a full TCA cycle increased significantly in the presence of ADP (Fig. 5.9 A<sub>1</sub>, B<sub>1</sub>), indicating that this enzyme is the first step in controlling glutamine metabolism. The presence of extramitochondrial glutamate also activated the secretion of aspartate (Fig. 5.9 A<sub>2</sub>, B<sub>2</sub>), reversely as in the case with aspartate feeding (Fig. 5.4 A<sub>3</sub>, B<sub>3</sub>), when glutamate was produced. Most likely, the aspartate-glutamate carrier equilibrates the mitochondrial concentrations of these two amino acids and its response is influenced only by their intracompartmental concentrations.

Glutamate was taken up in modest amounts in the absence of ADP, and aspartate was produced in nearly equimolar amounts, considering the confidence intervals of the rates computed for glutamate uptake and aspartate production (Table 5.2). Glutamate concentration could not be determined reliably when using ADP (Supplem. Fig. S5.1, 9b). Nevertheless, an increased production of aspartate was observed, which indicates that glutamate uptake increased considerably by adding ADP. This means that the preferred uptake system for glutamate is the glutamate-aspartate carrier and not the glutamate carrier (Fiermonte et al., 2002).

### 5.3.9. Serine

Serine was taken up by the permeabilized cells in moderate amounts (Table 5.2). Consistent with previous studies (Appling, 1991; Barlowe and Appling, 1988; Narkewicz et al., 1996), serine is converted by mitochondrial serine hydroxymethyltransferase to produce glycine and C<sub>1</sub> units, that can subsequently be converted to and secreted as formate (not measured) (Fig. 5.2) (Kelley et al., 2002). Only 59% of the glycine that could be potentially produced was secreted. The remaining glycine was most likely converted by the glycine cleavage system into C<sub>1</sub> units and  $\text{CO}_2$ . The NADH produced in the glycine cleavage reaction is then consumed by the PCX-MDH-ME cycle to maintain the metabolic steady state in the mitochondria. Regeneration of tetrahydrofolate from

## 5. Identification of elementary flux modes in mitochondria

methyltetrahydrofolate produces NADPH that contributes significantly to the mitochondrial metabolism under *in vivo* conditions (Lewis et al., 2014).

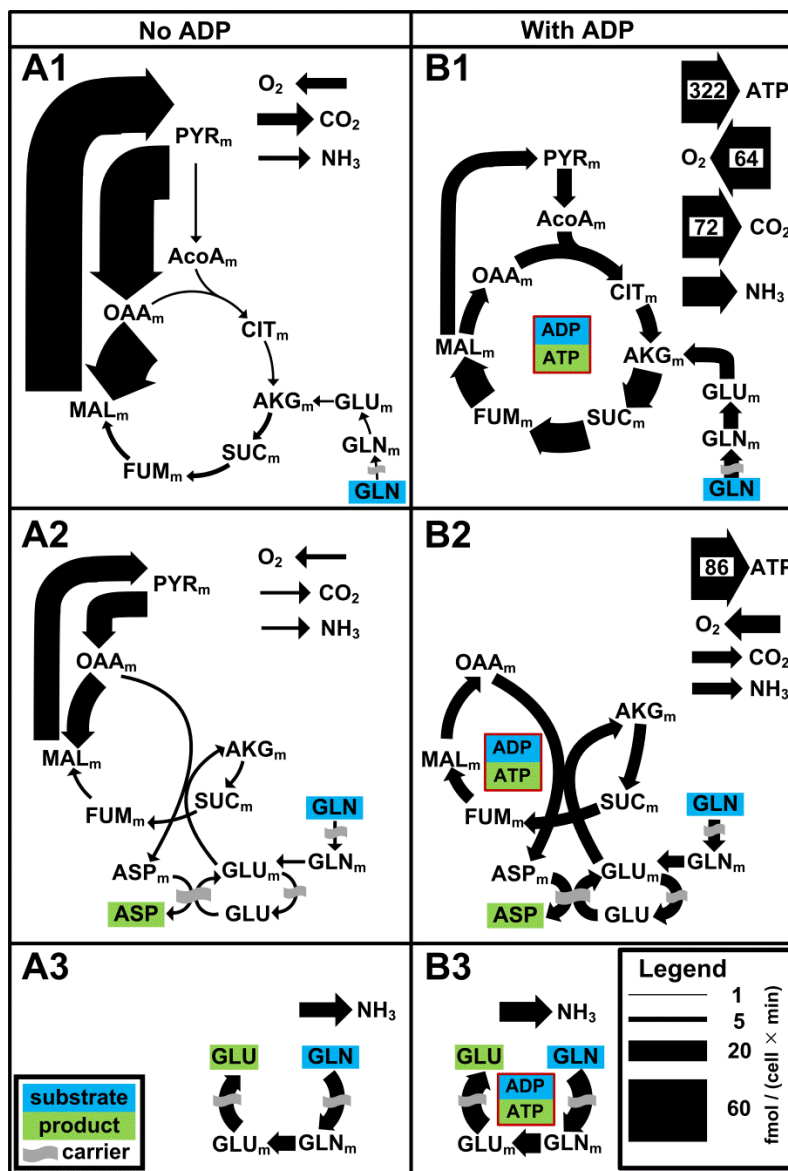


**Figure 5.9.** Metabolic fluxes of the mitochondrial elementary modes that metabolize glutamine to CO<sub>2</sub> (A1, B1), glutamine to aspartate and CO<sub>2</sub> (A2, B2) and glutamine to glutamate (A3, B3). The modes in the A-column do not use supplied ADP, and the modes in the B-column contained ADP as substrate. The fluxes higher than 60 fmol/ (cell × min) are indicated by numbers on the corresponding arrow. Subscripts: *m* – mitochondrial. Abbreviations: AcoA – acetyl-CoA; AKG – α-ketoglutarate; ASP – aspartate; CIT – citrate; FUM – fumarate; GLN – glutamine; GLU – glutamate; MAL – malate; OAA – oxaloacetate; PYR – pyruvate; SUC – succinate.

### 5.4. Conclusions

Selectively permeabilized CHO-K1 cells proved to be a useful system for detailed studies of the mitochondrial metabolism. The permeabilized cells retain functional mitochondria that are able to process at metabolic steady state various single substrates or combinations of carbon sources. By using EMA it was evidenced that the mitochondrial reactions involved in the TCA cycle, anaplerotic and cataplerotic reactions, amino acid metabolism, as well as the oxidative phosphorylation and mitochondrial transport are active. Beyond demonstrating the functionality of mitochondrial metabolic pathways, EMA was used to support the observations from earlier screening experiments (Wahrheit et al., 2015). Additionally, the contributions of separate pathways at processing a certain substrate or combination of substrates could be quantified.

In the absence of ADP, substrate uptake was limited in most cases. Full metabolization to CO<sub>2</sub> has been observed for pyruvate, citrate,  $\alpha$ -ketoglutarate, C<sub>4</sub>-dicarboxylic acids and glutamate. This requires an active PCX-MDH-ME cycle that disposes of the ATP generated by oxidative phosphorylation. The PCX-MDH-ME cycle is the limiting step in processing substrates, as the accumulation of ATP and NADH inhibits key enzymes involved in the TCA cycle. Since uncoupling proteins were not found to be expressed in wild-type CHO cells (Pecqueur et al., 2008) uncoupling can be excluded in our experiments.

Stimulation by ADP enhanced respiration and the metabolization to CO<sub>2</sub> of most substrates, as shown by Wahrheit et al. (2015), with considerable differences for  $\alpha$ -ketoglutarate and citrate and less for C<sub>4</sub>-dicarboxylic acids. The differences are explained by the way in which the enzymes of the TCA cycle are controlled. In the first part of the TCA cycle, IDH and AKGDH are positively modulated by substrate and cofactor availability. The fluxes of the second part of the TCA cycle involving the inter-conversion of C<sub>4</sub>-dicarboxylates seem to be determined primarily by the concentration of C<sub>4</sub>-dicarboxylates. The high concentrations of C<sub>4</sub>-dicarboxylates could inhibit enzymes that do not process them directly. This effect may lead indirectly to a reduced TCA cycle flux.

## 5. Identification of elementary flux modes in mitochondria

---

Glutamine metabolism is controlled by GDH and by removing glutamate from the mitochondria via the glutamate carrier. The summarized conclusions are organized by the feeding experiments that support them in Supplem. Table S5.4.

A question mark that is left after analyzing our results is related to the regulatory role played by the mitochondrial carriers. Little is known about their function to control metabolite concentrations for achieving a specific metabolic state in the mitochondria. Knowledge about regulation of mitochondrial transporters would improve the understanding of the mitochondrial metabolic system. Complex regulatory effects that span over more reactions are difficult to establish without further information about transporter properties. The discovery and characterization of new mitochondrial carriers able to transport the tested substrates and observed products would expand the number of elementary modes that are computed. The findings obtained using our approach indicate a limiting role of the pyruvate carrier, a high sensitivity of the aspartate-glutamate antiporter for balancing the content of these amino acids in the mitochondria, and a potential cooperation between the citrate and the dicarboxylate carrier. Also, determining intracompartmental concentrations under selected feeding conditions would be of great value at establishing the control checkpoints in the mitochondrial metabolism. Off-gas analysis of  $O_2$  and  $CO_2$  would add extra constraints to the linear system used to calculate the mode fluxes, making possible the resolution of more complex modes, where e.g. more substrates are taken up together. Sampling ADP and ATP concentrations would enable the quantification of uncoupling effects particularly for the study of certain diseases or toxic effects of test compounds.

Using selectively permeabilized cells and flux analysis methods provides a great system for metabolic studies that aim at understanding diseases related to mitochondrial dysfunctions or at debottlenecking the metabolic connection between mitochondria and cytosol. By removing the background noise of cytosolic reactions, it becomes possible to study the effect of transport or enzyme inhibitors and of genetic modifications of the mitochondrial enzymes on the mitochondrial metabolism.



### Supplementary data 5

**Supplem. Figure S5.1. Experimental (o) and fitted (-) extracellular concentrations in the experiments with permeabilized CHO-K1 cells.**  $r$  – production rate [fmol/ (cell  $\times$  min)]. The brackets contain the 95% confidence interval for the rate.

**Supplem. Table S5.1. Selection of the elementary modes that can describe the observed metabolite uptake and production.** The modes are selected accordingly to the following criteria: u - the metabolite is taken up; p - the metabolite is produced; xu - the metabolite is not taken up; xp - the metabolite is not produced; iu - the metabolite is or is not taken up; ip - the metabolite is or is not produced.

**Supplem. Table S5.2. Mitochondrial fluxes** [fmol / cell  $\times$  min] in selectively permeabilized CHO-K1 cells under various feeding conditions. The fluxes were computed using the determined extracellular rates and the stoichiometry indicated by reactions R1-R50. By addition of ADP it was assumed that the flux R44=0.

**Supplem. Table S5.3. Stoichiometry of the modes selected using the Table S1 and the contribution to each mode to the total flux** in each feeding experiment using selectively permeabilized CHO-K1 cells [fmol / cell  $\times$  min].

**Supplem. Table S5.4. Conclusions on mitochondrial enzymes and transporters activity and about regulation of the mitochondrial metabolism** resulted by applying elementary mode analysis to the observations from feeding experiments with selectively permeabilized CHO-K1 cells. The gray areas indicate the experiments on which each corresponding conclusion was based.

## Chapter 6

### 6. Conclusions and outlook

In the present work, systems biology tools were developed and applied using CHO-K1 as a model mammalian system to study metabolic compartmentation between mitochondria and cytosol. The focus was to use mathematical modeling first to reveal details about the topology of compartmented metabolic networks in eukaryotes and second, what role plays compartmentation at controlling metabolic fluxes and metabolite availability in the larger scheme of cellular metabolism.

The systems biology tools that were applied are (1) non-stationary  $^{13}\text{C}$  metabolic flux analysis (Inst- $^{13}\text{C}$ MFA), (2) dynamic metabolic flux analysis (dyMFA) and (3) elementary mode analysis (EMA). A software platform for Inst- $^{13}\text{C}$ MFA was developed and tested first on *S. cerevisiae*. The model was then extended to include the dynamics of extracellular isotopomers by including growth, changes in the extracellular concentrations and metabolite exchange with the media. The mass isotopomers of extracellular metabolites in a batch culture of CHO-K1 cells was sufficient to compute the metabolic fluxes for a detailed, compartmented network. Even though some metabolites are taken up with net fluxes, they were found labeled in the extracellular media. Sometimes, like in the case of pyruvate, they were exchanged with a very high flux. This means that the media is not only a source of substrates for the cells, but it is also an important environment, playing the role of another compartment.

By applying what was named “high resolution Inst- $^{13}\text{C}$ MFA”, which is Inst- $^{13}\text{C}$ MFA using both intra- and extracellular labeling from parallel labeling experiments using different labeled substrates, it resulted that the metabolism of CHO-K1 cells is not only compartmented, but also most likely spatially structured. Enzyme association and metabolite channeling create microenvironments that separate metabolite pools in the same compartment. Pyruvate channeling was determined in both cytosol and mitochondria. In the cytosol, a possible association of glycolytic enzymes to the cell

membrane produced secreted lactate labeled differently than the cytosolic pool. The assumption of glycolytic pyruvate-to-secreted lactate channeling is also supported by the very low cytosolic concentrations that were estimated for these organic acids.

CHO-K1 cells growing in the exponential phase require high amounts of NADPH to be consumed by fatty acids synthesis and to mitigate the oxidative stress related to high mitochondrial respiration and protein folding and unfolding futile cycles (Klein et al., 2015). The main source of cytosolic NADPH is a high PPP activity, similar to cancer cells. No or little cytosolic activity of ME and IDH was estimated using Inst-<sup>13</sup>CMFA, these two enzymes being the only other possible sources of NADPH. Cytosolic ME activity was not detected experimentally (Wahrheit et al., 2014b) nor simulated, but high cytosolic activity of IDH determined by (Wahrheit et al., 2014b) did not reflect in flux estimations. It is possible that cytosolic IDH has more a protective role than as a NADPH producer/consumer (Lee et al., 2002). Although the *in vivo* activities of mitochondrial ME and PCX were modest, their activity together with that of MDH formed a futile cycle which ran at high flux. This cycle has the purpose to recycle ADP from ATP when ADP is not provided together with the metabolized mitochondrial substrate. The flux values are the maximum possible when in the mode flux calculation it is considered that uncoupling and proton leakage do not occur.

Inst-<sup>13</sup>CMFA revealed that some pathways for synthesis and degradation of non-essential amino acids occur simultaneously, but in different compartments. Key metabolites, e.g. malate and glutamate, are cycled via several mitochondrial carriers between mitochondria and cytosol. A dynamic control of the cytosolic and mitochondrial NADH pools could be a reason for this observation, as these two metabolites are part of the aspartate-malate shuttle. The aspartate-glutamate mitochondrial carrier contributes to the shuttle activity by controlling the content of these two amino acids in the compartments, as it resulted from studies using selectively permeabilized cells. Selectively permeabilized cells consumed substrates at considerably higher rates than those estimated *in vivo*. An exception is uptake of pyruvate by the mitochondria, which

was comparable in both cases. Mitochondrial uptake of pyruvate combined with the activity of the PDH complex is most likely the bottleneck in the split of pyruvate between glycolysis and the TCA cycle. Because of its complex regulation pattern, PDH was already indicated as bottleneck reaction in the pyruvate metabolism of cancer cells (Israel and Schwartz, 2011). However, as it was shown in Chapter 5, the control of metabolism does not operate through individual reactions. The example of aspartate being taken up by mitochondria only in the presence of aspartate is an important indication of systemic interactions. Enzyme co-regulation, transporter cooperation and metabolite inhibition/stimulation effects are all advocates for employing systemic characterizations of mammalian cells instead of gene-focused or reaction-focused approaches. This is especially important when the goal is to understand the causes/effects of a disease or to optimize the cell for production of biopharmaceuticals.

Labeling experiments where exchange with the media occurs must consider the influence of the extracellular labeling. As this process becomes dynamic due to changes in the extracellular concentrations and cell growth, only a dynamic model can accurately describe the labeling state of the cell. In this context, INST-<sup>13</sup>CMFA proved to be an effective tool for estimating metabolic fluxes considering the narrow confidence intervals that were computed. Experiments using selectively permeabilized cells provided direct access to the mitochondrial metabolism and contributed to establishing the topology of the mitochondrial metabolism. This led to revealing not only the activity of certain enzymes or transporters, but the activity of whole mitochondrial pathways. The key highlights of the methods that were described in this thesis are:

- INST-<sup>13</sup>CMFA using only extracellular labeling: can be applied industrially, useful to reveal compartmented fluxes, can be used to estimate the fluxes of metabolite exchange with the media.
- High resolution INST-<sup>13</sup>CMFA: estimate metabolic fluxes in a complex network with small confidence intervals, estimate reaction reversibility, estimate fluxes and exchange

at the cytosol/mitochondria boundary, estimate intracompartmental concentrations, can be used to uncover details about metabolite channeling.

- Dynamic metabolic flux analysis: determine metabolic switches, correlate switches with changes in metabolite availability and with cell growth.
- EMA applied to analyze feeding experiments using selectively permeabilized cells: reveal the activity of whole mitochondrial pathways (including transporters), reveal regulatory effects observed by using more mitochondrial substrates.

Mammalian metabolism is a complex system that is tightly controlled at several levels. In this framework, compartmentation allows the cells to maintain stable states, e.g. exponential growth, under highly dynamic extracellular conditions where substrates are depleted and secreted products accumulate. For this reasons, the methods that were employed herein would be greatly complemented by larger scale models, which are able to simulate growth in a comprehensive manner. Genome scale initiatives have already been set in place for plant cells (de Oliveira Dal'Molin and Nielsen, 2013), the human genome reconstruction is already available owing to a concerted scientific effort (Mo et al., 2007; Thiele et al., 2013), based on which a mouse reconstruction was also built (Sigurdsson et al., 2010). Given the immense economic importance of this cell line, it is to be expected that a genome scale model of the CHO cell line will soon be available (Borth, 2014; Kaas et al., 2014). However, if genome scale models are to be used for fluxomics, the same problems related to alternative pathways and cycles will be encountered. Such fluxes cannot be solved by flux balancing. To minimize this uncertainty, a future option for comprehensive genome-scale fluxomics is combining genome scale models with  $^{13}\text{C}$ MFA. The labeling information can be used in the objective function that constrains the flux space. Genome scale atom networks could then be built to describe the atom mapping throughout the whole network. Mathematical frameworks that condensate atoms into metabolic units, similar to the elementary metabolite units introduced by Antoniewicz et al. (Antoniewicz et al., 2007), could greatly reduce the computational costs and make such applications feasible.

Flux analysis offers only a static image of the metabolism. Advanced dynamical models of the metabolism could evolve from semi-empirical fitting to considering reaction kinetics (Chen et al., 2012), even at genome scale (Chakrabarti et al., 2013). Recent progress was made by applying metabolic flux analysis and kinetic modeling to understand the shift in to lactate consumption in mouse myeloma cells (Mulukutla et al., 2012). Besides the computational costs, kinetic modeling requires the determination of intracompartmental concentrations. There has been much progress in this area, including the development of sensors sensitive to intracompartmental concentrations (Frommer et al., 2009) or of protocols for sampling intracellular concentrations (Wahrheit and Heinzle, 2013; Wahrheit and Heinzle, 2014a).

Improvements in experimental methods would bring an essential contribution to constructing realistic metabolic models. There are still many mitochondrial carriers that have not yet been annotated (Table 1.1) or characterized, and this fact introduces a great deal of uncertainty in models that include compartmentation. The development of methods for determining *in vivo* multi-enzyme complexes or enzyme-transporter association would contribute to adding a spatial component to cell models. Quantifying the electron chain uncoupling (Brand and Esteves, 2005), oxidative stress (Adam-Vizi, 2005; Milne et al., 2007) or the activity of futile cycles (Locasale and Cantley, 2011) will permit a better stoichiometric quantification of the energy metabolism of mammalian cells, which is the core of mitochondria-related diseases and aging.

In the spirit of systems biology, meaning embracing complexity, model layering should be the next natural step in dealing with the compartmentation of the living into organelles, cells, tissues, organs and bodies. Several types of mathematical models of different resolution could be integrated to exchange parameters and create complete organ or even body models (Bordbar et al., 2011; Eissing et al., 2011) that could constitute excellent platforms for *in silico* testing. This ambitious goal would lead to the minimization of animal testing, optimized time for strain engineering and to the design of personalized therapies or diagnosis platforms.

## Research activities

(Poster) **Nicolae A.**, Hans M., Wittmann C., Heinzle E. (2010), *Characterization of Saccharomyces cerevisiae metabolic network using a dynamic isotopomer model*, SBM (2010), Paris.

Wahrheit J., **Nicolae A.**, Heinzle E. (2011), *Eukaryotic metabolism: measuring compartment fluxes*, Biotechnol J. 2011 Sep;6(9):1071-85. doi: 10.1002/biot.201100032. Epub 2011 Aug 29.

(Poster) Wahrheit J., **Nicolae A.**, Heinzle E. (2013), *Investigation of glutamine metabolism in CHO cells by dynamic metabolic flux analysis*, BMC Proceedings, 7(Suppl 6):P44.  
<http://www.biomedcentral.com/1753-6561/7/S6/P44>

Wahrheit J., **Nicolae A.**, Heinzle E. (2014), *Dynamics of growth and metabolism controlled by glutamine availability in Chinese hamster ovary cells*, Appl Microbiol Biotechnol. DOI 10.1007/s00253-013-5452-2.

**Nicolae A.**, Wahrheit J., Bahnemann J., Zeng A.P., Heinzle E. (2014), *Non-stationary  $^{13}\text{C}$  metabolic flux analysis of Chinese hamster ovary cells in batch culture using extracellular labeling highlights metabolic reversibility and compartmentation*, BMC Sys Biol, 2014, 8:50 doi:10.1186/1752-0509-8-50.

(Poster) Wahrheit J., **Nicolae A.**, Nonnenmacher Y., Heinzle E. (2014), *Mitochondrial network analysis using highthroughput respiration screening and elementary mode analysis yields detailed information about TCA cycle activities*, SBMC 2014, Berlin.

---

## Appendix

**Supplem. Table S1.1. Average biomass composition of the CHO-K1 cell**

| Component     | pg/cell                          |
|---------------|----------------------------------|
| Dry weight    | 290                              |
| Proteins      | 171.86                           |
| Carbohydrates | 22.4 (Altamirano et al., 2001a)  |
| Lipids        | 24.64 (Altamirano et al., 2001a) |
| DNA           | 13.41                            |
| RNA           | 5.79                             |

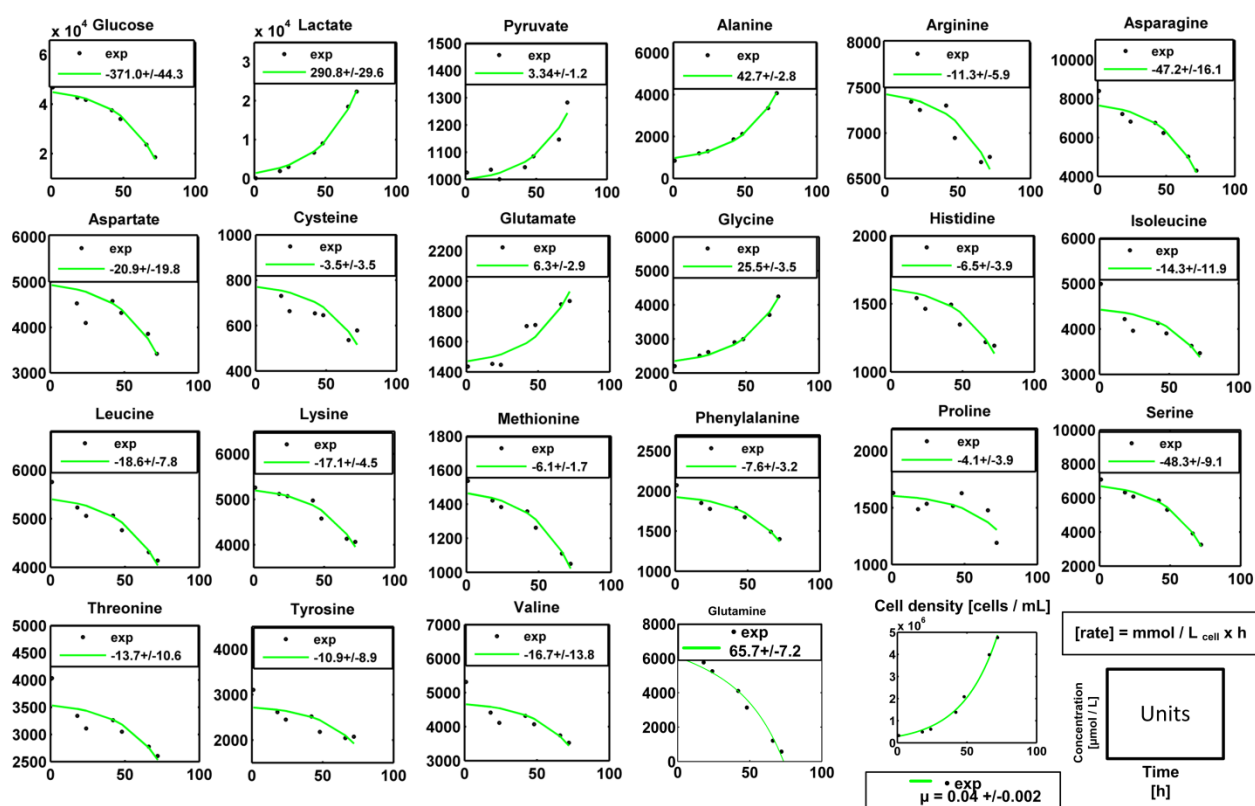


**Supplem. Table S1.2.** Precursor requirements for the synthesis of macromolecules in the CHO-K1 cell line

| Precursor              | Average composition<br>[pmol/cell] | Macromolecule<br>(unit of quantitative reference)          |
|------------------------|------------------------------------|------------------------------------------------------------|
| Alanine                | 0.103670                           | Proteins<br>(mole of amino acid)                           |
| Arginine               | 0.081327                           |                                                            |
| Asparagine / aspartate | 0.130177                           |                                                            |
| Glutamine / glutamate  | 0.151689                           |                                                            |
| Glycine                | 0.140649                           |                                                            |
| Histidine              | 0.031833                           |                                                            |
| Isoleucine             | 0.055419                           |                                                            |
| Leucine                | 0.108359                           |                                                            |
| Lysine                 | 0.089150                           |                                                            |
| Methionine             | 0.009462                           |                                                            |
| Phenylalanine          | 0.047120                           |                                                            |
| Proline                | 0.046327                           |                                                            |
| Serine                 | 0.076950                           |                                                            |
| Threonine              | 0.063611                           |                                                            |
| Tryptophane            | 0.001068                           |                                                            |
| Tyrosine               | 0.053013                           |                                                            |
| Cysteine               | 0.079279                           |                                                            |
| Valine                 | 0.078340                           |                                                            |
| Glucose-6-phosphate    | 0.138272                           | Carbohydrates<br>(mole of glucose)                         |
| Lipids                 | 0.035671                           | Lipids<br>(1 mole = $C_{38.925}H_{74.2}O_{6.95}P_{0.85}$ ) |
| DNA                    | 0.042851                           | DNA<br>(ribose-5-phosphate)                                |
| RNA                    | 0.017826                           | RNA<br>(ribose-5-phosphate)                                |

## Appendix to Chapter 3

**Supplem. Fig. S3.1. Complete culture profile of CHO-K1 cells during the exponential growth phase.** The lines represent the fitted concentration profiles to the experimental values (dots) and in the boxes are the determined extracellular rates [mmol/(L cell  $\times$  h)] together with the 95% confidence intervals. Glutamine uptake was determined by considering a spontaneous degradation rate of  $0.0033 \text{ h}^{-1}$ . The exponential growth phase is shown in the last plot.



**Supplem. Table S3. 1. List of reactions in the non-compartmented central carbon metabolism of CHO-K1 (Table S3.1.1). List of metabolic reactions, fluxes and reversibilities in the compartmented central carbon metabolism of CHO-K1 cells (Table S3.1.2).** Carbon transfer rules are provided in the parentheses after each reaction. Reversible reactions are designated by double arrows. Reversibility (rev) is computed as the ratio between the reverse flux and the net flux. lb – lower boundary; ub – upper boundary. Subscripts meaning: *c* – cytosolic; *ex* – extracellular; *m* – mitochondrial; Abbreviations: AcoA – acetyl-CoA; ALA – alanine; ASN – asparagine; ASP – aspartate; CIT – citrate; FUM – fumarate; GLC – glucose; G6P – glucose-6-phosphate; PG – phosphoglycerate; PEP – phosphoenolpyruvate; GLN – glutamine; GLU – glutamate; GLY – glycine; ICI – isocitrate; ILE – isoleucine; LAC – lactate; LEU – leucine; LYS – lysine; MAL – malate; MET – methionine; OAA – oxaloacetate; PHE – phenylalanine; PYR – pyruvate; SER – serine; SUC – succinate; THR – threonine; TYR – tyrosine; VAL – valine.

**Table S3.1.1**

| Flux | Reaction                                                           |
|------|--------------------------------------------------------------------|
| v1   | $GLC_{ex}(abcdef) \rightarrow G6P(abcdef)$                         |
| v2   | $G6P(abcdef) \rightarrow PG(abc) + PG(def)$                        |
| v3   | $3\ G6P(abcdef) \rightarrow 5\ PG(def) + 3\ CO_2(a)$               |
| v4   | $G6P(abcdef) \rightarrow Biomass$                                  |
| v5   | $PG(abc) \rightarrow PEP(abc)$                                     |
| v6   | $PEP(abc) \rightarrow PYR(abc)$                                    |
| v7   | $PYR(abc) \rightarrow AcoA(bc) + CO_2(a)$                          |
| v8   | $OAA(abcd) + AcoA(ef) \rightarrow CIT(efbcda)$                     |
| v9   | $CIT(abcdef) \rightarrow AKG(abcde) + CO_2(f)$                     |
| v10  | $AKG(abcde) \rightarrow 0.5\ MAL(abcd) + 0.5\ MAL(dcba) + CO_2(e)$ |
| v11  | $MAL(abcd) \leftrightarrow OAA(abcd)$                              |
| v12  | $PYR(abc) \leftrightarrow LAC(abc)$                                |
| v13  | $LAC(abc) \leftrightarrow LAC_{ex}(abc)$                           |
| v14  | $OAA(abcd) \rightarrow PEP(abc) + CO_2(d)$                         |
| v15  | $MAL(abcd) \rightarrow PYR(abc) + CO_2(d)$                         |
| v16  | $PYR(abc) + CO_2(d) \rightarrow OAA(abcd)$                         |
| v17  | $PG(abc) \rightarrow SER(abc)$                                     |
| v18  | $SER(abc) \leftrightarrow GLY(ab) + MTHF(c)$                       |
| v19  | $SER_{ex}(abc) \leftrightarrow SER(abc)$                           |
| v20  | $SER(abc) \rightarrow Biomass$                                     |
| v21  | $GLY(abc) \leftrightarrow GLY_{ex}(abc)$                           |
| v22  | $GLY(abc) \rightarrow Biomass$                                     |
| v23  | $SER(abc) \rightarrow PYR(abc)$                                    |
| v24  | $PYR(abc) + GLU(defgh) \leftrightarrow ALA(abc) + AKG(defgh)$      |
| v25  | $ALA(abc) \leftrightarrow ALA_{ex}(abc)$                           |
| v26  | $ALA(abc) \rightarrow Biomass$                                     |
| v27  | $PYR(abc) \leftrightarrow PYR_{ex}(abc)$                           |
| v28  | $ASP(abcd) + AKG(efghi) \leftrightarrow OAA(abcd) + GLU(efghi)$    |
| v29  | $ASN(abcd) \rightarrow ASP(abcd)$                                  |
| v30  | $ASP_{ex}(abcd) \leftrightarrow ASP(abcd)$                         |
| v31  | $ASP(abcd) \rightarrow Biomass$                                    |
| v32  | $AKG(abcde) \leftrightarrow GLU(abcde)$                            |
| v33  | $GLU(abcde) \leftrightarrow GLU_{ex}(abcde)$                       |

|     |                                                                                |
|-----|--------------------------------------------------------------------------------|
| v34 | $GLU(abcde) \rightarrow \text{Biomass}$                                        |
| v35 | $GLN(abcde) \rightarrow GLU(abcde)$                                            |
| v36 | $GLN_{ex}(abcde) \leftrightarrow GLN(abcde)$                                   |
| v37 | $AcoA(ab) \rightarrow \text{Biomass}$                                          |
| v38 | $AA_{ex}(ILE, VAL, MET, THR, TYR, PHE) \rightarrow MAL(AA \text{ catabolism})$ |
| v39 | $AA_{ex}(LEU, ILE, LYS, TYR, PHE) \rightarrow ACOA(AA \text{ catabolism})$     |
| v40 | $AKG(abcde) \rightarrow GLU(abcde)(AA \text{ catabolism})$                     |
| v41 | $AA(PRO, HIS, ARG) \rightarrow GLU(AA \text{ catabolism})$                     |
| v42 | $G6P(abcdef) \rightarrow \text{carbohydrates}$                                 |

Table S3.1.1

| Flux | Reaction                                                               | Flux<br>[mmol/L<br>cell·h] | lb<br>[mmol/L<br>cell·h] | ub<br>[mmol/L<br>cell·h] | rev  | rev lb | rev ub |
|------|------------------------------------------------------------------------|----------------------------|--------------------------|--------------------------|------|--------|--------|
| v1   | $GLC_{ex}(abcdef) \rightarrow G6P(abcdef)$                             | 371.0                      | 326.7                    | 415.3                    | 0    | 0      | 0      |
| v2   | $G6P(abcdef) \rightarrow PG(abc) + PG(def)$                            | 65.8                       | 25.2                     | 96.5                     | 0    | 0      | 0      |
| v3   | $3 G6P(abcdef) \rightarrow 5 PG(def) + 3 CO_2(a)$                      | 97.5                       | 87.6                     | 111.0                    | 0    | 0      | 0      |
| v4   | $G6P(abcdef) \rightarrow \text{Biomass}$                               | 3.9                        | -                        | -                        | 0    | -      | -      |
| v5   | $PG(abc) \rightarrow PEP_c(abc)$                                       | 597.9                      | 585.7                    | 607.5                    | 0    | 0      | 0      |
| v6   | $PEP_c(abc) \rightarrow PYR_{ci}(abc)$                                 | 540.3                      | 528.1                    | 549.8                    | 0    | 0      | 0      |
| v7   | $PYR_{ci}(abc) \rightarrow PYR_m(abc)$                                 | 375.2                      | 363.0                    | 384.7                    | 0    | 0      | 0      |
| v8   | $PYR_m(abc) \rightarrow AcoA_m(bc) + CO_2(a)$                          | 455.8                      | 442.4                    | 466.9                    | 0    | 0      | 0      |
| v9   | $OAA_m(abcd) + AcoA_m(ef) \rightarrow CIT_m(efbcda)$                   | 548.7                      | 529.5                    | 556.9                    | 0    | 0      | 0      |
| v10  | $CIT_m(abcdef) \rightarrow AKG_m(abcde) + CO_2(f)$                     | 441.7                      | 422.8                    | 450.2                    | 0    | 0      | 0      |
| v11  | $AKG_m(abcde) \rightarrow 0.5 MAL_m(abcd) + 0.5 MAL_m(dcba) + CO_2(e)$ | 571.3                      | 555.8                    | 581.1                    | 0    | 0      | 0      |
| v12  | $MAL_m(abcd) \leftrightarrow OAA_m(abcd)$                              | 474.4                      | 473.0                    | 486.0                    | 14.3 | 0.16   | >100   |
| v13  | $PYR_{c2}(abc) \leftrightarrow LAC_c(abc)$                             | 290.8                      | 261.1                    | 320.4                    | 15.3 | 0      | >100   |
| v14  | $LAC_c(abc) \leftrightarrow LAC_{ex}(abc)$                             | 290.8                      | 261.1                    | 320.4                    | n.d. | n.d.   | n.d.   |
| v15  | $OAA_c(abcd) \rightarrow PEP_c(abc) + CO_2(d)$                         | 65.0                       | 35.5                     | 72.2                     | 0    | 0      | 0      |
| v16  | $MAL_c(abcd) \rightarrow PYR_{ci}(abc) + CO_2(d)$                      | 16.4                       | 9.4                      | 45.8                     | 0    | 0      | 0      |
| v17  | $OAA_c(abcd) \leftrightarrow MAL_c(abcd)$                              | 19.3                       | 10.9                     | 50.7                     | n.d. | n.d.   | n.d.   |
| v18  | $PYR_m(abc) + CO_2(d) \rightarrow OAA_m(abcd)$                         | 59.6                       | 52.9                     | 64.1                     | 0    | 0      | 0      |
| v19  | $MAL_m(abcd) \rightarrow PYR_m(abc) + CO_2(d)$                         | 149.4                      | 142.8                    | 154.0                    | 0    | 0      | 0      |
| v20  | $PG(abc) \rightarrow SER(abc)$                                         | 21.2                       | 19.9                     | 21.9                     | 0    | 0      | 0      |
| v21  | $SER(abc) \leftrightarrow GLY(ab) + MTHF(c)$                           | 34.5                       | 33.3                     | 35.2                     | 4.03 | 3.43   | 4.75   |
| v22  | $SER_{ex}(abc) \leftrightarrow SER(abc)$                               | 48.3                       | 39.2                     | 57.4                     | 33.5 | 14.0   | 98.5   |
| v23  | $SER(abc) \rightarrow \text{Biomass}$                                  | 4.9                        | -                        | -                        | 0    | -      | -      |
| v24  | $GLY(abc) \leftrightarrow GLY_{ex}(abc)$                               | 25.5                       | 22.0                     | 29.0                     | 4.6  | 2.2    | 6.9    |
| v25  | $GLY(abc) \rightarrow \text{Biomass}$                                  | 9.0                        | -                        | -                        | 0    | -      | -      |
| v26  | $SER(abc) \rightarrow PYR_{ci}(abc)$                                   | 30.0                       | 28.8                     | 30.8                     | 0    | 0      | 0      |

|     |                                                                                  |       |       |       |                                   |                      |                      |
|-----|----------------------------------------------------------------------------------|-------|-------|-------|-----------------------------------|----------------------|----------------------|
| v27 | $PYR_{ci}(abc) + GLU_c(defgh) \leftrightarrow ALA_c(abc) + AKG_c(defgh)$         | 40.1  | 38.3  | 129.2 | 36.6                              | 17.3                 | >100                 |
| v28 | $ALA_c(abc) \leftrightarrow ALA_{ex}(abc)$                                       | 42.7  | 39.9  | 45.5  | 0.154·<br>·e <sup>(t*0.036)</sup> | 0.142<br>(0.038<br>) | 0.169<br>(0.04<br>2) |
| v29 | $ALA_c(abc) \rightarrow Biomass$                                                 | 6.7   | -     | -     | 0                                 | -                    | -                    |
| v30 | $ALA_m(abc) \leftrightarrow ALA_c(abc)$                                          | 9.5   | -10.6 | 13.6  | 0.15                              | 0                    | 1.15                 |
| v31 | $PYR_m(abc) + GLU_m(defgh) \leftrightarrow ALA_m(abc) + AKG_m(defgh)$            | 9.5   | -10.6 | 13.6  | n.d.                              | -                    | -                    |
| v32 | $PYR_{ci}(abc) \leftrightarrow PYR_{ex}(abc)$                                    | 3.3   | 2.1   | 4.56  | 2700/t                            | 2055/t               | 2808/<br>t           |
| v33 | $ASP_c(abcd) + AKG_c(efghi) \leftrightarrow OAA_c(abcd) + GLU_c(efghi)$          | 45.3  | 31.9  | 48.3  | 19.3                              | 1.3                  | >100                 |
| v34 | $ASP_c(abcd) + AKG_m(edghi) \rightarrow OAA_m(abcd) + GLU_m(efghi)$              | 14.5  | 11.4  | 27.9  | 0                                 | 0                    | 0                    |
| v35 | $ASN(abcd) \rightarrow ASP_c(abcd)$                                              | 47.2  | 31.1  | 63.2  | 0                                 | 0                    | 0                    |
| v36 | $ASP_{ex}(abcd) \leftrightarrow ASP_c(abcd)$                                     | 20.9  | 1.1   | 40.7  | 0.7                               | 0.34                 | 0.84                 |
| v37 | $ASP_c(abcd) \rightarrow Biomass$                                                | 8.4   | -     | -     | 0                                 | -                    | -                    |
| v38 | $MAL_c(abcd) \leftrightarrow MAL_m(abcd)$                                        | 2.9   | 0.9   | 5.0   | 6.9                               | 0.8                  | 15.1                 |
| v39 | $CIT_m(abcdef) \rightarrow CIT_c(abcdef)$                                        | 106.6 | 40.1  | n.d.  | 0                                 | 0                    | 0                    |
| v40 | $CIT_c(abcdef) \rightarrow AKG_c(abcde) + CO_2(e)$                               | 67.6  | 1     | n.d.  | 0                                 | 0                    | 0                    |
| v41 | $AKG_m(abcde) \leftrightarrow AKG_c(abcde)$                                      | 26.3  | -62.8 | 53.5  | 8.2                               | 2.15                 | >100                 |
| v42 | $AKG_c(abcde) \leftrightarrow GLU_c(abcde)$                                      | 71.2  | 62.7  | 78.8  | n.d.                              | -                    | -                    |
| v43 | $GLU_c(abcde) \rightarrow GLU_m(abcde)$                                          | 74.8  | 66.4  | 82.5  | 0                                 | 0                    | 0                    |
| v44 | $GLU_m(abcde) \leftrightarrow AKG_m(abcde)$                                      | 161.0 | 158.5 | 179.8 | n.d.                              | -                    | -                    |
| v45 | $GLU_c(abcde) \leftrightarrow GLU_{ex}(abcde)$                                   | 6.3   | 3.4   | 9.3   | 1.3                               | 1.2                  | 1.6                  |
| v46 | $GLU_c(abcde) \rightarrow Biomass$                                               | 9.7   | -     | -     | 0                                 | -                    | -                    |
| v47 | $GLN_c(abcde) \rightarrow GLU_c(abcde)$                                          | 14.6  | 13.3  | 15.8  | 0                                 | 0                    | 0                    |
| v48 | $GLN_c(abcde) \rightarrow GLU_m(abcde)$                                          | 81.0  | 80.1  | 82.4  | 0                                 | 0                    | 0                    |
| v49 | $GLN_{ex}(abcde) \leftrightarrow GLN_c(abcde)$                                   | 66.4  | 50.3  | 82.4  | 1.28                              | 1.02                 | 1.78                 |
| v50 | $CIT_c(abcdef) \rightarrow OAA_c(fcde) + AcoAc(ab)$                              | 39.1  | -     | -     | 0                                 | -                    | -                    |
| v51 | $AcoAc(ab) \rightarrow Biomass$                                                  | 39.1  | -     | -     | 0                                 | -                    | -                    |
| v52 | $AA_{ex}(ILE, VAL, MET, THR, TYR, PHE) \rightarrow MAL_m(AA \text{ catabolism})$ | 49.6  | 5.1   | 99.9  | 0                                 | -                    | -                    |
| v53 | $AA_{ex}(LEU, ILE, LYS, TYR, PHE) \rightarrow ACOA_m(AA \text{ catabolism})$     | 92.6  | 27.9  | 161.4 | 0                                 | -                    | -                    |
| v54 | $AKG_c(abcde) \rightarrow GLU_c(abcde) (AA \text{ catabolism})$                  | 38.7  | 5.2   | 75.6  | 0                                 | -                    | -                    |
| v55 | $AA(PRO, HIS, ARG) \rightarrow GLU_c(AA \text{ catabolism})$                     | 11.6  | 0.8   | 25.3  | 0                                 | -                    | -                    |
| v56 | $PYR_{ci}(abcd) \leftrightarrow ALA_c(abcd)$                                     | 0     | -     | -     | 0                                 | -                    | -                    |
| v57 | $PYR_m(abc) \leftrightarrow LAC(abc)$                                            | 0     | -     | -     | 0                                 | -                    | -                    |

---

|     |                                                |       |       |       |      |   |      |
|-----|------------------------------------------------|-------|-------|-------|------|---|------|
| v58 | $PYR_{c1}(abc) \leftrightarrow PYR_{c2}(abc)$  | 168.1 | 149.2 | 174.8 | 0.13 | 0 | 0.41 |
| v59 | $PEP(abc) \rightarrow PYR_{c2}(abc)$           | 122.7 | 103.8 | 129.4 | 0    | 0 | 0    |
| v60 | $G6P(abcdef) \rightarrow \text{carbohydrates}$ | 8.9   | -     | -     | 0    | 0 | 0    |

**Supplem. Table S3.2.** Experimental (exp) and simulated (sim) mass isotopomer distributions of extracellular metabolites and used standard deviations (SD).

| exp<br>Time [h]    | Lactate |       |       |       | Alanine |       |       |       | Aspartate |       |       |       |       |
|--------------------|---------|-------|-------|-------|---------|-------|-------|-------|-----------|-------|-------|-------|-------|
|                    | Mo      | M1    | M2    | M3    | Mo      | M1    | M2    | M3    | Mo        | M1    | M2    | M3    | M4    |
| 1                  | 0.889   | 0.027 | 0.003 | 0.081 | 0.963   | 0.031 | 0.002 | 0.004 | 0.972     | 0.028 | 0.000 | 0.000 | 0.000 |
| 18                 | 0.345   | 0.013 | 0.029 | 0.613 | 0.802   | 0.024 | 0.007 | 0.167 | 0.973     | 0.026 | 0.000 | 0.001 | 0.000 |
| 24                 | 0.267   | 0.012 | 0.037 | 0.684 | 0.728   | 0.023 | 0.010 | 0.239 | 0.965     | 0.032 | 0.000 | 0.002 | 0.000 |
| 42                 | 0.150   | 0.011 | 0.051 | 0.788 | 0.512   | 0.019 | 0.018 | 0.451 | 0.950     | 0.038 | 0.007 | 0.004 | 0.001 |
| 48                 | 0.128   | 0.012 | 0.055 | 0.805 | 0.409   | 0.018 | 0.024 | 0.549 | 0.948     | 0.038 | 0.007 | 0.005 | 0.001 |
| 66                 | 0.092   | 0.012 | 0.057 | 0.839 | 0.206   | 0.015 | 0.034 | 0.745 | 0.936     | 0.039 | 0.011 | 0.011 | 0.004 |
| 72                 | 0.082   | 0.012 | 0.058 | 0.848 | 0.149   | 0.014 | 0.038 | 0.799 | 0.932     | 0.035 | 0.014 | 0.014 | 0.005 |
| sim<br>Time [h]    | Lactate |       |       |       | Alanine |       |       |       | Aspartate |       |       |       |       |
|                    | Mo      | M1    | M2    | M3    | Mo      | M1    | M2    | M3    | Mo        | M1    | M2    | M3    | M4    |
| 1                  | 0.897   | 0.030 | 0.002 | 0.070 | 0.966   | 0.033 | 0.000 | 0.001 | 0.972     | 0.028 | 0.000 | 0.000 | 0.000 |
| 18                 | 0.301   | 0.020 | 0.025 | 0.654 | 0.824   | 0.030 | 0.006 | 0.140 | 0.969     | 0.029 | 0.001 | 0.001 | 0.000 |
| 24                 | 0.247   | 0.020 | 0.028 | 0.706 | 0.742   | 0.029 | 0.009 | 0.219 | 0.967     | 0.030 | 0.002 | 0.001 | 0.000 |
| 42                 | 0.169   | 0.019 | 0.032 | 0.780 | 0.475   | 0.026 | 0.021 | 0.478 | 0.959     | 0.032 | 0.005 | 0.004 | 0.001 |
| 48                 | 0.156   | 0.019 | 0.033 | 0.792 | 0.392   | 0.025 | 0.025 | 0.558 | 0.954     | 0.033 | 0.007 | 0.005 | 0.002 |
| 66                 | 0.131   | 0.019 | 0.035 | 0.814 | 0.207   | 0.024 | 0.035 | 0.734 | 0.929     | 0.038 | 0.016 | 0.013 | 0.004 |
| 72                 | 0.125   | 0.020 | 0.036 | 0.819 | 0.170   | 0.025 | 0.038 | 0.767 | 0.915     | 0.042 | 0.021 | 0.017 | 0.005 |
| exp SD<br>Time [h] | Lactate |       |       |       | Alanine |       |       |       | Aspartate |       |       |       |       |
|                    | Mo      | M1    | M2    | M3    | Mo      | M1    | M2    | M3    | Mo        | M1    | M2    | M3    | M4    |
| 1                  | 0.039   | 0.005 | 0.005 | 0.005 | 0.036   | 0.022 | 0.009 | 0.005 | 0.011     | 0.022 | 0.005 | 0.005 | 0.010 |
| 18                 | 0.038   | 0.020 | 0.022 | 0.038 | 0.041   | 0.011 | 0.005 | 0.037 | 0.022     | 0.007 | 0.005 | 0.008 | 0.021 |
| 24                 | 0.035   | 0.008 | 0.035 | 0.044 | 0.021   | 0.010 | 0.024 | 0.032 | 0.006     | 0.023 | 0.023 | 0.005 | 0.026 |
| 42                 | 0.035   | 0.006 | 0.042 | 0.040 | 0.036   | 0.022 | 0.024 | 0.025 | 0.024     | 0.005 | 0.023 | 0.021 | 0.022 |
| 48                 | 0.023   | 0.024 | 0.026 | 0.028 | 0.026   | 0.007 | 0.023 | 0.036 | 0.022     | 0.011 | 0.010 | 0.005 | 0.025 |
| 66                 | 0.036   | 0.006 | 0.038 | 0.037 | 0.023   | 0.022 | 0.021 | 0.005 | 0.025     | 0.009 | 0.022 | 0.022 | 0.024 |
| 72                 | 0.005   | 0.022 | 0.030 | 0.035 | 0.038   | 0.009 | 0.024 | 0.028 | 0.009     | 0.023 | 0.005 | 0.006 | 0.024 |

**(Table S3.2.cont.)**

| exp      | Glutamate |       |       |       |       |       | Glutamine |       |       |       |       |       |
|----------|-----------|-------|-------|-------|-------|-------|-----------|-------|-------|-------|-------|-------|
| Time [h] | Mo        | M1    | M2    | M3    | M4    | M5    | Mo        | M1    | M2    | M3    | M4    | M5    |
| 1        | 0.943     | 0.048 | 0.000 | 0.009 | 0.000 | 0.000 | 0.956     | 0.042 | 0.000 | 0.000 | 0.002 | 0.000 |
| 18       | 0.915     | 0.050 | 0.020 | 0.011 | 0.003 | 0.001 | 0.953     | 0.043 | 0.000 | 0.001 | 0.002 | 0.000 |
| 24       | 0.895     | 0.052 | 0.034 | 0.011 | 0.005 | 0.002 | 0.951     | 0.043 | 0.002 | 0.001 | 0.003 | 0.000 |
| 42       | 0.848     | 0.050 | 0.065 | 0.017 | 0.014 | 0.007 | 0.927     | 0.057 | 0.011 | 0.001 | 0.004 | 0.001 |
| 48       | 0.830     | 0.041 | 0.080 | 0.024 | 0.017 | 0.009 | 0.937     | 0.045 | 0.007 | 0.002 | 0.007 | 0.001 |
| 66       | 0.699     | 0.048 | 0.146 | 0.036 | 0.045 | 0.026 | 0.898     | 0.043 | 0.026 | 0.009 | 0.016 | 0.007 |
| 72       | 0.634     | 0.049 | 0.175 | 0.045 | 0.059 | 0.038 | 0.780     | 0.054 | 0.078 | 0.023 | 0.042 | 0.024 |
| sim      | Glutamate |       |       |       |       |       | Glutamine |       |       |       |       |       |

| Time [h] | Mo        | M1    | M2    | M3    | M4    | M5    | Mo        | M1    | M2    | M3    | M4    | M5    |
|----------|-----------|-------|-------|-------|-------|-------|-----------|-------|-------|-------|-------|-------|
| 1        | 0.957     | 0.042 | 0.000 | 0.000 | 0.000 | 0.000 | 0.958     | 0.042 | 0.000 | 0.000 | 0.000 | 0.000 |
| 18       | 0.932     | 0.045 | 0.014 | 0.004 | 0.004 | 0.001 | 0.955     | 0.043 | 0.002 | 0.000 | 0.001 | 0.000 |
| 24       | 0.917     | 0.047 | 0.021 | 0.006 | 0.008 | 0.001 | 0.952     | 0.043 | 0.003 | 0.001 | 0.001 | 0.000 |
| 42       | 0.845     | 0.053 | 0.054 | 0.019 | 0.024 | 0.005 | 0.941     | 0.044 | 0.008 | 0.003 | 0.004 | 0.001 |
| 48       | 0.812     | 0.055 | 0.069 | 0.025 | 0.032 | 0.007 | 0.934     | 0.044 | 0.011 | 0.004 | 0.005 | 0.001 |
| 66       | 0.680     | 0.065 | 0.128 | 0.050 | 0.063 | 0.014 | 0.879     | 0.049 | 0.036 | 0.014 | 0.018 | 0.004 |
| 72       | 0.627     | 0.069 | 0.150 | 0.060 | 0.076 | 0.017 | 0.793     | 0.056 | 0.073 | 0.030 | 0.039 | 0.009 |
| Exp SD   | Glutamate |       |       |       |       |       | Glutamine |       |       |       |       |       |
| Time [h] | Mo        | M1    | M2    | M3    | M4    | M5    | Mo        | M1    | M2    | M3    | M4    | M5    |
| 1        | 0.005     | 0.005 | 0.009 | 0.008 | 0.023 | 0.007 | 0.009     | 0.005 | 0.008 | 0.005 | 0.005 | 0.023 |
| 18       | 0.020     | 0.005 | 0.005 | 0.026 | 0.025 | 0.010 | 0.024     | 0.005 | 0.023 | 0.022 | 0.005 | 0.007 |
| 24       | 0.023     | 0.011 | 0.010 | 0.010 | 0.005 | 0.024 | 0.022     | 0.023 | 0.006 | 0.005 | 0.005 | 0.022 |
| 42       | 0.023     | 0.005 | 0.023 | 0.009 | 0.010 | 0.023 | 0.008     | 0.024 | 0.025 | 0.005 | 0.005 | 0.023 |
| 48       | 0.039     | 0.036 | 0.039 | 0.011 | 0.009 | 0.008 | 0.006     | 0.025 | 0.025 | 0.010 | 0.005 | 0.005 |
| 66       | 0.028     | 0.033 | 0.041 | 0.025 | 0.010 | 0.024 | 0.030     | 0.005 | 0.025 | 0.005 | 0.035 | 0.005 |
| 72       | 0.037     | 0.034 | 0.030 | 0.023 | 0.005 | 0.005 | 0.035     | 0.005 | 0.007 | 0.023 | 0.026 | 0.022 |

(Table S3.2.cont.)

| exp      | Glycine |       |       | Serine |       |       |       | Pyruvate |       |       |       |       |
|----------|---------|-------|-------|--------|-------|-------|-------|----------|-------|-------|-------|-------|
| Time [h] | Mo      | M1    | M2    | Mo     | M1    | M2    | M3    | Mo       | M1    | M2    | M3    | M5    |
| 1        | 0.984   | 0.016 | 0.000 | 0.993  | 0.007 | 0.000 | 0.000 | 0.873    | 0.027 | 0.002 | 0.098 | 0.000 |
| 18       | 0.977   | 0.017 | 0.006 | 0.969  | 0.013 | 0.000 | 0.018 | 0.318    | 0.014 | 0.025 | 0.643 | 0.000 |
| 24       | 0.975   | 0.016 | 0.009 | 0.958  | 0.016 | 0.000 | 0.026 | 0.241    | 0.012 | 0.029 | 0.717 | 0.000 |
| 42       | 0.961   | 0.017 | 0.022 | 0.913  | 0.029 | 0.010 | 0.049 | 0.177    | 0.012 | 0.034 | 0.777 | 0.001 |
| 48       | 0.950   | 0.018 | 0.032 | 0.885  | 0.035 | 0.017 | 0.063 | 0.160    | 0.012 | 0.037 | 0.791 | 0.001 |
| 66       | 0.904   | 0.018 | 0.079 | 0.757  | 0.084 | 0.056 | 0.103 | 0.149    | 0.013 | 0.041 | 0.797 | 0.007 |
| 72       | 0.879   | 0.017 | 0.104 | 0.670  | 0.118 | 0.085 | 0.128 | 0.124    | 0.014 | 0.051 | 0.811 | 0.024 |
| sim      | Glycine |       |       | Serine |       |       |       | Pyruvate |       |       |       |       |
| Time [h] | Mo      | M1    | M2    | Mo     | M1    | M2    | M3    | Mo       | M1    | M2    | M3    | M5    |
| 1        | 0.978   | 0.022 | 0.000 | 0.992  | 0.007 | 0.000 | 0.000 | 0.887    | 0.030 | 0.003 | 0.080 | 0.000 |
| 18       | 0.978   | 0.019 | 0.003 | 0.978  | 0.009 | 0.002 | 0.012 | 0.293    | 0.022 | 0.027 | 0.659 | 0.000 |
| 24       | 0.977   | 0.018 | 0.005 | 0.969  | 0.010 | 0.003 | 0.018 | 0.228    | 0.021 | 0.030 | 0.720 | 0.000 |
| 42       | 0.966   | 0.014 | 0.020 | 0.925  | 0.020 | 0.010 | 0.045 | 0.160    | 0.021 | 0.035 | 0.784 | 0.001 |
| 48       | 0.958   | 0.013 | 0.029 | 0.900  | 0.028 | 0.015 | 0.057 | 0.153    | 0.021 | 0.036 | 0.789 | 0.001 |
| 66       | 0.905   | 0.011 | 0.084 | 0.754  | 0.084 | 0.053 | 0.108 | 0.137    | 0.024 | 0.038 | 0.801 | 0.004 |
| 72       | 0.873   | 0.011 | 0.116 | 0.665  | 0.124 | 0.079 | 0.132 | 0.129    | 0.025 | 0.040 | 0.806 | 0.009 |
| exp SD   | Glycine |       |       | Serine |       |       |       | Pyruvate |       |       |       |       |
| Time [h] | Mo      | M1    | M2    | Mo     | M1    | M2    | M3    | Mo       | M1    | M2    | M3    | M5    |
| 1        | 0.010   | 0.022 | 0.022 | 0.025  | 0.006 | 0.005 | 0.005 | 0.032    | 0.025 | 0.011 | 0.024 | 0.023 |
| 18       | 0.024   | 0.026 | 0.011 | 0.011  | 0.007 | 0.022 | 0.022 | 0.005    | 0.023 | 0.020 | 0.042 | 0.007 |
| 24       | 0.024   | 0.025 | 0.006 | 0.035  | 0.025 | 0.005 | 0.005 | 0.023    | 0.024 | 0.040 | 0.036 | 0.022 |
| 42       | 0.023   | 0.008 | 0.007 | 0.007  | 0.022 | 0.005 | 0.009 | 0.031    | 0.021 | 0.022 | 0.038 | 0.023 |

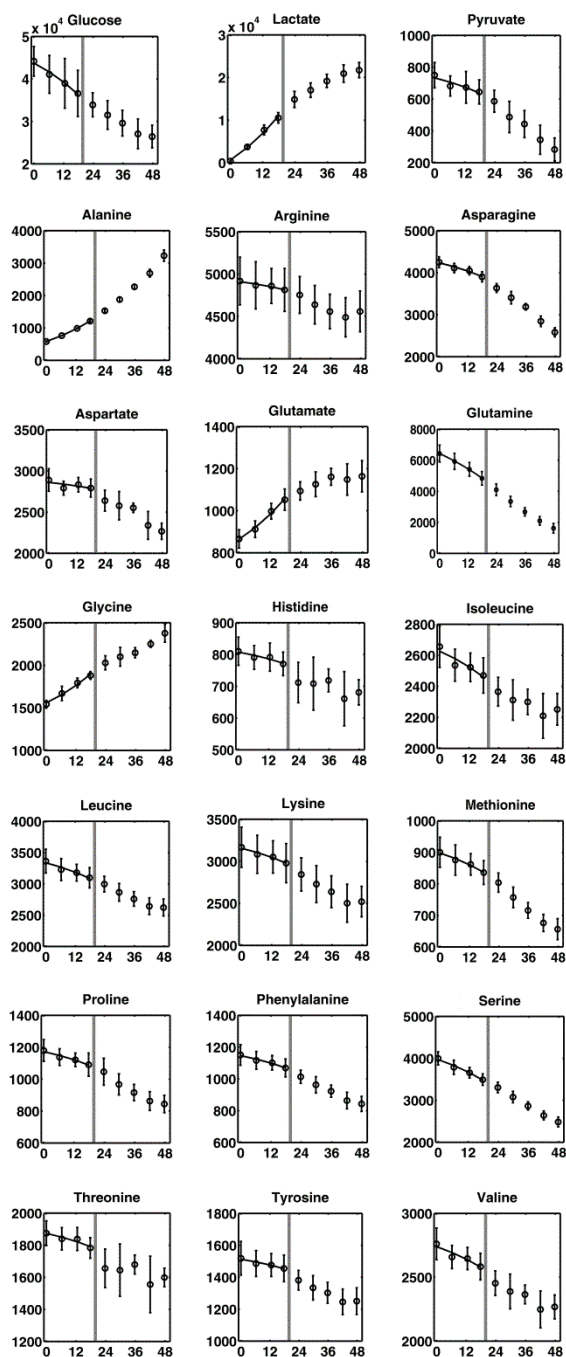


---

|    |       |       |       |       |       |       |       |       |       |       |       |       |
|----|-------|-------|-------|-------|-------|-------|-------|-------|-------|-------|-------|-------|
| 48 | 0.005 | 0.025 | 0.008 | 0.007 | 0.005 | 0.005 | 0.010 | 0.045 | 0.022 | 0.024 | 0.040 | 0.005 |
| 66 | 0.022 | 0.026 | 0.010 | 0.024 | 0.008 | 0.005 | 0.024 | 0.021 | 0.025 | 0.025 | 0.038 | 0.005 |
| 72 | 0.022 | 0.010 | 0.005 | 0.024 | 0.021 | 0.005 | 0.005 | 0.007 | 0.005 | 0.029 | 0.030 | 0.022 |

## Appendix to Chapter 4

**Supplem. Figure 4.1.** Cultivation profile of the CHO-K1 cells culture during 48 h in 250 ml baffled shake flask with a working volume of 120 mL. The represented extracellular concentrations are in [ $\mu\text{mol} / \text{L}$ ] and the time is in [h]. The values represent the average from 4 parallel cultivations. The curves are the fitted values of extracellular concentrations simulating an exponential growth model with balanced growth (metabolic steady state) over the first 18 h.



**Supplem. Table S4. 1. List of reactions used in the stoichiometric model for dynamic metabolic flux analysis.** Reactions represented with a simple arrow were constrained to be unidirectional, while those represented by double arrow can be reversible. Abbreviations: AcoA – acetyl-CoA; ALA – alanine; ASN – asparagine; ASP – aspartate; CIT – citrate; CYS – cysteine; DHAP – dihydroxyacetone-3-phosphate; FUM – fumarate; GLC – glucose; G6P – glucose-6-phosphate; GAP – glycerine aldehyde 3-phosphate; GLN – glutamine; GLU – glutamate; GLY – glycine; HIS – histidine; ICI – isocitrate; ILE – isoleucine; LAC – lactate; LEU – leucine; LYS – lysine; MAL – malate; MET – methionine; MTHF – methyltetrahydrofolate; OAA – oxaloacetate; PEP – phosphoenolpyruvate; PG – phosphoglycerate; PHE – phenylalanine; PYR – pyruvate; R5P – ribose-5-phosphate; S7P – sedoheptulose-7-phosphate; SER – serine; SUC – succinate; THR – threonine; TYR – tyrosine; VAL – valine.

| Reaction                                                                                                  |
|-----------------------------------------------------------------------------------------------------------|
| $GLC_{ex} \rightarrow G6P$                                                                                |
| $G6P \rightarrow F6P$                                                                                     |
| $F6P \rightarrow GAP + DHAP$                                                                              |
| $DHAP \leftrightarrow GAP$                                                                                |
| $GAP \rightarrow 1,3PG$                                                                                   |
| $1,3PG \rightarrow 3PG$                                                                                   |
| $3PG \rightarrow PEP$                                                                                     |
| $PEP \rightarrow PYR$                                                                                     |
| $G6P \rightarrow \text{Carbohydrates}$                                                                    |
| $PYR \rightarrow AcoA + CO_2$                                                                             |
| $OAA + AcoA \rightarrow CIT$                                                                              |
| $CIT \rightarrow AKG + CO_2$                                                                              |
| $AKG \rightarrow SUC + CO_2$                                                                              |
| $SUC \rightarrow FUM$                                                                                     |
| $FUM \rightarrow MAL$                                                                                     |
| $MAL \leftrightarrow OAA$                                                                                 |
| $PEP \leftrightarrow OAA$ (generic C3 – C4 reaction)                                                      |
| $PYR \leftrightarrow LAC$                                                                                 |
| $G6P \rightarrow R5P + CO_2$                                                                              |
| $2R5P \leftrightarrow S7P + GAP$                                                                          |
| $GAP + S7P \leftrightarrow F6P + E4P$                                                                     |
| $R5P + E4P \leftrightarrow F6P + GAP$                                                                     |
| $R5P + 1.215 GLN + 0.5 GLY + 1.285 ASP + 0.715 NH_3 + 0.285 MTHF \rightarrow DNA + 1.215 GLU + 0.785 FUM$ |
| $R5P + 1.215 GLN + 0.5 GLY + 1.285 ASP + 0.715 NH_3 \rightarrow RNA + 1.215 GLU + 0.785 FUM$              |
| $0.775 DHAP + 17.075 AcoA + 0.15 SER \rightarrow Lipids$                                                  |
| $ALA \rightarrow \text{Proteins}$                                                                         |
| $ASP \rightarrow \text{Proteins}$                                                                         |
| $CYS \rightarrow \text{Proteins}$                                                                         |
| $GLU \rightarrow \text{Proteins}$                                                                         |
| $GLY \rightarrow \text{Proteins}$                                                                         |
| $HIS \rightarrow \text{Proteins}$                                                                         |
| $ILE \rightarrow \text{Proteins}$                                                                         |
| $LEU \rightarrow \text{Proteins}$                                                                         |
| $MET \rightarrow \text{Proteins}$                                                                         |
| $LYS \rightarrow \text{Proteins}$                                                                         |
| $PHE \rightarrow \text{Proteins}$                                                                         |

$PRO \rightarrow Proteins$   
 $SER \rightarrow Proteins$   
 $THR \rightarrow Proteins$   
 $TYR \rightarrow Proteins$   
 $VAL \rightarrow Proteins$   
 $ALA + AKG \leftrightarrow PYR + GLU$   
 $ASP + AKG \leftrightarrow OAA + GLU$   
 $ASP + NH_3 \leftrightarrow ASN$   
 $ARG \rightarrow GLU$  (arginine catabolism)  
 $CYS \rightarrow PYR$  (cysteine catabolism)  
 $GLN \leftrightarrow GLU + NH_3$   
 $LEU + AKG \rightarrow 3 AcoA + GLU$  (leucine catabolism)  
 $VAL + AKG \rightarrow SUC + CO_2 + GLU$   
 $GLU \rightarrow AKG + NH_3$   
 $SER \leftrightarrow GLY + MTHF$   
 $HIS \rightarrow GLU + MTHF$  (histidine catabolism)  
 $LYS + AKG \rightarrow 2 AcoA + 2 CO_2 + GLU$  (lysine catabolism)  
 $MET + AKG \rightarrow SUC + MTHF + GLU$  (methionine catabolism)  
 $PHE + AKG \rightarrow TYR + GLU$   
 $PRO \rightarrow GLU$   
 $SER \rightarrow PYR + NH_3$  (serine catabolism)  
 $THR \rightarrow SUC$  (threonine catabolism)  
 $TYR \rightarrow 2 AcoA + FUM + CO_2 + GLU$  (tyrosine catabolism)  
 $GLN_{ex} \rightarrow GLN$   
 $LAC_{ex} \rightarrow LAC$   
 $PYR_{ex} \rightarrow PYR$   
 $NH_3 \rightarrow NH_{3ex}$   
 $ALA_{ex} \leftrightarrow ALA$   
 $ASP_{ex} \leftrightarrow ASP$   
 $ASN_{ex} \rightarrow ASN$   
 $ARG_{ex} \rightarrow ARG$   
 $CYS_{ex} \rightarrow CYS$   
 $GLU_{ex} \leftrightarrow GLU$   
 $GLY_{ex} \leftrightarrow GLY$   
 $HIS_{ex} \rightarrow HIS$   
 $ILE_{ex} \rightarrow ILE$   
 $LEU_{ex} \rightarrow LEU$   
 $LYE_{ex} \rightarrow LYS$   
 $MET_{ex} \rightarrow MET$   
 $PHE_{ex} \rightarrow PHE$   
 $PRO_{ex} \rightarrow PRO$   
 $SER_{ex} \rightarrow SER$   
 $THR_{ex} \rightarrow THR$   
 $TYR_{ex} \rightarrow TYR$   
 $VAL_{ex} \rightarrow VAL$   
 $MTHF_{sink} \leftrightarrow MTHF$

**Supplem. Table S4.2.** List of reactions, fluxes and reversibilities in the central carbon metabolism of CHO-K1 estimated for the first 2 – 18 h cultivation period. Carbon transfer rules are given in parentheses for each reaction. Reversible reactions are indicated by double arrows. Reversibility (rev) is computed as the ratio between the reverse flux and the net flux. The 95% confidence interval was evaluated by refitting the model until the minimized objective function took the value of  $\chi^2(0.95, \text{nr. experimental points} - \text{nr. parameters})$ . lb – lower boundary; ub – upper boundary; Subscripts meaning: c – cytosolic; ex – extracellular; m – mitochondrial; Abbreviations: AcoA – acetyl-CoA; ALA – alanine; ASN – asparagine; ASP – aspartate; CIT – citrate; FUM – fumarate; GLC – glucose; G6P – glucose-6-phosphate; PG – phosphoglycerate; PEP – phosphoenolpyruvate; GLN – glutamine; GLU – glutamate; GLY – glycine; ICI – isocitrate; ILE – isoleucine; LAC – lactate; LEU – leucine; LYS – lysine; MAL – malate; MET – methionine; OAA – oxaloacetate; PHE – phenylalanine; PYR – pyruvate; SER – serine; SUC – succinate; THR – threonine; TYR – tyrosine; VAL – valine.

| Flux | Reaction                                                                                                              | Flux<br>[mmol/L<br>cell $\times$ h] | lb<br>[mmol/L<br>cell $\times$ h] | ub<br>[mmol/L<br>cell $\times$ h] | rev  | rev<br>lb | rev<br>ub |
|------|-----------------------------------------------------------------------------------------------------------------------|-------------------------------------|-----------------------------------|-----------------------------------|------|-----------|-----------|
| v1   | $GLC_{ex}(abcdef) + ATP_c \rightarrow G6P(abcdef) + ADP_c$                                                            | 289.7                               | 246.3                             | 333.0                             | 0    | 0         | 0         |
| v2   | $G6P(abcdef) + ADP_c + 2 NAD^+_c \rightarrow PG(abc) + PG(def) + ATP_c + 2 NADH_c$                                    | 24.3                                | 18.6                              | 29.2                              | 0    | 0         | 0         |
| v3   | $3 G6P(abcdef) + 3 ADP_c + 5 NAD^+_c + 6 NADP^+_c \rightarrow 5 PG(def) + 3 CO_2(a) + 3 ATP_c + 5 NADH_c + 6 NADPH_c$ | 87.4                                | 85.4                              | 89.6                              | 0    | 0         | 0         |
| v4   | $G6P(abcdef) + 6.43 ATP_c + 0.72 NADH_c \rightarrow (DNA, RNA) + 6.43 ADP_c + 0.72 NAD^+_c$                           | 3.3                                 | 3.3                               | 3.3                               | 0    | 0         | 0         |
| v5   | $PG(abc) \rightarrow PEP_c(abc)$                                                                                      | 464.9                               | 464.7                             | 465.0                             | 0    | 0         | 0         |
| v6   | $PEP_c(abc) + ADP_c \rightarrow PYR_{ci}(abc) + ATP_c$                                                                | 498.2                               | 492.3                             | 500.2                             | 0    | 0         | 0         |
| v7   | $PYR_{ci}(abc) \rightarrow PYR_{m2}(abc)$                                                                             | 118.9                               | 113.7                             | 119.0                             | 0    | 0         | 0         |
| v8   | $PYR_{m2}(abc) + NAD^+_m \rightarrow AcoA_m(bc) + CO_2(a) + NADH_m$                                                   | 77.5                                | 77.2                              | 77.6                              | 0    | 0         | 0         |
| v9   | $OAA_m(abcd) + AcoA_m(ef) \rightarrow CIT_m(efbcda)$                                                                  | 100.8                               | 100.6                             | 100.9                             | 0    | 0         | 0         |
| v10  | $CIT_m(abcdef) + NAD(P)^+_m \rightarrow AKG_m(abcde) + CO_2(f) + NAD(P)H_m$                                           | 58.7                                | 57.0                              | 67.7                              | 0    | 0         | 0         |
| v11  | $AKG_m(abcde) + NAD^+_m \rightarrow 0.5 MAL_m(abcd) + 0.5 MAL_m(dcba) + CO_2(e) + NADH_m$                             | 105.6                               | 105.4                             | 105.7                             | 0    | 0         | 0         |
| v12  | $MAL_m(abcd) + NAD^+_m \leftrightarrow OAA_m(abcd) + NADH$                                                            | 191.6                               | 185.1                             | 198.9                             | 10.3 | 10.2      | 11.3      |

|     |                                                                          |       |       |       |                      |                      |                       |
|-----|--------------------------------------------------------------------------|-------|-------|-------|----------------------|----------------------|-----------------------|
| v13 | $PYR_{c2}(abc) + NADH_c \leftrightarrow LAC_{c2}(abc) + NAD^+_c$         | 431.7 | 391.0 | 472.3 | 31.9                 | 18.6                 | 32.0                  |
| v14 | $LAC_c(abc) \leftrightarrow LAC_{ex}(abc)$                               | 431.7 | 391.0 | 472.3 | 28.2                 | 28.1                 | 28.3                  |
| v15 | $OAA_c(abcd) + GDP_c \rightarrow PEP_c(abc) + CO_2(d) + GTP_c$           | 66.4  | 61.2  | 68.5  | 0                    | 0                    | 0                     |
| v16 | $MAL_c(abcd) + NADP^+_c \rightarrow PYR_{ci}(abc) + CO_2(d) + NADPH_c$   | 5.4   | 0     | 11.0  | 0                    | 0                    | 0                     |
| v17 | $OAA_c(abcd) + NADH_c \leftrightarrow MAL_c(abcd) + NAD^+_c$             | 90.5  | 88.6  | 90.7  | 22.7                 | 21.7                 | 23.0                  |
| v18 | $PYR_{mi}(abc) + CO_2(d) + GTP_m \rightarrow OAA_m(abcd) + GDP_m$        | 23.1  | 15.1  | 24.8  | 0                    | 0                    | 0                     |
| v19 | $MAL_m(abcd) + NADP^+_m \rightarrow PYR_{mi}(abc) + CO_2(d) + NADPH_m$   | 8.3   | 5.9   | 9.2   | 0                    | 0                    | 0                     |
| v20 | $PG(abc) + NH_3_c \rightarrow SER(abc)$                                  | 20.5  | 20.4  | 20.5  | 0                    | 0                    | 0                     |
| v21 | $SER(abc) \leftrightarrow GLY(ab) + MTHF(c)$                             | 21.9  | 21.9  | 21.9  | 3.8                  | 3.2                  | 3.8                   |
| v22 | $SER_{ex}(abc) \leftrightarrow SER(abc)$                                 | 20.8  | 17.8  | 23.4  | 13.3                 | 13.1                 | 13.9                  |
| v23 | $SER(abc) + 4 ATP_c \rightarrow Proteins + 4 ADP_c$                      | 4.2   | 4.1   | 4.2   | 0                    | 0                    | 0                     |
| v24 | $GLY(abc) \leftrightarrow GLY_{ex}(abc)$                                 | 14.3  | 8.7   | 19.9  | 2.9                  | 1.9                  | 3.1                   |
| v25 | $GLY(abc) + 4 ATP_c \rightarrow Proteins + 4 ADP_c$                      | 7.6   | 7.5   | 7.7   | 0                    | 0                    | 0                     |
| v26 | $SER(abc) \rightarrow PYR_{ci} + NH_3_c(abc)$                            | 15.2  | 15.1  | 15.2  | 0                    | 0                    | 0                     |
| v27 | $PYR_{ci}(abc) + GLU_c(defgh) \leftrightarrow ALA_c(abc) + AKG_c(defgh)$ | 5.3   | 4.4   | 6.0   | 0.5                  | 0.4                  | 0.5                   |
| v28 | $ALA_c(abc) \leftrightarrow ALA_{ex}(abc)$                               | 26.3  | 26.1  | 26.5  | 2.7                  | 2.7                  | 4.1                   |
| v29 | $ALA_c(abc) + 4 ATP_c \rightarrow Proteins + 4 ADP_c$                    | 5.6   | 5.4   | 5.8   | 0                    | 0                    | 0                     |
| v30 | $ALA_m(abc) \leftrightarrow ALA_c(abc)$                                  | 26.6  | 25.9  | 27.5  | 3.7                  | 3.5                  | 4.7                   |
| v31 | $PYR_{mi}(abc) + GLU_m(defgh) \leftrightarrow ALA_m(abc) + AKG_m(defgh)$ | 26.6  | 25.9  | 27.5  | 14.4                 | 12.9                 | 14.6                  |
| v32 | $PYR_{ex}(abc) \leftrightarrow PYR_{ci}(abc)$                            | 4.0   | 2.2   | 5.8   | 1714/<br>time<br>[h] | 1700/<br>time<br>[h] | >2500/<br>time<br>[h] |
| v33 | $ASP_c(abcd) + AKG_c(efghi) \leftrightarrow OAA_c(abcd) + GLU_c(efghi)$  | 123.8 | 118.8 | 124.0 | 30.0                 | 1.9                  | n.d.                  |
| v34 | $OAA_m(abcd) + GLU_m(efghi) \leftrightarrow ASP_m(abcd) + AKG_m(efghi)$  | 113.8 | 108.8 | 114.0 | 62.5                 | 0                    | n.d.                  |
| v35 | $ASN(abcd) \rightarrow ASP_c(abcd)$                                      | 13.9  | 11.4  | 16.5  | 0                    | 0                    | 0                     |
| v36 | $ASP_{ex}(abcd) \leftrightarrow ASP_c(abcd)$                             | 3.1   | 0.0   | 6.7   | 5.8                  | 4.4                  | 6.4                   |

|     |                                                                                                                       |       |       |       |      |      |      |
|-----|-----------------------------------------------------------------------------------------------------------------------|-------|-------|-------|------|------|------|
| v37 | $ASP_c(abcd) + 4 ATP_c \rightarrow Proteins + 4 ADP_c$                                                                | 7.1   | 7.0   | 7.2   | 0    | 0    | 0    |
| v38 | $MAL_m(abcd) \leftrightarrow MAL_c(abcd)$                                                                             | 58.1  | 53.1  | 58.2  | 30.5 | 29.5 | n.d. |
| v39 | $CIT_m(abcdef) + MAL_c(ghij) \rightarrow CIT_c(abcdef) + MAL_m(ghij)$                                                 | 42.1  | 33.1  | 43.7  | 0    | 0    | 0    |
| v40 | $CIT_c(abcdef) + NADPH_c \rightarrow AKG_c(abcde) + CO_2(e) + NADP^+_c$                                               | 9.0   | 0     | 10.6  | 3.1  | 2.9  | 3.1  |
| v41 | $AKG_m(abcde) + MAL_c(fghi) \leftrightarrow AKG_c(abcde) + MAL_m(fghi)$                                               | 101.1 | 100.3 | 105.7 | 18.0 | 17.9 | 18.1 |
| v42 | $AKG_c(abcde) + NH_{3c} + NAD(P)H_c \leftrightarrow GLU_c(abcde) + NAD(P)^+_c$                                        | 0     | 0     | 0     | n.d. | -    | -    |
| v43 | $GLU_m(abcde) \rightarrow GLU_c(abcde)$                                                                               | 156.1 | 155.7 | 156.1 | 2.4  | 0    | 2.7  |
| v44 | $GLU_m(abcde) + NAD(P)^+_m \leftrightarrow AKG_m(abcde) + NAD(P)H_m + NH_{3m}$                                        | 7.5   | 7.5   | 7.6   | 9.5  | 7.1  | 9.5  |
| v45 | $GLU_c(abcde) \leftrightarrow GLU_{ex}(abcde)$                                                                        | 8.1   | 7.2   | 8.9   | 1.3  | 1.3  | 1.3  |
| v46 | $GLU_c(abcde) + 4 ATP_c \rightarrow Proteins + 4 ADP_c$                                                               | 8.2   | 7.9   | 8.5   | 0    | 0    | 0    |
| v47 | $GLU_c(abcde) + NH_{3c} + ATP_c \rightarrow GLN_c(abcde) + ADP_c$                                                     | 136.8 | 136.4 | 137.2 | 5.2  | 4.6  | 5.2  |
| v48 | $GLN_m(abcde) \rightarrow GLU_m(abcde) + NH_{3m}$                                                                     | 190.3 | 189.9 | 190.7 | 0    | 0    | 0    |
| v49 | $GLN_{ex}(abcde) \leftrightarrow GLN_c(abcde)$                                                                        | 53.5  | 51.3  | 55.6  | 0.6  | 0.5  | 0.6  |
| v50 | $CIT_c(abcdef) + ATP_c \rightarrow OAA_c(fcde) + AcoA_c(ab) + ADP_c$                                                  | 33.1  | 32.7  | 33.5  | 0    | 0    | 0    |
| v51 | $AcoA_c(ab) + 1.08 ATP_c + 0.09 NADH_c + 1.61 NADPH_c \rightarrow Lipids + 1.08 ADP_c + 0.09 NAD^+_c + 1.61 NADP^+_c$ | 33.1  | 32.7  | 33.5  | 0    | 0    | 0    |
| v52 | $AA_{ex}(ILE, VAL, MET, THR, TYR, PHE) \rightarrow SUC_m(AA \text{ catabolism})$                                      | 8.9   | 4.9   | 12.9  | 0    | 0    | 0    |
| v53 | $AA_{ex}(LEU, ILE, LYS, TYR, PHE) \rightarrow ACOA_m(AA \text{ catabolism})$                                          | 23.3  | 10.6  | 36.0  | 0    | 0    | 0    |
| v54 | $AKG_c(abcde) \rightarrow GLU_c(abcde) (AA \text{ catabolism})$                                                       | 12.2  | 3.4   | 20.5  | 0    | 0    | 0    |
| v55 | $AA(PRO, HIS, ARG) \rightarrow GLU_c(AA \text{ catabolism})$                                                          | 0.7   | 0     | 3.1   | 0    | 0    | 0    |
| v56 | $SUC_m(abcd) + ADP_m + FAD_m \leftrightarrow FUM_m(abcd) + ATP_m + FADH_{2m}$                                         | 114.5 | 114.3 | 114.6 | 0    | 0    | 0    |
| v57 | $FUM_m(abcd) \leftrightarrow MAL_m(abcd)$                                                                             | 114.7 | 114.5 | 114.8 | 47.6 | 45.5 | 83.6 |
| v58 | $PYR_{c1}(abc) \leftrightarrow PYR_{c2}(abc)$                                                                         | 398.5 | 398.0 | 398.6 | 0.13 | 0    | 0.13 |
| v59 | $PEP_c(abc) \rightarrow PYR_{c2}(abc)$                                                                                | 33.2  | 33.1  | 33.7  | 0    | 0    | 0    |

|     |                                                                         |       |       |       |      |      |      |
|-----|-------------------------------------------------------------------------|-------|-------|-------|------|------|------|
| v60 | $AA_{ex}(abcd) \rightarrow FUM_m(abcd)$ (AA catabolism)                 | 0.2   | 0.1   | 0.3   | 0    | 0    | 0    |
| v61 | $GLU_c(abcde) + ASP_m(efgh) \leftrightarrow GLU_m(abcde) + ASP_c(efgh)$ | 113.8 | 108.8 | 114.0 | 5.6  | 5.6  | 5.6  |
| v62 | $PYR_{m2}(abc) \leftrightarrow PYR_{m1}(abc)$                           | 41.4  | 36.4  | 41.5  | 0.06 | 0    | 0.06 |
|     | $PYR_{c1}(abc) \leftrightarrow LAC_{c1}(abc)$                           | -     | -     | -     | 60.0 | 59.9 | 60.2 |
|     | $PYR_{m1}(abc) \leftrightarrow LAC_m(abc)$                              | -     | -     | -     | 71.3 | 68.9 | 80.0 |



**Supplem. Table S4.3.** Experimental (exp) and simulated (sim) mass isotopomer distributions of extracellular metabolites and standard deviations (SD) used in simulations. (\_ex – extracellular; \_cell – intracellular);

| Time [h] | [U- <sup>13</sup> C <sub>6</sub> ] Glucose |                |                |                |                |                |                |                |            |                |                |
|----------|--------------------------------------------|----------------|----------------|----------------|----------------|----------------|----------------|----------------|------------|----------------|----------------|
| exp      | Lactate_ex                                 |                |                |                | Alanine_ex     |                |                |                | Glycine_ex |                |                |
|          | Mo                                         | M <sub>1</sub> | M <sub>2</sub> | M <sub>3</sub> | M <sub>1</sub> | M <sub>2</sub> | M <sub>3</sub> | M <sub>4</sub> | Mo         | M <sub>1</sub> | M <sub>2</sub> |
| 0        | 0.967                                      | 0.033          | 0.000          | 0.000          | 0.967          | 0.033          | 0.000          | 0.000          | 0.978      | 0.022          | 0.000          |
| 2        | 0.709                                      | 0.030          | 0.016          | 0.245          | 0.891          | 0.035          | 0.007          | 0.067          | 0.970      | 0.026          | 0.004          |
| 4        | 0.504                                      | 0.023          | 0.028          | 0.445          | 0.824          | 0.033          | 0.011          | 0.132          | 0.967      | 0.026          | 0.007          |
| 6        | 0.350                                      | 0.018          | 0.037          | 0.595          | 0.774          | 0.032          | 0.014          | 0.180          | 0.964      | 0.026          | 0.010          |
| 12       | 0.214                                      | 0.015          | 0.046          | 0.725          | 0.604          | 0.028          | 0.025          | 0.343          | 0.953      | 0.026          | 0.021          |
| 18       | 0.169                                      | 0.015          | 0.050          | 0.766          | 0.491          | 0.025          | 0.033          | 0.450          | 0.943      | 0.026          | 0.030          |
| sim      |                                            |                |                |                |                |                |                |                |            |                |                |
| 0        | 0.967                                      | 0.033          | 0.000          | 0.000          | 0.967          | 0.033          | 0.000          | 0.000          | 0.978      | 0.022          | 0.000          |
| 2        | 0.660                                      | 0.023          | 0.010          | 0.306          | 0.927          | 0.032          | 0.002          | 0.039          | 0.975      | 0.022          | 0.003          |
| 4        | 0.474                                      | 0.020          | 0.018          | 0.488          | 0.853          | 0.031          | 0.006          | 0.110          | 0.971      | 0.022          | 0.007          |
| 6        | 0.370                                      | 0.019          | 0.023          | 0.588          | 0.779          | 0.032          | 0.010          | 0.179          | 0.968      | 0.022          | 0.011          |
| 12       | 0.238                                      | 0.019          | 0.030          | 0.712          | 0.599          | 0.033          | 0.021          | 0.348          | 0.953      | 0.022          | 0.025          |
| 18       | 0.188                                      | 0.019          | 0.033          | 0.759          | 0.474          | 0.034          | 0.028          | 0.464          | 0.933      | 0.022          | 0.045          |
| SD       |                                            |                |                |                |                |                |                |                |            |                |                |
| 0        | 0.01                                       | 0.01           | 0.01           | 0.01           | 0.01           | 0.01           | 0.01           | 0.01           | 0.01       | 0.01           | 0.01           |
| 2        | 0.01                                       | 0.01           | 0.01           | 0.01           | 0.01           | 0.01           | 0.01           | 0.01           | 0.01       | 0.01           | 0.01           |
| 4        | 0.01                                       | 0.01           | 0.01           | 0.01           | 0.01           | 0.01           | 0.01           | 0.01           | 0.01       | 0.01           | 0.01           |
| 6        | 0.01                                       | 0.01           | 0.01           | 0.01           | 0.01           | 0.01           | 0.01           | 0.01           | 0.01       | 0.01           | 0.01           |
| 12       | 0.01                                       | 0.01           | 0.01           | 0.01           | 0.01           | 0.01           | 0.01           | 0.01           | 0.01       | 0.01           | 0.01           |
| 18       | 0.01                                       | 0.01           | 0.01           | 0.01           | 0.01           | 0.01           | 0.01           | 0.01           | 0.01       | 0.01           | 0.01           |

**Supplem. Table S4.3.(cont.)**

| Time [h] | [U- <sup>13</sup> C <sub>6</sub> ] Glucose |                |                |                |              |                |                |                |                |  |
|----------|--------------------------------------------|----------------|----------------|----------------|--------------|----------------|----------------|----------------|----------------|--|
| exp      | Serine_ex                                  |                |                |                | Aspartate_ex |                |                |                |                |  |
|          | Mo                                         | M <sub>1</sub> | M <sub>2</sub> | M <sub>3</sub> | Mo           | M <sub>1</sub> | M <sub>2</sub> | M <sub>3</sub> | M <sub>4</sub> |  |
| 0.000    | 0.967                                      | 0.033          | 0.000          | 0.000          | 0.956        | 0.043          | 0.001          | 0.000          | 0.000          |  |
| 0.004    | 0.954                                      | 0.035          | 0.003          | 0.007          | 0.951        | 0.047          | 0.002          | 0.000          | 0.000          |  |
| 0.007    | 0.944                                      | 0.037          | 0.004          | 0.014          | 0.949        | 0.047          | 0.002          | 0.001          | 0.000          |  |
| 0.010    | 0.937                                      | 0.039          | 0.005          | 0.019          | 0.948        | 0.048          | 0.003          | 0.001          | 0.000          |  |
| 0.021    | 0.902                                      | 0.045          | 0.013          | 0.041          | 0.938        | 0.049          | 0.009          | 0.004          | 0.001          |  |
| 0.030    | 0.868                                      | 0.054          | 0.021          | 0.057          | 0.942        | 0.044          | 0.007          | 0.006          | 0.001          |  |
| sim      |                                            |                |                |                |              |                |                |                |                |  |
| 0.000    | 0.967                                      | 0.033          | 0.000          | 0.000          | 0.972        | 0.028          | 0.000          | 0.000          | 0.000          |  |
| 0.003    | 0.958                                      | 0.034          | 0.002          | 0.007          | 0.971        | 0.029          | 0.001          | 0.000          | 0.000          |  |
| 0.007    | 0.947                                      | 0.036          | 0.003          | 0.014          | 0.968        | 0.029          | 0.002          | 0.001          | 0.000          |  |
| 0.011    | 0.936                                      | 0.037          | 0.005          | 0.022          | 0.964        | 0.029          | 0.004          | 0.002          | 0.001          |  |
| 0.025    | 0.895                                      | 0.046          | 0.013          | 0.046          | 0.949        | 0.031          | 0.012          | 0.006          | 0.002          |  |
| 0.045    | 0.844                                      | 0.058          | 0.024          | 0.074          | 0.931        | 0.033          | 0.021          | 0.011          | 0.004          |  |
| SD       |                                            |                |                |                |              |                |                |                |                |  |
| 0.01     | 0.01                                       | 0.01           | 0.01           | 0.01           | 0.01         | 0.01           | 0.01           | 0.01           | 0.01           |  |
| 0.01     | 0.01                                       | 0.01           | 0.01           | 0.01           | 0.01         | 0.01           | 0.01           | 0.01           | 0.01           |  |
| 0.01     | 0.01                                       | 0.01           | 0.01           | 0.01           | 0.01         | 0.01           | 0.01           | 0.01           | 0.01           |  |

|      |      |      |      |      |      |      |      |      |      |
|------|------|------|------|------|------|------|------|------|------|
| 0.01 | 0.01 | 0.01 | 0.01 | 0.01 | 0.01 | 0.01 | 0.01 | 0.01 | 0.01 |
| 0.01 | 0.01 | 0.01 | 0.01 | 0.01 | 0.01 | 0.01 | 0.01 | 0.01 | 0.01 |
| 0.01 | 0.01 | 0.01 | 0.01 | 0.01 | 0.01 | 0.01 | 0.01 | 0.01 | 0.01 |

Supplem. Table S4.3.(cont.)

| Time<br>[h] | [U- <sup>13</sup> C <sub>6</sub> ] Glucose |                |                |                |                |                |              |                |                |                |                |                |
|-------------|--------------------------------------------|----------------|----------------|----------------|----------------|----------------|--------------|----------------|----------------|----------------|----------------|----------------|
| exp         | Glutamate_ex                               |                |                |                |                |                | Glutamine_ex |                |                |                |                |                |
|             | Mo                                         | M <sub>1</sub> | M <sub>2</sub> | M <sub>3</sub> | M <sub>4</sub> | M <sub>5</sub> | Mo           | M <sub>1</sub> | M <sub>2</sub> | M <sub>3</sub> | M <sub>4</sub> | M <sub>5</sub> |
| 0           | 0.946                                      | 0.053          | 0.001          | 0.000          | 0.000          | 0.000          | 0.946        | 0.053          | 0.001          | 0.000          | 0.000          | 0.000          |
| 2           | 0.923                                      | 0.043          | 0.004          | 0.025          | 0.003          | 0.002          | 0.938        | 0.056          | 0.002          | 0.000          | 0.003          | 0.000          |
| 4           | 0.915                                      | 0.045          | 0.008          | 0.026          | 0.003          | 0.002          | 0.936        | 0.057          | 0.003          | 0.000          | 0.003          | 0.000          |
| 6           | 0.908                                      | 0.047          | 0.011          | 0.028          | 0.004          | 0.002          | 0.935        | 0.058          | 0.003          | 0.000          | 0.003          | 0.001          |
| 12          | 0.880                                      | 0.046          | 0.036          | 0.028          | 0.007          | 0.003          | 0.945        | 0.052          | 0.000          | 0.000          | 0.003          | 0.000          |
| 18          | 0.841                                      | 0.053          | 0.059          | 0.031          | 0.011          | 0.005          | 0.936        | 0.054          | 0.005          | 0.001          | 0.004          | 0.001          |
| sim         |                                            |                |                |                |                |                |              |                |                |                |                |                |
| 0           | 0.958                                      | 0.042          | 0.000          | 0.000          | 0.000          | 0.000          | 0.958        | 0.042          | 0.000          | 0.000          | 0.000          | 0.000          |
| 2           | 0.954                                      | 0.043          | 0.003          | 0.000          | 0.000          | 0.000          | 0.957        | 0.043          | 0.001          | 0.000          | 0.000          | 0.000          |
| 4           | 0.943                                      | 0.045          | 0.010          | 0.001          | 0.001          | 0.000          | 0.955        | 0.043          | 0.002          | 0.000          | 0.000          | 0.000          |
| 6           | 0.929                                      | 0.047          | 0.018          | 0.003          | 0.002          | 0.000          | 0.951        | 0.043          | 0.004          | 0.001          | 0.000          | 0.000          |
| 12          | 0.884                                      | 0.053          | 0.044          | 0.010          | 0.008          | 0.002          | 0.939        | 0.045          | 0.011          | 0.002          | 0.002          | 0.000          |
| 18          | 0.837                                      | 0.059          | 0.069          | 0.017          | 0.014          | 0.003          | 0.923        | 0.047          | 0.020          | 0.005          | 0.004          | 0.001          |
| SD          |                                            |                |                |                |                |                |              |                |                |                |                |                |
| 0           | 0.01                                       | 0.01           | 0.01           | 0.01           | 0.01           | 0.01           | 0.01         | 0.01           | 0.01           | 0.01           | 0.01           | 0.01           |
| 2           | 0.01                                       | 0.01           | 0.01           | 0.01           | 0.01           | 0.01           | 0.01         | 0.01           | 0.01           | 0.01           | 0.01           | 0.01           |
| 4           | 0.01                                       | 0.01           | 0.01           | 0.01           | 0.01           | 0.01           | 0.01         | 0.01           | 0.01           | 0.01           | 0.01           | 0.01           |
| 6           | 0.01                                       | 0.01           | 0.01           | 0.01           | 0.01           | 0.01           | 0.01         | 0.01           | 0.01           | 0.01           | 0.01           | 0.01           |
| 12          | 0.01                                       | 0.01           | 0.01           | 0.01           | 0.01           | 0.01           | 0.01         | 0.01           | 0.01           | 0.01           | 0.01           | 0.01           |
| 18          | 0.01                                       | 0.01           | 0.01           | 0.01           | 0.01           | 0.01           | 0.01         | 0.01           | 0.01           | 0.01           | 0.01           | 0.01           |

Supplem. Table S4.3.(cont.)

| Time<br>[h] | [U- <sup>13</sup> C <sub>6</sub> ] Glucose |                |                |                |              |                |                |                |
|-------------|--------------------------------------------|----------------|----------------|----------------|--------------|----------------|----------------|----------------|
| exp         | Pyruvate_cell                              |                |                |                | Lactate_cell |                |                |                |
|             | Mo                                         | M <sub>1</sub> | M <sub>2</sub> | M <sub>3</sub> | Mo           | M <sub>1</sub> | M <sub>2</sub> | M <sub>3</sub> |
| 0           | 0.967                                      | 0.033          | 0.000          | 0.000          | 0.967        | 0.033          | 0.000          | 0.000          |
| 2           | 0.624                                      | 0.035          | 0.024          | 0.317          | 0.447        | 0.027          | 0.061          | 0.466          |
| 4           | 0.459                                      | 0.029          | 0.037          | 0.475          | 0.412        | 0.026          | 0.052          | 0.510          |
| 6           | 0.404                                      | 0.029          | 0.038          | 0.529          | 0.400        | 0.025          | 0.057          | 0.519          |
| 12          | 0.378                                      | 0.028          | 0.040          | 0.554          | 0.368        | 0.024          | 0.062          | 0.546          |
| 18          | 0.352                                      | 0.025          | 0.040          | 0.584          | 0.334        | 0.025          | 0.064          | 0.577          |
| sim         |                                            |                |                |                |              |                |                |                |
| 0           | 0.967                                      | 0.033          | 0.000          | 0.000          | 0.967        | 0.033          | 0.000          | 0.000          |
| 2           | 0.608                                      | 0.028          | 0.016          | 0.347          | 0.576        | 0.027          | 0.016          | 0.381          |
| 4           | 0.481                                      | 0.031          | 0.025          | 0.462          | 0.442        | 0.029          | 0.026          | 0.502          |
| 6           | 0.425                                      | 0.033          | 0.030          | 0.513          | 0.387        | 0.030          | 0.030          | 0.552          |
| 12          | 0.340                                      | 0.034          | 0.036          | 0.590          | 0.310        | 0.032          | 0.036          | 0.623          |
| 18          | 0.289                                      | 0.035          | 0.040          | 0.636          | 0.264        | 0.033          | 0.040          | 0.663          |
| SD          |                                            |                |                |                |              |                |                |                |
| 0           | 0.03                                       | 0.03           | 0.03           | 0.03           | 0.03         | 0.03           | 0.03           | 0.03           |
| 2           | 0.03                                       | 0.03           | 0.03           | 0.03           | 0.03         | 0.03           | 0.03           | 0.03           |

|    |      |      |      |      |      |      |      |      |
|----|------|------|------|------|------|------|------|------|
| 4  | 0.03 | 0.03 | 0.03 | 0.03 | 0.03 | 0.03 | 0.03 | 0.03 |
| 6  | 0.03 | 0.03 | 0.03 | 0.03 | 0.03 | 0.03 | 0.03 | 0.03 |
| 12 | 0.03 | 0.03 | 0.03 | 0.03 | 0.03 | 0.03 | 0.03 | 0.03 |
| 18 | 0.03 | 0.03 | 0.03 | 0.03 | 0.03 | 0.03 | 0.03 | 0.03 |

Supplem. Table S4.3.(cont.)

| Time [h] | [U- <sup>13</sup> C <sub>6</sub> ] Glucose |                |                |                |                |             |                |                |                |                |
|----------|--------------------------------------------|----------------|----------------|----------------|----------------|-------------|----------------|----------------|----------------|----------------|
| exp      | Fumarate_cell                              |                |                |                |                | Malate_cell |                |                |                |                |
|          | Mo                                         | M <sub>1</sub> | M <sub>2</sub> | M <sub>3</sub> | M <sub>4</sub> | Mo          | M <sub>1</sub> | M <sub>2</sub> | M <sub>3</sub> | M <sub>4</sub> |
| 0        | 0.956                                      | 0.043          | 0.001          | 0.000          | 0.000          | 0.956       | 0.043          | 0.001          | 0.000          | 0.000          |
| 2        | 0.810                                      | 0.055          | 0.077          | 0.053          | 0.006          | 0.778       | 0.061          | 0.086          | 0.060          | 0.015          |
| 4        | 0.751                                      | 0.056          | 0.099          | 0.082          | 0.012          | 0.725       | 0.059          | 0.107          | 0.089          | 0.020          |
| 6        | 0.722                                      | 0.056          | 0.117          | 0.088          | 0.017          | 0.701       | 0.059          | 0.123          | 0.093          | 0.024          |
| 12       | 0.688                                      | 0.058          | 0.140          | 0.091          | 0.023          | 0.665       | 0.061          | 0.148          | 0.097          | 0.030          |
| 18       | 0.662                                      | 0.060          | 0.157          | 0.094          | 0.027          | 0.627       | 0.066          | 0.171          | 0.101          | 0.036          |
| sim      |                                            |                |                |                |                |             |                |                |                |                |
| 0        | 0.972                                      | 0.028          | 0.000          | 0.000          | 0.000          | 0.957       | 0.043          | 0.000          | 0.000          | 0.000          |
| 2        | 0.797                                      | 0.054          | 0.103          | 0.038          | 0.008          | 0.797       | 0.054          | 0.102          | 0.039          | 0.008          |
| 4        | 0.710                                      | 0.062          | 0.145          | 0.065          | 0.018          | 0.710       | 0.062          | 0.144          | 0.065          | 0.018          |
| 6        | 0.683                                      | 0.062          | 0.154          | 0.077          | 0.024          | 0.683       | 0.063          | 0.153          | 0.077          | 0.024          |
| 12       | 0.656                                      | 0.062          | 0.161          | 0.090          | 0.031          | 0.656       | 0.062          | 0.160          | 0.091          | 0.031          |
| 18       | 0.639                                      | 0.062          | 0.166          | 0.099          | 0.035          | 0.639       | 0.062          | 0.165          | 0.099          | 0.035          |
| SD       |                                            |                |                |                |                |             |                |                |                |                |
| 0        | 0.03                                       | 0.03           | 0.03           | 0.03           | 0.03           | 0.03        | 0.03           | 0.03           | 0.03           | 0.03           |
| 2        | 0.03                                       | 0.03           | 0.03           | 0.03           | 0.03           | 0.03        | 0.03           | 0.03           | 0.03           | 0.03           |
| 4        | 0.03                                       | 0.03           | 0.03           | 0.03           | 0.03           | 0.03        | 0.03           | 0.03           | 0.03           | 0.03           |
| 6        | 0.03                                       | 0.03           | 0.03           | 0.03           | 0.03           | 0.03        | 0.03           | 0.03           | 0.03           | 0.03           |
| 12       | 0.03                                       | 0.03           | 0.03           | 0.03           | 0.03           | 0.03        | 0.03           | 0.03           | 0.03           | 0.03           |
| 18       | 0.03                                       | 0.03           | 0.03           | 0.03           | 0.03           | 0.03        | 0.03           | 0.03           | 0.03           | 0.03           |

Supplem. Table S4.3.(cont.)

| Time [h] | [U- <sup>13</sup> C <sub>6</sub> ] Glucose |                |                |                |                |                |              |                |                |                |                |                |                |
|----------|--------------------------------------------|----------------|----------------|----------------|----------------|----------------|--------------|----------------|----------------|----------------|----------------|----------------|----------------|
| exp      | AKG_cell                                   |                |                |                |                |                | Citrate_cell |                |                |                |                |                |                |
|          | Mo                                         | M <sub>1</sub> | M <sub>2</sub> | M <sub>3</sub> | M <sub>4</sub> | M <sub>5</sub> | Mo           | M <sub>1</sub> | M <sub>2</sub> | M <sub>3</sub> | M <sub>4</sub> | M <sub>5</sub> | M <sub>6</sub> |
| 0        | 0.946                                      | 0.053          | 0.001          | 0.000          | 0.000          | 0.000          | 0.935        | 0.063          | 0.002          | 0.000          | 0.000          | 0.000          | 0.000          |
| 2        | 0.796                                      | 0.090          | 0.063          | 0.027          | 0.014          | 0.010          | 0.426        | 0.062          | 0.377          | 0.059          | 0.045          | 0.028          | 0.003          |
| 4        | 0.656                                      | 0.107          | 0.146          | 0.039          | 0.032          | 0.020          | 0.334        | 0.054          | 0.411          | 0.070          | 0.069          | 0.054          | 0.008          |
| 6        | 0.688                                      | 0.104          | 0.123          | 0.053          | 0.019          | 0.013          | 0.269        | 0.049          | 0.440          | 0.071          | 0.091          | 0.068          | 0.013          |
| 12       | 0.618                                      | 0.099          | 0.162          | 0.059          | 0.036          | 0.026          | 0.227        | 0.050          | 0.444          | 0.069          | 0.115          | 0.076          | 0.020          |
| 18       | 0.544                                      | 0.103          | 0.185          | 0.070          | 0.057          | 0.040          | 0.195        | 0.050          | 0.449          | 0.073          | 0.133          | 0.080          | 0.021          |
| sim      |                                            |                |                |                |                |                |              |                |                |                |                |                |                |
| 0        | 0.947                                      | 0.053          | 0.000          | 0.000          | 0.000          | 0.000          | 0.942        | 0.059          | 0.000          | 0.000          | 0.000          | 0.000          | 0.000          |
| 2        | 0.756                                      | 0.078          | 0.139          | 0.017          | 0.009          | 0.001          | 0.464        | 0.066          | 0.367          | 0.044          | 0.041          | 0.015          | 0.003          |
| 4        | 0.653                                      | 0.090          | 0.187          | 0.039          | 0.027          | 0.005          | 0.326        | 0.066          | 0.419          | 0.066          | 0.080          | 0.034          | 0.009          |
| 6        | 0.624                                      | 0.091          | 0.196          | 0.047          | 0.035          | 0.008          | 0.289        | 0.065          | 0.426          | 0.072          | 0.093          | 0.043          | 0.013          |
| 12       | 0.600                                      | 0.091          | 0.202          | 0.053          | 0.043          | 0.011          | 0.263        | 0.063          | 0.424          | 0.076          | 0.103          | 0.053          | 0.017          |
| 18       | 0.585                                      | 0.092          | 0.206          | 0.057          | 0.048          | 0.013          | 0.252        | 0.063          | 0.419          | 0.079          | 0.109          | 0.059          | 0.019          |
| SD       |                                            |                |                |                |                |                |              |                |                |                |                |                |                |
| 0        | 0.03                                       | 0.03           | 0.03           | 0.03           | 0.03           | 0.03           | 0.03         | 0.03           | 0.03           | 0.03           | 0.03           | 0.03           | 0.03           |

|    |   |   |   |   |   |   |      |      |      |      |      |      |      |
|----|---|---|---|---|---|---|------|------|------|------|------|------|------|
| 2  | 1 | 1 | 1 | 1 | 1 | 1 | 0.03 | 0.03 | 0.03 | 0.03 | 0.03 | 0.03 | 0.03 |
| 4  | 1 | 1 | 1 | 1 | 1 | 1 | 0.03 | 0.03 | 0.03 | 0.03 | 0.03 | 0.03 | 0.03 |
| 6  | 1 | 1 | 1 | 1 | 1 | 1 | 0.03 | 0.03 | 0.03 | 0.03 | 0.03 | 0.03 | 0.03 |
| 12 | 1 | 1 | 1 | 1 | 1 | 1 | 0.03 | 0.03 | 0.03 | 0.03 | 0.03 | 0.03 | 0.03 |
| 18 | 1 | 1 | 1 | 1 | 1 | 1 | 0.03 | 0.03 | 0.03 | 0.03 | 0.03 | 0.03 | 0.03 |

Supplem. Table S4.3.(cont.)

| Time [h] | [U- <sup>13</sup> C <sub>6</sub> ] Glucose |                |                |                |              |                |                |             |                |                |                |
|----------|--------------------------------------------|----------------|----------------|----------------|--------------|----------------|----------------|-------------|----------------|----------------|----------------|
| exp      | Alanine_cell                               |                |                |                | Glycine_cell |                |                | Serine_cell |                |                |                |
|          | Mo                                         | M <sub>1</sub> | M <sub>2</sub> | M <sub>3</sub> | Mo           | M <sub>1</sub> | M <sub>2</sub> | Mo          | M <sub>1</sub> | M <sub>2</sub> | M <sub>3</sub> |
| 0        | 0.967                                      | 0.033          | 0.000          | 0.000          | 0.978        | 0.022          | 0.000          | 0.967       | 0.033          | 0.000          | 0.000          |
| 2        | 0.547                                      | 0.078          | 0.107          | 0.267          | 0.939        | 0.019          | 0.042          | 0.882       | 0.050          | 0.016          | 0.053          |
| 4        | 0.526                                      | 0.043          | 0.094          | 0.337          | 0.916        | 0.022          | 0.062          | 0.875       | 0.045          | 0.013          | 0.066          |
| 6        | 0.310                                      | 0.055          | 0.232          | 0.404          | 0.917        | 0.018          | 0.065          | 0.849       | 0.054          | 0.023          | 0.074          |
| 12       | 0.391                                      | 0.056          | 0.149          | 0.404          | 0.900        | 0.019          | 0.080          | 0.826       | 0.062          | 0.028          | 0.084          |
| 18       | 0.350                                      | 0.076          | 0.171          | 0.402          | 0.880        | 0.021          | 0.098          | 0.796       | 0.073          | 0.040          | 0.091          |
| sim      |                                            |                |                |                |              |                |                |             |                |                |                |
| 0        | 0.967                                      | 0.033          | 0.000          | 0.000          | 0.978        | 0.022          | 0.000          | 0.967       | 0.033          | 0.000          | 0.000          |
| 2        | 0.739                                      | 0.030          | 0.010          | 0.221          | 0.930        | 0.022          | 0.048          | 0.888       | 0.044          | 0.012          | 0.055          |
| 4        | 0.633                                      | 0.032          | 0.018          | 0.317          | 0.923        | 0.022          | 0.055          | 0.877       | 0.047          | 0.015          | 0.061          |
| 6        | 0.570                                      | 0.033          | 0.022          | 0.376          | 0.916        | 0.022          | 0.062          | 0.866       | 0.050          | 0.017          | 0.067          |
| 12       | 0.447                                      | 0.034          | 0.030          | 0.489          | 0.892        | 0.022          | 0.087          | 0.826       | 0.061          | 0.027          | 0.086          |
| 18       | 0.366                                      | 0.035          | 0.036          | 0.563          | 0.861        | 0.022          | 0.117          | 0.775       | 0.076          | 0.041          | 0.108          |
| SD       |                                            |                |                |                |              |                |                |             |                |                |                |
| 0        | 0.03                                       | 0.03           | 0.03           | 0.03           | 0.03         | 0.03           | 0.03           | 0.03        | 0.03           | 0.03           | 0.03           |
| 2        | 1                                          | 1              | 1              | 1              | 0.03         | 0.03           | 0.03           | 0.03        | 0.03           | 0.03           | 0.03           |
| 4        | 1                                          | 1              | 1              | 1              | 0.03         | 0.03           | 0.03           | 0.03        | 0.03           | 0.03           | 0.03           |
| 6        | 1                                          | 1              | 1              | 1              | 0.03         | 0.03           | 0.03           | 0.03        | 0.03           | 0.03           | 0.03           |
| 12       | 1                                          | 1              | 1              | 1              | 0.03         | 0.03           | 0.03           | 0.03        | 0.03           | 0.03           | 0.03           |
| 18       | 1                                          | 1              | 1              | 1              | 0.03         | 0.03           | 0.03           | 0.03        | 0.03           | 0.03           | 0.03           |

Supplem. Table S4.3.(cont.)

| Time [h] | [U- <sup>13</sup> C <sub>6</sub> ] Glucose |                |                |                |                |                |                |                |                |                |                |
|----------|--------------------------------------------|----------------|----------------|----------------|----------------|----------------|----------------|----------------|----------------|----------------|----------------|
| exp      | Aspartate_cell                             |                |                |                |                | Glutamate_cell |                |                |                |                |                |
|          | Mo                                         | M <sub>1</sub> | M <sub>2</sub> | M <sub>3</sub> | M <sub>4</sub> | Mo             | M <sub>1</sub> | M <sub>2</sub> | M <sub>3</sub> | M <sub>4</sub> | M <sub>5</sub> |
| 0        | 0.956                                      | 0.043          | 0.001          | 0.000          | 0.000          | 0.946          | 0.053          | 0.001          | 0.000          | 0.000          | 0.000          |
| 2        | 0.780                                      | 0.061          | 0.093          | 0.060          | 0.007          | 0.731          | 0.063          | 0.162          | 0.024          | 0.014          | 0.006          |
| 4        | 0.721                                      | 0.058          | 0.113          | 0.096          | 0.014          | 0.677          | 0.056          | 0.190          | 0.034          | 0.030          | 0.013          |
| 6        | 0.690                                      | 0.057          | 0.130          | 0.101          | 0.022          | 0.645          | 0.053          | 0.205          | 0.040          | 0.039          | 0.019          |
| 12       | 0.644                                      | 0.062          | 0.159          | 0.104          | 0.031          | 0.585          | 0.055          | 0.230          | 0.050          | 0.054          | 0.026          |
| 18       | 0.606                                      | 0.067          | 0.189          | 0.105          | 0.033          | 0.534          | 0.058          | 0.244          | 0.061          | 0.069          | 0.034          |
| sim      |                                            |                |                |                |                |                |                |                |                |                |                |
| 0        | 0.972                                      | 0.028          | 0.000          | 0.000          | 0.000          | 0.954          | 0.046          | 0.000          | 0.000          | 0.000          | 0.000          |
| 2        | 0.797                                      | 0.054          | 0.101          | 0.039          | 0.008          | 0.758          | 0.077          | 0.138          | 0.017          | 0.009          | 0.001          |
| 4        | 0.712                                      | 0.062          | 0.142          | 0.066          | 0.018          | 0.655          | 0.089          | 0.186          | 0.039          | 0.026          | 0.005          |
| 6        | 0.685                                      | 0.062          | 0.151          | 0.078          | 0.024          | 0.627          | 0.090          | 0.195          | 0.047          | 0.035          | 0.008          |
| 12       | 0.658                                      | 0.062          | 0.158          | 0.091          | 0.031          | 0.603          | 0.090          | 0.201          | 0.053          | 0.043          | 0.011          |
| 18       | 0.641                                      | 0.062          | 0.163          | 0.100          | 0.035          | 0.587          | 0.091          | 0.205          | 0.057          | 0.048          | 0.013          |
| SD       |                                            |                |                |                |                |                |                |                |                |                |                |

|    |      |      |      |      |      |      |      |      |      |      |      |
|----|------|------|------|------|------|------|------|------|------|------|------|
| 0  | 0.03 | 0.03 | 0.03 | 0.03 | 0.03 | 0.03 | 0.03 | 0.03 | 0.03 | 0.03 | 0.03 |
| 2  | 0.03 | 0.03 | 0.03 | 0.03 | 0.03 | 0.03 | 0.03 | 0.03 | 0.03 | 0.03 | 0.03 |
| 4  | 0.03 | 0.03 | 0.03 | 0.03 | 0.03 | 0.03 | 0.03 | 0.03 | 0.03 | 0.03 | 0.03 |
| 6  | 0.03 | 0.03 | 0.03 | 0.03 | 0.03 | 0.03 | 0.03 | 0.03 | 0.03 | 0.03 | 0.03 |
| 12 | 0.03 | 0.03 | 0.03 | 0.03 | 0.03 | 0.03 | 0.03 | 0.03 | 0.03 | 0.03 | 0.03 |
| 18 | 0.03 | 0.03 | 0.03 | 0.03 | 0.03 | 0.03 | 0.03 | 0.03 | 0.03 | 0.03 | 0.03 |

Supplem. Table S4.3.(cont.)

| Time<br>[h] | [U- <sup>13</sup> C <sub>5</sub> ] Glutamine |       |       |       |            |       |       |       |            |       |       |
|-------------|----------------------------------------------|-------|-------|-------|------------|-------|-------|-------|------------|-------|-------|
| exp         | Lactate_ex                                   |       |       |       | Alanine_ex |       |       |       | Glycine_ex |       |       |
|             | Mo                                           | M1    | M2    | M3    | Mo         | M1    | M2    | M3    | Mo         | M1    | M2    |
| 0           | 0.967                                        | 0.033 | 0.000 | 0.000 | 0.967      | 0.033 | 0.000 | 0.000 | 0.978      | 0.022 | 0.000 |
| 2           | 0.957                                        | 0.036 | 0.002 | 0.005 | 0.960      | 0.036 | 0.001 | 0.002 | 0.976      | 0.024 | 0.000 |
| 6           | 0.945                                        | 0.037 | 0.006 | 0.012 | 0.952      | 0.038 | 0.003 | 0.006 | 0.974      | 0.026 | 0.000 |
| 12          | 0.936                                        | 0.039 | 0.007 | 0.018 | 0.941      | 0.041 | 0.006 | 0.013 | 0.973      | 0.026 | 0.001 |
| 18          | 0.927                                        | 0.042 | 0.009 | 0.022 | 0.933      | 0.042 | 0.007 | 0.018 | 0.971      | 0.027 | 0.002 |
| sim         |                                              |       |       |       |            |       |       |       |            |       |       |
| 0           | 0.967                                        | 0.033 | 0.000 | 0.000 | 0.967      | 0.033 | 0.000 | 0.000 | 0.978      | 0.022 | 0.000 |
| 2           | 0.959                                        | 0.032 | 0.002 | 0.007 | 0.963      | 0.032 | 0.001 | 0.004 | 0.978      | 0.022 | 0.000 |
| 6           | 0.938                                        | 0.033 | 0.007 | 0.021 | 0.943      | 0.034 | 0.006 | 0.017 | 0.978      | 0.022 | 0.000 |
| 12          | 0.926                                        | 0.035 | 0.010 | 0.028 | 0.918      | 0.037 | 0.012 | 0.033 | 0.978      | 0.022 | 0.000 |
| 18          | 0.922                                        | 0.036 | 0.012 | 0.031 | 0.901      | 0.039 | 0.016 | 0.043 | 0.978      | 0.022 | 0.000 |
| SD          |                                              |       |       |       |            |       |       |       |            |       |       |
| 0           | 0.01                                         | 0.01  | 0.01  | 0.01  | 0.01       | 0.01  | 0.01  | 0.01  | 0.01       | 0.01  | 0.01  |
| 2           | 0.01                                         | 0.01  | 0.01  | 0.01  | 0.01       | 0.01  | 0.01  | 0.01  | 0.01       | 0.01  | 0.01  |
| 6           | 0.01                                         | 0.01  | 0.01  | 0.01  | 0.01       | 0.01  | 0.01  | 0.01  | 0.01       | 0.01  | 0.01  |
| 12          | 0.01                                         | 0.01  | 0.01  | 0.01  | 0.01       | 0.01  | 0.01  | 0.01  | 0.01       | 0.01  | 0.01  |
| 18          | 0.01                                         | 0.01  | 0.01  | 0.01  | 0.01       | 0.01  | 0.01  | 0.01  | 0.01       | 0.01  | 0.01  |

Supplem. Table S4.3.(cont.)

| Time<br>[h] | [U- <sup>13</sup> C <sub>5</sub> ] Glutamine |       |       |       |              |       |       |       |       |  |
|-------------|----------------------------------------------|-------|-------|-------|--------------|-------|-------|-------|-------|--|
| exp         | Serine_ex                                    |       |       |       | Aspartate_ex |       |       |       |       |  |
|             | Mo                                           | M1    | M2    | M3    | Mo           | M1    | M2    | M3    | M4    |  |
| 0           | 0.967                                        | 0.033 | 0.000 | 0.000 | 0.956        | 0.043 | 0.001 | 0.000 | 0.000 |  |
| 2           | 0.962                                        | 0.036 | 0.002 | 0.000 | 0.946        | 0.050 | 0.001 | 0.000 | 0.002 |  |
| 6           | 0.961                                        | 0.037 | 0.002 | 0.000 | 0.945        | 0.048 | 0.001 | 0.001 | 0.006 |  |
| 12          | 0.967                                        | 0.033 | 0.000 | 0.000 | 0.935        | 0.045 | 0.004 | 0.004 | 0.013 |  |
| 18          | 0.964                                        | 0.034 | 0.002 | 0.000 | 0.925        | 0.047 | 0.005 | 0.005 | 0.018 |  |
| sim         |                                              |       |       |       |              |       |       |       |       |  |
| 0           | 0.967                                        | 0.033 | 0.000 | 0.000 | 0.972        | 0.028 | 0.000 | 0.000 | 0.000 |  |
| 2           | 0.967                                        | 0.032 | 0.000 | 0.000 | 0.969        | 0.029 | 0.000 | 0.000 | 0.002 |  |
| 6           | 0.967                                        | 0.032 | 0.000 | 0.000 | 0.956        | 0.030 | 0.003 | 0.002 | 0.009 |  |
| 12          | 0.967                                        | 0.032 | 0.000 | 0.000 | 0.934        | 0.033 | 0.008 | 0.004 | 0.021 |  |
| 18          | 0.968                                        | 0.032 | 0.000 | 0.000 | 0.908        | 0.036 | 0.014 | 0.007 | 0.035 |  |
| SD          |                                              |       |       |       |              |       |       |       |       |  |
| 0           | 0.01                                         | 0.01  | 0.01  | 0.01  | 0.01         | 0.01  | 0.01  | 0.01  | 0.01  |  |
| 2           | 0.01                                         | 0.01  | 0.01  | 0.01  | 0.01         | 0.01  | 0.01  | 0.01  | 0.01  |  |
| 6           | 0.01                                         | 0.01  | 0.01  | 0.01  | 0.01         | 0.01  | 0.01  | 0.01  | 0.01  |  |
| 12          | 0.01                                         | 0.01  | 0.01  | 0.01  | 0.01         | 0.01  | 0.01  | 0.01  | 0.01  |  |

|    |      |      |      |      |      |      |      |      |      |
|----|------|------|------|------|------|------|------|------|------|
| 18 | 0.01 | 0.01 | 0.01 | 0.01 | 0.01 | 0.01 | 0.01 | 0.01 | 0.01 |
|----|------|------|------|------|------|------|------|------|------|

Supplem. Table S4.3.(cont.)

| Time [h] | [U- <sup>13</sup> C <sub>5</sub> ] Glutamine |       |       |       |       |       |              |       |       |       |       |       |
|----------|----------------------------------------------|-------|-------|-------|-------|-------|--------------|-------|-------|-------|-------|-------|
| exp      | Glutamate_ex                                 |       |       |       |       |       | Glutamine_ex |       |       |       |       |       |
|          | Mo                                           | M1    | M2    | M3    | M4    | M5    | Mo           | M1    | M2    | M3    | M4    | M5    |
| 0        | 0.946                                        | 0.053 | 0.001 | 0.000 | 0.000 | 0.000 | 0.000        | 0.000 | 0.000 | 0.004 | 0.092 | 0.904 |
| 2        | 0.916                                        | 0.057 | 0.000 | 0.004 | 0.003 | 0.020 | 0.003        | 0.000 | 0.001 | 0.009 | 0.108 | 0.879 |
| 6        | 0.874                                        | 0.053 | 0.000 | 0.011 | 0.008 | 0.053 | 0.004        | 0.001 | 0.001 | 0.009 | 0.106 | 0.879 |
| 12       | 0.809                                        | 0.049 | 0.003 | 0.024 | 0.015 | 0.100 | 0.006        | 0.001 | 0.001 | 0.009 | 0.107 | 0.876 |
| 18       | 0.720                                        | 0.048 | 0.010 | 0.037 | 0.019 | 0.166 | 0.008        | 0.001 | 0.002 | 0.010 | 0.105 | 0.874 |
| sim      |                                              |       |       |       |       |       |              |       |       |       |       |       |
| 0        | 0.958                                        | 0.042 | 0.000 | 0.000 | 0.000 | 0.000 | 0.000        | 0.000 | 0.000 | 0.000 | 0.096 | 0.904 |
| 2        | 0.941                                        | 0.042 | 0.000 | 0.002 | 0.002 | 0.013 | 0.005        | 0.000 | 0.000 | 0.000 | 0.096 | 0.899 |
| 6        | 0.885                                        | 0.043 | 0.004 | 0.011 | 0.008 | 0.048 | 0.010        | 0.001 | 0.001 | 0.002 | 0.095 | 0.890 |
| 12       | 0.799                                        | 0.046 | 0.011 | 0.026 | 0.018 | 0.100 | 0.020        | 0.004 | 0.003 | 0.006 | 0.095 | 0.873 |
| 18       | 0.715                                        | 0.049 | 0.018 | 0.040 | 0.028 | 0.150 | 0.032        | 0.006 | 0.005 | 0.012 | 0.094 | 0.851 |
| SD       |                                              |       |       |       |       |       |              |       |       |       |       |       |
| 0        | 0.01                                         | 0.01  | 0.01  | 0.01  | 0.01  | 0.01  | 0.01         | 0.01  | 0.01  | 0.01  | 0.01  | 0.01  |
| 2        | 0.01                                         | 0.01  | 0.01  | 0.01  | 0.01  | 0.01  | 0.01         | 0.01  | 0.01  | 0.01  | 0.01  | 0.01  |
| 6        | 0.01                                         | 0.01  | 0.01  | 0.01  | 0.01  | 0.01  | 0.01         | 0.01  | 0.01  | 0.01  | 0.01  | 0.01  |
| 12       | 0.01                                         | 0.01  | 0.01  | 0.01  | 0.01  | 0.01  | 0.01         | 0.01  | 0.01  | 0.01  | 0.01  | 0.01  |
| 18       | 0.01                                         | 0.01  | 0.01  | 0.01  | 0.01  | 0.01  | 0.01         | 0.01  | 0.01  | 0.01  | 0.01  | 0.01  |

Supplem. Table S4.3.(cont.)

| Time [h] | [U- <sup>13</sup> C <sub>5</sub> ] Glutamine |       |       |       |              |       |       |       |
|----------|----------------------------------------------|-------|-------|-------|--------------|-------|-------|-------|
| exp      | Pyruvate_cell                                |       |       |       | Lactate_cell |       |       |       |
|          | Mo                                           | M1    | M2    | M3    | Mo           | M1    | M2    | M3    |
| 0        | 0.967                                        | 0.033 | 0.000 | 0.000 | 0.967        | 0.033 | 0.000 | 0.000 |
| 2        | 0.864                                        | 0.084 | 0.018 | 0.034 | 0.871        | 0.085 | 0.036 | 0.008 |
| 6        | 0.902                                        | 0.065 | 0.010 | 0.023 | 0.912        | 0.057 | 0.028 | 0.004 |
| 12       | 0.857                                        | 0.098 | 0.015 | 0.030 | 0.926        | 0.046 | 0.017 | 0.012 |
| 18       | 0.929                                        | 0.038 | 0.006 | 0.027 | 0.939        | 0.035 | 0.006 | 0.020 |
| sim      |                                              |       |       |       |              |       |       |       |
| 0        | 0.967                                        | 0.033 | 0.000 | 0.000 | 0.967        | 0.033 | 0.000 | 0.000 |
| 2        | 0.923                                        | 0.034 | 0.010 | 0.033 | 0.926        | 0.034 | 0.009 | 0.031 |
| 6        | 0.896                                        | 0.039 | 0.017 | 0.047 | 0.900        | 0.039 | 0.017 | 0.045 |
| 12       | 0.885                                        | 0.041 | 0.020 | 0.054 | 0.889        | 0.041 | 0.019 | 0.051 |
| 18       | 0.878                                        | 0.043 | 0.022 | 0.057 | 0.883        | 0.042 | 0.021 | 0.054 |
| SD       |                                              |       |       |       |              |       |       |       |
| 0        | 0.03                                         | 0.03  | 0.03  | 0.03  | 0.03         | 0.03  | 0.03  | 0.03  |
| 2        | 0.03                                         | 0.03  | 0.03  | 0.03  | 0.03         | 0.03  | 0.03  | 0.03  |
| 6        | 0.03                                         | 0.03  | 0.03  | 0.03  | 0.03         | 0.03  | 0.03  | 0.03  |
| 12       | 0.03                                         | 0.03  | 0.03  | 0.03  | 0.03         | 0.03  | 0.03  | 0.03  |
| 18       | 0.03                                         | 0.03  | 0.03  | 0.03  | 0.03         | 0.03  | 0.03  | 0.03  |

Supplem. Table S4.3.(cont.)

| Time [h] | [U- <sup>13</sup> C <sub>5</sub> ] Glutamine |       |       |       |       |             |       |       |       |       |
|----------|----------------------------------------------|-------|-------|-------|-------|-------------|-------|-------|-------|-------|
| exp      | Fumarate_cell                                |       |       |       |       | Malate_cell |       |       |       |       |
|          | Mo                                           | M1    | M2    | M3    | M4    | Mo          | M1    | M2    | M3    | M4    |
| 0        | 0.956                                        | 0.043 | 0.001 | 0.000 | 0.000 | 0.956       | 0.043 | 0.001 | 0.000 | 0.000 |
| 2        | 0.584                                        | 0.058 | 0.076 | 0.057 | 0.225 | 0.552       | 0.071 | 0.076 | 0.064 | 0.237 |
| 6        | 0.515                                        | 0.059 | 0.082 | 0.080 | 0.264 | 0.498       | 0.066 | 0.082 | 0.083 | 0.271 |
| 12       | 0.464                                        | 0.068 | 0.100 | 0.075 | 0.293 | 0.489       | 0.058 | 0.094 | 0.072 | 0.288 |
| 18       | 0.461                                        | 0.073 | 0.109 | 0.072 | 0.285 | 0.443       | 0.083 | 0.111 | 0.072 | 0.290 |
| sim      |                                              |       |       |       |       |             |       |       |       |       |
| 0        | 0.972                                        | 0.028 | 0.000 | 0.000 | 0.000 | 0.957       | 0.043 | 0.000 | 0.000 | 0.000 |
| 2        | 0.563                                        | 0.063 | 0.078 | 0.047 | 0.249 | 0.568       | 0.063 | 0.078 | 0.047 | 0.244 |
| 6        | 0.498                                        | 0.083 | 0.104 | 0.054 | 0.261 | 0.503       | 0.083 | 0.104 | 0.054 | 0.256 |
| 12       | 0.492                                        | 0.085 | 0.108 | 0.055 | 0.260 | 0.496       | 0.085 | 0.107 | 0.055 | 0.256 |
| 18       | 0.488                                        | 0.087 | 0.111 | 0.056 | 0.258 | 0.492       | 0.088 | 0.110 | 0.056 | 0.254 |
| SD       |                                              |       |       |       |       |             |       |       |       |       |
| 0        | 0.03                                         | 0.03  | 0.03  | 0.03  | 0.03  | 0.03        | 0.03  | 0.03  | 0.03  | 0.03  |
| 2        | 0.03                                         | 0.03  | 0.03  | 0.03  | 0.03  | 0.03        | 0.03  | 0.03  | 0.03  | 0.03  |
| 6        | 0.03                                         | 0.03  | 0.03  | 0.03  | 0.03  | 0.03        | 0.03  | 0.03  | 0.03  | 0.03  |
| 12       | 0.03                                         | 0.03  | 0.03  | 0.03  | 0.03  | 0.03        | 0.03  | 0.03  | 0.03  | 0.03  |
| 18       | 0.03                                         | 0.03  | 0.03  | 0.03  | 0.03  | 0.03        | 0.03  | 0.03  | 0.03  | 0.03  |

Supplem. Table S4.3.(cont.)

| Time [h] | [U- <sup>13</sup> C <sub>5</sub> ] Glutamine |       |       |       |       |       |              |       |       |       |       |       |       |
|----------|----------------------------------------------|-------|-------|-------|-------|-------|--------------|-------|-------|-------|-------|-------|-------|
| exp      | AKG_cell                                     |       |       |       |       |       | Citrate_cell |       |       |       |       |       |       |
|          | Mo                                           | M1    | M2    | M3    | M4    | M5    | Mo           | M1    | M2    | M3    | M4    | M5    | M6    |
| 0        | 0.946                                        | 0.053 | 0.001 | 0.000 | 0.000 | 0.000 | 0.935        | 0.063 | 0.002 | 0.000 | 0.000 | 0.000 | 0.000 |
| 2        | 0.253                                        | 0.081 | 0.088 | 0.282 | 0.041 | 0.254 | 0.539        | 0.073 | 0.079 | 0.062 | 0.193 | 0.047 | 0.006 |
| 6        | 0.173                                        | 0.114 | 0.093 | 0.395 | 0.036 | 0.189 | 0.485        | 0.071 | 0.084 | 0.081 | 0.212 | 0.058 | 0.009 |
| 12       | 0.119                                        | 0.158 | 0.051 | 0.545 | 0.009 | 0.118 | 0.420        | 0.082 | 0.101 | 0.085 | 0.228 | 0.072 | 0.011 |
| 18       | 0.126                                        | 0.194 | 0.056 | 0.584 | 0.011 | 0.029 | 0.403        | 0.090 | 0.110 | 0.088 | 0.233 | 0.064 | 0.011 |
| sim      |                                              |       |       |       |       |       |              |       |       |       |       |       |       |
| 0        | 0.947                                        | 0.053 | 0.000 | 0.000 | 0.000 | 0.000 | 0.942        | 0.059 | 0.000 | 0.000 | 0.000 | 0.000 | 0.000 |
| 2        | 0.367                                        | 0.043 | 0.028 | 0.091 | 0.070 | 0.401 | 0.514        | 0.083 | 0.076 | 0.051 | 0.208 | 0.050 | 0.019 |
| 6        | 0.288                                        | 0.062 | 0.050 | 0.114 | 0.077 | 0.409 | 0.433        | 0.100 | 0.108 | 0.062 | 0.221 | 0.053 | 0.024 |
| 12       | 0.283                                        | 0.065 | 0.053 | 0.117 | 0.077 | 0.405 | 0.426        | 0.102 | 0.111 | 0.064 | 0.220 | 0.053 | 0.024 |
| 18       | 0.281                                        | 0.068 | 0.055 | 0.119 | 0.077 | 0.399 | 0.422        | 0.104 | 0.114 | 0.065 | 0.219 | 0.052 | 0.024 |
| SD       |                                              |       |       |       |       |       |              |       |       |       |       |       |       |
| 0        | 0.03                                         | 0.03  | 0.03  | 0.03  | 0.03  | 0.03  | 0.03         | 0.03  | 0.03  | 0.03  | 0.03  | 0.03  | 0.03  |
| 2        | 1                                            | 1     | 1     | 1     | 1     | 1     | 0.03         | 0.03  | 0.03  | 0.03  | 0.03  | 0.03  | 0.03  |
| 6        | 1                                            | 1     | 1     | 1     | 1     | 1     | 0.03         | 0.03  | 0.03  | 0.03  | 0.03  | 0.03  | 0.03  |
| 12       | 1                                            | 1     | 1     | 1     | 1     | 1     | 0.03         | 0.03  | 0.03  | 0.03  | 0.03  | 0.03  | 0.03  |
| 18       | 1                                            | 1     | 1     | 1     | 1     | 1     | 0.03         | 0.03  | 0.03  | 0.03  | 0.03  | 0.03  | 0.03  |

Supplem. Table S4.3.(cont.)

| Time [h] | [U- <sup>13</sup> C <sub>5</sub> ] Glutamine |              |             |
|----------|----------------------------------------------|--------------|-------------|
| exp      | Alanine_cell                                 | Glycine_cell | Serine_cell |

|     | Mo    | M1    | M2    | M3    | Mo    | M1    | M2    | Mo    | M1    | M2    | M3    |
|-----|-------|-------|-------|-------|-------|-------|-------|-------|-------|-------|-------|
| 0   | 0.967 | 0.033 | 0.000 | 0.000 | 0.978 | 0.022 | 0.000 | 0.967 | 0.033 | 0.000 | 0.000 |
| 2   | 0.818 | 0.097 | 0.044 | 0.041 | 0.954 | 0.029 | 0.017 | 0.959 | 0.038 | 0.001 | 0.002 |
| 6   | 0.775 | 0.104 | 0.056 | 0.066 | 0.965 | 0.029 | 0.006 | 0.949 | 0.042 | 0.004 | 0.005 |
| 12  | 0.794 | 0.063 | 0.031 | 0.112 | 0.974 | 0.024 | 0.002 | 0.933 | 0.042 | 0.007 | 0.018 |
| 18  | 0.857 | 0.082 | 0.019 | 0.042 | 0.980 | 0.020 | 0.000 | 0.966 | 0.033 | 0.000 | 0.002 |
| sim |       |       |       |       |       |       |       |       |       |       |       |
| 0   | 0.967 | 0.033 | 0.000 | 0.000 | 0.978 | 0.022 | 0.000 | 0.967 | 0.033 | 0.000 | 0.000 |
| 2   | 0.937 | 0.034 | 0.007 | 0.022 | 0.978 | 0.022 | 0.000 | 0.967 | 0.032 | 0.000 | 0.000 |
| 6   | 0.913 | 0.038 | 0.013 | 0.036 | 0.978 | 0.022 | 0.000 | 0.968 | 0.032 | 0.000 | 0.000 |
| 12  | 0.896 | 0.040 | 0.017 | 0.046 | 0.978 | 0.022 | 0.000 | 0.968 | 0.032 | 0.000 | 0.000 |
| 18  | 0.885 | 0.042 | 0.020 | 0.053 | 0.978 | 0.022 | 0.000 | 0.968 | 0.032 | 0.000 | 0.000 |
| SD  |       |       |       |       |       |       |       |       |       |       |       |
| 0   | 0.03  | 0.03  | 0.03  | 0.03  | 0.03  | 0.03  | 0.03  | 0.03  | 0.03  | 0.03  | 0.03  |
| 2   | 1     | 1     | 1     | 1     | 0.03  | 0.03  | 0.03  | 0.03  | 0.03  | 0.03  | 0.03  |
| 6   | 1     | 1     | 1     | 1     | 0.03  | 0.03  | 0.03  | 0.03  | 0.03  | 0.03  | 0.03  |
| 12  | 1     | 1     | 1     | 1     | 0.03  | 0.03  | 0.03  | 0.03  | 0.03  | 0.03  | 0.03  |
| 18  | 1     | 1     | 1     | 1     | 0.03  | 0.03  | 0.03  | 0.03  | 0.03  | 0.03  | 0.03  |

Supplem. Table S4.3.(cont.)

| Time<br>[h] | [U- <sup>13</sup> C <sub>5</sub> ] Glutamine |       |       |       |       |                |       |       |       |       |       |
|-------------|----------------------------------------------|-------|-------|-------|-------|----------------|-------|-------|-------|-------|-------|
| exp         | Aspartate_cell                               |       |       |       |       | Glutamate_cell |       |       |       |       |       |
|             | Mo                                           | M1    | M2    | M3    | M4    | Mo             | M1    | M2    | M3    | M4    | M5    |
| 0           | 0.956                                        | 0.043 | 0.001 | 0.000 | 0.000 | 0.946          | 0.053 | 0.001 | 0.000 | 0.000 | 0.000 |
| 2           | 0.555                                        | 0.066 | 0.091 | 0.064 | 0.223 | 0.314          | 0.055 | 0.117 | 0.107 | 0.047 | 0.361 |
| 6           | 0.497                                        | 0.063 | 0.107 | 0.082 | 0.252 | 0.283          | 0.047 | 0.053 | 0.110 | 0.052 | 0.455 |
| 12          | 0.460                                        | 0.071 | 0.114 | 0.069 | 0.286 | 0.270          | 0.052 | 0.047 | 0.129 | 0.043 | 0.458 |
| 18          | 0.462                                        | 0.077 | 0.116 | 0.062 | 0.283 | 0.273          | 0.064 | 0.054 | 0.138 | 0.037 | 0.433 |
| sim         |                                              |       |       |       |       |                |       |       |       |       |       |
| 0           | 0.972                                        | 0.028 | 0.000 | 0.000 | 0.000 | 0.954          | 0.046 | 0.000 | 0.000 | 0.000 | 0.000 |
| 2           | 0.574                                        | 0.064 | 0.077 | 0.047 | 0.239 | 0.366          | 0.043 | 0.028 | 0.091 | 0.070 | 0.404 |
| 6           | 0.509                                        | 0.083 | 0.103 | 0.054 | 0.251 | 0.287          | 0.062 | 0.049 | 0.113 | 0.077 | 0.412 |
| 12          | 0.503                                        | 0.085 | 0.106 | 0.055 | 0.251 | 0.282          | 0.064 | 0.052 | 0.116 | 0.077 | 0.408 |
| 18          | 0.499                                        | 0.088 | 0.109 | 0.056 | 0.249 | 0.280          | 0.067 | 0.055 | 0.119 | 0.077 | 0.402 |
| SD          |                                              |       |       |       |       |                |       |       |       |       |       |
| 0           | 0.03                                         | 0.03  | 0.03  | 0.03  | 0.03  | 0.03           | 0.03  | 0.03  | 0.03  | 0.03  | 0.03  |
| 2           | 0.03                                         | 0.03  | 0.03  | 0.03  | 0.03  | 0.03           | 0.03  | 0.03  | 0.03  | 0.03  | 0.03  |
| 6           | 0.03                                         | 0.03  | 0.03  | 0.03  | 0.03  | 0.03           | 0.03  | 0.03  | 0.03  | 0.03  | 0.03  |
| 12          | 0.03                                         | 0.03  | 0.03  | 0.03  | 0.03  | 0.03           | 0.03  | 0.03  | 0.03  | 0.03  | 0.03  |
| 18          | 0.03                                         | 0.03  | 0.03  | 0.03  | 0.03  | 0.03           | 0.03  | 0.03  | 0.03  | 0.03  | 0.03  |



**Supplem. Table S4.4. Extracellular concentrations sampled in a 100 mL shake flask culture of CHO-K1 cells. (AVG – average from 4 parallel cultivations; SD – standard deviation)**

|     | Time [h] | Cells/mL | Glucose  | Lactate  | Pyruvate | Alanine  | Arginine | Asparagine |
|-----|----------|----------|----------|----------|----------|----------|----------|------------|
| AVG | 0        | 1.55E+06 | 4.42E+04 | 3.74E+02 | 7.50E+02 | 5.80E+02 | 4.92E+03 | 4.25E+03   |
|     | 6.25     | 2.23E+06 | 4.11E+04 | 3.71E+03 | 6.82E+02 | 7.61E+02 | 4.87E+03 | 4.11E+03   |
|     | 12.5     | 2.58E+06 | 3.90E+04 | 7.68E+03 | 6.74E+02 | 9.87E+02 | 4.86E+03 | 4.05E+03   |
|     | 17.75    | 2.98E+06 | 3.66E+04 | 1.05E+04 | 6.45E+02 | 1.21E+03 | 4.81E+03 | 3.90E+03   |
|     | 23.75    | 3.60E+06 | 3.39E+04 | 1.49E+04 | 5.86E+02 | 1.53E+03 | 4.75E+03 | 3.63E+03   |
|     | 29.75    | 4.30E+06 | 3.15E+04 | 1.70E+04 | 4.87E+02 | 1.87E+03 | 4.64E+03 | 3.40E+03   |
|     | 35.75    | 5.45E+06 | 2.96E+04 | 1.92E+04 | 4.43E+02 | 2.27E+03 | 4.56E+03 | 3.19E+03   |
|     | 42       | 6.55E+06 | 2.71E+04 | 2.09E+04 | 3.44E+02 | 2.69E+03 | 4.49E+03 | 2.84E+03   |
|     | 47.75    | 8.40E+06 | 2.64E+04 | 2.17E+04 | 2.84E+02 | 3.23E+03 | 4.56E+03 | 2.58E+03   |
|     |          |          |          |          |          |          |          |            |
| SD  | 0        | 0.00E+00 | 3.49E+03 | 3.64E+01 | 7.96E+01 | 1.43E+01 | 2.81E+02 | 1.29E+02   |
|     | 6.25     | 2.53E+05 | 4.44E+03 | 2.98E+02 | 6.32E+01 | 6.29E+00 | 2.78E+02 | 1.12E+02   |
|     | 12.5     | 1.76E+05 | 5.84E+03 | 1.16E+03 | 9.92E+01 | 1.30E+01 | 2.06E+02 | 9.74E+01   |
|     | 17.75    | 1.71E+05 | 5.43E+03 | 1.22E+03 | 7.56E+01 | 2.94E+01 | 2.53E+02 | 1.19E+02   |
|     | 23.75    | 2.16E+05 | 2.82E+03 | 1.88E+03 | 6.86E+01 | 4.69E+01 | 2.17E+02 | 1.04E+02   |
|     | 29.75    | 4.58E+05 | 3.37E+03 | 1.68E+03 | 9.80E+01 | 7.71E+01 | 2.27E+02 | 1.47E+02   |
|     | 35.75    | 6.81E+05 | 3.02E+03 | 1.54E+03 | 8.50E+01 | 7.45E+01 | 2.03E+02 | 7.62E+01   |
|     | 42       | 6.40E+05 | 3.49E+03 | 2.04E+03 | 9.10E+01 | 1.16E+02 | 2.31E+02 | 1.23E+02   |
|     | 47.75    | 1.52E+06 | 2.65E+03 | 1.77E+03 | 7.18E+01 | 1.73E+02 | 2.40E+02 | 1.07E+02   |
|     |          |          |          |          |          |          |          |            |

**Supplem. Table S4.4. (cont.)**

|     | Time [h] | Aspartic Acid | Cysteine | Glutamic Acid | Glutamine | Glycine  | Histidine |
|-----|----------|---------------|----------|---------------|-----------|----------|-----------|
| AVG | 0        | 2.89E+03      | 1.29E+01 | 8.66E+02      | 6.43E+03  | 1.54E+03 | 8.10E+02  |
|     | 6.25     | 2.79E+03      | 1.31E+01 | 9.12E+02      | 5.93E+03  | 1.67E+03 | 7.91E+02  |
|     | 12.5     | 2.83E+03      | 1.29E+01 | 9.98E+02      | 5.41E+03  | 1.79E+03 | 7.92E+02  |
|     | 17.75    | 2.79E+03      | 1.33E+01 | 1.05E+03      | 4.84E+03  | 1.88E+03 | 7.70E+02  |
|     | 23.75    | 2.64E+03      | 1.44E+01 | 1.09E+03      | 4.10E+03  | 2.03E+03 | 7.12E+02  |
|     | 29.75    | 2.58E+03      | 1.47E+01 | 1.13E+03      | 3.34E+03  | 2.10E+03 | 7.08E+02  |
|     | 35.75    | 2.55E+03      | 1.37E+01 | 1.16E+03      | 2.68E+03  | 2.15E+03 | 7.18E+02  |
|     | 42       | 2.34E+03      | 1.48E+01 | 1.15E+03      | 2.09E+03  | 2.25E+03 | 6.61E+02  |
|     | 47.75    | 2.27E+03      | 1.19E+01 | 1.16E+03      | 1.62E+03  | 2.38E+03 | 6.81E+02  |
|     |          |               |          |               |           |          |           |
| SD  | 0        | 1.36E+02      | 1.54E+00 | 4.33E+01      | 5.47E+02  | 4.46E+01 | 4.45E+01  |
|     | 6.25     | 8.39E+01      | 1.79E+00 | 3.92E+01      | 5.21E+02  | 8.31E+01 | 3.72E+01  |
|     | 12.5     | 8.76E+01      | 2.00E+00 | 3.73E+01      | 4.41E+02  | 5.74E+01 | 4.40E+01  |
|     | 17.75    | 1.09E+02      | 2.12E+00 | 5.04E+01      | 4.35E+02  | 4.48E+01 | 3.72E+01  |
|     | 23.75    | 1.27E+02      | 2.26E+00 | 4.32E+01      | 3.73E+02  | 8.22E+01 | 6.33E+01  |
|     | 29.75    | 1.72E+02      | 3.10E+00 | 5.85E+01      | 3.32E+02  | 1.10E+02 | 8.34E+01  |
|     | 35.75    | 5.70E+01      | 2.89E+00 | 4.03E+01      | 2.65E+02  | 5.91E+01 | 3.59E+01  |
|     | 42       | 1.69E+02      | 4.01E+00 | 7.44E+01      | 2.74E+02  | 3.93E+01 | 8.53E+01  |
|     | 47.75    | 9.87E+01      | 2.27E+00 | 7.40E+01      | 3.08E+02  | 1.05E+02 | 3.97E+01  |
|     |          |               |          |               |           |          |           |

Supplem. Table S4.4. (cont.)

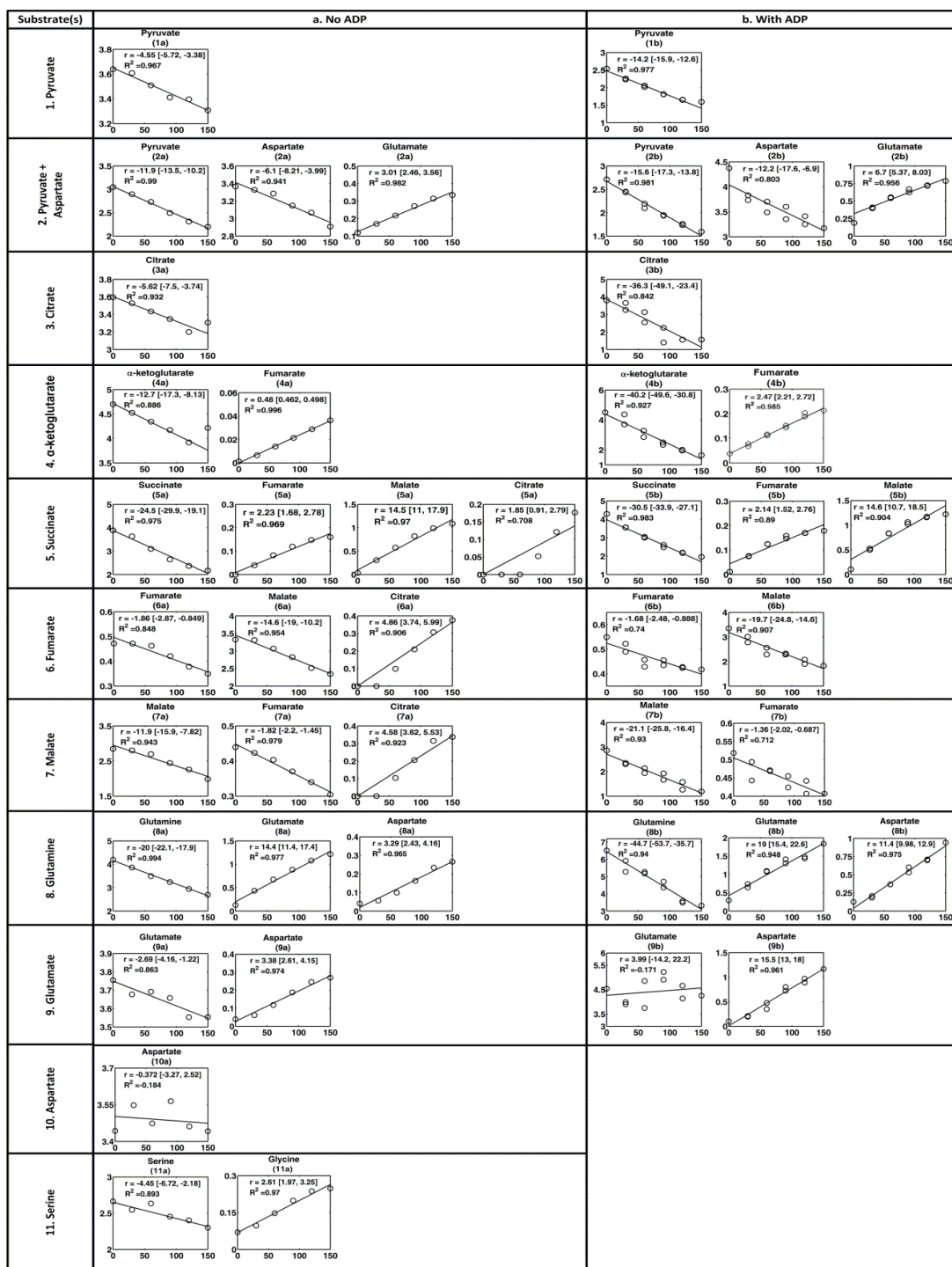
|            | Time [h] | Isoleucine | Leucine  | Lysine   | Methionine | Phenylalanine | Proline  |
|------------|----------|------------|----------|----------|------------|---------------|----------|
| <b>AVG</b> | 0        | 2.66E+03   | 3.36E+03 | 3.17E+03 | 9.00E+02   | 1.15E+03      | 1.18E+03 |
|            | 6.25     | 2.54E+03   | 3.23E+03 | 3.08E+03 | 8.76E+02   | 1.12E+03      | 1.14E+03 |
|            | 12.5     | 2.52E+03   | 3.18E+03 | 3.05E+03 | 8.62E+02   | 1.10E+03      | 1.12E+03 |
|            | 17.75    | 2.47E+03   | 3.10E+03 | 2.98E+03 | 8.36E+02   | 1.07E+03      | 1.09E+03 |
|            | 23.75    | 2.37E+03   | 3.00E+03 | 2.84E+03 | 8.04E+02   | 1.01E+03      | 1.05E+03 |
|            | 29.75    | 2.31E+03   | 2.87E+03 | 2.73E+03 | 7.57E+02   | 9.63E+02      | 9.67E+02 |
|            | 35.75    | 2.30E+03   | 2.76E+03 | 2.64E+03 | 7.16E+02   | 9.23E+02      | 9.16E+02 |
|            | 42       | 2.21E+03   | 2.64E+03 | 2.50E+03 | 6.76E+02   | 8.64E+02      | 8.63E+02 |
|            | 47.75    | 2.25E+03   | 2.62E+03 | 2.52E+03 | 6.56E+02   | 8.43E+02      | 8.45E+02 |
|            |          |            |          |          |            |               |          |
| <b>SD</b>  | 0        | 1.34E+02   | 1.89E+02 | 2.38E+02 | 4.76E+01   | 6.47E+01      | 6.79E+01 |
|            | 6.25     | 1.03E+02   | 1.75E+02 | 2.26E+02 | 4.81E+01   | 5.57E+01      | 5.23E+01 |
|            | 12.5     | 9.22E+01   | 1.34E+02 | 1.92E+02 | 3.39E+01   | 4.56E+01      | 4.27E+01 |
|            | 17.75    | 1.14E+02   | 1.62E+02 | 2.32E+02 | 3.77E+01   | 5.62E+01      | 7.27E+01 |
|            | 23.75    | 9.28E+01   | 1.25E+02 | 1.98E+02 | 3.03E+01   | 4.10E+01      | 8.46E+01 |
|            | 29.75    | 1.30E+02   | 1.41E+02 | 2.20E+02 | 3.24E+01   | 5.13E+01      | 6.62E+01 |
|            | 35.75    | 8.19E+01   | 1.15E+02 | 1.89E+02 | 2.48E+01   | 3.80E+01      | 5.05E+01 |
|            | 42       | 1.44E+02   | 1.33E+02 | 2.26E+02 | 2.71E+01   | 5.19E+01      | 5.86E+01 |
|            | 47.75    | 1.02E+02   | 1.36E+02 | 1.81E+02 | 3.32E+01   | 4.69E+01      | 5.42E+01 |

Supplem. Table S4.4. (cont.)

|            | Time [h] | Serine   | Threonine | Tryptophane | Tyrosine | Valine   |
|------------|----------|----------|-----------|-------------|----------|----------|
| <b>AVG</b> | 0        | 4.00E+03 | 1.87E+03  | 3.18E+02    | 1.52E+03 | 2.76E+03 |
|            | 6.25     | 3.79E+03 | 1.84E+03  | 3.13E+02    | 1.49E+03 | 2.66E+03 |
|            | 12.5     | 3.66E+03 | 1.84E+03  | 3.15E+02    | 1.48E+03 | 2.65E+03 |
|            | 17.75    | 3.49E+03 | 1.78E+03  | 3.11E+02    | 1.46E+03 | 2.58E+03 |
|            | 23.75    | 3.30E+03 | 1.66E+03  | 2.98E+02    | 1.38E+03 | 2.45E+03 |
|            | 29.75    | 3.08E+03 | 1.64E+03  | 2.85E+02    | 1.33E+03 | 2.39E+03 |
|            | 35.75    | 2.87E+03 | 1.68E+03  | 2.78E+02    | 1.30E+03 | 2.37E+03 |
|            | 42       | 2.64E+03 | 1.56E+03  | 2.63E+02    | 1.25E+03 | 2.25E+03 |
|            | 47.75    | 2.48E+03 | 1.60E+03  | 2.58E+02    | 1.25E+03 | 2.27E+03 |
|            |          |          |           |             |          |          |
| <b>SD</b>  | 0        | 1.55E+02 | 7.63E+01  | 3.01E+01    | 1.05E+02 | 1.24E+02 |
|            | 6.25     | 1.68E+02 | 7.01E+01  | 2.92E+01    | 8.12E+01 | 9.09E+01 |
|            | 12.5     | 1.26E+02 | 7.19E+01  | 2.42E+01    | 7.17E+01 | 8.70E+01 |
|            | 17.75    | 1.37E+02 | 6.40E+01  | 2.03E+01    | 8.32E+01 | 1.04E+02 |
|            | 23.75    | 1.25E+02 | 1.20E+02  | 1.37E+01    | 6.13E+01 | 9.61E+01 |
|            | 29.75    | 1.36E+02 | 1.63E+02  | 1.59E+01    | 7.64E+01 | 1.36E+02 |
|            | 35.75    | 9.68E+01 | 5.89E+01  | 1.20E+01    | 6.53E+01 | 7.33E+01 |
|            | 42       | 1.05E+02 | 1.76E+02  | 2.11E+01    | 8.01E+01 | 1.44E+02 |
|            | 47.75    | 1.16E+02 | 5.79E+01  | 2.28E+01    | 8.35E+01 | 9.37E+01 |

## Appendix to Chapter 5

**Supplem. Figure S5.1.** Experimental (o) and fitted (–) extracellular concentrations in the experiments with permeabilized CHO-K1 cells.  $r$  – production rate [fmol/ (cell  $\times$  min)]. The brackets contain the 95% confidence interval for the rate.



**Supplem. Table S5.1. Selection of the elementary modes that can describe the observed metabolite uptake and production.** The modes are selected accordingly to the following criteria: u - the metabolite is taken up; p - the metabolite is produced; xu - the metabolite is not taken up; xp - the metabolite is not produced; iu - the metabolite is or is not taken up; ip - the metabolite is or is not produced.

| SUBSTATE(S) /<br>PRODUCT(S) | pyruvate<br>/ - | pyruvate,<br>ADP / ATP | pyruvate,<br>aspartate /<br>glutamate | pyruvate,<br>aspartate, ADP /<br>glutamate, ATP | citrate<br>/ - | citrate,<br>ADP /<br>ATP |
|-----------------------------|-----------------|------------------------|---------------------------------------|-------------------------------------------------|----------------|--------------------------|
| External Flux               | 1a              | 1b                     | 2a                                    | 2b                                              | 3a             | 3b                       |
| Pyruvate                    | u / xp          | u / xp                 | iu / xp                               | iu / xp                                         | xu / xp        | xu / xp                  |
| Malate                      | xu / xp         | xu / xp                | xu / xp                               | xu / xp                                         | xu / xp        | xu / xp                  |
| Succinate                   | xu / xp         | xu / xp                | xu / xp                               | xu / xp                                         | xu / xp        | xu / xp                  |
| Fumarate                    | xu / xp         | xu / xp                | xu / xp                               | xu / xp                                         | xu / xp        | xu / xp                  |
| Citrate                     | xu / xp         | xu / xp                | xu / xp                               | xu / xp                                         | u / xp         | u / xp                   |
| Aspartate                   | xu / xp         | xu / xp                | iu / xp                               | iu / xp                                         | xu / xp        | xu / xp                  |
| $\alpha$ -ketoglutarate     | xu / xp         | xu / xp                | xu / xp                               | xu / xp                                         | xu / xp        | xu / xp                  |
| Glutamate                   | xu / xp         | xu / xp                | xu / ip                               | xu / ip                                         | xu / xp        | xu / xp                  |
| Glutamine                   | xu / xp         | xu / xp                | xu / xp                               | xu / xp                                         | xu / xp        | xu / xp                  |
| CO <sub>2</sub>             | iu / ip         | iu / ip                | iu / ip                               | iu / ip                                         | iu / ip        | iu / ip                  |
| Serine                      | xu / xp         | xu / xp                | xu / xp                               | xu / xp                                         | xu / xp        | xu / xp                  |
| Glycine                     | xu / xp         | xu / xp                | xu / xp                               | xu / xp                                         | xu / xp        | xu / xp                  |
| C <sub>1</sub>              | xu / xp         | xu / xp                | xu / xp                               | xu / xp                                         | xu / xp        | xu / xp                  |
| O <sub>2</sub>              | iu / xp         | iu / xp                | iu / xp                               | iu / xp                                         | iu / xp        | iu / xp                  |
| NH <sub>3</sub>             | xp / xp         | xp / xp                | xp / xp                               | xp / xp                                         | xu / xp        | xu / xp                  |
| ADP                         | xu / xp         | u / xp                 | xu / xp                               | u / xp                                          | xu / xp        | u / xp                   |
| ATP                         | xu / xp         | xu / ip                | xu / xp                               | xu / ip                                         | xu / xp        | xu / ip                  |

(cont. Table S5.1)

| SUBSTATE(S) /<br>PRODUCT(S) | $\alpha$ -<br>ketoglutarate<br>/ - | $\alpha$ -<br>ketoglutarate<br>, ADP /<br>fumarate,<br>ATP | succinate<br>/<br>fumarate<br>, malate,<br>citrate | succinate<br>, ADP /<br>fumarate,<br>malate,<br>citrate,<br>ATP | malate<br>(fumarate<br>) / citrate | malate<br>(fumarate)<br>, ADP /<br>citrate,<br>ATP |
|-----------------------------|------------------------------------|------------------------------------------------------------|----------------------------------------------------|-----------------------------------------------------------------|------------------------------------|----------------------------------------------------|
| External Flux               | 4a                                 | 4b                                                         | 5a                                                 | 5b                                                              | 6a/7a                              | 6b/7b                                              |
| Pyruvate                    | xu / xp                            | xu / xp                                                    | xu / xp                                            | xu / xp                                                         | xu / xp                            | xu / xp                                            |
| Malate                      | xu / xp                            | xu / xp                                                    | xu / ip                                            | xu / ip                                                         | u / xp                             | u / xp                                             |
| Succinate                   | xu / xp                            | xu / xp                                                    | u / xp                                             | u / xp                                                          | xu / xp                            | xu / xp                                            |
| Fumarate                    | xu / xp                            | xu / ip                                                    | xu / ip                                            | xu / ip                                                         | xu / xp                            | xu / xp                                            |
| Citrate                     | xu / xp                            | xu / xp                                                    | xu / ip                                            | xu / ip                                                         | xu / ip                            | xu / ip                                            |
| Aspartate                   | xu / xp                            | xu / xp                                                    | xu / xp                                            | xu / xp                                                         | xu / xp                            | xu / xp                                            |
| $\alpha$ -ketoglutarate     | u / xp                             | u / xp                                                     | xu / xp                                            | xu / xp                                                         | xu / xp                            | xu / xp                                            |

|                 |         |         |         |         |         |         |
|-----------------|---------|---------|---------|---------|---------|---------|
| Glutamate       | xu / xp | xu / xp | xu / xp | xu / xp | xu / xp | xu / xp |
| Glutamine       | xu / xp | xu / xp | xu / xp | xu / xp | xu / xp | xu / xp |
| CO <sub>2</sub> | iu / ip | iu / ip | iu / ip | iu / ip | iu / ip | iu / ip |
| Serine          | xu / xp | xu / xp | xu / xp | xu / xp | xu / xp | xu / xp |
| Glycine         | xu / xp | xu / xp | xu / xp | xu / xp | xu / xp | xu / xp |
| C <sub>1</sub>  | xu / xp | xu / xp | xu / xp | xu / xp | xu / xp | xu / xp |
| O <sub>2</sub>  | iu / xp | iu / xp | iu / xp | iu / xp | iu / xp | iu / xp |
| NH <sub>3</sub> | xu / xp | xu / xp | xu / xp | xu / xp | xu / xp | xu / xp |
| ADP             | xu / xp | u / xp  | xu / xp | xu / xp | xu / xp | xu / xp |
| ATP             | xu / xp | xu / ip | xu / xp | xu / ip | xu / xp | xu / ip |

(cont. Table S5.1)

| SUBSTATE(S) /<br>PRODUCT(S) | glutamine /<br>glutamate,<br>aspartate | glutamine, ADP /<br>glutamate,<br>aspartate, ATP | glutamate /<br>aspartate | glutamate,<br>ADP /<br>aspartate, ATP | serine /<br>glycine |
|-----------------------------|----------------------------------------|--------------------------------------------------|--------------------------|---------------------------------------|---------------------|
| External Flux               | 8a                                     | 8b                                               | 9a                       | 9b                                    | 11a                 |
| Pyruvate                    | xu / xp                                | xu / xp                                          | xu / xp                  | xu / xp                               | xu / xp             |
| Malate                      | xu / xp                                | xu / xp                                          | xu / xp                  | xu / xp                               | xu / xp             |
| Succinate                   | xu / xp                                | xu / xp                                          | xu / xp                  | xu / xp                               | xu / xp             |
| Fumarate                    | xu / xp                                | xu / xp                                          | xu / xp                  | xu / xp                               | xu / xp             |
| Citrate                     | xu / xp                                | xu / xp                                          | xu / xp                  | xu / xp                               | xu / xp             |
| Aspartate                   | xu / ip                                | xu / ip                                          | xu / ip                  | xu / ip                               | xu / xp             |
| α-ketoglutarate             | xu / xp                                | xu / xp                                          | xu / xp                  | xu / xp                               | xu / xp             |
| Glutamate                   | xu / ip                                | xu / ip                                          | xu / xp                  | u / xp                                | xu / xp             |
| Glutamine                   | u / xp                                 | u / xp                                           | xu / xp                  | xu / xp                               | xu / xp             |
| CO <sub>2</sub>             | iu / ip                                | iu / ip                                          | iu / ip                  | iu / ip                               | iu / ip             |
| Serine                      | xu / xp                                | xu / xp                                          | xu / xp                  | xu / xp                               | u / xp              |
| Glycine                     | xu / xp                                | xu / xp                                          | xu / xp                  | xu / xp                               | xu / ip             |
| C <sub>1</sub>              | xu / xp                                | xu / xp                                          | xu / xp                  | xu / xp                               | xu / ip             |
| O <sub>2</sub>              | iu / xp                                | iu / xp                                          | iu / xp                  | iu / xp                               | xu / xp             |
| NH <sub>3</sub>             | xu / ip                                | xu / ip                                          | xu / ip                  | xu / ip                               | xu / ip             |
| ADP                         | xu / xp                                | iu / xp                                          | xu / xp                  | u / xp                                | xu / xp             |
| ATP                         | xu / xp                                | xu / ip                                          | xu / xp                  | xu / ip                               | xu / xp             |

**Supplem. Table S5.2. Mitochondrial fluxes** [fmol / cell  $\times$  min] in selectively permeabilized CHO-K1 cells under various feeding conditions. The fluxes were computed using the determined extracellular rates and the stoichiometry indicated by reactions R1-R50. By addition of ADP it was assumed that the flux R44=0.

| Reaction                                       | Uptake /<br>Production             | pyruvate<br>/ - | pyruvate,<br>aspartate /<br>glutamate | citrate<br>/ - | $\alpha$ -<br>ketoglutarate /<br>- |
|------------------------------------------------|------------------------------------|-----------------|---------------------------------------|----------------|------------------------------------|
|                                                | Exp. No.                           |                 |                                       |                |                                    |
|                                                | Flux [fmol /<br>cell $\times$ min] | 1a              | 2a                                    | 3a             | 4a                                 |
| --> PYRc                                       | R1                                 | 4.6             | 11.9                                  | 0              | 0                                  |
| <--> MALc                                      | R2                                 | 0               | 0                                     | 0              | 0                                  |
| <--> SUCc                                      | R3                                 | 0               | 0                                     | 0              | 0                                  |
| <--> FUMc                                      | R4                                 | 0               | 0                                     | 0              | -0.48                              |
| <--> CITc                                      | R5                                 | 0               | 0                                     | 5.6            | 0                                  |
| <--> ASPc                                      | R6                                 | 0               | 6.1                                   | 0              | 0                                  |
| --> AKGc                                       | R7                                 | 0               | 0                                     | 0              | 12.7                               |
| <--> GLUc                                      | R8                                 | 0               | -3                                    | 0              | 0                                  |
| --> GLNc                                       | R9                                 | 0               | 0                                     | 0              | 0                                  |
| <--> SERc                                      | R11                                | 0               | 0                                     | 0              | 0                                  |
| <--> GLYc                                      | R12                                | 0               | 0                                     | 0              | 0                                  |
| <--> ADPc                                      | R24                                | 0               | 0                                     | 0              | 0                                  |
| <--> CO2c                                      | R10                                | -13.8           | -45.1                                 | -33.6          | -61.58                             |
| <--> C1c                                       | R13                                | 0               | 0                                     | 0              | 0                                  |
| C1c <--> C1m                                   | R14                                | 0               | 0                                     | 0              | 0                                  |
| GLYc <--> GLYm                                 | R15                                | 0               | 0                                     | 0              | 0                                  |
| SERc <--> SERm                                 | R16                                | 0               | 0                                     | 0              | 0                                  |
| CO2c <--> CO2m                                 | R17                                | -13.8           | -45.1                                 | -33.6          | -61.58                             |
| SERm <--> GLYm + MTHFm                         | R18                                | 0               | 0                                     | 0              | 0                                  |
| MTHFm --> C1m + THFm                           | R19                                | 0               | 0                                     | 0              | 0                                  |
| GLYm + THFm + NADm --><br>MTHFm + CO2m + NADHm | R20                                | 0               | 0                                     | 0              | 0                                  |
| --> O2m                                        | R21                                | 11.5            | 34.55                                 | 25.2           | 49.36                              |
| <--> NH3c                                      | R22                                | 0               | -3.1                                  | 0              | 0                                  |
| NH3c <--> NH3m                                 | R23                                | 0               | -3.1                                  | 0              | 0                                  |
| <--> ATPc                                      | R25                                | 0               | 0                                     | 0              | 0                                  |
| ADPc + ATPm <--> ADPm +<br>ATPc                | R26                                | 0               | 0                                     | 0              | 0                                  |
| PYRc --> PYRm                                  | R27                                | 4.6             | 11.9                                  | 0              | 0                                  |
| FUMc <--> FUMm                                 | R28                                | 0               | 0                                     | 0              | -0.48                              |
| MALc <--> MALm                                 | R29                                | 0               | 0                                     | 5.6            | 12.7                               |

|                                                                |     |       |         |        |         |
|----------------------------------------------------------------|-----|-------|---------|--------|---------|
| SUCc <--> SUCm                                                 | R30 | 0     | 0       | 0      | 0       |
| MALm + AKGc --> MALc + AKGm                                    | R31 | 0     | 0       | 0      | 12.7    |
| ASPm + GLUc <--> ASPc + GLUm                                   | R32 | 0     | -6.1    | 0      | 0       |
| CITm + MALc <--> CITc + MALm                                   | R33 | 0     | 0       | -5.6   | 0       |
| GLNc --> GLNm                                                  | R34 | 0     | 0       | 0      | 0       |
| GLUc <--> GLUm                                                 | R35 | 0     | 3.1     | 0      | 0       |
| PYRm + NADm --> ACOAm + NADHm + CO <sub>2</sub> m              | R36 | 4.6   | 15      | 5.6    | 12.22   |
| ACOAm + OAAm --> CITm                                          | R37 | 4.6   | 15      | 5.6    | 12.22   |
| CITm + NADm --> AKGm + NADHm + CO <sub>2</sub> m               | R38 | 4.6   | 15      | 11.2   | 12.22   |
| AKGm + ADPm + NADm --> SUCm + ATPm + NADHm + CO <sub>2</sub> m | R39 | 4.6   | 12      | 11.2   | 24.92   |
| SUCm + FADm <--> FUMm + FADHm                                  | R40 | 4.6   | 12      | 11.2   | 24.92   |
| FUMm <--> MALm                                                 | R41 | 4.6   | 12      | 11.2   | 24.44   |
| MALm + NADm <--> OAAm + NADHm                                  | R42 | -52.9 | -163.85 | -120.4 | -234.58 |
| MALm + NADPm --> PYRm + CO <sub>2</sub> m + NADPHm             | R43 | 57.5  | 175.85  | 131.6  | 259.02  |
| PYRm + CO <sub>2</sub> m + ATPm --> OAAm + ADPm                | R44 | 57.5  | 172.75  | 126    | 246.8   |
| AKGm + ASPm <--> GLUm + OAAm                                   | R45 | 0     | 6.1     | 0      | 0       |
| GLUm + NADm <--> AKGm + NH <sub>3</sub> m + NADHm              | R46 | 0     | 3.1     | 0      | 0       |
| GLNm --> GLUm + NH <sub>3</sub> m                              | R47 | 0     | 0       | 0      | 0       |
| 2 NADHm + O <sub>2</sub> m + 5 ADPm --> 2 NADm + 5 ATPm        | R48 | 9.2   | 28.55   | 19.6   | 36.9    |
| 2 FADHm + O <sub>2</sub> m + 3 ADPm --> 2 FADm + 3 ATPm        | R49 | 2.3   | 6       | 5.6    | 12.46   |
| NADPHm + NADm <--> NADPm + NADHm                               | R50 | 57.5  | 175.85  | 131.6  | 259.02  |

(cont. Table S5.2)

| Reaction                                       | succinate /<br>fumarate,<br>malate,<br>citrate | malate<br>(fumarate)<br>/ citrate | glutamine /<br>glutamate,<br>aspartate | glutamate<br>/ aspartate | serine /<br>glycine |
|------------------------------------------------|------------------------------------------------|-----------------------------------|----------------------------------------|--------------------------|---------------------|
|                                                | 5a                                             | 6a/7a                             | 8a                                     | 9a                       | 11a                 |
| --> PYRc                                       | 0                                              | 0                                 | 0                                      | 0                        | 0                   |
| <--> MALc                                      | -14.5                                          | 16.5                              | 0                                      | 0                        | 0                   |
| <--> SUCc                                      | 24.5                                           | 0                                 | 0                                      | 0                        | 0                   |
| <--> FUMc                                      | -2.2                                           | 0                                 | 0                                      | 0                        | 0                   |
| <--> CITc                                      | -1.9                                           | -4.9                              | 0                                      | 0                        | 0                   |
| <--> ASPc                                      | 0                                              | 0                                 | -3.3                                   | -3.38                    | 0                   |
| --> AKGc                                       | 0                                              | 0                                 | 0                                      | 0                        | 0                   |
| <--> GLUc                                      | 0                                              | 0                                 | -14.4                                  | 2.29                     | 0                   |
| --> GLNc                                       | 0                                              | 0                                 | 20                                     | 0                        | 0                   |
| <--> SERc                                      | 0                                              | 0                                 | 0                                      | 0                        | 4.5                 |
| <--> GLYc                                      | 0                                              | 0                                 | 0                                      | 0                        | -2.6                |
| <--> ADPc                                      | 0                                              | 0                                 | 0                                      | 0                        | 0                   |
| <--> CO2c                                      | -19.8                                          | -36.6                             | -14.8                                  | 2.07                     | -1.9                |
| <--> C1c                                       | 0                                              | 0                                 | 0                                      | 0                        | -6.4                |
| C1c <--> C1m                                   | 0                                              | 0                                 | 0                                      | 0                        | -6.4                |
| GLYc <--> GLYm                                 | 0                                              | 0                                 | 0                                      | 0                        | -2.6                |
| SERc <--> SERm                                 | 0                                              | 0                                 | 0                                      | 0                        | 4.5                 |
| CO2c <--> CO2m                                 | -19.8                                          | -36.6                             | -14.8                                  | 2.07                     | -1.9                |
| SERm <--> GLYm + MTHFm                         | 0                                              | 0                                 | 0                                      | 0                        | 4.5                 |
| MTHFm --> C1m + THFm                           | 0                                              | 0                                 | 0                                      | 0                        | 6.4                 |
| GLYm + THFm + NADm --><br>MTHFm + CO2m + NADHm | 0                                              | 0                                 | 0                                      | 0                        | 1.9                 |
| --> O2m                                        | 27.1                                           | 27.45                             | 15.3                                   | 0.165                    | 0.95                |
| <--> NH3c                                      | 0                                              | 0                                 | -22.3                                  | 1.09                     | 0                   |
| NH3c <--> NH3m                                 | 0                                              | 0                                 | -22.3                                  | 1.09                     | 0                   |
| <--> ATPc                                      | 0                                              | 0                                 | 0                                      | 0                        | 0                   |
| ADPc + ATPm <--> ADPm +<br>ATPc                | 0                                              | 0                                 | 0                                      | 0                        | 0                   |
| PYRc --> PYRm                                  | 0                                              | 0                                 | 0                                      | 0                        | 0                   |
| FUMc <--> FUMm                                 | -2.2                                           | 0                                 | 0                                      | 0                        | 0                   |
| MALc <--> MALm                                 | -16.4                                          | 11.6                              | 0                                      | 0                        | 0                   |
| SUCc <--> SUCm                                 | 24.5                                           | 0                                 | 0                                      | 0                        | 0                   |
| MALm + AKGc --> MALc +                         | 0                                              | 0                                 | 0                                      | 0                        | 0                   |



|                                                                |        |         |       |        |       |
|----------------------------------------------------------------|--------|---------|-------|--------|-------|
| AKGm                                                           |        |         |       |        |       |
| ASPm + GLUc <--> ASPc + GLUm                                   | 0      | 0       | 3.3   | 3.38   | 0     |
| CITm + MALc <--> CITc + MALm                                   | 1.9    | 4.9     | 0     | 0      | 0     |
| GLNc --> GLNm                                                  | 0      | 0       | 20    | 0      | 0     |
| GLUc <--> GLUm                                                 | 0      | 0       | -17.7 | -1.09  | 0     |
| PYRm + NADm --> ACOAm + NADHm + CO <sub>2</sub> m              | 5.9    | 11.6    | 2.3   | -1.09  | 0     |
| ACOAm + OAAm --> CITm                                          | 5.9    | 11.6    | 2.3   | -1.09  | 0     |
| CITm + NADm --> AKGm + NADHm + CO <sub>2</sub> m               | 4      | 6.7     | 2.3   | -1.09  | 0     |
| AKGm + ADPm + NADm --> SUCm + ATPm + NADHm + CO <sub>2</sub> m | 4      | 6.7     | 7.9   | 1.2    | 0     |
| SUCm + FADm <--> FUMm + FADHm                                  | 28.5   | 6.7     | 7.9   | 1.2    | 0     |
| FUMm <--> MALm                                                 | 26.3   | 6.7     | 7.9   | 1.2    | 0     |
| MALm + NADm <--> OAAm + NADHm                                  | -105.1 | -125.65 | -70.9 | 1.465  | -4.75 |
| MALm + NADPm --> PYRm + CO <sub>2</sub> m + NADPHm             | 116.9  | 148.85  | 78.8  | -0.265 | 4.75  |
| PYRm + CO <sub>2</sub> m + ATPm --> OAAm + ADPm                | 111    | 137.25  | 76.5  | 0.825  | 4.75  |
| AKGm + ASPm <--> GLUm + OAAm                                   | 0      | 0       | -3.3  | -3.38  | 0     |
| GLUm + NADm <--> AKGm + NH <sub>3</sub> m + NADHm              | 0      | 0       | 2.3   | -1.09  | 0     |
| GLNm --> GLUm + NH <sub>3</sub> m                              | 0      | 0       | 20    | 0      | 0     |
| 2 NADHm + O <sub>2</sub> m + 5 ADPm --> 2 NADm + 5 ATPm        | 12.85  | 24.1    | 11.35 | -0.435 | 0.95  |
| 2 FADHm + O <sub>2</sub> m + 3 ADPm --> 2 FADm + 3 ATPm        | 14.25  | 3.35    | 3.95  | 0.6    | 0     |
| NADPHm + NADm <--> NADPm + NADHm                               | 116.9  | 148.85  | 78.8  | -0.265 | 4.75  |

(cont. Table S5.2)

| Reaction                                                    | Uptake /<br>Production      | pyruvate,<br>pyruvate, aspartate, ADP /<br>ADP / ATP glutamate, ATP citrate, ADP /<br>ATP |         |      |
|-------------------------------------------------------------|-----------------------------|-------------------------------------------------------------------------------------------|---------|------|
|                                                             | Exp. No.                    |                                                                                           |         |      |
|                                                             | Flux [fmol /<br>cell × min] | 1b                                                                                        | 2b      | 3b   |
| --> PYRc                                                    | R1                          | 14.2                                                                                      | 15.6    | 0    |
| <--> MALc                                                   | R2                          | 0                                                                                         | 0       | 0    |
| <--> SUCc                                                   | R3                          | 0                                                                                         | 0       | 0    |
| <--> FUMc                                                   | R4                          | 0                                                                                         | 0       | 0    |
| <--> CITc                                                   | R5                          | 0                                                                                         | 0       | 38   |
| <--> ASPc                                                   | R6                          | 0                                                                                         | 12.2    | 0    |
| --> AKGc                                                    | R7                          | 0                                                                                         | 0       | 0    |
| <--> GLUc                                                   | R8                          | 0                                                                                         | -6.7    | 0    |
| --> GLNc                                                    | R9                          | 0                                                                                         | 0       | 0    |
| <--> SERc                                                   | R11                         | 0                                                                                         | 0       | 0    |
| <--> GLYc                                                   | R12                         | 0                                                                                         | 0       | 0    |
| PYRm + CO <sub>2</sub> m + ATPm --><br>OAAm + ADPm          | R44                         | 0                                                                                         | 0       | 0    |
| <--> CO <sub>2</sub> c                                      | R10                         | -42.6                                                                                     | -62.1   | -228 |
| <--> C <sub>1</sub> c                                       | R13                         | 0                                                                                         | 0       | 0    |
| C <sub>1</sub> c <--> C <sub>1</sub> m                      | R14                         | 0                                                                                         | 0       | 0    |
| GLYc <--> GLYm                                              | R15                         | 0                                                                                         | 0       | 0    |
| SERc <--> SERm                                              | R16                         | 0                                                                                         | 0       | 0    |
| CO <sub>2</sub> c <--> CO <sub>2</sub> m                    | R17                         | -42.6                                                                                     | -62.1   | -228 |
| SERm <--> GLYm + MTHFm                                      | R18                         | 0                                                                                         | 0       | 0    |
| MTHFm --> C <sub>1</sub> m + THFm                           | R19                         | 0                                                                                         | 0       | 0    |
| GLYm + THFm + NADm --><br>MTHFm + CO <sub>2</sub> m + NADHm | R20                         | 0                                                                                         | 0       | 0    |
| --> O <sub>2</sub> m                                        | R21                         | 35.5                                                                                      | 45.45   | 171  |
| <--> NH <sub>3</sub> c                                      | R22                         | 0                                                                                         | -5.5    | 0    |
| NH <sub>3</sub> c <--> NH <sub>3</sub> m                    | R23                         | 0                                                                                         | -5.5    | 0    |
| <--> ADPc                                                   | R24                         | 177.5                                                                                     | 227.25  | 855  |
| <--> ATPc                                                   | R25                         | -177.5                                                                                    | -227.25 | -855 |
| ADPc + ATPm <--> ADPm +<br>ATPc                             | R26                         | 177.5                                                                                     | 227.25  | 855  |
| PYRc --> PYRm                                               | R27                         | 14.2                                                                                      | 15.6    | 0    |
| FUMc <--> FUMm                                              | R28                         | 0                                                                                         | 0       | 0    |
| MALc <--> MALm                                              | R29                         | 0                                                                                         | 0       | 38   |
| SUCc <--> SUCm                                              | R30                         | 0                                                                                         | 0       | 0    |

|                                                                |     |      |       |     |
|----------------------------------------------------------------|-----|------|-------|-----|
| MALm + AKGc --> MALc + AKGm                                    | R31 | 0    | 0     | 0   |
| ASPm + GLUc <--> ASPc + GLUm                                   | R32 | 0    | -12.2 | 0   |
| CITm + MALc <--> CITc + MALm                                   | R33 | 0    | 0     | -38 |
| GLNc --> GLNm                                                  | R34 | 0    | 0     | 0   |
| GLUc <--> GLUm                                                 | R35 | 0    | 5.5   | 0   |
| PYRm + NADm --> ACOAm + NADHm + CO <sub>2</sub> m              | R36 | 14.2 | 21.1  | 38  |
| ACOAm + OAAm --> CITm                                          | R37 | 14.2 | 21.1  | 38  |
| CITm + NADm --> AKGm + NADHm + CO <sub>2</sub> m               | R38 | 14.2 | 21.1  | 76  |
| AKGm + ADPm + NADm --> SUCm + ATPm + NADHm + CO <sub>2</sub> m | R39 | 14.2 | 14.4  | 76  |
| SUCm + FADm <--> FUMm + FADHm                                  | R40 | 14.2 | 14.4  | 76  |
| FUMm <--> MALm                                                 | R41 | 14.2 | 14.4  | 76  |
| MALm + NADm <--> OAAm + NADHm                                  | R42 | 14.2 | 8.9   | 38  |
| MALm + NADPm --> PYRm + CO <sub>2</sub> m + NADPHm             | R43 | 0    | 5.5   | 38  |
| AKGm + ASPm <--> GLUm + OAAm                                   | R45 | 0    | 12.2  | 0   |
| GLUm + NADm <--> AKGm + NH <sub>3</sub> m + NADHm              | R46 | 0    | 5.5   | 0   |
| GLNm --> GLUm + NH <sub>3</sub> m                              | R47 | 0    | 0     | 0   |
| 2 NADHm + O <sub>2</sub> m + 5 ADPm --> 2 NADm + 5 ATPm        | R48 | 28.4 | 38.25 | 133 |
| 2 FADHm + O <sub>2</sub> m + 3 ADPm --> 2 FADm + 3 ATPm        | R49 | 7.1  | 7.2   | 38  |
| NADPHm + NADm <--> NADPm + NADHm                               | R50 | 0    | 5.5   | 38  |

(cont. Table S5.2)

| Reaction                                                    | Uptake /<br>Production             | $\alpha$ -ketoglutarate,<br>ADP /<br>fumarate, ATP | succinate,<br>ADP /<br>fumarate,<br>malate,<br>citrate,<br>ATP | malate<br>(fumarate),<br>ADP /<br>citrate,<br>ATP | glutamine,<br>ADP /<br>glutamate,<br>aspartate,<br>ATP |
|-------------------------------------------------------------|------------------------------------|----------------------------------------------------|----------------------------------------------------------------|---------------------------------------------------|--------------------------------------------------------|
|                                                             | Exp. No.                           |                                                    |                                                                |                                                   |                                                        |
|                                                             | Flux [fmol /<br>cell $\times$ min] | 4b                                                 | 5b                                                             | 6b/7b                                             | 8b                                                     |
| --> PYRc                                                    | R1                                 | 0                                                  | 0                                                              | 0                                                 | 0                                                      |
| <--> MALc                                                   | R2                                 | 0                                                  | -14.6                                                          | 21.4                                              | 0                                                      |
| <--> SUCc                                                   | R3                                 | 0                                                  | 30.5                                                           | 0                                                 | 0                                                      |
| <--> FUMc                                                   | R4                                 | -2.5                                               | -2.1                                                           | 0                                                 | 0                                                      |
| <--> CITc                                                   | R5                                 | 0                                                  | -1.9                                                           | -4.9                                              | 0                                                      |
| <--> ASPc                                                   | R6                                 | 0                                                  | 0                                                              | 0                                                 | -11.4                                                  |
| --> AKGc                                                    | R7                                 | 40.2                                               | 0                                                              | 0                                                 | 0                                                      |
| <--> GLUc                                                   | R8                                 | 0                                                  | 0                                                              | 0                                                 | -19                                                    |
| --> GLNc                                                    | R9                                 | 0                                                  | 0                                                              | 0                                                 | 44.7                                                   |
| <--> SERc                                                   | R11                                | 0                                                  | 0                                                              | 0                                                 | 0                                                      |
| <--> GLYc                                                   | R12                                | 0                                                  | 0                                                              | 0                                                 | 0                                                      |
| PYRm + CO <sub>2</sub> m + ATPm --><br>OAAm + ADPm          | R44                                | 0                                                  | 0                                                              | 0                                                 | 0                                                      |
| <--> CO <sub>2</sub> c                                      | R10                                | -191                                               | -43.8                                                          | -56.2                                             | -82.9                                                  |
| <--> C1c                                                    | R13                                | 0                                                  | 0                                                              | 0                                                 | 0                                                      |
| C1c <--> C1m                                                | R14                                | 0                                                  | 0                                                              | 0                                                 | 0                                                      |
| GLYc <--> GLYm                                              | R15                                | 0                                                  | 0                                                              | 0                                                 | 0                                                      |
| SERc <--> SERm                                              | R16                                | 0                                                  | 0                                                              | 0                                                 | 0                                                      |
| CO <sub>2</sub> c <--> CO <sub>2</sub> m                    | R17                                | -191                                               | -43.8                                                          | -56.2                                             | -82.9                                                  |
| SERm <--> GLYm + MTHFm                                      | R18                                | 0                                                  | 0                                                              | 0                                                 | 0                                                      |
| MTHFm --> C1m + THFm                                        | R19                                | 0                                                  | 0                                                              | 0                                                 | 0                                                      |
| GLYm + THFm + NADm --><br>MTHFm + CO <sub>2</sub> m + NADHm | R20                                | 0                                                  | 0                                                              | 0                                                 | 0                                                      |
| --> O <sub>2</sub> m                                        | R21                                | 153.3                                              | 48.1                                                           | 42.15                                             | 81.45                                                  |
| <--> NH <sub>3</sub> c                                      | R22                                | 0                                                  | 0                                                              | 0                                                 | -59                                                    |
| NH <sub>3</sub> c <--> NH <sub>3</sub> m                    | R23                                | 0                                                  | 0                                                              | 0                                                 | -59                                                    |
| <--> ADPc                                                   | R24                                | 766.5                                              | 210                                                            | 210.75                                            | 407.25                                                 |
| <--> ATPc                                                   | R25                                | -766.5                                             | -210                                                           | -210.75                                           | -407.25                                                |
| ADPc + ATPm <--> ADPm +<br>ATPc                             | R26                                | 766.5                                              | 210                                                            | 210.75                                            | 407.25                                                 |
| PYRc --> PYRm                                               | R27                                | 0                                                  | 0                                                              | 0                                                 | 0                                                      |
| FUMc <--> FUMm                                              | R28                                | -2.5                                               | -2.1                                                           | 0                                                 | 0                                                      |
| MALc <--> MALm                                              | R29                                | 40.2                                               | -16.5                                                          | 16.5                                              | 0                                                      |

|                                                                |     |        |       |       |       |
|----------------------------------------------------------------|-----|--------|-------|-------|-------|
| SUCc <--> SUCm                                                 | R30 | 0      | 30.5  | 0     | 0     |
| MALm + AKGc --> MALc + AKGm                                    | R31 | 40.2   | 0     | 0     | 0     |
| ASPm + GLUc <--> ASPc + GLUm                                   | R32 | 0      | 0     | 0     | 11.4  |
| CITm + MALc <--> CITc + MALm                                   | R33 | 0      | 1.9   | 4.9   | 0     |
| GLNc --> GLNm                                                  | R34 | 0      | 0     | 0     | 44.7  |
| GLUc <--> GLUm                                                 | R35 | 0      | 0     | 0     | -30.4 |
| PYRm + NADm --> ACOAm + NADHm + CO <sub>2</sub> m              | R36 | 37.7   | 11.9  | 16.5  | 14.3  |
| ACOAm + OAAm --> CITm                                          | R37 | 37.7   | 11.9  | 16.5  | 14.3  |
| CITm + NADm --> AKGm + NADHm + CO <sub>2</sub> m               | R38 | 37.7   | 10    | 11.6  | 14.3  |
| AKGm + ADPm + NADm --> SUCm + ATPm + NADHm + CO <sub>2</sub> m | R39 | 77.9   | 10    | 11.6  | 40    |
| SUCm + FADm <--> FUMm + FADHm                                  | R40 | 77.9   | 40.5  | 11.6  | 40    |
| FUMm <--> MALm                                                 | R41 | 75.4   | 38.4  | 11.6  | 40    |
| MALm + NADm <--> OAAm + NADHm                                  | R42 | 37.7   | 11.9  | 16.5  | 25.7  |
| MALm + NADPm --> PYRm + CO <sub>2</sub> m + NADPHm             | R43 | 37.7   | 11.9  | 16.5  | 14.3  |
| AKGm + ASPm <--> GLUm + OAAm                                   | R45 | 0      | 0     | 0     | -11.4 |
| GLUm + NADm <--> AKGm + NH <sub>3</sub> m + NADHm              | R46 | 0      | 0     | 0     | 14.3  |
| GLNm --> GLUm + NH <sub>3</sub> m                              | R47 | 0      | 0     | 0     | 44.7  |
| 2 NADHm + O <sub>2</sub> m + 5 ADPm --> 2 NADm + 5 ATPm        | R48 | 114.35 | 27.85 | 36.35 | 61.45 |
| 2 FADHm + O <sub>2</sub> m + 3 ADPm --> 2 FADm + 3 ATPm        | R49 | 38.95  | 20.25 | 5.8   | 20    |
| NADPHm + NADm <--> NADPm + NADHm                               | R50 | 37.7   | 11.9  | 16.5  | 14.3  |

**Supplem. Table S5.3. Stoichiometry of the modes selected using the Table S1 and the contribution to each mode to the total flux in each feeding experiment using selectively permeabilized CHO-K1 cells [fmol / cell × min].**

| Reaction                                          | Mode<br>1 | Mode<br>2 | Mode<br>3 | Mode<br>4 | Mode<br>5 | Mode<br>6 | Mode<br>7 | Mode<br>8 | Mode<br>9 | Mode<br>10 |
|---------------------------------------------------|-----------|-----------|-----------|-----------|-----------|-----------|-----------|-----------|-----------|------------|
| --> PYRc                                          | 1         | 1         | 1         | 0         | 0         | 1         | 0         | 0         | 0         | 0          |
| <--> MALc                                         | 0         | 0         | 0         | 0         | 0         | 0         | 0         | 0         | 0         | 0          |
| <--> SUCc                                         | 0         | 0         | 0         | 0         | 0         | 0         | 0         | 0         | 0         | 0          |
| <--> FUMc                                         | 0         | 0         | 0         | 0         | 0         | 0         | 0         | 0         | 0         | 0          |
| <--> CITc                                         | 0         | 0         | 0         | 0         | 0         | 0         | 0         | 0         | 1         | 1          |
| <--> ASPc                                         | 0         | 0         | 1         | 1         | 1         | 1         | 1         | 1         | 0         | 0          |
| --> AKGc                                          | 0         | 0         | 0         | 0         | 0         | 0         | 0         | 0         | 0         | 0          |
| <--> GLUc                                         | 0         | 0         | -1        | -0.5      | 0         | -1        | 0         | -0.5      | 0         | 0          |
| --> GLNc                                          | 0         | 0         | 0         | 0         | 0         | 0         | 0         | 0         | 0         | 0          |
| <--> CO2c                                         | -3        | -3        | -2        | -1.5      | -4        | 2         | -4        | -1.5      | -6        | -6         |
| <--> SERc                                         | 0         | 0         | 0         | 0         | 0         | 0         | 0         | 0         | 0         | 0          |
| <--> GLYc                                         | 0         | 0         | 0         | 0         | 0         | 0         | 0         | 0         | 0         | 0          |
| <--> C1c                                          | 0         | 0         | 0         | 0         | 0         | 0         | 0         | 0         | 0         | 0          |
| C1c <--> C1m                                      | 0         | 0         | 0         | 0         | 0         | 0         | 0         | 0         | 0         | 0          |
| GLYc <--> GLYm                                    | 0         | 0         | 0         | 0         | 0         | 0         | 0         | 0         | 0         | 0          |
| SERc <--> SERm                                    | 0         | 0         | 0         | 0         | 0         | 0         | 0         | 0         | 0         | 0          |
| CO2c <--> CO2m                                    | -3        | -3        | -2        | -1.5      | -4        | -2        | -4        | -1.5      | -6        | -6         |
| SERm <--> GLYm + MTHFm                            | 0         | 0         | 0         | 0         | 0         | 0         | 0         | 0         | 0         | 0          |
| MTHFm --> C1m + THFm                              | 0         | 0         | 0         | 0         | 0         | 0         | 0         | 0         | 0         | 0          |
| GLYm + THFm + NADm --> MTHFm + CO2m + NADHm + NH3 | 0         | 0         | 0         | 0         | 0         | 0         | 0         | 0         | 0         | 0          |
| --> O2m                                           | 2.5       | 2.5       | 1         | 0.75      | 3         | 1         | 3         | 0.75      | 4.5       | 4.5        |
| <--> NH3c                                         | 0         | 0         | 0         | -0.5      | -1        | 0         | -1        | -0.5      | 0         | 0          |
| NH3c <--> NH3m                                    | 0         | 0         | 0         | -0.5      | -1        | 0         | -1        | -0.5      | 0         | 0          |
| <--> ADPc                                         | 0         | 12.5      | 0         | 0         | 0         | 5         | 15        | 3.75      | 0         | 22.5       |
| <--> ATPc                                         | 0         | -12.5     | 0         | 0         | 0         | -5        | -15       | -3.55     | 0         | -22.5      |
| ADPc + ATPm <--> ADPm + ATPc                      | 0         | 12.5      | 0         | 0         | 0         | 5         | 15        | 3.75      | 0         | 22.5       |
| PYRc --> PYRm                                     | 1         | 1         | 1         | 0         | 0         | 1         | 0         | 0         | 0         | 0          |
| FUMc <--> FUMm                                    | 0         | 0         | 0         | 0         | 0         | 0         | 0         | 0         | 0         | 0          |
| MALc <--> MALm                                    | 0         | 0         | 0         | 0         | 0         | 0         | 0         | 0         | 1         | 1          |
| SUCc <--> SUCm                                    | 0         | 0         | 0         | 0         | 0         | 0         | 0         | 0         | 0         | 0          |
| MALm + AKGc --> MALc + AKGm                       | 0         | 0         | 0         | 0         | 0         | 0         | 0         | 0         | 0         | 0          |
| ASPm + GLUc <--> ASPc + GLUm                      | 0         | 0         | -1        | -1        | -1        | -1        | -1        | -1        | 0         | 0          |
| CITm + MALc <--> CITc + MALm                      | 0         | 0         | 0         | 0         | 0         | 0         | 0         | 0         | -1        | -1         |
| GLNc --> GLNm                                     | 0         | 0         | 0         | 0         | 0         | 0         | 0         | 0         | 0         | 0          |
| GLUc <--> GLUm                                    | 0         | 0         | 0         | 0.5       | 1         | 0         | 1         | 0.5       | 0         | 0          |
| PYRm + NADm --> ACOAm + NADHm + CO2m              | 1         | 1         | 1         | 0.5       | 1         | 1         | 1         | 0.5       | 1         | 1          |

|                                                                                                                                       |       |     |    |       |     |   |     |      |       |     |
|---------------------------------------------------------------------------------------------------------------------------------------|-------|-----|----|-------|-----|---|-----|------|-------|-----|
| ACOA <sub>m</sub> + OAA <sub>m</sub> --> CIT <sub>m</sub>                                                                             | 1     | 1   | 1  | 0.5   | 1   | 1 | 1   | 0.5  | 1     | 1   |
| CIT <sub>m</sub> + NAD <sub>m</sub> --> AKG <sub>m</sub> + NADH <sub>m</sub>                                                          | 1     | 1   | 1  | 0.5   | 1   | 1 | 1   | 0.5  | 2     | 2   |
| + CO <sub>2m</sub>                                                                                                                    |       |     |    |       |     |   |     |      |       |     |
| AKG <sub>m</sub> + ADP <sub>m</sub> + NAD <sub>m</sub> --> SUC <sub>m</sub> + ATP <sub>m</sub> + NADH <sub>m</sub> + CO <sub>2m</sub> | 1     | 1   | 0  | 0     | 1   | 1 | 1   | 0    | 2     | 2   |
| SUC <sub>m</sub> + FAD <sub>m</sub> <--> FUM <sub>m</sub> + FADH <sub>m</sub>                                                         | 1     | 1   | 0  | 0     | 1   | 0 | 1   | 0    | 2     | 2   |
| FUM <sub>m</sub> <--> MAL <sub>m</sub>                                                                                                | 1     | 1   | 0  | 0     | 1   | 0 | 1   | 0    | 2     | 2   |
| MAL <sub>m</sub> + NAD <sub>m</sub> <--> OAA <sub>m</sub> + NADH <sub>m</sub>                                                         | -11.5 | 1   | -5 | -4.25 | -15 | 0 | 0   | -0.5 | -21.5 | 1   |
| MAL <sub>m</sub> + NADP <sub>m</sub> --> PYR <sub>m</sub> + CO <sub>2m</sub> + NADPH <sub>m</sub>                                     | 12.5  | 0   | 5  | 4.25  | 16  | 0 | 1   | 0.5  | 23.5  | 1   |
| PYR <sub>m</sub> + CO <sub>2m</sub> + ATP <sub>m</sub> --> OAA <sub>m</sub> + ADP <sub>m</sub>                                        | 12.5  | 0   | 5  | 3.75  | 15  | 0 | 0   | 0    | 22.5  | 0   |
| AKG <sub>m</sub> + ASP <sub>m</sub> <--> GLU <sub>m</sub> + OAA <sub>m</sub>                                                          | 0     | 0   | 1  | 1     | 1   | 1 | 1   | 1    | 0     | 0   |
| GLU <sub>m</sub> + NAD <sub>m</sub> <--> AKG <sub>m</sub> + NH <sub>3m</sub> + NADH <sub>m</sub>                                      | 0     | 0   | 0  | 0.5   | 1   | 0 | 1   | 0.5  | 0     | 0   |
| GLN <sub>m</sub> --> GLU <sub>m</sub> + NH <sub>3m</sub>                                                                              | 0     | 0   | 0  | 0     | 0   | 0 | 0   | 0    | 0     | 0   |
| 2 NADH <sub>m</sub> + O <sub>2m</sub> + 5 ADP <sub>m</sub> --> 2 NAD <sub>m</sub> + 5 ATP <sub>m</sub>                                | 2     | 2   | 1  | 0.75  | 2.5 | 1 | 2.5 | 0.75 | 3.5   | 3.5 |
| 2 FADH <sub>m</sub> + O <sub>2m</sub> + 3 ADP <sub>m</sub> --> 2 FAD <sub>m</sub> + 3 ATP <sub>m</sub>                                | 0.5   | 0.5 | 0  | 0     | 0.5 | 0 | 0.5 | 0    | 1     | 1   |
| NADPH <sub>m</sub> + NAD <sub>m</sub> <--> NADP <sub>m</sub> + NADH <sub>m</sub>                                                      | 12.5  | 0   | 5  | 4.25  | 16  | 0 | 1   | 0.5  | 23.5  | 1   |

(cont. Table S5.3)

| Reaction                                                   | Mode 11 | Mode 12 | Mode 13 | Mode 14 | Mode 15 | Mode 16 | Mode 17 | Mode 18 | Mode 19 | Mode 20 |
|------------------------------------------------------------|---------|---------|---------|---------|---------|---------|---------|---------|---------|---------|
| --> PYR <sub>c</sub>                                       | 0       | 0       | 0       | 0       | 0       | 0       | 0       | 0       | 0       | 0       |
| <--> MAL <sub>c</sub>                                      | 0       | 0       | 0       | 0       | 0       | -1      | 0       | 0       | 0       | -1      |
| <--> SUC <sub>c</sub>                                      | 0       | 0       | 0       | 0       | 1       | 1       | 1       | 1       | 1       | 1       |
| <--> FUM <sub>c</sub>                                      | 0       | -1      | 0       | -1      | 0       | 0       | 0       | -1      | 0       | 0       |
| <--> CIT <sub>c</sub>                                      | 0       | 0       | 0       | 0       | 0       | 0       | -0.5    | 0       | 0       | 0       |
| <--> ASP <sub>c</sub>                                      | 0       | 0       | 0       | 0       | 0       | 0       | 0       | 0       | 0       | 0       |
| --> AKG <sub>c</sub>                                       | 1       | 1       | 1       | 1       | 0       | 0       | 0       | 0       | 0       | 0       |
| <--> GLU <sub>c</sub>                                      | 0       | 0       | 0       | 0       | 0       | 0       | 0       | 0       | 0       | 0       |
| --> GLN <sub>c</sub>                                       | 0       | 0       | 0       | 0       | 0       | 0       | 0       | 0       | 0       | 0       |
| <--> CO <sub>2c</sub>                                      | -5      | -1      | -5      | -1      | -4      | 0       | -1      | 0       | -4      | 0       |
| <--> SER <sub>c</sub>                                      | 0       | 0       | 0       | 0       | 0       | 0       | 0       | 0       | 0       | 0       |
| <--> GLY <sub>c</sub>                                      | 0       | 0       | 0       | 0       | 0       | 0       | 0       | 0       | 0       | 0       |
| <--> C <sub>1c</sub>                                       | 0       | 0       | 0       | 0       | 0       | 0       | 0       | 0       | 0       | 0       |
| C <sub>1c</sub> <--> C <sub>1m</sub>                       | 0       | 0       | 0       | 0       | 0       | 0       | 0       | 0       | 0       | 0       |
| GLY <sub>c</sub> <--> GLY <sub>m</sub>                     | 0       | 0       | 0       | 0       | 0       | 0       | 0       | 0       | 0       | 0       |
| SER <sub>c</sub> <--> SER <sub>m</sub>                     | 0       | 0       | 0       | 0       | 0       | 0       | 0       | 0       | 0       | 0       |
| CO <sub>2c</sub> <--> CO <sub>2m</sub>                     | -5      | -1      | -5      | -1      | -4      | 0       | -1      | 0       | -4      | 0       |
| SER <sub>m</sub> <--> GLY <sub>m</sub> + MTHF <sub>m</sub> | 0       | 0       | 0       | 0       | 0       | 0       | 0       | 0       | 0       | 0       |
| MTHF <sub>m</sub> --> C <sub>1m</sub> + THF <sub>m</sub>   | 0       | 0       | 0       | 0       | 0       | 0       | 0       | 0       | 0       | 0       |

|                                                                                  |     |     |     |     |       |      |      |      |       |      |
|----------------------------------------------------------------------------------|-----|-----|-----|-----|-------|------|------|------|-------|------|
| GLYm + THFm + NADm --><br>MTHFm + CO <sub>2</sub> m + NADHm +<br>NH <sub>3</sub> | 0   | 0   | 0   | 0   | 0     | 0    | 0    | 0    | 0     | 0    |
| --> O <sub>2</sub> m                                                             | 4   | 1   | 4   | 1   | 3.5   | 0.5  | 1.25 | 0.5  | 3.5   | 0.5  |
| <--> NH <sub>3</sub> c                                                           | 0   | 0   | 0   | 0   | 0     | 0    | 0    | 0    | 0     | 0    |
| NH <sub>3</sub> c <--> NH <sub>3</sub> m                                         | 0   | 0   | 0   | 0   | 0     | 0    | 0    | 0    | 0     | 0    |
| <--> ADPc                                                                        | 0   | 0   | 20  | 5   | 0     | 0    | 0    | 0    | 16.5  | 1.5  |
| <--> ATPc                                                                        | 0   | 0   | -20 | -5  | 0     | 0    | 0    | 0    | -16.5 | -1.5 |
| ADPc + ATPm <--> ADPm +<br>ATPc                                                  | 0   | 0   | 20  | 5   | 0     | 0    | 0    | 0    | 16.5  | 1.5  |
| PYRc --> PYRm                                                                    | 0   | 0   | 0   | 0   | 0     | 0    | 0    | 0    | 0     | 0    |
| FUMc <--> FUMm                                                                   | 0   | -1  | 0   | -1  | 0     | 0    | 0    | -1   | 0     | 0    |
| MALc <--> MALm                                                                   | 1   | 1   | 1   | 1   | 0     | -1   | -0.5 | 0    | 0     | -1   |
| SUCc <--> SUCm                                                                   | 0   | 0   | 0   | 0   | 1     | 1    | 1    | 1    | 1     | 1    |
| MALm + AKGc --> MALc +<br>AKGm                                                   | 1   | 1   | 1   | 1   | 0     | 0    | 0    | 0    | 0     | 0    |
| ASPm + GLUc <--> ASPc +<br>GLUm                                                  | 0   | 0   | 0   | 0   | 0     | 0    | 0    | 0    | 0     | 0    |
| CITm + MALc <--> CITc +<br>MALm                                                  | 0   | 0   | 0   | 0   | 0     | 0    | 0.5  | 0    | 0     | 0    |
| GLNc --> GLNm                                                                    | 0   | 0   | 0   | 0   | 0     | 0    | 0    | 0    | 0     | 0    |
| GLUc <--> GLUm                                                                   | 0   | 0   | 0   | 0   | 0     | 0    | 0    | 0    | 0     | 0    |
| PYRm + NADm --> ACOAm +<br>NADHm + CO <sub>2</sub> m                             | 1   | 0   | 1   | 0   | 1     | 0    | 0.5  | 0    | 1     | 0    |
| ACOAm + OAAm --> CITm                                                            | 1   | 0   | 1   | 0   | 1     | 0    | 0.5  | 0    | 1     | 0    |
| CITm + NADm --> AKGm +<br>NADHm + CO <sub>2</sub> m                              | 1   | 0   | 1   | 0   | 1     | 0    | 0    | 0    | 1     | 0    |
| AKGm + ADPm + NADm --><br>SUCm + ATPm + NADHm +<br>CO <sub>2</sub> m             | 2   | 1   | 2   | 1   | 1     | 0    | 0    | 0    | 1     | 0    |
| SUCm + FADm <--> FUMm +<br>FADHm                                                 | 2   | 1   | 2   | 1   | 2     | 1    | 1    | 1    | 2     | 1    |
| FUMm <--> MALm                                                                   | 2   | 0   | 2   | 0   | 2     | 1    | 1    | 0    | 2     | 1    |
| MALm + NADm <--> OAAm +<br>NADHm                                                 | -19 | -5  | 1   | 0   | -15.5 | -1.5 | 4.75 | -1.5 | 1     | 0    |
| MALm + NADPm --> PYRm +<br>CO <sub>2</sub> m + NADPHm                            | 21  | 5   | 1   | 0   | 17.5  | 1.5  | 5.75 | 1.5  | 1     | 0    |
| PYRm + CO <sub>2</sub> m + ATPm --><br>OAAm + ADPm                               | 20  | 5   | 0   | 0   | 16.5  | 1.5  | 5.25 | 1.5  | 0     | 0    |
| AKGm + ASPm <--> GLUm +<br>OAAm                                                  | 0   | 0   | 0   | 0   | 0     | 0    | 0    | 0    | 0     | 0    |
| GLUm + NADm <--> AKGm +<br>NH <sub>3</sub> m + NADHm                             | 0   | 0   | 0   | 0   | 0     | 0    | 0    | 0    | 0     | 0    |
| GLNm --> GLUm + NH <sub>3</sub> m                                                | 0   | 0   | 0   | 0   | 0     | 0    | 0    | 0    | 0     | 0    |
| 2 NADHm + O <sub>2</sub> m + 5 ADPm --><br>2 NADm + 5 ATPm                       | 3   | 0.5 | 3   | 0.5 | 2.5   | 0    | 0.75 | 0    | 2.5   | 0    |
| 2 FADHm + O <sub>2</sub> m + 3 ADPm --><br>2 FADm + 3 ATPm                       | 1   | 0.5 | 1   | 0.5 | 1     | -0.5 | 0.5  | 0.5  | 1     | 0.5  |



|                                     |    |   |   |   |      |     |      |     |   |   |
|-------------------------------------|----|---|---|---|------|-----|------|-----|---|---|
| NADPHm + NADm <--><br>NADPm + NADHm | 21 | 5 | 1 | 0 | 17.5 | 1.5 | 5.75 | 1.5 | 1 | 0 |
|-------------------------------------|----|---|---|---|------|-----|------|-----|---|---|

(cont. Table S5.3)

| Reaction                                                | Mode<br>21 | Mode<br>22 | Mode<br>23 | Mode<br>24 | Mode<br>25 | Mode<br>26 | Mode<br>27 | Mode<br>28 | Mode<br>29 | Mode<br>30 |
|---------------------------------------------------------|------------|------------|------------|------------|------------|------------|------------|------------|------------|------------|
| --> PYRc                                                | 0          | 0          | 0          | 0          | 0          | 0          | 0          | 0          | 0          | 0          |
| <--> MALc                                               | 0          | 0          | 1          | 1          | 1          | 1          | 0          | 0          | 0          | 0          |
| <--> SUCc                                               | 1          | 1          | 0          | 0          | 0          | 0          | 0          | 0          | 0          | 0          |
| <--> FUMc                                               | 0          | -1         | 0          | 0          | 0          | 0          | 1          | 1          | 1          | 1          |
| <--> CITc                                               | -0.5       | 0          | 0          | -0.5       | 0          | -0.5       | 0          | -0.5       | 0          | -0.5       |
| <--> ASPc                                               | 0          | 0          | 0          | 0          | 0          | 0          | 0          | 0          | 0          | 0          |
| --> AKGc                                                | 0          | 0          | 0          | 0          | 0          | 0          | 0          | 0          | 0          | 0          |
| <--> GLUc                                               | 0          | 0          | 0          | 0          | 0          | 0          | 0          | 0          | 0          | 0          |
| --> GLNc                                                | 0          | 0          | 0          | 0          | 0          | 0          | 0          | 0          | 0          | 0          |
| <--> CO2c                                               | -1         | 0          | -4         | -1         | -4         | -1         | -4         | -1         | -4         | -1         |
| <--> SERc                                               | 0          | 0          | 0          | 0          | 0          | 0          | 0          | 0          | 0          | 0          |
| <--> GLYc                                               | 0          | 0          | 0          | 0          | 0          | 0          | 0          | 0          | 0          | 0          |
| <--> C1c                                                | 0          | 0          | 0          | 0          | 0          | 0          | 0          | 0          | 0          | 0          |
| C1c <--> C1m                                            | 0          | 0          | 0          | 0          | 0          | 0          | 0          | 0          | 0          | 0          |
| GLYc <--> GLYm                                          | 0          | 0          | 0          | 0          | 0          | 0          | 0          | 0          | 0          | 0          |
| SERc <--> SERm                                          | 0          | 0          | 0          | 0          | 0          | 0          | 0          | 0          | 0          | 0          |
| CO2c <--> CO2m                                          | -1         | 0          | -4         | -1         | -4         | -1         | -4         | -1         | -4         | -1         |
| SERm <--> GLYm + MTHFm                                  | 0          | 0          | 0          | 0          | 0          | 0          | 0          | 0          | 0          | 0          |
| MTHFm --> C1m + THFm                                    | 0          | 0          | 0          | 0          | 0          | 0          | 0          | 0          | 0          | 0          |
| GLYm + THFm + NADm --><br>MTHFm + CO2m + NADHm +<br>NH3 | 0          | 0          | 0          | 0          | 0          | 0          | 0          | 0          | 0          | 0          |
| --> O2m                                                 | 1.25       | 0.5        | 3          | 0.75       | 3          | 0.75       | 3          | 0.75       | 3          | 0.75       |
| <--> NH3c                                               | 0          | 0          | 0          | 0          | 0          | 0          | 0          | 0          | 0          | 0          |
| NH3c <--> NH3m                                          | 0          | 0          | 0          | 0          | 0          | 0          | 0          | 0          | 0          | 0          |
| <--> ADPc                                               | 5.75       | 1.5        | 0          | 0          | 15         | 3.75       | 0          | 0          | 15         | 3.75       |
| <--> ATPc                                               | -5.75      | -1.5       | 0          | 0          | -15        | -3.75      | 0          | 0          | -15        | -3.75      |
| ADPc + ATPm <--> ADPm +<br>ATPc                         | 5.75       | 1.5        | 0          | 0          | 15         | 3.75       | 0          | 0          | 15         | 3.75       |
| PYRc --> PYRm                                           | 0          | 0          | 0          | 0          | 0          | 0          | 0          | 0          | 0          | 0          |
| FUMc <--> FUMm                                          | 0          | -1         | 0          | 0          | 0          | 0          | 1          | 1          | 1          | 1          |
| MALc <--> MALm                                          | -0.5       | 0          | 1          | 0.5        | 1          | 0.5        | 0          | -0.5       | 0          | -0.5       |
| SUCc <--> SUCm                                          | 1          | 1          | 0          | 0          | 0          | 0          | 0          | 0          | 0          | 0          |
| MALm + AKGc --> MALc +<br>AKGm                          | 0          | 0          | 0          | 0          | 0          | 0          | 0          | 0          | 0          | 0          |
| ASPm + GLUc <--> ASPc + GLUm                            | 0          | 0          | 0          | 0          | 0          | 0          | 0          | 0          | 0          | 0          |
| CITm + MALc <--> CITc + MALm                            | 0.5        | 0          | 0          | 0.5        | 0          | 0.5        | 0          | 0.5        | 0          | 0.5        |
| GLNc --> GLNm                                           | 0          | 0          | 0          | 0          | 0          | 0          | 0          | 0          | 0          | 0          |
| GLUc <--> GLUm                                          | 0          | 0          | 0          | 0          | 0          | 0          | 0          | 0          | 0          | 0          |

|                                                                |      |     |     |       |     |      |     |       |     |      |
|----------------------------------------------------------------|------|-----|-----|-------|-----|------|-----|-------|-----|------|
| PYRm + NADm --> ACOAm + NADHm + CO <sub>2</sub> m              | 0.5  | 0   | 1   | 0.5   | 1   | 0.5  | 1   | 0.5   | 1   | 0.5  |
| ACOAm + OAAm --> CITm                                          | 0.5  | 0   | 1   | 0.5   | 1   | 0.5  | 1   | 0.5   | 1   | 0.5  |
| CITm + NADm --> AKGm + NADHm + CO <sub>2</sub> m               | 0    | 0   | 1   | 0     | 1   | 0    | 1   | 0     | 1   | 0    |
| AKGm + ADPm + NADm --> SUCm + ATPm + NADHm + CO <sub>2</sub> m | 0    | 0   | 1   | 0     | 1   | 0    | 1   | 0     | 1   | 0    |
| SUCm + FADm <--> FUMm + FADHm                                  | 1    | 1   | 1   | 0     | 1   | 0    | 1   | 0     | 1   | 0    |
| FUMm <--> MALm                                                 | 1    | 0   | 1   | 0     | 1   | 0    | 2   | 1     | 2   | 1    |
| MALm + NADm <--> OAAm + NADHm                                  | 0.5  | 0   | -14 | -3.25 | 1   | 0.5  | -14 | -3.25 | 1   | 0.5  |
| MALm + NADPm --> PYRm + CO <sub>2</sub> m + NADPHm             | 0.5  | 0   | 16  | 4.25  | 1   | 0.5  | 16  | 4.25  | 1   | 0.5  |
| PYRm + CO <sub>2</sub> m + ATPm --> OAAm + ADPm                | 0    | 0   | 15  | 3.75  | 0   | 0    | 15  | 3.75  | 0   | 0    |
| AKGm + ASPm <--> GLUm + OAAm                                   | 0    | 0   | 0   | 0     | 0   | 0    | 0   | 0     | 0   | 0    |
| GLUm + NADm <--> AKGm + NH <sub>3</sub> m + NADHm              | 0    | 0   | 0   | 0     | 0   | 0    | 0   | 0     | 0   | 0    |
| GLNm --> GLUm + NH <sub>3</sub> m                              | 0    | 0   | 0   | 0     | 0   | 0    | 0   | 0     | 0   | 0    |
| 2 NADHm + O <sub>2</sub> m + 5 ADPm --> 2 NADm + 5 ATPm        | 0.75 | 0   | 2.5 | 0.75  | 2.5 | 0.75 | 2.5 | 0.75  | 2.5 | 0.75 |
| 2 FADHm + O <sub>2</sub> m + 3 ADPm --> 2 FADm + 3 ATPm        | 0.5  | 0.5 | 0.5 | 0     | 0.5 | 0    | 0.5 | 0     | 0.5 | 0    |
| NADPHm + NADm <--> NADPm + NADHm                               | 0.5  | 0   | 16  | 4.25  | 1   | 0.5  | 16  | 4.25  | 1   | 0.5  |

(cont. Table S5.3)

| Reaction / Mode →                        | 31 | 32 | 33 | 34 | 35 | 36 | 37 | 38 | 39 | 40 | 41 | 42 |
|------------------------------------------|----|----|----|----|----|----|----|----|----|----|----|----|
| --> PYRc                                 | 0  | 0  | 0  | 0  | 0  | 0  | 0  | 0  | 0  | 0  | 0  | 0  |
| <--> MALc                                | 0  | 0  | 0  | 0  | 0  | 0  | 0  | 0  | 0  | 0  | 0  | 0  |
| <--> SUCc                                | 0  | 0  | 0  | 0  | 0  | 0  | 0  | 0  | 0  | 0  | 0  | 0  |
| <--> FUMc                                | 0  | 0  | 0  | 0  | 0  | 0  | 0  | 0  | 0  | 0  | 0  | 0  |
| <--> CITc                                | 0  | 0  | 0  | 0  | 0  | 0  | 0  | 0  | 0  | 0  | 0  | 0  |
| <--> ASPc                                | 0  | -1 | 0  | 0  | -1 | 0  | 0  | -1 | 0  | -1 | 0  | 0  |
| --> AKGc                                 | 0  | 0  | 0  | 0  | 0  | 0  | 0  | 0  | 0  | 0  | 0  | 0  |
| <--> GLUc                                | 0  | 0  | -1 | 0  | 0  | -1 | 1  | 1  | 1  | 1  | 0  | 0  |
| --> GLNc                                 | 1  | 1  | 1  | 1  | 1  | 1  | 0  | 0  | 0  | 0  | 0  | 0  |
| <--> CO <sub>2</sub> c                   | -5 | -1 | 0  | -5 | -1 | 0  | -5 | -1 | -5 | -1 | 0  | -1 |
| <--> SERc                                | 0  | 0  | 0  | 0  | 0  | 0  | 0  | 0  | 0  | 0  | 1  | 1  |
| <--> GLYc                                | 0  | 0  | 0  | 0  | 0  | 0  | 0  | 0  | 0  | 0  | -1 | 0  |
| <--> C <sub>1</sub> c                    | 0  | 0  | 0  | 0  | 0  | 0  | 0  | 0  | 0  | 0  | -1 | -2 |
| C <sub>1</sub> c <--> C <sub>1</sub> m   | 0  | 0  | 0  | 0  | 0  | 0  | 0  | 0  | 0  | 0  | -1 | -2 |
| GLYc <--> GLYm                           | 0  | 0  | 0  | 0  | 0  | 0  | 0  | 0  | 0  | 0  | -1 | 0  |
| SERc <--> SERm                           | 0  | 0  | 0  | 0  | 0  | 0  | 0  | 0  | 0  | 0  | 1  | 1  |
| CO <sub>2</sub> c <--> CO <sub>2</sub> m | -5 | -1 | 0  | -5 | -1 | 0  | 0  | -1 | 0  | -1 | 0  | -1 |

|                                                      |       |     |    |       |     |    |      |      |       |     |   |   |     |
|------------------------------------------------------|-------|-----|----|-------|-----|----|------|------|-------|-----|---|---|-----|
| SERm <--> GLYm + MTHFm                               | 0     | 0   | 0  | 0     | 0   | 0  | 0    | 0    | 0     | 0   | 0 | 1 | 1   |
| MTHFm --> C1m + THFm                                 | 0     | 0   | 0  | 0     | 0   | 0  | 0    | 0    | 0     | 0   | 0 | 1 | 2   |
| GLYm + THFm + NADm --><br>MTHFm + CO2m + NADHm + NH3 | 0     | 0   | 0  | 0     | 0   | 0  | 0    | 0    | 0     | 0   | 0 | 0 | 1   |
| --> O2m                                              | 4.5   | 1.5 | 0  | 4.5   | 1.5 | 0  | 4.5  | 1.5  | 4.5   | 1.5 | 0 | 0 | 0.5 |
| <--> NH3c                                            | -2    | -1  | -1 | -2    | -1  | -1 | -1   | 0    | -1    | 0   | 0 | 0 | -1  |
| NH3c <--> NH3m                                       | -2    | -1  | -1 | -2    | -1  | -1 | -1   | 0    | -1    | 0   | 0 | 0 | -1  |
| <--> ADPc                                            | 0     | 0   | 0  | 22.5  | 7.5 | 0  | 0    | 0    | 22.5  | 7.5 | 0 | 0 | 0   |
| <--> ATPc                                            | 0     | 0   | 0  | -22.5 | 7.5 | 0  | 0    | 0    | -22.5 | 7.5 | 0 | 0 | 0   |
| ADPc + ATPm <--> ADPm + ATPc                         | 0     | 0   | 0  | 22.5  | 7.5 | 0  | 0    | 0    | 22.5  | 7.5 | 0 | 0 | 0   |
| PYRc --> PYRm                                        | 0     | 0   | 0  | 0     | 0   | 0  | 0    | 0    | 0     | 0   | 0 | 0 | 0   |
| FUMc <--> FUMm                                       | 0     | 0   | 0  | 0     | 0   | 0  | 0    | 0    | 0     | 0   | 0 | 0 | 0   |
| MALc <--> MALm                                       | 0     | 0   | 0  | 0     | 0   | 0  | 0    | 0    | 0     | 0   | 0 | 0 | 0   |
| SUCc <--> SUCm                                       | 0     | 0   | 0  | 0     | 0   | 0  | 0    | 0    | 0     | 0   | 0 | 0 | 0   |
| MALm + AKGc --> MALc + AKGm                          | 0     | 0   | 0  | 0     | 0   | 0  | 0    | 0    | 0     | 0   | 0 | 0 | 0   |
| ASPm + GLUc <--> ASPc + GLUm                         | 0     | 1   | 0  | 0     | 1   | 0  | 0    | 1    | 0     | 1   | 0 | 0 | 0   |
| CITm + MALc <--> CITc + MALm                         | 0     | 0   | 0  | 0     | 0   | 0  | 0    | 0    | 0     | 0   | 0 | 0 | 0   |
| GLNc --> GLNm                                        | 1     | 1   | 1  | 1     | 1   | 1  | 0    | 0    | 0     | 0   | 0 | 0 | 0   |
| GLUc <--> GLUm                                       | 0     | -1  | -1 | 0     | -1  | -1 | 1    | 0    | 1     | 0   | 0 | 0 | 0   |
| PYRm + NADm --> ACOAm +<br>NADHm + CO2m              | 1     | 0   | 0  | 1     | 0   | 0  | 1    | 0    | 1     | 0   | 0 | 0 | 0   |
| ACOAm + OAAm --> CITm                                | 1     | 0   | 0  | 1     | 0   | 0  | 1    | 0    | 1     | 0   | 0 | 0 | 0   |
| CITm + NADm --> AKGm +<br>NADHm + CO2m               | 1     | 0   | 0  | 1     | 0   | 0  | 1    | 0    | 1     | 0   | 0 | 0 | 0   |
| AKGm + ADPm + NADm --> SUCm<br>+ ATPm + NADHm + CO2m | 2     | 1   | 0  | 2     | 1   | 0  | 2    | 1    | 2     | 1   | 0 | 0 | 0   |
| SUCm + FADm <--> FUMm +<br>FADHm                     | 2     | 1   | 0  | 2     | 1   | 0  | 2    | 1    | 2     | 1   | 0 | 0 | 0   |
| FUMm <--> MALm                                       | 2     | 1   | 0  | 2     | 1   | 0  | 2    | 1    | 2     | 1   | 0 | 0 | 0   |
| MALm + NADm <--> OAAm +<br>NADHm                     | -21.5 | 6.5 | 0  | 1     | 1   | 0  | 21.5 | -6.5 | 1     | 1   | 0 | 0 | 2.5 |
| MALm + NADPm --> PYRm +<br>CO2m + NADPHm             | 23.5  | 7.5 | 0  | 1     | 0   | 0  | 23.5 | 7.5  | 1     | 0   | 0 | 0 | 2.5 |
| PYRm + CO2m + ATPm --> OAAm<br>+ ADPm                | 22.5  | 7.5 | 0  | 0     | 0   | 0  | 22.5 | 7.5  | 0     | 0   | 0 | 0 | 2.5 |
| AKGm + ASPm <--> GLUm +<br>OAAm                      | 0     | -1  | 0  | 0     | -1  | 0  | 0    | -1   | 0     | -1  | 0 | 0 | 0   |
| GLUm + NADm <--> AKGm +<br>NH3m + NADHm              | 1     | 0   | 0  | 1     | 0   | 0  | 1    | 0    | 1     | 0   | 0 | 0 | 0   |
| GLNm --> GLUm + NH3m                                 | 1     | 1   | 1  | 1     | 1   | 1  | 0    | 0    | 0     | 0   | 0 | 0 | 0   |
| 2 NADHm + O2m + 5 ADPm --> 2<br>NADm + 5 ATPm        | 3.5   | 1   | 0  | 3.5   | 1   | 0  | 3.5  | 1    | 3.5   | 1   | 0 | 0 | 0.5 |
| 2 FADHm + O2m + 3 ADPm --> 2<br>FADm + 3 ATPm        | 1     | 0.5 | 0  | 1     | 0.5 | 0  | 1    | 0.5  | 1     | 0.5 | 0 | 0 | 0   |
| NADPHm + NADm <--> NADPm +<br>NADHm                  | 23.5  | 7.5 | 0  | 1     | 0   | 0  | 23.5 | 7.5  | 1     | 0   | 0 | 0 | 2.5 |

| Experiment | 1a                               | 1b   | 2a <sup>*1</sup> | 2b <sup>*2</sup> | 3a   | 3b | 4a   | 4b    | 5a   | 5b <sup>*3</sup> | 6a/7a | 6b/7b <sup>*4</sup> | 8a   | 8b   | 9a   | 9b | 12a |
|------------|----------------------------------|------|------------------|------------------|------|----|------|-------|------|------------------|-------|---------------------|------|------|------|----|-----|
|            | Contribution [fmol / cell × min] |      |                  |                  |      |    |      |       |      |                  |       |                     |      |      |      |    |     |
| Mode 1     | 4.6                              | 0    | 11.9             | 0                | 0    | 0  | 0    | 0     | 0    | 0                | 0     | 0                   | 0    | 0    | 0    | 0  | 0   |
| Mode 2     | 0                                | 14.2 | 0                | 15.6             | 0    | 0  | 0    | 0     | 0    | 0                | 0     | 0                   | 0    | 0    | 0    | 0  | 0   |
| Mode 3     | 0                                | 0    | 0                | 0                | 0    | 0  | 0    | 0     | 0    | 0                | 0     | 0                   | 0    | 0    | 0    | 0  | 0   |
| Mode 4     | 0                                | 0    | 6.1              | 0                | 0    | 0  | 0    | 0     | 0    | 0                | 0     | 0                   | 0    | 0    | 0    | 0  | 0   |
| Mode 5     | 0                                | 0    | 0                | 0                | 0    | 0  | 0    | 0     | 0    | 0                | 0     | 0                   | 0    | 0    | 0    | 0  | 0   |
| Mode 6     | 0                                | 0    | 0                | 0                | 0    | 0  | 0    | 0     | 0    | 0                | 0     | 0                   | 0    | 0    | 0    | 0  | 0   |
| Mode 7     | 0                                | 0    | 0                | 0                | 0    | 0  | 0    | 0     | 0    | 0                | 0     | 0                   | 0    | 0    | 0    | 0  | 0   |
| Mode 8     | 0                                | 0    | 0                | 12.2             | 0    | 0  | 0    | 0     | 0    | 0                | 0     | 0                   | 0    | 0    | 0    | 0  | 0   |
| Mode 9     | 0                                | 0    | 0                | 0                | 5.62 | 0  | 0    | 0     | 0    | 0                | 0     | 0                   | 0    | 0    | 0    | 0  | 0   |
| Mode 10    | 0                                | 0    | 0                | 0                | 0    | 38 | 0    | 0     | 0    | 0                | 0     | 0                   | 0    | 0    | 0    | 0  | 0   |
| Mode 11    | 0                                | 0    | 0                | 0                | 0    | 0  | 12.3 | 0     | 0    | 0                | 0     | 0                   | 0    | 0    | 0    | 0  | 0   |
| Mode 12    | 0                                | 0    | 0                | 0                | 0    | 0  | 0.4  | 0     | 0    | 0                | 0     | 0                   | 0    | 0    | 0    | 0  | 0   |
| Mode 13    | 0                                | 0    | 0                | 0                | 0    | 0  | 0    | 37.73 | 0    | 0                | 0     | 0                   | 0    | 0    | 0    | 0  | 0   |
| Mode 14    | 0                                | 0    | 0                | 0                | 0    | 0  | 0    | 2.47  | 0    | 0                | 0     | 0                   | 0    | 0    | 0    | 0  | 0   |
| Mode 15    | 0                                | 0    | 0                | 0                | 0    | 0  | 0    | 0     | 4.07 | 0                | 0     | 0                   | 0    | 0    | 0    | 0  | 0   |
| Mode 16    | 0                                | 0    | 0                | 0                | 0    | 0  | 0    | 0     | 14.5 | 0                | 0     | 0                   | 0    | 0    | 0    | 0  | 0   |
| Mode 17    | 0                                | 0    | 0                | 0                | 0    | 0  | 0    | 0     | 3.7  | 0                | 0     | 0                   | 0    | 0    | 0    | 0  | 0   |
| Mode 18    | 0                                | 0    | 0                | 0                | 0    | 0  | 0    | 0     | 2.23 | 0                | 0     | 0                   | 0    | 0    | 0    | 0  | 0   |
| Mode 19    | 0                                | 0    | 0                | 0                | 0    | 0  | 0    | 0     | 0    | 10.6             | 0     | 0                   | 0    | 0    | 0    | 0  | 0   |
| Mode 20    | 0                                | 0    | 0                | 0                | 0    | 0  | 0    | 0     | 0    | 14.6             | 0     | 0                   | 0    | 0    | 0    | 0  | 0   |
| Mode 21    | 0                                | 0    | 0                | 0                | 0    | 0  | 0    | 0     | 0    | 3.7              | 0     | 0                   | 0    | 0    | 0    | 0  | 0   |
| Mode 22    | 0                                | 0    | 0                | 0                | 0    | 0  | 0    | 0     | 0    | 2.14             | 0     | 0                   | 0    | 0    | 0    | 0  | 0   |
| Mode 23    | 0                                | 0    | 0                | 0                | 0    | 0  | 0    | 0     | 0    | 0                | 7     | 0                   | 0    | 0    | 0    | 0  | 0   |
| Mode 24    | 0                                | 0    | 0                | 0                | 0    | 0  | 0    | 0     | 0    | 0                | 9.72  | 0                   | 0    | 0    | 0    | 0  | 0   |
| Mode 25    | 0                                | 0    | 0                | 0                | 0    | 0  | 0    | 0     | 0    | 0                | 0     | 11.6                | 0    | 0    | 0    | 0  | 0   |
| Mode 26    | 0                                | 0    | 0                | 0                | 0    | 0  | 0    | 0     | 0    | 0                | 0     | 9.72                | 0    | 0    | 0    | 0  | 0   |
| Mode 27    | 0                                | 0    | 0                | 0                | 0    | 0  | 0    | 0     | 0    | 0                | 0     | 0                   | 0    | 0    | 0    | 0  | 0   |
| Mode 28    | 0                                | 0    | 0                | 0                | 0    | 0  | 0    | 0     | 0    | 0                | 0     | 0                   | 0    | 0    | 0    | 0  | 0   |
| Mode 29    | 0                                | 0    | 0                | 0                | 0    | 0  | 0    | 0     | 0    | 0                | 0     | 0                   | 0    | 0    | 0    | 0  | 0   |
| Mode 30    | 0                                | 0    | 0                | 0                | 0    | 0  | 0    | 0     | 0    | 0                | 0     | 0                   | 0    | 0    | 0    | 0  | 0   |
| Mode 31    | 0                                | 0    | 0                | 0                | 0    | 0  | 0    | 0     | 0    | 0                | 0     | 0                   | 2.31 | 0    | 0    | 0  | 0   |
| Mode 32    | 0                                | 0    | 0                | 0                | 0    | 0  | 0    | 0     | 0    | 0                | 0     | 0                   | 3.29 | 0    | 0    | 0  | 0   |
| Mode 33    | 0                                | 0    | 0                | 0                | 0    | 0  | 0    | 0     | 0    | 0                | 0     | 0                   | 14.4 | 0    | 0    | 0  | 0   |
| Mode 34    | 0                                | 0    | 0                | 0                | 0    | 0  | 0    | 0     | 0    | 0                | 0     | 0                   | 0    | 14.3 | 0    | 0  | 0   |
| Mode 35    | 0                                | 0    | 0                | 0                | 0    | 0  | 0    | 0     | 0    | 0                | 0     | 0                   | 0    | 11.4 | 0    | 0  | 0   |
| Mode 36    | 0                                | 0    | 0                | 0                | 0    | 0  | 0    | 0     | 0    | 0                | 0     | 0                   | 0    | 19   | 0    | 0  | 0   |
| Mode 37    | 0                                | 0    | 0                | 0                | 0    | 0  | 0    | 0     | 0    | 0                | 0     | 0                   | 0    | 0    | 2.69 | 0  | 0   |
| Mode 38    | 0                                | 0    | 0                | 0                | 0    | 0  | 0    | 0     | 0    | 0                | 0     | 0                   | 0    | 0    | 0    | 0  | 0   |
| Mode 39    | 0                                | 0    | 0                | 0                | 0    | 0  | 0    | 0     | 0    | 0                | 0     | 0                   | 0    | 0    | 0    | 0  | 0   |
| Mode 40    | 0                                | 0    | 0                | 0                | 0    | 0  | 0    | 0     | 0    | 0                | 0     | 0                   | 0    | 0    | 0    | 0  | 0   |

|         |   |   |   |   |   |   |   |   |   |   |   |   |   |   |   |   |   |      |
|---------|---|---|---|---|---|---|---|---|---|---|---|---|---|---|---|---|---|------|
| Mode 41 | o | o | o | o | o | o | o | o | o | o | o | o | o | o | o | o | o | 2.61 |
| Mode 42 | o | o | o | o | o | o | o | o | o | o | o | o | o | o | o | o | o | 1.84 |

\*<sup>1</sup> In the experiments 2a and 2b it is assumed that the modes that take up ASP and PYR together are not active (Mode 3 and Mode 6) . Also, the modes that use ASP to produce only CO<sub>2</sub> (Mode 5 and Mode 7) are considered inactive when computing the contribution factors.

\*<sup>2</sup> In the experiments 5b, 6b and 7b the CIT concentration could not be determined. Mode contribution factors were computed assuming the same factors for CIT production as in 5a, 6a and 7a respectively.

\*<sup>3</sup> In the experiment 9b, GLU concentration could not be determined reliably, therefore the mode flux was not computed.

\*<sup>4</sup> The contribution of Modes 27-30 to FUM metabolism could not be determined due to extracellular conversion of FUM to MAL.

**Supplem. Table S5.4. Conclusions on mitochondrial enzymes and transporters activity and about regulation of the mitochondrial metabolism** resulted by applying elementary mode analysis to the observations from feeding experiments with selectively permeabilized CHO-K1 cells. The gray areas indicate the experiments on which each corresponding conclusion was based.

| Experiment No.                            | 1a                                                                                                                                                                                                   | 1b            | 2a                                            | 2b                       | 3a                                                 | 3b           | 4a                      | 4b                           | 5a        | 5b             | 6a/7a             | 6b/7b                  | 8a        | 8b             | 9a        | 9b             | 11a    |
|-------------------------------------------|------------------------------------------------------------------------------------------------------------------------------------------------------------------------------------------------------|---------------|-----------------------------------------------|--------------------------|----------------------------------------------------|--------------|-------------------------|------------------------------|-----------|----------------|-------------------|------------------------|-----------|----------------|-----------|----------------|--------|
| Substrate                                 | pyruvate                                                                                                                                                                                             | pyruvate, ADP | pyruvate, aspartate                           | pyruvate, aspartate, ADP | citrate                                            | citrate, ADP | $\alpha$ -ketoglutarate | $\alpha$ -ketoglutarate, ADP | succinate | succinate, ADP | malate / fumarate | malate / fumarate, ADP | glutamine | glutamine, ADP | glutamate | glutamate, ADP | serine |
| Citrate synthase flux [fmol / cell x min] | 4.6                                                                                                                                                                                                  | 14.2          | 15                                            | 21.1                     | 5.6                                                | 38           | 12.22                   | 37.7                         | 5.9       | 11.9           | 11.6              | 16.5                   | 2.3       | 14.3           | -         | -              | 0      |
|                                           | Uptake rates increased by adding ADP. This happens because (1) ADP is a substrate for oxidative phosphorylation and allows regeneration of NAD <sup>+</sup> and (2) ADP stimulates PDH, IDH and AKGH |               |                                               |                          |                                                    |              |                         |                              |           |                |                   |                        |           |                |           |                |        |
|                                           | In the experiments where ADP was not supplied, the highly active PCX-MDH-ME cycle disposed of the ATP                                                                                                |               |                                               |                          |                                                    |              |                         |                              |           |                |                   |                        |           |                |           |                |        |
|                                           | ME provides PYR for replenishing the TCA                                                                                                                                                             |               |                                               |                          |                                                    |              |                         |                              |           |                |                   |                        |           |                |           |                |        |
|                                           | Reducing equivalents are transferred from NADPH to NAD <sup>+</sup> via the NNT or using cycling by NAD <sup>-</sup> and NADP-dependent IDH isoenzymes                                               |               |                                               |                          |                                                    |              |                         |                              |           |                |                   |                        |           |                |           |                |        |
|                                           |                                                                                                                                                                                                      |               |                                               |                          | Full metabolization to CO <sub>2</sub> is possible |              |                         |                              |           |                |                   |                        |           |                |           |                |        |
|                                           | PYR and ASP had a reciprocal stimulating effect. This effect did not manifest for PYR in the presence of ADP. ASP was not taken up without PYR.                                                      |               |                                               |                          |                                                    |              |                         |                              |           |                |                   |                        |           |                |           |                |        |
|                                           |                                                                                                                                                                                                      |               | ASP and PYR are metabolized by separate modes |                          |                                                    |              |                         |                              |           |                |                   |                        |           |                |           |                |        |

|                                                                                                                                                                                                      |                                                                                      |  |
|------------------------------------------------------------------------------------------------------------------------------------------------------------------------------------------------------|--------------------------------------------------------------------------------------|--|
|                                                                                                                                                                                                      | GLU is re-transported into the mitochondria via the GLU carrier                      |  |
| PYR uptake is limited in all stimulating conditions (ADP, ASP, ASP+ADP) by the MPC. PYR uptake is in the same range with the uptake <i>in vivo</i> by the CHO-K1 mitochondria (Nicolae et al., 2014) |                                                                                      |  |
|                                                                                                                                                                                                      | Either complete reuptake of MAL occurs or CIT is transported without antiport        |  |
|                                                                                                                                                                                                      | Highest complete TCA cycle flux, both with and w/o ADP                               |  |
|                                                                                                                                                                                                      | High TCA cycle flux confirms that IDH and AKGDH are the bottlenecks of the TCA cycle |  |
|                                                                                                                                                                                                      | High cytosolic concentrations of AKG did not inhibit ME                              |  |
|                                                                                                                                                                                                      | Transported via the C4-dicarboxylate carrier (antiport with phosphate)               |  |
|                                                                                                                                                                                                      | Extramitochondrial conversion of FUM to MAL                                          |  |

(cont. Table S5.4)

| Experiment No.                            | 1a                                                                                                        | 1b            | 2a                  | 2b                       | 3a                                                                                   | 3b           | 4a                                                      | 4b                   | 5a                                                                                                                                 | 5b             | 6a/7a             | 6b/7b                                       | 8a        | 8b             | 9a        | 9b             | 11a    |  |
|-------------------------------------------|-----------------------------------------------------------------------------------------------------------|---------------|---------------------|--------------------------|--------------------------------------------------------------------------------------|--------------|---------------------------------------------------------|----------------------|------------------------------------------------------------------------------------------------------------------------------------|----------------|-------------------|---------------------------------------------|-----------|----------------|-----------|----------------|--------|--|
| Substrate                                 | pyruvate                                                                                                  | pyruvate, ADP | pyruvate, aspartate | pyruvate, aspartate, ADP | citrate                                                                              | citrate, ADP | α-ketoglutarate                                         | α-ketoglutarate, ADP | succinate                                                                                                                          | succinate, ADP | malate / fumarate | malate / fumarate, ADP                      | glutamine | glutamine, ADP | glutamate | glutamate, ADP | serine |  |
| Citrate synthase flux [fmol / cell x min] | 4.6                                                                                                       | 14.2          | 15                  | 21.1                     | 5.6                                                                                  | 38           | 12.22                                                   | 37.7                 | 5.9                                                                                                                                | 11.9           | 11.6              | 16.5                                        | 2.3       | 14.3           | -         | -              | 0      |  |
|                                           |                                                                                                           |               |                     |                          | Either complete reuptake of MAL occurs or CIT is transported without antiport        |              |                                                         |                      |                                                                                                                                    |                |                   |                                             |           |                |           |                |        |  |
|                                           |                                                                                                           |               |                     |                          | Highest complete TCA cycle flux, both with and w/o ADP                               |              |                                                         |                      |                                                                                                                                    |                |                   |                                             |           |                |           |                |        |  |
|                                           |                                                                                                           |               |                     |                          | High TCA cycle flux confirms that IDH and AKGDH are the bottlenecks of the TCA cycle |              |                                                         |                      |                                                                                                                                    |                |                   |                                             |           |                |           |                |        |  |
|                                           |                                                                                                           |               |                     |                          |                                                                                      |              | High cytosolic concentrations of AKG did not inhibit ME |                      |                                                                                                                                    |                |                   |                                             |           |                |           |                |        |  |
|                                           |                                                                                                           |               |                     |                          |                                                                                      |              |                                                         |                      | Transported via the C4-dicarboxylate carrier (antiport with phosphate)                                                             |                |                   |                                             |           |                |           |                |        |  |
|                                           |                                                                                                           |               |                     |                          |                                                                                      |              |                                                         |                      |                                                                                                                                    |                |                   | Extramitochondrial conversion of FUM to MAL |           |                |           |                |        |  |
|                                           |                                                                                                           |               |                     |                          |                                                                                      |              |                                                         |                      | MAL/CIT secretion is favored instead of a full TCA cycle                                                                           |                |                   |                                             |           |                |           |                |        |  |
|                                           | First half of TCA cycle is controlled by (allosteric) effectors: ADP, ATP, NADH --> "effector-controlled" |               |                     |                          |                                                                                      |              |                                                         |                      |                                                                                                                                    |                |                   |                                             |           |                |           |                |        |  |
|                                           |                                                                                                           |               |                     |                          |                                                                                      |              |                                                         |                      | The TCA part involving the C4-dicarboxylates is controlled by the concentration of dicarboxylates and not by ADP (, ATP, NADH) --> |                |                   |                                             |           |                |           |                |        |  |



|  |                                                                                      |                                                                                            |                                                                                                       |                                                                                            |
|--|--------------------------------------------------------------------------------------|--------------------------------------------------------------------------------------------|-------------------------------------------------------------------------------------------------------|--------------------------------------------------------------------------------------------|
|  |                                                                                      |                                                                                            | "concentration-controlled" second half of TCA cycle                                                   |                                                                                            |
|  |                                                                                      |                                                                                            | The C4-dicarboxylates may inhibit enzymes involved in the TCA cycle that do not process then directly |                                                                                            |
|  |                                                                                      |                                                                                            |                                                                                                       | Most of the GLN was converted to GLU, then exported via the GLU carrier                    |
|  |                                                                                      | Control by GDH reduces the TCA cycle flux on GLN compared to when AKG is used as substrate |                                                                                                       | Control by GDH reduces the TCA cycle flux on GLN compared to when AKG is used as substrate |
|  |                                                                                      |                                                                                            |                                                                                                       | Extracellular GLU induced ASP secretion                                                    |
|  | GLU uptake occurs via the GLU-ASP carrier; GLU production occurs via the GLU carrier |                                                                                            |                                                                                                       | GLU uptake occurs via the GLU-ASP carrier; GLU production occurs via the GLU carrier       |
|  |                                                                                      |                                                                                            |                                                                                                       | Serine was converted by mSH MT to glycine                                                  |
|  |                                                                                      |                                                                                            |                                                                                                       | Glycine was partially cleaved to C1 and CO2                                                |

---

## References

### [A]

- Adam-Vizi, V., 2005. Production of reactive oxygen species in brain mitochondria: contribution by electron transport chain and non-electron transport chain sources. *Antioxid Redox Signal.* 7, 1140-9.
- Ahn, W. S., Antoniewicz, M. R., 2011. Metabolic flux analysis of CHO cells at growth and non-growth phases using isotopic tracers and mass spectrometry. *Metab Eng.* 13, 598-609.
- Ahn, W. S., Antoniewicz, M. R., 2012. Towards dynamic metabolic flux analysis in CHO cell cultures. *Biotechnol J.* 7, 61-74.
- Ahn, W. S., Antoniewicz, M. R., 2013. Parallel labeling experiments with [1,2-(13)C]glucose and [U-(13)C]glutamine provide new insights into CHO cell metabolism. *Metab Eng.* 15, 34-47.
- al-Habori, M., 1995. Microcompartmentation, metabolic channelling and carbohydrate metabolism. *Int J Biochem Cell Biol.* 27, 123-32.
- Allen, D. K., Shachar-Hill, Y., Ohlrogge, J. B., 2007. Compartment-specific labeling information in 13C metabolic flux analysis of plants. *Phytochemistry.* 68, 2197-210.
- Altamirano, C., Cairo, J. J., Godia, F., 2001a. Decoupling cell growth and product formation in Chinese hamster ovary cells through metabolic control. *Biotechnol Bioeng.* 76, 351-60.
- Altamirano, C., Illanes, A., Casablancas, A., Gamez, X., Cairo, J. J., Godia, C., 2001b. Analysis of CHO cells metabolic redistribution in a glutamate-based defined medium in continuous culture. *Biotechnol Prog.* 17, 1032-41.
- Amaral, A. I., Teixeira, A. P., Sonnewald, U., Alves, P. M., 2011. Estimation of intracellular fluxes in cerebellar neurons after hypoglycemia: Importance of the pyruvate recycling pathway and glutamine oxidation. *J Neurosci Res.* 89, 700-10.
- Anastasiou, D., Poulogiannis, G., Asara, J. M., Boxer, M. B., Jiang, J. K., Shen, M., Bellinger, G., Sasaki, A. T., Locasale, J. W., Auld, D. S., Thomas, C. J., Vander Heiden, M. G., Cantley, L. C., 2011. Inhibition of pyruvate kinase M2 by reactive oxygen species contributes to cellular antioxidant responses. *Science.* 334, 1278-83.
- Antoniewicz, M. R., 2013a. Dynamic metabolic flux analysis--tools for probing transient states of metabolic networks. *Curr Opin Biotechnol.* 24, 973-8.
- Antoniewicz, M. R., 2013b. Using multiple tracers for 13C metabolic flux analysis. *Methods Mol Biol.* 985, 353-65.
- Antoniewicz, M. R., Kelleher, J. K., Stephanopoulos, G., 2006. Determination of confidence intervals of metabolic fluxes estimated from stable isotope measurements. *Metab Eng.* 8, 324-37.
- Antoniewicz, M. R., Kelleher, J. K., Stephanopoulos, G., 2007. Elementary metabolite units (EMU): a novel framework for modeling isotopic distributions. *Metab Eng.* 9, 68-86.
- Appling, D. R., 1991. Compartmentation of folate-mediated one-carbon metabolism in eukaryotes. *FASEB J.* 5, 2645-51.

### [B]

- Baba, N., Sharma, H. M., 1971. Histochemistry of lactic dehydrogenase in heart and pectoralis muscles of rat. *J Cell Biol.* 51, 621-35.
- Bahnemann, J., Kayo, S., Wahrheit, J., Heinzle, E., Pörtner, R., Zeng, A.-P., 2014. In search of an effective cell disruption method to isolate intact mitochondria from Chinese hamster ovary cells. *Eng. Life Sci.* 14, 161-169.

- Balaban, R. S., 2006. Modeling mitochondrial function. *Am J Physiol Cell Physiol.* 291, C1107-13.
- Balaban, R. S., 2010. The mitochondrial proteome: a dynamic functional program in tissues and disease states. *Environ Mol Mutagen.* 51, 352-9.
- Barden, R. E., Fung, C. H., Utter, M. F., Scrutton, M. C., 1972. Pyruvate carboxylase from chicken liver. Steady state kinetic studies indicate a "two-site" ping-pong mechanism. *J Biol Chem.* 247, 1323-33.
- Barlowe, C. K., Appling, D. R., 1988. In vitro evidence for the involvement of mitochondrial folate metabolism in the supply of cytoplasmic one-carbon units. *Biofactors.* 1, 171-6.
- Baycin-Hizal, D., Tabb, D. L., Chaerkady, R., Chen, L., Lewis, N. E., Nagarajan, H., Sarkaria, V., Kumar, A., Wolozny, D., Colao, J., Jacobson, E., Tian, Y., O'Meally, R. N., Krag, S. S., Cole, R. N., Palsson, B. O., Zhang, H., Betenbaugh, M., 2012. Proteomic analysis of Chinese hamster ovary cells. *J Proteome Res.* 11, 5265-76.
- Becker, J., Hackl, M., Rupp, O., Jakobi, T., Schneider, J., Szczepanowski, R., Bekel, T., Borth, N., Goesmann, A., Grillari, J., Kaltschmidt, C., Noll, T., Puhler, A., Tauch, A., Brinkrolf, K., 2011. Unraveling the Chinese hamster ovary cell line transcriptome by next-generation sequencing. *J Biotechnol.* 156, 227-35.
- Belle, A., Tanay, A., Bitincka, L., Shamir, R., O'Shea, E. K., 2006. Quantification of protein half-lives in the budding yeast proteome. *Proc Natl Acad Sci U S A.* 103, 13004-9.
- Bensaad, K., Tsuruta, A., Selak, M. A., Vidal, M. N., Nakano, K., Bartrons, R., Gottlieb, E., Vousden, K. H., 2006. TIGAR, a p53-inducible regulator of glycolysis and apoptosis. *Cell.* 126, 107-20.
- Beuster, G., Zarse, K., Kaleta, C., Thierbach, R., Kiehntopf, M., Steinberg, P., Schuster, S., Ristow, M., 2011. Inhibition of alanine aminotransferase in silico and in vivo promotes mitochondrial metabolism to impair malignant growth. *J Biol Chem.* 286, 22323-30.
- Birch, J. R., Racher, A. J., 2006. Antibody production. *Adv Drug Deliv Rev.* 58, 671-85.
- Blake, J. A., Bult, C. J., Eppig, J. T., Kadin, J. A., Richardson, J. E., 2014. The Mouse Genome Database: integration of and access to knowledge about the laboratory mouse. *Nucleic Acids Res.* 42, D810-7.
- Bonarius, H. P., Hatzimanikatis, V., Meesters, K. P., de Gooijer, C. D., Schmid, G., Tramper, J., 1996. Metabolic flux analysis of hybridoma cells in different culture media using mass balances. *Biotechnol Bioeng.* 50, 299-318.
- Bonarius, H. P., Ozemre, A., Timmerarends, B., Skrabal, P., Tramper, J., Schmid, G., Heinzle, E., 2001. Metabolic-flux analysis of continuously cultured hybridoma cells using (13)CO(2) mass spectrometry in combination with (13)C-lactate nuclear magnetic resonance spectroscopy and metabolite balancing. *Biotechnol Bioeng.* 74, 528-38.
- Bonarius, H. P., Timmerarends, B., de Gooijer, C. D., Tramper, J., 1998. Metabolite-balancing techniques vs. 13C tracer experiments to determine metabolic fluxes in hybridoma cells. *Biotechnol Bioeng.* 58, 258-62.
- Bordbar, A., Feist, A. M., Usaite-Black, R., Woodcock, J., Palsson, B. O., Famili, I., 2011. A multi-tissue type genome-scale metabolic network for analysis of whole-body systems physiology. *BMC Syst Biol.* 5, 180.
- Borth, N., 2014. Opening the black box: Chinese hamster ovary research goes genome scale. *Pharmaceutical Bioprocessing.* 2, 367-369.
- Boss, O., Hagen, T., Lowell, B. B., 2000. Uncoupling proteins 2 and 3: potential regulators of mitochondrial energy metabolism. *Diabetes.* 49, 143-56.
- Boss, O., Samec, S., Paoloni-Giacobino, A., Rossier, C., Dulloo, A., Seydoux, J., Muzzin, P., Giacobino, J. P., 1997. Uncoupling protein-3: a new member of the mitochondrial carrier family with tissue-specific expression. *FEBS Lett.* 408, 39-42.

- Brand, M. D., Esteves, T. C., 2005. Physiological functions of the mitochondrial uncoupling proteins UCP2 and UCP3. *Cell Metab.* 2, 85-93.
- Bratic, A., Larsson, N. G., 2013. The role of mitochondria in aging. *J Clin Invest.* 123, 951-7.
- Bricker, D. K., Taylor, E. B., Schell, J. C., Orsak, T., Boutron, A., Chen, Y. C., Cox, J. E., Cardon, C. M., Van Vranken, J. G., Dephoure, N., Redin, C., Boudina, S., Gygi, S. P., Brivet, M., Thummel, C. S., Rutter, J., 2012. A mitochondrial pyruvate carrier required for pyruvate uptake in yeast, *Drosophila*, and humans. *Science.* 337, 96-100.
- Brinkrolf, K., Rupp, O., Laux, H., Kollin, F., Ernst, W., Linke, B., Kofler, R., Romand, S., Hesse, F., Budach, W. E., Galosy, S., Muller, D., Noll, T., Wienberg, J., Jostock, T., Leonard, M., Grillari, J., Tauch, A., Goesmann, A., Helk, B., Mott, J. E., Puhler, A., Borth, N., 2013. Chinese hamster genome sequenced from sorted chromosomes. *Nat Biotechnol.* 31, 694-5.
- Brooks, G. A., Dubouchaud, H., Brown, M., Sicurello, J. P., Butz, C. E., 1999. Role of mitochondrial lactate dehydrogenase and lactate oxidation in the intracellular lactate shuttle. *Proc Natl Acad Sci U S A.* 96, 1129-34.
- Brown, A. J., Sweeney, B., Mainwaring, D. O., James, D. C., 2014. Synthetic promoters for CHO cell engineering. *Biotechnol Bioeng.* 111, 1638-47.
- Bucher, T., Brauser, B., Conze, A., Klein, F., Langguth, O., Sies, H., 1972. State of oxidation-reduction and state of binding in the cytosolic NADH-system as disclosed by equilibration with extracellular lactate-pyruvate in hemoglobin-free perfused rat liver. *European Journal of Biochemistry.* 27, 301-17.
- Bugrim, A., Nikolskaya, T., Nikolsky, Y., 2004. Early prediction of drug metabolism and toxicity: systems biology approach and modeling. *Drug Discov Today.* 9, 127-35.
- Butler, M., Meneses-Acosta, A., 2012. Recent advances in technology supporting biopharmaceutical production from mammalian cells. *Appl Microbiol Biotechnol.* 96, 885-94.

## [C]

- Cakir, T., Tacer, C. S., Ulgen, K. O., 2004. Metabolic pathway analysis of enzyme-deficient human red blood cells. *Biosystems.* 78, 49-67.
- Calvo, S., Jain, M., Xie, X., Sheth, S. A., Chang, B., Goldberger, O. A., Spinazzola, A., Zeviani, M., Carr, S. A., Mootha, V. K., 2006. Systematic identification of human mitochondrial disease genes through integrative genomics. *Nat Genet.* 38, 576-82.
- Campanella, M. E., Chu, H., Low, P. S., 2005. Assembly and regulation of a glycolytic enzyme complex on the human erythrocyte membrane. *Proc Natl Acad Sci U S A.* 102, 2402-7.
- Carinhas, N., Duarte, T. M., Barreiro, L. C., Carrondo, M. J., Alves, P. M., Teixeira, A. P., 2013. Metabolic signatures of GS-CHO cell clones associated with butyrate treatment and culture phase transition. *Biotechnol Bioeng.* 110, 3244-57.
- Carinhas, N., Oliveira, R., Alves, P. M., Carrondo, M. J., Teixeira, A. P., 2012. Systems biotechnology of animal cells: the road to prediction. *Trends Biotechnol.* 30, 377-85.
- Carlson, R., Fell, D., Sreenc, F., 2002. Metabolic pathway analysis of a recombinant yeast for rational strain development. *Biotechnol Bioeng.* 79, 121-34.
- Cascante, M., Cortes, A., 1988. Kinetic studies of chicken and turkey liver mitochondrial aspartate aminotransferase. *Biochem J.* 250, 805-12.
- Cassard, A. M., Bouillaud, F., Mattei, M. G., Hentz, E., Raimbault, S., Thomas, M., Ricquier, D., 1990. Human uncoupling protein gene: structure, comparison with rat gene, and assignment to the long arm of chromosome 4. *J Cell Biochem.* 43, 255-64.

- Castegna, A., Scarcia, P., Agrimi, G., Palmieri, L., Rottensteiner, H., Spera, I., Germinario, L., Palmieri, F., 2010. Identification and functional characterization of a novel mitochondrial carrier for citrate and oxoglutarate in *Saccharomyces cerevisiae*. *J Biol Chem*. 285, 17359-70.
- Castrillo, J. I., Oliver, S. G., 2011. Yeast systems biology: the challenge of eukaryotic complexity. *Methods Mol Biol*. 759, 3-28.
- Cavero, S., Voza, A., del Arco, A., Palmieri, L., Villa, A., Blanco, E., Runswick, M. J., Walker, J. E., Cerdan, S., Palmieri, F., Satrustegui, J., 2003. Identification and metabolic role of the mitochondrial aspartate-glutamate transporter in *Saccharomyces cerevisiae*. *Mol Microbiol*. 50, 1257-69.
- Ceccarelli, C., Grodsky, N. B., Ariyaratne, N., Colman, R. F., Bahnson, B. J., 2002. Crystal structure of porcine mitochondrial NADP+-dependent isocitrate dehydrogenase complexed with Mn<sup>2+</sup> and isocitrate. Insights into the enzyme mechanism. *J Biol Chem*. 277, 43454-62.
- Chakrabarti, A., Miskovic, L., Soh, K. C., Hatzimanikatis, V., 2013. Towards kinetic modeling of genome-scale metabolic networks without sacrificing stoichiometric, thermodynamic and physiological constraints. *Biotechnol J*. 8, 1043-57.
- Chang, Y., Suthers, P. F., Maranas, C. D., 2008. Identification of optimal measurement sets for complete flux elucidation in metabolic flux analysis experiments. *Biotechnol Bioeng*. 100, 1039-49.
- Chen, J., Zheng, H., Liu, H., Niu, J., Liu, J., Shen, T., Rui, B., Shi, Y., 2007. Improving metabolic flux estimation via evolutionary optimization for convex solution space. *Bioinformatics*. 23, 1115-23.
- Chen, N., Koumpouras, G. C., Polizzi, K. M., Kontoravdi, C., 2012. Genome-based kinetic modeling of cytosolic glucose metabolism in industrially relevant cell lines: *Saccharomyces cerevisiae* and Chinese hamster ovary cells. *Bioprocess Biosyst Eng*. 35, 1023-33.
- Christie, K. R., Weng, S., Balakrishnan, R., Costanzo, M. C., Dolinski, K., Dwight, S. S., Engel, S. R., Feierbach, B., Fisk, D. G., Hirschman, J. E., Hong, E. L., Issel-Tarver, L., Nash, R., Sethuraman, A., Starr, B., Theesfeld, C. L., Andrada, R., Binkley, G., Dong, Q., Lane, C., Schroeder, M., Botstein, D., Cherry, J. M., 2004. *Saccharomyces* Genome Database (SGD) provides tools to identify and analyze sequences from *Saccharomyces cerevisiae* and related sequences from other organisms. *Nucleic Acids Res*. 32, D311-4.
- Cruz, F., Villalba, M., Garcia-Espinosa, M. A., Ballesteros, P., Bogonez, E., Satrustegui, J., Cerdan, S., 2001. Intracellular compartmentation of pyruvate in primary cultures of cortical neurons as detected by (13)C NMR spectroscopy with multiple (13)C labels. *J Neurosci Res*. 66, 771-81.
- Cybulski, R. L., Fisher, R. R., 1977. Mitochondrial neutral amino acid transport: evidence for a carrier mediated mechanism. *Biochemistry*. 16, 5116-20.

## [D]

- Da Cruz, S., Xenarios, I., Langridge, J., Vilbois, F., Parone, P. A., Martinou, J. C., 2003. Proteomic analysis of the mouse liver mitochondrial inner membrane. *J Biol Chem*. 278, 41566-71.
- de Forges, H., Bouissou, A., Perez, F., 2012. Interplay between microtubule dynamics and intracellular organization. *Int J Biochem Cell Biol*. 44, 266-74.
- de Oliveira Dal'Molin, C. G., Nielsen, L. K., 2013. Plant genome-scale metabolic reconstruction and modelling. *Curr Opin Biotechnol*. 24, 271-7.
- De Palma, A., Prezioso, G., Scalera, V., 2005. Kinetic evidence for the uniport mechanism hypothesis in the mitochondrial tricarboxylate transport system. *J Bioenerg Biomembr*. 37, 279-87.
- Dean, J., Reddy, P., 2013. Metabolic analysis of antibody producing CHO cells in fed-batch production. *Biotechnol Bioeng*. 110, 1735-47.

- DeBerardinis, R. J., Thompson, C. B., 2012. Cellular metabolism and disease: what do metabolic outliers teach us? *Cell*. 148, 1132-44.
- del Arco, A., Satrustegui, J., 2004. Identification of a novel human subfamily of mitochondrial carriers with calcium-binding domains. *J Biol Chem*. 279, 24701-13.
- Deshpande, R., Yang, T. H., Heinzle, E., 2009. Towards a metabolic and isotopic steady state in CHO batch cultures for reliable isotope-based metabolic profiling. *Biotechnol J*. 4, 247-63.
- Deshpande, R. R., *Mammalian Cell Culture: High Throughput Applications of Oxygen Sensor Plates and Cellular Physiological Studies Using <sup>13</sup>C-Labeling* Universität des Saarlandes, Saarbrücken, 2008.
- Di Noia, M. A., Todisco, S., Cirigliano, A., Rinaldi, T., Agrimi, G., Iacobazzi, V., Palmieri, F., 2014. The human SLC25A33 and SLC25A36 genes of solute carrier family 25 encode two mitochondrial pyrimidine nucleotide transporters. *J Biol Chem*. 289, 33137-48.
- Dietmair, S., Nielsen, L. K., Timmins, N. E., 2012. Mammalian cells as biopharmaceutical production hosts in the age of omics. *Biotechnol J*. 7, 75-89.
- Dietmair, S., Timmins, N. E., Gray, P. P., Nielsen, L. K., Kromer, J. O., 2010. Towards quantitative metabolomics of mammalian cells: development of a metabolite extraction protocol. *Anal Biochem*. 404, 155-64.
- Dolce, V., Fiermonte, G., Messina, A., Palmieri, F., 1991. Nucleotide sequence of a human heart cDNA encoding the mitochondrial phosphate carrier. *DNA Seq*. 2, 133-5.
- Du, J., Cleghorn, W. M., Contreras, L., Lindsay, K., Rountree, A. M., Chertov, A. O., Turner, S. J., Sahaboglu, A., Linton, J., Sadilek, M., Satrustegui, J., Sweet, I. R., Paquet-Durand, F., Hurley, J. B., 2013. Inhibition of mitochondrial pyruvate transport by zaprinast causes massive accumulation of aspartate at the expense of glutamate in the retina. *J Biol Chem*. 288, 36129-40.
- Duarte, T. M., Carinhas, N., Barreiro, L. C., Carrondo, M. J., Alves, P. M., Teixeira, A. P., 2014. Metabolic responses of CHO cells to limitation of key amino acids. *Biotechnol Bioeng*. 111, 2095-106.
- Duchen, M. R., 2004. Roles of mitochondria in health and disease. *Diabetes*. 53 Suppl 1, S96-102.

## [E]

- Eissing, T., Kuepfer, L., Becker, C., Block, M., Coboeken, K., Gaub, T., Goerlitz, L., Jaeger, J., Loosen, R., Ludewig, B., Meyer, M., Niederalt, C., Sevestre, M., Siegmund, H. U., Solodenko, J., Thelen, K., Telle, U., Weiss, W., Wendl, T., Willmann, S., Lippert, J., 2011. A computational systems biology software platform for multiscale modeling and simulation: integrating whole-body physiology, disease biology, and molecular reaction networks. *Front Physiol*. 2, 4.
- Else, P. L., Hulbert, A. J., 1985. An allometric comparison of the mitochondria of mammalian and reptilian tissues: the implications for the evolution of endothermy. *J Comp Physiol B*. 156, 3-11.

## [F]

- Fan, L., I. Kadura, et al. 2012. Improving the efficiency of CHO cell line generation using glutamine synthetase gene knockout cells. *Biotechnol Bioeng* 109(4): 1007-1015.
- Fang, J., Hsu, B. Y., MacMullen, C. M., Poncz, M., Smith, T. J., Stanley, C. A., 2002. Expression, purification and characterization of human glutamate dehydrogenase (GDH) allosteric regulatory mutations. *Biochem J*. 363, 81-7.
- Fiermonte, G., De Leonadis, F., Todisco, S., Palmieri, L., Lasorsa, F. M., Palmieri, F., 2004. Identification of the mitochondrial ATP-Mg/Pi transporter. Bacterial expression, reconstitution, functional characterization, and tissue distribution. *J Biol Chem*. 279, 30722-30.

- Fiermonte, G., Dolce, V., Arrigoni, R., Runswick, M. J., Walker, J. E., Palmieri, F., 1999. Organization and sequence of the gene for the human mitochondrial dicarboxylate carrier: evolution of the carrier family. *Biochem J.* 344 Pt 3, 953-60.
- Fiermonte, G., Dolce, V., David, L., Santorelli, F. M., Dionisi-Vici, C., Palmieri, F., Walker, J. E., 2003. The mitochondrial ornithine transporter. Bacterial expression, reconstitution, functional characterization, and tissue distribution of two human isoforms. *J Biol Chem.* 278, 32778-83.
- Fiermonte, G., Dolce, V., Palmieri, L., Ventura, M., Runswick, M. J., Palmieri, F., Walker, J. E., 2001. Identification of the human mitochondrial oxodicarboxylate carrier. Bacterial expression, reconstitution, functional characterization, tissue distribution, and chromosomal location. *J Biol Chem.* 276, 8225-30.
- Fiermonte, G., Palmieri, L., Dolce, V., Lasorsa, F. M., Palmieri, F., Runswick, M. J., Walker, J. E., 1998. The sequence, bacterial expression, and functional reconstitution of the rat mitochondrial dicarboxylate transporter cloned via distant homologs in yeast and *Caenorhabditis elegans*. *J Biol Chem.* 273, 24754-9.
- Fiermonte, G., Palmieri, L., Todisco, S., Agrimi, G., Palmieri, F., Walker, J. E., 2002. Identification of the mitochondrial glutamate transporter. Bacterial expression, reconstitution, functional characterization, and tissue distribution of two human isoforms. *J Biol Chem.* 277, 19289-94.
- Flamholz, A., Phillips, R., Milo, R., 2014. The quantified cell. *Mol Biol Cell.* 25, 3497-500.
- Follstad, B. D., Stephanopoulos, G., 1998. Effect of reversible reactions on isotope label redistribution--analysis of the pentose phosphate pathway. *European Journal of Biochemistry.* 252, 360-71.
- Forth, T., McConkey, G. A., Westhead, D. R., 2010. MetNetMaker: a free and open-source tool for the creation of novel metabolic networks in SBML format. *Bioinformatics.* 26, 2352-3.
- Frezza, C., Cipolat, S., Scorrano, L., 2007. Organelle isolation: functional mitochondria from mouse liver, muscle and cultured fibroblasts. *Nat Protoc.* 2, 287-95.
- Friedman, J. R., Nunnari, J., 2014. Mitochondrial form and function. *Nature.* 505, 335-43.
- Frommer, W. B., Davidson, M. W., Campbell, R. E., 2009. Genetically encoded biosensors based on engineered fluorescent proteins. *Chem Soc Rev.* 38, 2833-41.

[G]

- Gandhi, V. V., Samuels, D. C., 2011. A review comparing deoxyribonucleoside triphosphate (dNTP) concentrations in the mitochondrial and cytoplasmic compartments of normal and transformed cells. *Nucleosides Nucleotides Nucleic Acids.* 30, 317-39.
- Garcia, C. K., Goldstein, J. L., Pathak, R. K., Anderson, R. G., Brown, M. S., 1994. Molecular characterization of a membrane transporter for lactate, pyruvate, and other monocarboxylates: implications for the Cori cycle. *Cell.* 76, 865-73.
- Ghorbaniaghdam, A., Henry, O., Jolicoeur, M., 2013. A kinetic-metabolic model based on cell energetic state: study of CHO cell behavior under Na-butyrate stimulation. *Bioprocess Biosyst Eng.* 36, 469-87.
- Gladden, L. B., 2004. Lactate metabolism: a new paradigm for the third millennium. *J Physiol.* 558, 5-30.
- Gnoni, G. V., Priore, P., Geelen, M. J., Siculella, L., 2009. The mitochondrial citrate carrier: metabolic role and regulation of its activity and expression. *IUBMB Life.* 61, 987-94.
- Goudar, C., Biener, R., Boisart, C., Heidemann, R., Piret, J., de Graaf, A., Konstantinov, K., 2010. Metabolic flux analysis of CHO cells in perfusion culture by metabolite balancing and 2D [<sup>13</sup>C, <sup>1</sup>H] COSY NMR spectroscopy. *Metab Eng.* 12, 138-49.

- Gruetter, R., 2002. In vivo  $^{13}\text{C}$  NMR studies of compartmentalized cerebral carbohydrate metabolism. *Neurochem Int.* 41, 143-54.
- Gutierrez-Aguilar, M., Baines, C. P., 2013. Physiological and pathological roles of mitochondrial SLC25 carriers. *Biochem J.* 454, 371-86.

## [H]

- Hackl, M., Jakobi, T., Blom, J., Doppmeier, D., Brinkrolf, K., Szczepanowski, R., Bernhart, S. H., Honer Zu Siederdisen, C., Bort, J. A., Wieser, M., Kunert, R., Jeffs, S., Hofacker, I. L., Goesmann, A., Puhler, A., Borth, N., Grillari, J., 2011. Next-generation sequencing of the Chinese hamster ovary microRNA transcriptome: Identification, annotation and profiling of microRNAs as targets for cellular engineering. *J Biotechnol.* 153, 62-75.
- Halestrap, A. P., Price, N. T., 1999. The proton-linked monocarboxylate transporter (MCT) family: structure, function and regulation. *Biochem J.* 343 Pt 2, 281-99.
- Hamel, P., Saint-Georges, Y., de Pinto, B., Lachacinski, N., Altamura, N., Dujardin, G., 2004. Redundancy in the function of mitochondrial phosphate transport in *Saccharomyces cerevisiae* and *Arabidopsis thaliana*. *Mol Microbiol.* 51, 307-17.
- Hammond, S., Kaplarevic, M., Borth, N., Betenbaugh, M. J., Lee, K. H., 2012. Chinese hamster genome database: an online resource for the CHO community at [www.CHOgenome.org](http://www.CHOgenome.org). *Biotechnol Bioeng.* 109, 1353-6.
- Han, S. P., 1977. Globally Convergent Method for Nonlinear-Programming. *J Optimiz Theory App.* 22, 297-309.
- Hans, M., Metabolische Charakterisierung von Hefen. Quantifizierung intrazellulärer Metabolite sowie metabolischer Stoffflüsse in *Saccharomyces cerevisiae* und *Kluyveromyces marxianus*. Naturwissenschaftlich-Technischen Fakultät III, Vol. Doktor der Naturwissenschaften. Universität des Saarlandes, Saarbrücken, 2003.
- Hansen, H. A., Emborg, C., 1994. Extra- and intracellular amino acid concentrations in continuous Chinese hamster ovary cell culture. *Appl Microbiol Biotechnol.* 41, 560-4.
- Hashimoto, T., Brooks, G. A., 2008. Mitochondrial lactate oxidation complex and an adaptive role for lactate production. *Med Sci Sports Exerc.* 40, 486-94.
- Hashimoto, T., Hussien, R., Brooks, G. A., 2006. Colocalization of MCT1, CD147, and LDH in mitochondrial inner membrane of L6 muscle cells: evidence of a mitochondrial lactate oxidation complex. *Am J Physiol Endocrinol Metab.* 290, E1237-44.
- Hashimoto, T., Hussien, R., Cho, H. S., Kaufer, D., Brooks, G. A., 2008. Evidence for the mitochondrial lactate oxidation complex in rat neurons: demonstration of an essential component of brain lactate shuttles. *PLoS One.* 3, e2915.
- Hassanein, M., Hoeksema, M. D., Shiota, M., Qian, J., Harris, B. K., Chen, H., Clark, J. E., Alborn, W. E., Eisenberg, R., Massion, P. P., 2013. SLC1A5 mediates glutamine transport required for lung cancer cell growth and survival. *Clin Cancer Res.* 19, 560-70.
- Hatefi, Y., Galante, Y. M., 1977. Dehydrogenase and transhydrogenase properties of the soluble NADH dehydrogenase of bovine heart mitochondria. *Proc Natl Acad Sci U S A.* 74, 846-50.
- Hayduk, E. J., Choe, L. H., Lee, K. H., 2004. A two-dimensional electrophoresis map of Chinese hamster ovary cell proteins based on fluorescence staining. *Electrophoresis.* 25, 2545-56.
- Hayward, B. E., Hussain, A., Wilson, R. H., Lyons, A., Woodcock, V., McIntosh, B., Harris, T. J., 1986. The cloning and nucleotide sequence of cDNA for an amplified glutamine synthetase gene from the Chinese hamster. *Nucleic Acids Res.* 14, 999-1008.



- 
- Henry, C. S., Broadbelt, L. J., Hatzimanikatis, V., 2007. Thermodynamics-based metabolic flux analysis. *Biophys J.* 92, 1792-805.
- Henry, O., Jolicoeur, M., Kamen, A., 2011. Unraveling the metabolism of HEK-293 cells using lactate isotopomer analysis. *Bioprocess Biosyst Eng.* 34, 263-73.
- Herzig, S., Raemy, E., Montessuit, S., Veuthey, J. L., Zamboni, N., Westermann, B., Kunji, E. R., Martinou, J. C., 2012. Identification and functional expression of the mitochondrial pyruvate carrier. *Science.* 337, 93-6.
- Hildyard, J. C., Halestrap, A. P., 2003. Identification of the mitochondrial pyruvate carrier in *Saccharomyces cerevisiae*. *Biochem J.* 374, 607-11.
- Hinkle, P. C., 2005. P/O ratios of mitochondrial oxidative phosphorylation. *Biochim Biophys Acta.* 1706, 1-11.
- Hofmann, U., Maier, K., Niebel, A., Vacun, G., Reuss, M., Mauch, K., 2008. Identification of metabolic fluxes in hepatic cells from transient  $^{13}\text{C}$ -labeling experiments: Part I. Experimental observations. *Biotechnol Bioeng.* 100, 344-54.
- Holthuis, J. C., Ungermann, C., 2013. Cellular microcompartments constitute general suborganellar functional units in cells. *Biol Chem.* 394, 151-61.
- Horst, M., Knecht, E. C., Schu, P. V., 1999. Import into and degradation of cytosolic proteins by isolated yeast vacuoles. *Mol Biol Cell.* 10, 2879-89.
- Houldsworth, J., Attardi, G., 1988. Two distinct genes for ADP/ATP translocase are expressed at the mRNA level in adult human liver. *Proc Natl Acad Sci U S A.* 85, 377-81.
- Huizing, M., Iacobazzi, V., Ijlst, L., Savelkoul, P., Ruitenbeek, W., van den Heuvel, L., Indiveri, C., Smeitink, J., Trijbels, F., Wanders, R., Palmieri, F., 1997. Cloning of the human carnitine-acylcarnitine carrier cDNA and identification of the molecular defect in a patient. *Am J Hum Genet.* 61, 1239-45.
- Hussien, R., Brooks, G. A., 2011. Mitochondrial and plasma membrane lactate transporter and lactate dehydrogenase isoform expression in breast cancer cell lines. *Physiological Genomics.* 43, 255-64.

## [I]

- Iacobazzi, V., Palmieri, F., Runswick, M. J., Walker, J. E., 1992. Sequences of the human and bovine genes for the mitochondrial 2-oxoglutarate carrier. *DNA Seq.* 3, 79-88.
- Indiveri, C., Abruzzo, G., Stipani, I., Palmieri, F., 1998. Identification and purification of the reconstitutively active glutamine carrier from rat kidney mitochondria. *Biochem J.* 333 ( Pt 2), 285-90.
- Israel, M., Schwartz, L., 2011. The metabolic advantage of tumor cells. *Mol Cancer.* 10, 70.

## [J]

- Jandt, U., You, C., Zhang, Y. H., Zeng, A. P., 2013. Compartmentalization and metabolic channeling for multienzymatic biosynthesis: practical strategies and modeling approaches. *Adv Biochem Eng Biotechnol.* 137, 41-65.
- Jastroch, M., Divakaruni, A. S., Mookerjee, S., Treberg, J. R., Brand, M. D., 2010. Mitochondrial proton and electron leaks. *Essays Biochem.* 47, 53-67.
- Jayapal, K. P., Wlaschin, K. F., Hu, W.-S., Yap, M. G. S., 2007. Recombinant Protein Therapeutics from CHO Cells - 20 Years and Counting. *Chemical Engineering Progress.* 103, 40-47
- Jitrapakdee, S., Wallace, J. C., 1999. Structure, function and regulation of pyruvate carboxylase. *Biochem J.* 340 ( Pt 1), 1-16.
-

- Jorda, J., Rojas, H. C., Carnicer, M., Wahl, A., Ferrer, P., Albiol, J., 2014. Quantitative Metabolomics and Instationary  $^{13}\text{C}$ -Metabolic Flux Analysis Reveals Impact of Recombinant Protein Production on Trehalose and Energy Metabolism in *Pichia pastoris*. *Metabolites*. 4, 281-99.
- Jorda, J., Suarez, C., Carnicer, M., ten Pierick, A., Heijnen, J. J., van Gulik, W., Ferrer, P., Albiol, J., Wahl, A., 2013. Glucose-methanol co-utilization in *Pichia pastoris* studied by metabolomics and instationary (1)(3)C flux analysis. *BMC Syst Biol*. 7, 17.
- [K]
- Kaas, C. S., Fan, Y., Weilguny, D., Kristensen, C., Kildegaard, H. F., Andersen, M. R., 2014. Toward genome-scale models of the Chinese hamster ovary cells: incentives, status and perspectives. *Pharmaceutical Bioprocessing*. 2, 437-448.
- Kajihata, S., Furusawa, C., Matsuda, F., Shimizu, H., 2014. OpenMebius: an open source software for isotopically nonstationary  $^{13}\text{C}$ -based metabolic flux analysis. *Biomed Res Int*. 2014, 627014.
- Kaletka, C., de Figueiredo, L. F., Schuster, S., 2009. Can the whole be less than the sum of its parts? Pathway analysis in genome-scale metabolic networks using elementary flux patterns. *Genome Res*. 19, 1872-83.
- Kanehisa, M., Goto, S., Sato, Y., Kawashima, M., Furumichi, M., Tanabe, M., 2014. Data, information, knowledge and principle: back to metabolism in KEGG. *Nucleic Acids Res*. 42, D199-205.
- Kang, J., Samuels, D. C., 2008. The evidence that the DNC (SLC25A19) is not the mitochondrial deoxyribonucleotide carrier. *Mitochondrion*. 8, 103-8.
- Kantardjieff, A., Nissom, P. M., Chuah, S. H., Yusufi, F., Jacob, N. M., Mulukutla, B. C., Yap, M., Hu, W. S., 2009. Developing genomic platforms for Chinese hamster ovary cells. *Biotechnol Adv*. 27, 1028-35.
- Kaplan, R. S., Mayor, J. A., Gremse, D. A., Wood, D. O., 1995. High level expression and characterization of the mitochondrial citrate transport protein from the yeast *Saccharomyces cerevisiae*. *J Biol Chem*. 270, 4108-14.
- Karp, P. D., Paley, S. M., Krummenacker, M., Latendresse, M., Dale, J. M., Lee, T. J., Kaipa, P., Gilham, F., Spaulding, A., Popescu, L., Altman, T., Paulsen, I., Keseler, I. M., Caspi, R., 2010. Pathway Tools version 13.0: integrated software for pathway/genome informatics and systems biology. *Brief Bioinform*. 11, 40-79.
- Keech, D. B., Utter, M. F., 1963. Pyruvate Carboxylase. II. Properties. *J Biol Chem*. 238, 2609-14.
- Kell, D. B., 2006. Systems biology, metabolic modelling and metabolomics in drug discovery and development. *Drug Discov Today*. 11, 1085-92.
- Kelley, K. M., Hamann, J. J., Navarre, C., Gladden, L. B., 2002. Lactate metabolism in resting and contracting canine skeletal muscle with elevated lactate concentration. *J Appl Physiol* (1985). 93, 865-72.
- Kildegaard, H. F., Baycin-Hizal, D., Lewis, N. E., Betenbaugh, M. J., 2013. The emerging CHO systems biology era: harnessing the 'omics revolution for biotechnology. *Curr Opin Biotechnol*. 24, 1102-7.
- Kim, J. Y., Kim, Y. G., Lee, G. M., 2012. CHO cells in biotechnology for production of recombinant proteins: current state and further potential. *Appl Microbiol Biotechnol*. 93, 917-30.
- Klein, T., Niklas, J., Heinzle, E., 2015. Engineering the supply chain for protein production/secretion in yeasts and mammalian cells. *J Ind Microbiol Biotechnol*.
- Kline, E. S., Brandt, R. B., Laux, J. E., Spainhour, S. E., Higgins, E. S., Rogers, K. S., Tinsley, S. B., Waters, M. G., 1986. Localization of L-lactate dehydrogenase in mitochondria. *Arch Biochem Biophys*. 246, 673-80.
- Kobayashi, K., Saheki, T., Song, Y. Z., 1993. Citrin Deficiency.

- 
- Kroemer, G., Galluzzi, L., Brenner, C., 2007. Mitochondrial membrane permeabilization in cell death. *Physiol Rev.* 87, 99-163.
- Kuan, J., Saier, M. H., Jr., 1993. The mitochondrial carrier family of transport proteins: structural, functional, and evolutionary relationships. *Crit Rev Biochem Mol Biol.* 28, 209-33.
- Kuznetsov, A. V., Veksler, V., Gellerich, F. N., Saks, V., Margreiter, R., Kunz, W. S., 2008. Analysis of mitochondrial function in situ in permeabilized muscle fibers, tissues and cells. *Nat Protoc.* 3, 965-76.
- Kyoto Daigaku. Kagaku Kenkyūjo. Seitai Johogaku., KEGG, Kyoto encyclopedia of genes and genomes. The Center, Kyoto, 2001.
- [L]
- Lane, M., Gardner, D. K., 2005. Mitochondrial malate-aspartate shuttle regulates mouse embryo nutrient consumption. *J Biol Chem.* 280, 18361-7.
- Lawson, J. E., Douglas, M. G., 1988. Separate genes encode functionally equivalent ADP/ATP carrier proteins in *Saccharomyces cerevisiae*. Isolation and analysis of AAC2. *J Biol Chem.* 263, 14812-8.
- Lee, H. W., Christie, A., Starkey, J. A., Read, E. K., Yoon, S., 2015. Intracellular metabolic flux analysis of CHO cells supplemented with wheat hydrolysates for improved mAb production and cell-growth. *J Chem Technol Biot.* 90, 291-302.
- Lee, S. M., Koh, H. J., Park, D. C., Song, B. J., Huh, T. L., Park, J. W., 2002. Cytosolic NADP(+)-dependent isocitrate dehydrogenase status modulates oxidative damage to cells. *Free Radic Biol Med.* 32, 1185-96.
- Leighty, R. W., Antoniewicz, M. R., 2011. Dynamic metabolic flux analysis (DMFA): a framework for determining fluxes at metabolic non-steady state. *Metab Eng.* 13, 745-55.
- Lemasters, J. J., 2007. Modulation of mitochondrial membrane permeability in pathogenesis, autophagy and control of metabolism. *J Gastroenterol Hepatol.* 22 Suppl 1, S31-7.
- Lemire, J., Mailloux, R. J., Appanna, V. D., 2008. Mitochondrial lactate dehydrogenase is involved in oxidative-energy metabolism in human astrocytoma cells (CCF-STTG1). *PLoS One.* 3, e1550.
- Lequeux, G., Beauprez, J., Maertens, J., Van Horen, E., Soetaert, W., Vandamme, E., Vanrolleghem, P. A., 2010. Dynamic metabolic flux analysis demonstrated on cultures where the limiting substrate is changed from carbon to nitrogen and vice versa. *J Biomed Biotechnol.* 2010.
- Lewis, C. A., Parker, S. J., Fiske, B. P., McCloskey, D., Gui, D. Y., Green, C. R., Vokes, N. I., Feist, A. M., Vander Heiden, M. G., Metallo, C. M., 2014. Tracing compartmentalized NADPH metabolism in the cytosol and mitochondria of mammalian cells. *Mol Cell.* 55, 253-63.
- Lewis, N. E., Liu, X., Li, Y., Nagarajan, H., Yerganian, G., O'Brien, E., Bordbar, A., Roth, A. M., Rosenbloom, J., Bian, C., Xie, M., Chen, W., Li, N., Baycin-Hizal, D., Latif, H., Forster, J., Betenbaugh, M. J., Famili, I., Xu, X., Wang, J., Palsson, B. O., 2013. Genomic landscapes of Chinese hamster ovary cell lines as revealed by the *Cricetulus griseus* draft genome. *Nat Biotechnol.* 31, 759-65.
- Liu, L. a., Systems biology of recombinant protein production by fungi.
- Locasale, J. W., Cantley, L. C., 2011. Metabolic flux and the regulation of mammalian cell growth. *Cell Metab.* 14, 443-51.
- Lu, D., Mulder, H., Zhao, P., Burgess, S. C., Jensen, M. V., Kamzolova, S., Newgard, C. B., Sherry, A. D., 2002. <sup>13</sup>C NMR isotopomer analysis reveals a connection between pyruvate cycling and glucose-stimulated insulin secretion (GSIS). *Proc Natl Acad Sci U S A.* 99, 2708-13.
- Lu, S., Sun, X., Zhang, Y., 2005. Insight into metabolism of CHO cells at low glucose concentration on the basis of the determination of intracellular metabolites. *Process Biochemistry.* 40, 1917-1921.
-

---

Lucas, M., Laplace, L., Bennett, M. J., 2011. Plant systems biology: network matters. *Plant Cell Environ.* 34, 535-53.

[M]

Ma, F., Jazmin, L. J., Young, J. D., Allen, D. K., 2014. Isotopically nonstationary  $^{13}\text{C}$  flux analysis of changes in *Arabidopsis thaliana* leaf metabolism due to high light acclimation. *Proc Natl Acad Sci U S A.* 111, 16967-72.

Madden, E. A., Storrie, B., 1987. The preparative isolation of mitochondria from Chinese hamster ovary cells. *Anal Biochem.* 163, 350-7.

Madeira, V. M., 2012. Overview of mitochondrial bioenergetics. *Methods Mol Biol.* 810, 1-6.

Maier, K., Hofmann, U., Reuss, M., Mauch, K., 2008. Identification of metabolic fluxes in hepatic cells from transient  $^{13}\text{C}$ -labeling experiments: Part II. Flux estimation. *Biotechnol Bioeng.* 100, 355-70.

Malaisse, W. J., Zhang, Y., Sener, A., 2004. Enzyme-to-enzyme channeling in the early steps of glycolysis in rat pancreatic islets. *Endocrine.* 24, 105-9.

Margineantu, D. H., Brown, R. M., Brown, G. K., Marcus, A. H., Capaldi, R. A., 2002. Heterogeneous distribution of pyruvate dehydrogenase in the matrix of mitochondria. *Mitochondrion.* 1, 327-38.

Marobbio, C. M., Agrimi, G., Lasorsa, F. M., Palmieri, F., 2003. Identification and functional reconstitution of yeast mitochondrial carrier for S-adenosylmethionine. *Embo J.* 22, 5975-82.

Marobbio, C. M., Di Noia, M. A., Palmieri, F., 2006. Identification of a mitochondrial transporter for pyrimidine nucleotides in *Saccharomyces cerevisiae*: bacterial expression, reconstitution and functional characterization. *Biochem J.* 393, 441-6.

Marobbio, C. M., Vozza, A., Harding, M., Bisaccia, F., Palmieri, F., Walker, J. E., 2002. Identification and reconstitution of the yeast mitochondrial transporter for thiamine pyrophosphate. *Embo J.* 21, 5653-61.

Martinez, V. S., Dietmair, S., Quek, L. E., Hodson, M. P., Gray, P., Nielsen, L. K., 2013. Flux balance analysis of CHO cells before and after a metabolic switch from lactate production to consumption. *Biotechnol Bioeng.* 110, 660-6.

Mazurek, S., Zwerschke, W., Jansen-Durr, P., Eigenbrodt, E., 2001. Metabolic cooperation between different oncogenes during cell transformation: interaction between activated ras and HPV-16 E7. *Oncogene.* 20, 6891-8.

McKenna, M. C., Tildon, J. T., Stevenson, J. H., Huang, X., Kingwell, K. G., 1995. Regulation of mitochondrial and cytosolic malic enzymes from cultured rat brain astrocytes. *Neurochem Res.* 20, 1491-501.

Metallo, C. M., Gameiro, P. A., Bell, E. L., Mattaini, K. R., Yang, J., Hiller, K., Jewell, C. M., Johnson, Z. R., Irvine, D. J., Guarente, L., Kelleher, J. K., Vander Heiden, M. G., Iliopoulos, O., Stephanopoulos, G., 2012. Reductive glutamine metabolism by IDH1 mediates lipogenesis under hypoxia. *Nature.* 481, 380-4.

Metallo, C. M., Walther, J. L., Stephanopoulos, G., 2009. Evaluation of  $^{13}\text{C}$  isotopic tracers for metabolic flux analysis in mammalian cells. *J Biotechnol.* 144, 167-74.

Michal, G., Schomburg, D., 2012. *Biochemical Pathways: An Atlas of Biochemistry and Molecular Biology.* John Wiley & Sons, Ltd., West Sussex, United Kingdom.

Millard, P., Sokol, S., Letisse, F., Portais, J. C., 2014. IsoDesign: a software for optimizing the design of  $^{13}\text{C}$ -metabolic flux analysis experiments. *Biotechnol Bioeng.* 111, 202-8.

Milne, G. L., Sanchez, S. C., Musiek, E. S., Morrow, J. D., 2007. Quantification of F2-isoprostanes as a biomarker of oxidative stress. *Nat Protoc.* 2, 221-6.

- Mizuarai, S., Miki, S., Araki, H., Takahashi, K., Kotani, H., 2005. Identification of dicarboxylate carrier SLC25a10 as malate transporter in de novo fatty acid synthesis. *J Biol Chem.* 280, 32434-41.
- Mo, M. L., Jamshidi, N., Palsson, B. O., 2007. A genome-scale, constraint-based approach to systems biology of human metabolism. *Mol Biosyst.* 3, 598-603.
- Mootha, V. K., Bunkenborg, J., Olsen, J. V., Hjerrild, M., Wisniewski, J. R., Stahl, E., Bolouri, M. S., Ray, H. N., Sihag, S., Kamal, M., Patterson, N., Lander, E. S., Mann, M., 2003. Integrated analysis of protein composition, tissue diversity, and gene regulation in mouse mitochondria. *Cell.* 115, 629-40.
- Moreno-Sanchez, R., Marin-Hernandez, A., Saavedra, E., Pardo, J. P., Ralph, S. J., Rodriguez-Enriquez, S., 2014. Who controls the ATP supply in cancer cells? Biochemistry lessons to understand cancer energy metabolism. *Int J Biochem Cell Biol.* 50, 10-23.
- Morris, M. E., Felmlee, M. A., 2008. Overview of the proton-coupled MCT (SLC16A) family of transporters: characterization, function and role in the transport of the drug of abuse gamma-hydroxybutyric acid. *AAPS J.* 10, 311-21.
- Mozo, J., Ferry, G., Studeny, A., Pecqueur, C., Rodriguez, M., Boutin, J. A., Bouillaud, F., 2006. Expression of UCP3 in CHO cells does not cause uncoupling, but controls mitochondrial activity in the presence of glucose. *Biochem J.* 393, 431-9.
- Mulukutla, B. C., Gramer, M., Hu, W. S., 2012. On metabolic shift to lactate consumption in fed-batch culture of mammalian cells. *Metab Eng.* 14, 138-49.
- Murphy, T. A., Dang, C. V., Young, J. D., 2013. Isotopically nonstationary  $^{13}\text{C}$  flux analysis of Myc-induced metabolic reprogramming in B-cells. *Metab Eng.* 15, 206-17.

[N]

- Narkewicz, M. R., Sauls, S. D., Tjoa, S. S., Teng, C., Fennessey, P. V., 1996. Evidence for intracellular partitioning of serine and glycine metabolism in Chinese hamster ovary cells. *Biochem J.* 313 ( Pt 3), 991-6.
- Nassir, F., Ibdah, J. A., 2014. Role of mitochondria in alcoholic liver disease. *World J Gastroenterol.* 20, 2136-42.
- Neuner, A., Heinzle, E., 2011. Mixed glucose and lactate uptake by *Corynebacterium glutamicum* through metabolic engineering. *Biotechnol J.* 6, 318-29.
- Nicolae, A., Wahrheit, J., Bahnemann, J., Zeng, A. P., Heinzle, E., 2014. Non-stationary  $^{13}\text{C}$  metabolic flux analysis of Chinese hamster ovary cells in batch culture using extracellular labeling highlights metabolic reversibility and compartmentation. *BMC Syst Biol.* 8, 50.
- Niklas, J., Heinzle, E., 2012. Metabolic flux analysis in systems biology of Mammalian cells. *Adv Biochem Eng Biotechnol.* 127, 109-32.
- Niklas, J., Melnyk, A., Yuan, Y., Heinzle, E., 2011a. Selective permeabilization for the high-throughput measurement of compartmented enzyme activities in mammalian cells. *Anal Biochem.* 416, 218-27.
- Niklas, J., Sandig, V., Heinzle, E., 2011b. Metabolite channeling and compartmentation in the human cell line AGE1.HN determined by  $^{13}\text{C}$  labeling experiments and  $^{13}\text{C}$  metabolic flux analysis. *J Biosci Bioeng.* 112, 616-23.
- Niklas, J., Schrader, E., Sandig, V., Noll, T., Heinzle, E., 2011c. Quantitative characterization of metabolism and metabolic shifts during growth of the new human cell line AGE1.HN using time resolved metabolic flux analysis. *Bioprocess Biosyst Eng.*
- Noack, S., Noh, K., Moch, M., Oldiges, M., Wiechert, W., 2010. Stationary versus non-stationary ( $^{13}\text{C}$ )-MFA: A comparison using a consistent dataset. *J Biotechnol.*

- 
- Noh, K., Droste, P., Wiechert, W., 2015. Visual workflows for  $^{13}\text{C}$ -metabolic flux analysis. *Bioinformatics*. 31, 346-54.
- Noh, K., Gronke, K., Luo, B., Takors, R., Oldiges, M., Wiechert, W., 2007. Metabolic flux analysis at ultra short time scale: isotopically non-stationary  $^{13}\text{C}$  labeling experiments. *J Biotechnol*. 129, 249-67.
- Noh, K., Wahl, A., Wiechert, W., 2006. Computational tools for isotopically instationary  $^{13}\text{C}$  labeling experiments under metabolic steady state conditions. *Metab Eng*. 8, 554-77.
- Noh, K., Wiechert, W., 2006. Experimental design principles for isotopically instationary  $^{13}\text{C}$  labeling experiments. *Biotechnol Bioeng*. 94, 234-51.
- Noh, K., Wiechert, W., 2011. The benefits of being transient: isotope-based metabolic flux analysis at the short time scale. *Appl Microbiol Biotechnol*. 91, 1247-65.
- Nolan, R. P., Lee, K., 2010. Dynamic model of CHO cell metabolism. *Metab Eng*. 13, 108-24.
- Nyberg, G. B., Balcarcel, R. R., Follstad, B. D., Stephanopoulos, G., Wang, D. I., 1999. Metabolism of peptide amino acids by Chinese hamster ovary cells grown in a complex medium. *Biotechnol Bioeng*. 62, 324-35.

## [O]

- O'Donnell-Tormey, J., Nathan, C. F., Lanks, K., DeBoer, C. J., de la Harpe, J., 1987. Secretion of pyruvate. An antioxidant defense of mammalian cells. *J Exp Med*. 165, 500-14.
- Orman, M. A., Arai, K., Yarmush, M. L., Androulakis, I. P., Berthiaume, F., Ierapetritou, M. G., 2010. Metabolic flux determination in perfused livers by mass balance analysis: effect of fasting. *Biotechnol Bioeng*. 107, 825-35.
- Orman, M. A., Berthiaume, F., Androulakis, I. P., Ierapetritou, M. G., 2011. Advanced stoichiometric analysis of metabolic networks of mammalian systems. *Crit Rev Biomed Eng*. 39, 511-34.

## [P]

- Pagliarini, D. J., Calvo, S. E., Chang, B., Sheth, S. A., Vafai, S. B., Ong, S. E., Walford, G. A., Sugiana, C., Boneh, A., Chen, W. K., Hill, D. E., Vidal, M., Evans, J. G., Thorburn, D. R., Carr, S. A., Mootha, V. K., 2008. A mitochondrial protein compendium elucidates complex I disease biology. *Cell*. 134, 112-23.
- Palmieri, F., 2008. Diseases caused by defects of mitochondrial carriers: a review. *Biochim Biophys Acta*. 1777, 564-78.
- Palmieri, F., 2013. The mitochondrial transporter family SLC25: identification, properties and physiopathology. *Mol Aspects Med*. 34, 465-84.
- Palmieri, L., Agrimi, G., Runswick, M. J., Fearnley, I. M., Palmieri, F., Walker, J. E., 2001. Identification in *Saccharomyces cerevisiae* of two isoforms of a novel mitochondrial transporter for 2-oxoadipate and 2-oxoglutarate. *J Biol Chem*. 276, 1916-22.
- Palmieri, L., Lasorsa, F. M., De Palma, A., Palmieri, F., Runswick, M. J., Walker, J. E., 1997. Identification of the yeast ACR1 gene product as a succinate-fumarate transporter essential for growth on ethanol or acetate. *FEBS Lett*. 417, 114-8.
- Palmieri, L., Lasorsa, F. M., Voza, A., Agrimi, G., Fiermonte, G., Runswick, M. J., Walker, J. E., Palmieri, F., 2000. Identification and functions of new transporters in yeast mitochondria. *Biochim Biophys Acta*. 1459, 363-9.

- Palmieri, L., Vozza, A., Agrimi, G., De Marco, V., Runswick, M. J., Palmieri, F., Walker, J. E., 1999. Identification of the yeast mitochondrial transporter for oxaloacetate and sulfate. *J Biol Chem.* 274, 22184-90.
- Pannone, E., Fiermonte, G., Dolce, V., Rocchi, M., Palmieri, F., 1998. Assignment of the human dicarboxylate carrier gene (DIC) to chromosome 17 band 17q25.3. *Cytogenet Cell Genet.* 83, 238-9.
- Papin, J. A., Stelling, J., Price, N. D., Klamt, S., Schuster, S., Palsson, B. O., 2004. Comparison of network-based pathway analysis methods. *Trends Biotechnol.* 22, 400-5.
- Pecqueur, C., Bui, T., Gelly, C., Hauchard, J., Barbot, C., Bouillaud, F., Ricquier, D., Miroux, B., Thompson, C. B., 2008. Uncoupling protein-2 controls proliferation by promoting fatty acid oxidation and limiting glycolysis-derived pyruvate utilization. *FASEB J.* 22, 9-18.
- Perez-Bercoff, A., McLysaght, A., Conant, G. C., 2011. Patterns of indirect protein interactions suggest a spatial organization to metabolism. *Mol Biosyst.* 7, 3056-64.
- Peuhkurinen, K. J., Hiltunen, J. K., Hassinen, I. E., 1983. Metabolic compartmentation of pyruvate in the isolated perfused rat heart. *Biochem J.* 210, 193-8.
- Phelps, A., Schobert, C. T., Wohlrab, H., 1991. Cloning and characterization of the mitochondrial phosphate transport protein gene from the yeast *Saccharomyces cerevisiae*. *Biochemistry.* 30, 248-52.
- Philp, A., Macdonald, A. L., Watt, P. W., 2005. Lactate--a signal coordinating cell and systemic function. *J Exp Biol.* 208, 4561-75.
- Porcelli, V., Fiermonte, G., Longo, A., Palmieri, F., 2014. The Human Gene SLC25A29, of Solute Carrier Family 25, Encodes a Mitochondrial Transporter of Basic Amino Acids. *J Biol Chem.* 289, 13374-84.
- Prohl, C., Pelzer, W., Diekert, K., Kmita, H., Bedekovics, T., Kispal, G., Lill, R., 2001. The yeast mitochondrial carrier Leu5p and its human homologue Graves' disease protein are required for accumulation of coenzyme A in the matrix. *Mol Cell Biol.* 21, 1089-97.
- Provost, A., Bastin, G., Agathos, S. N., Schneider, Y. J., 2006. Metabolic design of macroscopic bioreaction models: application to Chinese hamster ovary cells. *Bioprocess Biosyst Eng.* 29, 349-66.
- Pruitt, K. D., Katz, K. S., Sicotte, H., Maglott, D. R., 2000. Introducing RefSeq and LocusLink: curated human genome resources at the NCBI. *Trends Genet.* 16, 44-7.
- Puck, T. T., 1985. Development of the chinese hamster ovary (CHO) cell for use in somatic cell genetics, ed. Gottesman MM, John Wiley & Sons, 37-64. In: Gottesman, M. M., (Ed.), *Molecular Cell Genetics*. John Wiley & Sons, New York, pp. 37-64.

## [Q]

- Quek, L. E., Dietmair, S., Kromer, J. O., Nielsen, L. K., 2009a. Metabolic flux analysis in mammalian cell culture. *Metab Eng.* 12, 161-71.
- Quek, L. E., Wittmann, C., Nielsen, L. K., Kromer, J. O., 2009b. OpenFLUX: efficient modelling software for <sup>13</sup>C-based metabolic flux analysis. *Microb Cell Fact.* 8, 25.

## [R]

- Raimundo, N., Baysal, B. E., Shadel, G. S., 2011. Revisiting the TCA cycle: signaling to tumor formation. *Trends Mol Med.* 17, 641-9.
- Ray, L. B., 2010. Metabolism Is Not Boring INTRODUCTION. *Science.* 330, 1337-1337.
- Ross, D. W., Mel, H. C., 1972. Growth dynamics of mitochondria in synchronized Chinese hamster cells. *Biophys J.* 12, 1562-72.

---

[S]

- Sagrista, M. L., Bozal, J., 1987. Lactate and malate dehydrogenase binding to the microsomal fraction from chicken liver. *Biochimie*. 69, 1207-15.
- Sanchis, D., Fleury, C., Chomiki, N., Goubern, M., Huang, Q., Neverova, M., Gregoire, F., Easlick, J., Raimbault, S., Levi-Meyrueis, C., Miroux, B., Collins, S., Seldin, M., Richard, D., Warden, C., Bouillaud, F., Ricquier, D., 1998. BMCP1, a novel mitochondrial carrier with high expression in the central nervous system of humans and rodents, and respiration uncoupling activity in recombinant yeast. *J Biol Chem*. 273, 34611-5.
- Sauer, U., Heinemann, M., Zamboni, N., 2007. Genetics. Getting closer to the whole picture. *Science*. 316, 550-1.
- Sazanov, L. A., Jackson, J. B., 1994. Proton-translocating transhydrogenase and NAD- and NADP-linked isocitrate dehydrogenases operate in a substrate cycle which contributes to fine regulation of the tricarboxylic acid cycle activity in mitochondria. *FEBS Lett*. 344, 109-16.
- Schafer, Z. T., Grassian, A. R., Song, L., Jiang, Z., Gerhart-Hines, Z., Irie, H. Y., Gao, S., Puigserver, P., Brugge, J. S., 2009. Antioxidant and oncogene rescue of metabolic defects caused by loss of matrix attachment. *Nature*. 461, 109-13.
- Schell, J. C., Rutter, J., 2013. The long and winding road to the mitochondrial pyruvate carrier. *Cancer Metab*. 1, 6.
- Schellenberger, J., Que, R., Fleming, R. M., Thiele, I., Orth, J. D., Feist, A. M., Zielinski, D. C., Bordbar, A., Lewis, N. E., Rahmanian, S., Kang, J., Hyduke, D. R., Palsson, B. O., 2011. Quantitative prediction of cellular metabolism with constraint-based models: the COBRA Toolbox v2.0. *Nat Protoc*. 6, 1290-307.
- Schiff, D., Purow, B. W., 2009. Neuro-oncology: Isocitrate dehydrogenase mutations in low-grade gliomas. *Nat Rev Neurol*. 5, 303-4.
- Schmidt, K., Carlsen, M., Nielsen, J., Villadsen, J., 1997. Modeling isotopomer distributions in biochemical networks using isotopomer mapping matrices. *Biotechnol Bioeng*. 55, 831-40.
- Schmidt, K., Nielsen, J., Villadsen, J., 1999. Quantitative analysis of metabolic fluxes in *Escherichia coli*, using two-dimensional NMR spectroscopy and complete isotopomer models. *J Biotechnol*. 71, 175-89.
- Schuster, S., Fell, D. A., Dandekar, T., 2000. A general definition of metabolic pathways useful for systematic organization and analysis of complex metabolic networks. *Nat Biotechnol*. 18, 326-32.
- Schwartz, J. M., Kanehisa, M., 2006. Quantitative elementary mode analysis of metabolic pathways: the example of yeast glycolysis. *BMC Bioinformatics*. 7, 186.
- Sellick, C. A., Croxford, A. S., Maqsood, A. R., Stephens, G., Westerhoff, H. V., Goodacre, R., Dickson, A. J., 2011a. Metabolite profiling of recombinant CHO cells: designing tailored feeding regimes that enhance recombinant antibody production. *Biotechnol Bioeng*. 108, 3025-31.
- Sellick, C. A., Hansen, R., Maqsood, A. R., Dunn, W. B., Stephens, G. M., Goodacre, R., Dickson, A. J., 2009. Effective quenching processes for physiologically valid metabolite profiling of suspension cultured Mammalian cells. *Anal Chem*. 81, 174-83.
- Sellick, C. A., Hansen, R., Stephens, G. M., Goodacre, R., Dickson, A. J., 2011b. Metabolite extraction from suspension-cultured mammalian cells for global metabolite profiling. *Nat. Protocols*. 6, 1241-1249.
- Sengupta, N., Rose, S. T., Morgan, J. A., 2010. Metabolic flux analysis of CHO cell metabolism in the late non-growth phase. *Biotechnol Bioeng*. 108, 82-92.
- Shampine, L. F., Reichelt, M. W., 1997. The MATLAB ODE suite. *Siam J Sci Comput*. 18, 1-22.



- Sheikholeslami, Z., Jolicoeur, M., Henry, O., 2013. Probing the metabolism of an inducible mammalian expression system using extracellular isotopomer analysis. *J Biotechnol.* 164, 469-78.
- Sheikholeslami, Z., Jolicoeur, M., Henry, O., 2014. Elucidating the effects of postinduction glutamine feeding on the growth and productivity of CHO cells. *Biotechnol Prog.* 30, 535-46.
- Sidorenko, Y., Wahl, A., Dauner, M., Genzel, Y., Reichl, U., 2008. Comparison of metabolic flux distributions for MDCK cell growth in glutamine- and pyruvate-containing media. *Biotechnol Prog.* 24, 311-20.
- Sigurdsson, M. I., Jamshidi, N., Steingrimsson, E., Thiele, I., Palsson, B. O., 2010. A detailed genome-wide reconstruction of mouse metabolism based on human Recon 1. *BMC Syst Biol.* 4, 140.
- Slade, P. G., Hajivandi, M., Bartel, C. M., Gorfien, S. F., 2012. Identifying the CHO secretome using mucin-type O-linked glycosylation and click-chemistry. *J Proteome Res.* 11, 6175-86.
- Srour, O., Young, J. D., Eldar, Y. C., 2011. Fluxomers: a new approach for  $^{13}\text{C}$  metabolic flux analysis. *BMC Syst Biol.* 5, 129.
- Strigun, A., Wahrheit, J., Beckers, S., Heinzle, E., Noor, F., 2011. Metabolic profiling using HPLC allows classification of drugs according to their mechanisms of action in HL-1 cardiomyocytes. *Toxicol Appl Pharmacol.* 252, 183-91.
- Strigun, A., Wahrheit, J., Niklas, J., Heinzle, E., Noor, F., 2012. Doxorubicin increases oxidative metabolism in HL-1 cardiomyocytes as shown by  $^{13}\text{C}$  metabolic flux analysis. *Toxicol Sci.* 125, 595-606.
- Strumilo, S., 2005. Short-term regulation of the alpha-ketoglutarate dehydrogenase complex by energy-linked and some other effectors. *Biochemistry (Mosc).* 70, 726-9.

[T]

- Templeton, N., Dean, J., Reddy, P., Young, J. D., 2013. Peak antibody production is associated with increased oxidative metabolism in an industrially relevant fed-batch CHO cell culture. *Biotechnol Bioeng.* 110, 2013-24.
- Terzer, M., Stelling, J., 2008. Large-scale computation of elementary flux modes with bit pattern trees. *Bioinformatics.* 24, 2229-35.
- Thiele, I., Price, N. D., Vo, T. D., Palsson, B. O., 2005. Candidate metabolic network states in human mitochondria. Impact of diabetes, ischemia, and diet. *J Biol Chem.* 280, 11683-95.
- Thiele, I., Swainston, N., Fleming, R. M., Hoppe, A., Sahoo, S., Aurich, M. K., Haraldsdottir, H., Mo, M. L., Rolfsson, O., Stobbe, M. D., Thorleifsson, S. G., Agren, R., Bolling, C., Bordel, S., Chavali, A. K., Dobson, P., Dunn, W. B., Endler, L., Hala, D., Hucka, M., Hull, D., Jameson, D., Jamshidi, N., Jonsson, J. J., Juty, N., Keating, S., Nookaew, I., Le Novere, N., Malys, N., Mazein, A., Papin, J. A., Price, N. D., Selkov, E., Sr., Sigurdsson, M. I., Simeonidis, E., Sonnenschein, N., Smallbone, K., Sorokin, A., van Beek, J. H., Weichart, D., Goryanin, I., Nielsen, J., Westerhoff, H. V., Kell, D. B., Mendes, P., Palsson, B. O., 2013. A community-driven global reconstruction of human metabolism. *Nat Biotechnol.* 31, 419-25.
- Timon-Gomez, A., Proft, M., Pascual-Ahuir, A., 2013. Differential regulation of mitochondrial pyruvate carrier genes modulates respiratory capacity and stress tolerance in yeast. *PLoS One.* 8, e79405.
- Titus, S. A., Moran, R. G., 2000. Retrovirally mediated complementation of the glyB phenotype. Cloning of a human gene encoding the carrier for entry of folates into mitochondria. *J Biol Chem.* 275, 36811-7.
- Todisco, S., Agrimi, G., Castegna, A., Palmieri, F., 2006. Identification of the mitochondrial NAD<sup>+</sup> transporter in *Saccharomyces cerevisiae*. *J Biol Chem.* 281, 1524-31.

- Tuttle, S., Stamato, T., Perez, M. L., Biaglow, J., 2000. Glucose-6-phosphate dehydrogenase and the oxidative pentose phosphate cycle protect cells against apoptosis induced by low doses of ionizing radiation. *Radiat Res.* 153, 781-7.
- Tyo, K. E., Liu, Z., Petranovic, D., Nielsen, J., 2012. Imbalance of heterologous protein folding and disulfide bond formation rates yields runaway oxidative stress. *BMC Biol.* 10, 16.

## [V]

- van Meer, G., Voelker, D. R., Feigenson, G. W., 2008. Membrane lipids: where they are and how they behave. *Nat Rev Mol Cell Biol.* 9, 112-24.
- van Roermund, C. W., Hettema, E. H., van den Berg, M., Tabak, H. F., Wanders, R. J., 1999. Molecular characterization of carnitine-dependent transport of acetyl-CoA from peroxisomes to mitochondria in *Saccharomyces cerevisiae* and identification of a plasma membrane carnitine transporter, Agp2p. *Embo J.* 18, 5843-52.
- Vander Heiden, M. G., Locasale, J. W., Swanson, K. D., Sharfi, H., Heffron, G. J., Amador-Noguez, D., Christofk, H. R., Wagner, G., Rabinowitz, J. D., Asara, J. M., Cantley, L. C., 2010. Evidence for an alternative glycolytic pathway in rapidly proliferating cells. *Science.* 329, 1492-9.
- Varma, A., Palsson, B. O., 1994. Metabolic Flux Balancing - Basic Concepts, Scientific and Practical Use. *Bio-Technol.* 12, 994-998.
- Vizan, P., Alcarraz-Vizan, G., Diaz-Moralli, S., Solovjeva, O. N., Frederiks, W. M., Cascante, M., 2009. Modulation of pentose phosphate pathway during cell cycle progression in human colon adenocarcinoma cell line HT29. *Int J Cancer.* 124, 2789-96.
- Vozza, A., Blanco, E., Palmieri, L., Palmieri, F., 2004. Identification of the mitochondrial GTP/GDP transporter in *Saccharomyces cerevisiae*. *J Biol Chem.* 279, 20850-7.

## [W]

- Wahrheit, J., Heinzle, E., 2013. Sampling and quenching of CHO suspension cells for the analysis of intracellular metabolites. *BMC Proc.* 7, 42.
- Wahrheit, J., Heinzle, E., 2014a. Quenching methods for the analysis of intracellular metabolites. *Methods Mol Biol.* 1104, 211-21.
- Wahrheit, J., Heinzle, E., 2014b. Quenching Methods for the Analysis of Intracellular Metabolites. In: Pörtner, R., (Ed.), *Animal Cell Biotechnology*. vol. 1104. Humana Press, pp. 211-221.
- Wahrheit, J., Nicolae, A., Heinzle, E., 2011a. Eukaryotic metabolism: measuring compartment fluxes. *Biotechnol J.* 6, 1071-85.
- Wahrheit, J., Nicolae, A., Heinzle, E., 2014a. Dynamics of growth and metabolism controlled by glutamine availability in Chinese hamster ovary cells. *Appl Microbiol Biotechnol.* 98, 1771-83.
- Wahrheit, J., Niklas, J., Heinzle, E., 2011b. Evaluation of sampling and quenching procedures for the analysis of intracellular metabolites in CHO suspension cells. *BMC Proc.* 5 Suppl 8, P82.
- Wahrheit, J., Niklas, J., Heinzle, E., 2014b. Metabolic control at the cytosol-mitochondria interface in different growth phases of CHO cells. *Metab Eng.* 23C, 9-21.
- Wahrheit, J., Nonnenmacher, Y., Sperber, S., Heinzle, E., 2015. High-throughput respiration screening of single mitochondrial substrates using permeabilized CHO cells highlights control of mitochondria metabolism. *Engineering in Life Sciences.* n/a-n/a.
- Wallace, D. C., 2012. Mitochondria and cancer. *Nat Rev Cancer.* 12, 685-98.
- Walsh, G., 2010. Biopharmaceutical benchmarks 2010. *Nat Biotechnol.* 28, 917-24.

- Walter, P., Stucki, J. W., 1970. Regulation of pyruvate carboxylase in rat liver mitochondria by adenine nucleotides and short chain fatty acids. *European Journal of Biochemistry*. 12, 508-19.
- Weibel, E. R., Staubli, W., Gnagi, H. R., Hess, F. A., 1969. Correlated morphometric and biochemical studies on the liver cell. I. Morphometric model, stereologic methods, and normal morphometric data for rat liver. *J Cell Biol*. 42, 68-91.
- Wellen, K. E., Thompson, C. B., 2010. Cellular metabolic stress: considering how cells respond to nutrient excess. *Mol Cell*. 40, 323-32.
- Wiback, S. J., Famili, I., Greenberg, H. J., Palsson, B. O., 2004. Monte Carlo sampling can be used to determine the size and shape of the steady-state flux space. *J Theor Biol*. 228, 437-47.
- Wiback, S. J., Mahadevan, R., Palsson, B. O., 2003. Reconstructing metabolic flux vectors from extreme pathways: defining the alpha-spectrum. *J Theor Biol*. 224, 313-24.
- Wiback, S. J., Palsson, B. O., 2002. Extreme pathway analysis of human red blood cell metabolism. *Biophys J*. 83, 808-18.
- Wiechert, W., de Graaf, A. A., 1997. Bidirectional reaction steps in metabolic networks: I. Modeling and simulation of carbon isotope labeling experiments. *Biotechnol Bioeng*. 55, 101-17.
- Wiechert, W., Noh, K., 2005. From stationary to instationary metabolic flux analysis. *Adv Biochem Eng Biotechnol*. 92, 145-72.
- Willemssen, A. M., Hendrickx, D. M., Hoefsloot, H. C., Hendriks, M. M., Wahl, S. A., Teusink, B., Smilde, A. K., van Kampen, A. H., 2015. MetDFBA: incorporating time-resolved metabolomics measurements into dynamic flux balance analysis. *Mol Biosyst*. 11, 137-45.
- Williamson, J. R., Cooper, R. H., 1980. Regulation of the citric acid cycle in mammalian systems. *FEBS Lett*. 117 Suppl, K73-85.
- Wittmann, C., Heinzle, E., 1999. Mass spectrometry for metabolic flux analysis. *Biotechnology and Bioengineering*. 62, 739-750.
- Wittmann, C., Heinzle, E., 2002. Genealogy profiling through strain improvement by using metabolic network analysis: metabolic flux genealogy of several generations of lysine-producing corynebacteria. *Appl Environ Microbiol*. 68, 5843-59.
- Wu, F., Yang, F., Vinnakota, K. C., Beard, D. A., 2007. Computer modeling of mitochondrial tricarboxylic acid cycle, oxidative phosphorylation, metabolite transport, and electrophysiology. *J Biol Chem*. 282, 24525-37.

## [X]

- Xie, L., Wang, D. I., 1996. Material balance studies on animal cell metabolism using a stoichiometrically based reaction network. *Biotechnol Bioeng*. 52, 579-90.
- Xu, X., Nagarajan, H., Lewis, N. E., Pan, S., Cai, Z., Liu, X., Chen, W., Xie, M., Wang, W., Hammond, S., Andersen, M. R., Neff, N., Passarelli, B., Koh, W., Fan, H. C., Wang, J., Gui, Y., Lee, K. H., Betenbaugh, M. J., Quake, S. R., Famili, I., Palsson, B. O., 2011. The genomic sequence of the Chinese hamster ovary (CHO)-K1 cell line. *Nat Biotechnol*. 29, 735-41.

## [Y]

- Yang, H., Mandy, D. E., Libourel, I. G., 2014. Optimal design of isotope labeling experiments. *Methods Mol Biol*. 1083, 133-47.
- Yang, T. H., Bolten, C. J., Coppi, M. V., Sun, J., Heinzle, E., 2009. Numerical bias estimation for mass spectrometric mass isotopomer analysis. *Anal Biochem*. 388, 192-203.

- Yang, T. H., Frick, O., Heinzle, E., 2008. Hybrid optimization for  $^{13}\text{C}$  metabolic flux analysis using systems parametrized by compactification. *BMC Syst Biol.* 2, 29.
- Young, J. D., 2014. INCA: a computational platform for isotopically non-stationary metabolic flux analysis. *Bioinformatics.* 30, 1333-5.
- [Z]
- Zamboni, N., 2011.  $^{13}\text{C}$  metabolic flux analysis in complex systems. *Curr Opin Biotechnol.* 22, 103-8.
- Zamboni, N., Fendt, S. M., Ruhl, M., Sauer, U., 2009.  $^{13}\text{C}$ -based metabolic flux analysis. *Nat Protoc.* 4, 878-92.
- Zamboni, N., Fischer, E., Sauer, U., 2005. FiatFlux--a software for metabolic flux analysis from  $^{13}\text{C}$ -glucose experiments. *BMC Bioinformatics.* 6, 209.
- Zamorano, F., Vande Wouwer, A., Jungers, R. M., Bastin, G., 2012. Dynamic metabolic models of CHO cell cultures through minimal sets of elementary flux modes. *J Biotechnol.*
- Zamorano, F., Wouwer, A. V., Bastin, G., 2010. A detailed metabolic flux analysis of an underdetermined network of CHO cells. *J Biotechnol.* 150, 497-508.
- Zara, V., Ferramosca, A., Papatheodorou, P., Palmieri, F., Rassow, J., 2005. Import of rat mitochondrial citrate carrier (CIC) at increasing salt concentrations promotes presequence binding to import receptor Tom20 and inhibits membrane translocation. *J Cell Sci.* 118, 3985-95.
- Zarrilli, R., Oates, E. L., McBride, O. W., Lerman, M. I., Chan, J. Y., Santisteban, P., Ursini, M. V., Notkins, A. L., Kohn, L. D., 1989. Sequence and chromosomal assignment of a novel cDNA identified by immunoscreening of a thyroid expression library: similarity to a family of mitochondrial solute carrier proteins. *Mol Endocrinol.* 3, 1498-505.
- Zhang, F., Sun, X., Yi, X., Zhang, Y., 2006. Metabolic characteristics of recombinant Chinese hamster ovary cells expressing glutamine synthetase in presence and absence of glutamine. *Cytotechnology.* 51, 21-8.
- Zhang, Y. H., 2011. Substrate channeling and enzyme complexes for biotechnological applications. *Biotechnol Adv.* 29, 715-25.
- Zhao, Q., Kurata, H., 2009. Maximum entropy decomposition of flux distribution at steady state to elementary modes. *Journal of Bioscience and Bioengineering.* 107, 84-89.
- Zhu, Y., King, B. L., Parvizi, B., Brunk, B. P., Stoeckert, C. J., Jr., Quackenbush, J., Richardson, J., Bult, C. J., 2003. Integrating computationally assembled mouse transcript sequences with the Mouse Genome Informatics (MGI) database. *Genome Biol.* 4, R16.
- Zupke, C., Stephanopoulos, G., 1994. Modeling of Isotope Distributions and Intracellular Fluxes in Metabolic Networks Using Atom Mapping Matrices. *Biotechnol Progr.* 10, 489-498.
- Zupke, C., Stephanopoulos, G., 1995. Intracellular flux analysis in hybridomas using mass balances and in vitro  $^{13}\text{C}$  nmr. *Biotechnol Bioeng.* 45, 292-303.
- Zurbriggen, M. D., Moor, A., Weber, W., 2012. Plant and bacterial systems biology as platform for plant synthetic bio(techno)logy. *J Biotechnol.* 160, 80-90.
- Zwingmann, C., Richter-Landsberg, C., Leibfritz, D., 2001.  $^{13}\text{C}$  isotopomer analysis of glucose and alanine metabolism reveals cytosolic pyruvate compartmentation as part of energy metabolism in astrocytes. *Glia.* 34, 200-12.

# Curriculum Vitae



---

## Work experience

**March 2015 - present**

Position **Research Associate**

Employer University of Luxembourg,  
Luxembourg Center for Systems Biomedicine

**November 2008 – September 2014**

Position **Scientific Research Assistant**

Employer Universität des Saarlandes, Technische Biochemie

**March 2007 – October 2008**

Position **Scientific Research Assistant**

Employer Institutul National pentru Cercetare – Dezvoltare in Stiinte  
Biologice  
(National Institute for Research and Development in  
Biological Sciences)

## Education

**November 2008 → 2015**

Title **Doctoral course for PhD in Biochemical Engineering**  
(Doktor-Ingenieur in Biowissenschaften)

Universität des Saarlandes

**2006 → 2008**

Title Master in Biotechnology

University Politehnica of Bucharest

**2001 → 2006**

Title Diploma Engineer of Chemical Engineering (with honors)  
University Politehnica of Bucharest

**1997 → 2001**

Title Baccalaureate (Secondary School Diploma)

“Mircea cel Batran” National College, Constanta

